UNIVERSITÀ DEGLI STUDI DI PALERMO

Dottorato in Ingegneria dell'Innovazione Tecnologica
Dipartimento di Ingegneria
ING-IND/25

Technologies for cultivation and exploitation of microalgae in industrial applications

IL DOTTORE
Dott. **Serena Lima**

IL COORDINATORE
Prof. Ing. Salvatore Gaglio

IL TUTOR
Prof. Ing. Alberto Brucato

CO TUTOR
Prof. Ing. Francesca Scargiali

CICLO XXXII
ANNO CONSEGUIMENTO TITOLO: 2020

Table of Contents

Acknowledgments

My gratitude goes to all the lab staff who helped me during my project in the time spend at the University of Palermo. I want to especially thank Giuseppe Fanale, Paolo Guerra, Andrea Vaccaro for their help and their precious advices. Many thanks to Ing. A. Siragusa and R. Arcuri for providing the sewage samples employed in my work and for performing the sewage analysis.

I wish to sincerely thank the staff of Colin Robinson lab at the Kent University, Canterbury, UK and I want to thank in particular Prof. Colin Robinson for hosting me in his lab during my first ten months of PhD and Julie Zedler for all the help, the advices and the courage she infused me while working together.

I would like to thank all the people that helped me during my months at the Nord University, Bodö, Norway and in particular Peter Schulze, Daniela Morales-Sanchez, Ralf Rautenberger and Prof. Kiron Viswanath for hosting me and sharing their precious knowledge with me. I also thank the staff of CCMAR, Faro, Portugal and in particular Lisa M. Schüler Tamára F. Santos and Prof. João C. S. Varela.

I wish to thank all the professors of my Department at Palermo University and in particular Giuseppe Caputo, Andrea Cipollina, Giorgio Micale and Alessandro Tamburini for their precious help and advice.

Thanks to all PhD students with whom I spent my time during the last three years and also the McS students that helped me during my work, namely Valentina Brunetto, Monica Richiusa, Evelin Costa, Pasquale Iannotta, Nadia Moukri, Francesco De Patrizio.

I wish to thank the post doc and friend Valeria Villanova for the precious help and for the many ideas she shared with me in the last years.

My grateful thanks go to Prof. Alberto Brucato, Prof. Francesca Scargiali and Prof. Franco Grisafi for the support given during all the three years of my PhD and the trust they always demonstrated to me.

My deepest thanks to my family: it is because of their help and support that my study period and my thesis work was possible. Thanks to Luigi Caleca for all the support, help and patience he demonstrated me during my PhD.

To all other persons involved in the project not mentioned above, I wish to address my sincere gratitude.

List of publications

Journal pubblications:

- G. Marotta, F. Scargiali, S. Lima, G. Caputo, F. Grisafi, A. Brucato, Vacuum air-lift bioreactor for microalgae production, Chem. Eng. Trans. 57 (2017) 925–930. doi:10.3303/CET1757155.
- S. Lima, C. Webb, E. Deery, C. Robinson, J. Zedler, Human Intrinsic Factor Expression for Bioavailable Vitamin B12 Enrichment in Microalgae, Biology (Basel). 7 (2018) 19. doi:10.3390/biology7010019.
- S. Lima, F. Grisafi, F. Scargiali, G. Caputo, A. Brucato, Growing Microalgae in a "Quasi-isoactinic" Photobioreactor, in: Chem. Eng. Trans., 2018: pp. 673–678. doi:10.3303/CET1864113.
- S. Lima, V. Villanova, M. Richiusa, F. Grisafi, F. Scargiali, A. Brucato, Pollutants Removal from Municipal Sewage by Means of Microalgae, in: Chem. Eng. Trans., 2019. doi:10.3303/CET1974208.

Under preparation or submitted:

- S. Lima, V. Villanova, A. Brucato, F. Grisafi, F. Scargiali. Microalgae as an effective tool for nutrient removal in municipal wastewater. Submitted for publication to *Algal Research.*
- S. Lima, P. S. C. Schulze, L. M. Schüler, R. Rautenberger, D. Morales-Sánchez, T. F. Santos, H. Pereira, J. C. S. Varela, F. Scargiali, R.H. Wijffels and K. Viswanath. Induction of proteins, polyunsaturated fatty acids and pigments in three microalgae using flashing light. Submitted for publication to *Biotechnology and Bioengineering*.
- D. Morales-Sánchez, L. Jep, S. Lima, P. S. C. Schulze, R.H. Wijffels, and K.Viswanath. Gene expression of *Nannochloropsis gaditana* under different flashing light. Under preparation.
- S. Lima, V. Villanova, F. Grisafi, A. Brucato, F. Scargiali. Combined effect of nutrient and flashing light frequency for a biochemical composition shift in *Nannochloropsis gaditana* grown in a "quasi-isoactinic" reactor. Submitted for publication to *Canadian Journal of Chemical Engineering*.

Partecipation to national conferences:

- Workshop Giovani AISAM 2019, Firenze 28/10/2019. Oral presentation: S. Lima, V. Villanova, F. Grisafi, A. Brucato, F. Scargiali. Effect of flashing light frequency on the induction of proteins, polyunsaturated fatty acids and pigments in three microalgae.
- GRICU School 2019, Palermo 3-7/07/2019. Poster presentation: S. Lima, F.

Scargiali, F. Grisafi, A. Brucato. Outcome of flashing light on microalgal growth: employing a « quasi-isoactinic » photobioreactor for investigating the growth kinetics and biochemical composition.

- GRICU School 2018, Pisa 16-19 may 2018, Poster presentation: Microalgae growth via a "quasi -isoactinic " photobioreactor : influence of dark-light cycles frequency.

Partecipation to International conferences:

- Conference Icheap 14, Bologna 26-29/05/2019, oral presentation: S. Lima, V. Villanova, M. Richiusa, F. Grisafi, F. Scargiali, A. Brucato. Pollutants removal from municipal sewage by means of microalgae.
- Eaba novel food for algae biomass workshop, Bruxelles 22-23/05/2019, pitch presentation: Microalgae research at the University of Palermo.
- IBIC 2018, Venezia 15 - 18 April, 2018, Oral presentation: S, Lima, F. Grisafi, F, Scargiali, G. Caputo, A. Brucato. Growing Microalgae in a "Quasi-isoactinic" photobioreactor.
- AlgaEurope Conference 2017, Berlin 5-7 December 2017, Oral presentation: Assessment of dark-light cycle effects on microalgae growth via a "quasi-isoactinic" photobioreactor.

Advances courses attended:

Title	Date and place
Course: Introduction to Learning, Teaching and Academic Environment	4/11/2016 18/11/2016 2/12/2016 University of Kent, Canterbury
Course: Critical Perspectives on Academic Practice	20/01/2017 3/02/2017 17/02/2017 University of Kent, Canterbury
PhD School: Multi-scale modelling for chemical engineering: From research in the lab to profitable applications	25-29/09/2017 Università degli Studi di Palermo
Seminar: Innovation ecosystem and tech-entrepeneurship in Israel	16/10/2017 Università degli Studi di Palermo
Seminar: Making Public Displays Interactive: From Application Design to Long-Term Deployment	26/10/2017 Università degli Studi di Palermo

Seminar: Phase Equilibrium Calculations with Equations of State	23/03/2018 Università degli Studi di Palermo
Seminar: Design and scale up of precipitation and crystallization processes: computational and experimental approaches	15/02/2018 Università degli Studi di Palermo
PhD School: Advanced chemical reactors , Circular economy concepts in process engineering.	16/05/18-19/05/18 Polo "Le Benedettine", Università di Pisa, Pisa
Seminars: "Cyclodextrins and catalysis: Recent advances and future opportunities" "Unusual Applications of Cyclodextrins in Organometallic Catalytic Processes"	7/06/2018 Università degli Studi di Palermo
Course: La comunicazione in pubblico	26-27/06/2018 Università degli Studi di Palermo
Corso di Formazione obbligatorio Generale e Specifica, per i lavoratori dell'Ateneo ed i soggetti ad essi equiparati.	16-17/07/2018 Università degli Studi di Palermo
Scuola di Calcolo con Matlab 2018	23-27/07/2018 Università degli Studi di Palermo
Eaba novel food for algae biomass workshop	22-23/05/2019 Bruxelles
PhD School: Il contributo dell'Ingegneria Chimica Italiana alla sostenibilità globale	30/06/2019-7/07/2019 Palermo

Aim of the thesis

Aim of the thesis

In the next decades human kind will face mainly three problems.

The first one is the increase of world temperature caused by the release in the atmosphere of greenhouse gases, phenomenon that is causing a potential disastrous climatic change. In the last period this theme has been highlighted by the media all over the world, also thanks to the young activist Greta Thunberg that put the spotlight on temperature rise. Unluckily, the phenomenon is not limited to headings in media: in September 2019, the Intergovernmental Panel on Climate Change (IPCC) exited their last report on the effect of climate change on the oceans and the cryosphere (IPCC, 2019a), after that of August 2019 concerning the effects on lands (IPCC, 2019b) and that of 2018 about the expected effects of a 1.5°C temperature increase on the planet (IPCC, 2018). These documents depict a clear and pessimistic scenario that indicates a very urgent need for action.

A further issue, partially connected to the first one, is the environment pollution caused mainly by the contamination of the hydric resources and by the accumulation of plastic materials. These issues are tightly connected to the massive industrialization occurred over the last two centuries, mainly, but not only, in western countries, but also to the population increase due in turn to the enhanced welfare. The pollution can be caused also by the agriculture and by the massive usage of fertilizers and chemicals employed to enforce the crop yields.

Then, there is the food crisis, which is spreading in developing countries. The need of food is going to increase in next years because of the exponential increase of human population, which will reach 10 billions in 2050 according to the Food and Agriculture Organization of the United Nations (FAO) (FAO, 2017). In this moment, in the western side of the world two millions people are dying every year because of the huge diffusion of malnutrition that causes overweight and death by chronic diseases. At the same time more than 820 millions of people do not have enough to eat, mainly in the developing countries (http://www.fao.org/state-of-food-security-nutrition/en/). Furthermore, the additional food that is going to be produced will cost a further increase of CO_2 emissions and relevant greenhouse effects, unless sustainably produced. It is to point out also that the increasing need of land areas for crop production causes destruction of forests; an example is the huge fire that hit the Amazon rainforest last summer and destroyed large part of it.

In this scenario, in the last decades microalgae gained a growing interest within the scientific community. They are microorganisms belonging to a variety of classes and phyla which perform photosynthesis, the surprising process occurring in our planet by which Life exists as we know it. They are responsible for the 50% of the global photosynthetic activity despite amounting only to the 0.2% of the biomass (Parker et al., 2008) and are the main CO_2/O_2 exchangers of the planet, with atmospheric CO_2 fixing

capability. Furthermore, they show several advantages compared to land plants; for example, they do not need arable lands for their growth and can employ wastewaters or salty water as a source of nutrients. Despite that, photosynthesis has some limitations; for example, only a fraction of the entire solar spectrum can be exploited and the photosynthetic antenna prevent the high-intensity caption of solar radiation. Furthermore, the concentration of CO_2, although relatively high as regards the greenhouse effect, is a limiting factor for the photosynthetic process. This is due to an evolutionary aspect, as Nature selected the *resilience* and not the *efficiency* in living organisms.

According to Prof. Guido Saracco, we need do like Nature, but possibly better than Nature (Saracco, 2017), that means that we need to exploit the photosynthetic mechanism and employ it for our purposes. To do that at best, we should modify the algal behaviour by employing biotechnological techniques or, as an alternative, by modifying the algal genome in such a way that they produce more efficiently the desired high-value biocompounds. In other words, we need to exploit the solar energy to transform it in what we need, by employing the microalgal cell as a high-value biorefinery. It is clear how, in this context, a strong interdisciplinarity is needed, as issues regarding chemical engineering, alternative energies, biology, biotechnology and molecular biology are involved.

The aim of my thesis is to work on how microalgae can help easing the future issues of human kind. Microalgal research and industrial cultivation is only a few tens of years old, so there still are several limitations and issues to solve. My research deals with the study of microalgal biology and with the development of technologies aimed at trying to make the best of them. My hope is that of devising tools able to promote the microalgal market in the world, as well as in southern Italy, as a sustainable source of healthy food, high-value biocompounds and biomass to be employed for various applications.

Contents

Contents

This thesis work is focused on technologies for the development of the microalgal industry. During this 3-years PhD work several themes were addressed.
Section 1 consists in a literature review concerning the general features of microalgae, their composition and a description of the photosynthetic process. Furthermore, themes such as biosynthetic pathways, growth kinetics, microalgae cultivation and their applications are reviewed.
Section 2 focuses on the genetic manipulation of microalgae aimed at producing a vitamin B12-enriched food supplement. In this case, the human intrinsic factor gene, was inserted in the genome of the microalgae *Chlamydomonas reinardhtii* in order to integrate new functions in this organism and path the way for the creation of a B12-enriched microalgal supplement. For sure, genetic engineering is going to play a role in the future of microalgal industry, but, while these technologies are developing, alternative strategies may consist in exploiting the present available photosynthetic microorganisms for obtaining the desired products.
For this reason, in Section 3, flashing light as lighting strategy was explored. In fact, light energy was provided in packages to three different microalgal species, *Nannochloropsis gaditana*, *Koliella antarctica*, *Tetraselmis chui*, to observe the enhanced production of high-value products such as chlorophylls, carotenoids and polyunsaturated fatty acids. Furthermore, this method represents a temporal dilution of light aimed at avoiding the saturation effect.
An alternative strategy for the exploitation of microalgal industry may consist in selecting and isolating indigenous species in an approach called *phycoprospecting*, discussed in Section 4. The concept of phycoprospecting relies on employing wastewaters as a nutrient source in order to create a sustainable process able to remediate polluted effluents while at the same time providing valuable compounds.
Lastly, in Section 5 the theme of outdoor photobioreactors for the production of microalgal biomass is addressed. The possibility to produce biomass and extend microalgal industry in Sicily, a region full of unexploited natural resources, was investigated.

Section 1: State of the art

1.1. Microalgae: a photosynthetic factory

Microalgae are a large class of photosynthetic microorganisms not belonging to the same phyletic group; this means that they have very different characteristics, both on a morphological than on a functional point of view. One diffused characteristic is being unicellular, even if we can go through a series of various cellular organizations and morphologies as shown in Figure 1.1 (Richmond and Hu, 2013).

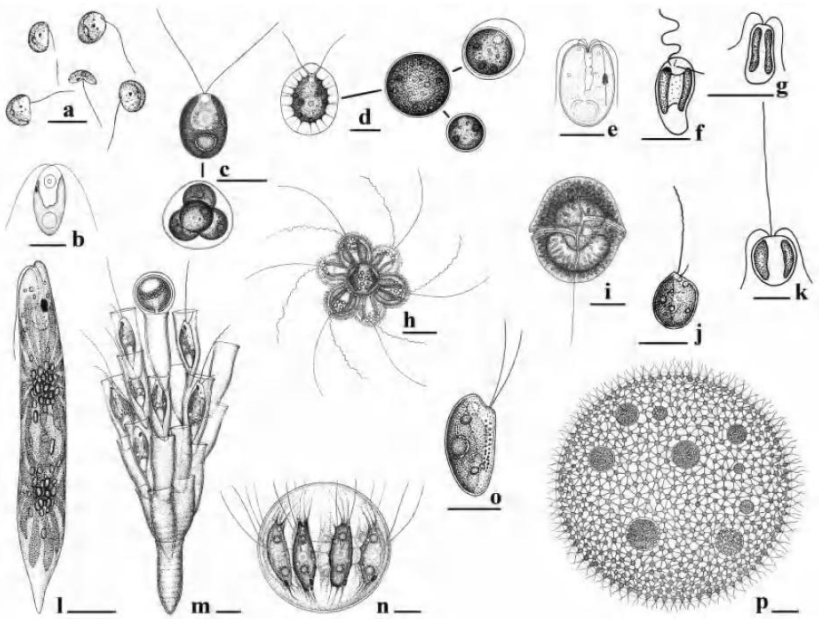

Figure 1.1: examples of flagellate microalgae diversity. a) *Pedinomonas* with one flagellum; b) *Dunaliella* with two flagella. Scale bar 5 µm; c) *Chlamydomonas* with two flagella or in the non flagellate version. Scale bar 10 µm; d) *Haematococcus* shown as a monoflagellate cell or as three non flagellate ones. Scale bar 10 µm; e) *Tetraselmis*, a quadriflagellate marine alga. Scale bar 5 µm; f) *Pavlova*, with two unequal flagella. Scale bar 5 µm; g) *Isochrysis*, with two flagella and two chloroplasts. Scale bar 5 µm; h) *Synura*, a colony with cells attached in the centrum. Scale bar 10 µm; i) *Gymnodium*, a dinoflagellate with several flagella. Scale bar 25 µm; l) *Ochromonas*, with two enequal flagella. Scale bar 10 µm; m) *Dinobryon*, an arbuscolar colony. Scale bar 10 µm; n) *Stephanosphaera*, a marine biflagellate. Scale bar 10 µm; o) *Rhodomonas*, a common marine biflagellate. Scale bar 10 µm; p) *Volvolox*, a large colonial flagellate with reproductive cells inside the otherwise hollow colony. Scale bar 35 µm. Reproduced from (Richmond and Hu, 2013).

The cell shape can vary and they are usually described as amoeboid, palmelloid, coccoid, filamentous, flagellate and sarcinoid. Furthermore, algae can exist as independent cells or they can be organized in more complex structures as shown in Figure 1.1p. They normally divide by an asexual reproduction but they can divide also through a sexual reproduction, similar to that belonging to other eukaryotes. Also the microalgae ultrastructure reflects their broad phylogenetic diversity. The main organelles of microalgal cells are:

- Plastids, the plants and algae light-harvesting organelles and, in particular, chloroplasts, the organelles responsible for the photosynthesis. They contain the chlorophyll and the photosynthesis occurs inside them. They are surrounded by a membrane and the inner part is called stroma, in which there are thylacoids, membranes in which the first steps of photosynthesis take place. The thylakoid arrangement varies among algal group (Kim and Archibald, 2009). Many thylacoids contain a pyrenoid, a CO_2-concentrating organelle in which the so called dark step of photosynthesis occurs, namely Calvin cycle. That's the step in which the fixation of CO_2 happens (Giordano et al., 2005).
- Mitochondrion, which has a central role in the energetic metabolism of the cell. In it, adenosine triphosphate (ATP) is produced (McBride et al., 2006).
- Nucleus, which is the organelle in which DNA is stored.
- Golgi body and endoplasmic reticulum, with functions of molecular products modification and secretion.
- Vacuoles, involved in the cell osmotic regulation.
- Flagella, own by swimming algae.

Under a biochemical point of view, algae contain all the major groups of macromolecules [*e.g.* carbohydrates, lipids, nucleic acids and proteins) but again they provide an exceptional diversity. They contain:

- Carbohydrates, such as starch or starch-like products. They are normally easy to observe in grains by using an optical microscope (Busi et al., 2014).
- Lipids, that occur in a variety of different compounds (Wood, 1974). The lipid composition varies depending on the microalgae species and on environmental conditions. As well known, microalgae respond to environmental stress by producing more lipids (Banerjee et al., 2017; Zhu et al., 2015). The research on this topic had a boost in the past years mainly because of the foreseen possibility to transform them in biodiesel. Now they are primarily considered as a nutritious source of essential fatty acids for human food.
- Proteins. In some cases, algae are very good sources of high-nutritional value protein. Some microalgae have a protein composition of 40 to 70% of the dry weight (Rebolloso-Fuentes et al., 2001) and algae such as *Chlorella* or *Tetraselmis* have percent of 50% in average (Becker, 2007; Tibbetts et al., 2015). They are often used as natural food supplement.
- Photosynthetic pigments. There are three major classes of them: chlorophylls, carotenoids and phycobilins. Chlorophylls present a tetrapyrrole ring with a central magnesium atom and a long-chain terpenoid alcohol. Chlorophyll *a* (Chl *a*) is present in the core center designated to

photosynthesis, while b and c are accessories and extend the range of light absorption. Carotenoids are a large group of chromophores constituted by two hexacarbon rings joined by an 18-carbon chain. They have some light-harvesting function next to some structural ones and together with the protection against stress irradiance. Phycobilins are linear tetrapyrroles present in cyanobacteria and red algae in the main antennae (Mulders et al., 2014).

1.2. The biology of photosynthesis

1.2.1. Overview

Oxygenic photosynthesis involves microorganisms such as microalgae and cyanobacteria. We refer to cyanobacteria as prokaryotic cells, in which there is no compartmentalization in organelles and in which we distinguish a nucleoid, where the genetic material is accumulated, and a chromoplast, peripherical and close to the cell wall, where the photosynthetic reactions occur. On the other way, we refer to microalgae as heterotrophic microorganisms that contain chloroplast as organelles responsible for the photosynthesis.

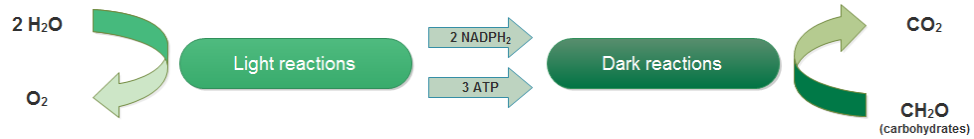

Figure 1.2 : Major products of the light and dark reactions of photosynthesis. The light reactions produce oxygen, two molecules of $NADPH_2$ and three molecules of ATP using the light energy and reducting water. $NADPH_2$ and ATP are used in the dark reactions to fix atmospheric CO_2 in organic matter (Richmond and Hu, 2013).

Photosynthesis is a process that converts solar energy and inorganic compounds in chemical energy and organic compounds. This process is essential for the life in Earth, and all the living being are somehow dependent on it. In this work, there is a focus on photosynthesis in microalgae, taking in consideration heterotrophic microorganisms not belonging to the same phyla. The process is composed by two series of reactions, as shown in Figure 1.2, the light and the dark reactions. In the light reactions the solar energy is converted in chemical energy in the form of 2 molecules of NADPH2 (nicotinamide adenine dinucleotide phosphate), cofactor in anabolic reactions that require it as reducing agent, and 3 molecules of ATPs, providing energy for the dark reactions. Water is used as donor of electrons and oxygen is generated as side-product. On the other way, dark reactions involve the fixation of atmospheric CO_2 in organic compounds.

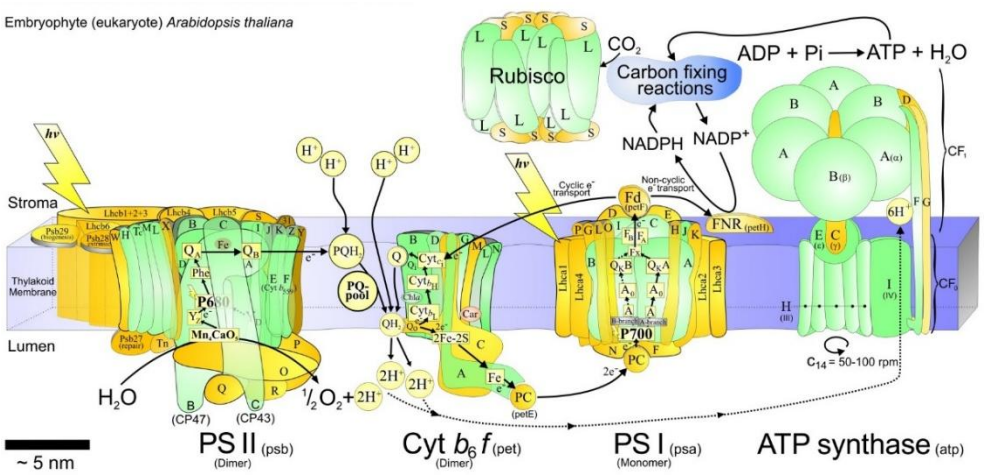

Figure 1.3**:** Arrangement of photosystems involved in the photosynthetic light reactions (Allen et al., 2011).

In Figure 1.3 the arrangement of photosystems is showed. One observes how, while light is harvested by photosystems II (PSII) and photosystem I (PSI), two electrons are extracted from water and reduced in oxygen. These are transported through a series of electrons carriers, including Plastoquinone (PQ), cytochrome b6/f (Cytbf), Plastocyanin (PC) to PSI where they are employed to produce NADPH. At the same time, protons (H+) are transported into the thylakoid lumen and a pH gradient is generated. This gradients allows ATP synthase to work.

1.2.2. Photochemical Pigments

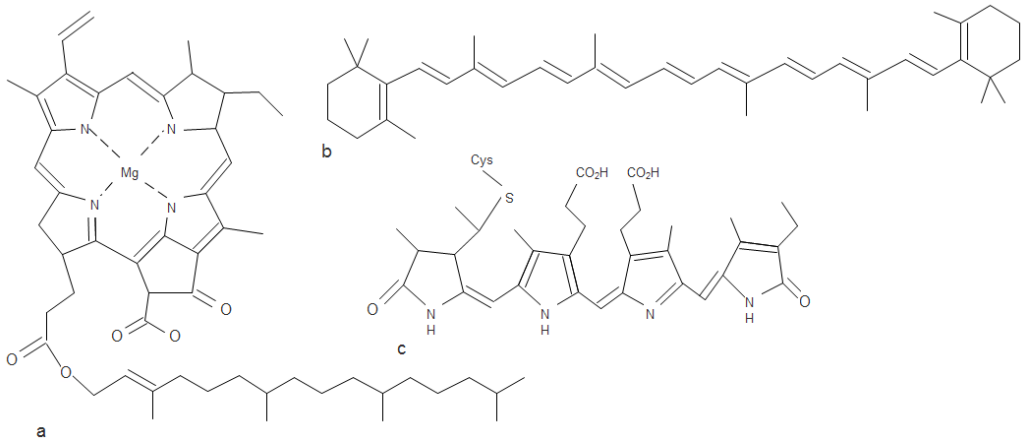

Figure 1.4: Molecular structures of the pigments in microalgae and cyanobacteria (a) Chl a representing the chlorophylls; (b) b-carotene, representing the carotenoids; (c) peptide-linked phycocyanobilin, representing the phycobiliproteins (Mulders et al., 2014).

Photosynthesis would not happen without some molecules specialized in harvesting light. These molecules are called photochemical pigments. There are three major classes of them: chlorophylls, carotenoids and phycobilinproteins. The difference amongst these groups relies on their chemical composition, as shown in Figure 1.4. In fact, chlorophylls present a long aromatic ring, the chlorin, which contains four pyrrole rings that surround a central magnesium atom and a long-chain terpenoid alcohol. Chl *a* is present in the core center designated to photosynthesis, while *b* to *f* can extend the range of light absorption and are located in the Light Harvesting Complexes (LCHs) close to the core center of PSII and I. Carotenoids are a large group of chromophores constituted by two hexacarbon rings joined by an 18-carbon chain. They have some light-harvesting function together with some structural ones and with the protection function against stress irradiance. Carotenoids are distinguished by different end-groups and divided in carotenes, that are true hydrocarbons, and xanthophylls, which contain oxygen atoms. Phycobiliproteins consist of two parts: a bilipigment, known as phycobilin, and a protein, which are covalently attached to each other via a cysteine amino acid. The phycobilin contains building blocks similar to those of chlorin, but they form an open linear structure. The common characteristic of the photochemical pigments is to owe a system of large conjugated double bounds, which can absorb specific wavelengths by excitation of the delocalized electrons. The not absorbed light is reflected, giving to the pigments their color.

1.2.3. Nature of light

In order to go through the photosynthetic mechanisms, one needs to focus on the nature of light. Light is an electromagnetic radiation, and visible light is only a small portion of the electromagnetic spectrum, as shown in Figure 1.5. Radiations have wavelengths going from 10^3 to 10^{-12} m; on the base of the wavelengths, the spectrum can be divided in several parts. Visible lights goes from the violet of about 380 nm to the far red at 750 nm, this range being usually expressed in nanometres (1 nm = 10^{-9} m). The visible light wavelengths correspond also to PAR (photosynthetic active radiation). This is the portion of the light spectrum employed in photosynthesis.

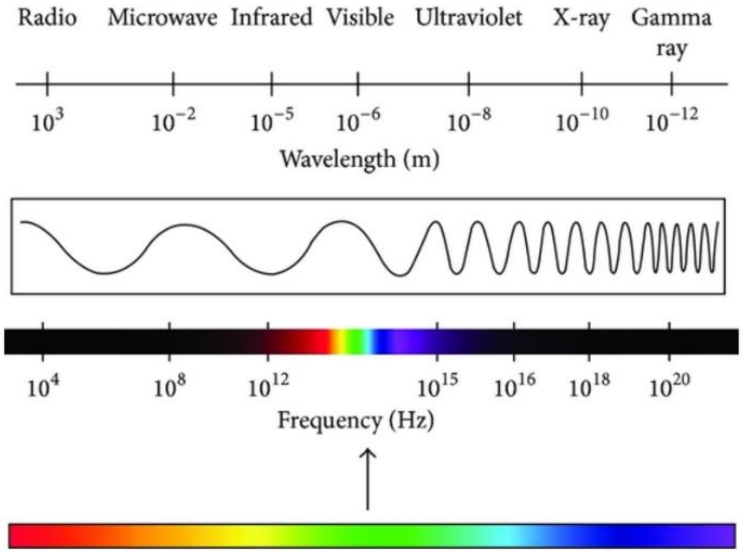

Figure 1.5 Electromagnetic Spectrum (Lewicka et al., 2015).

According to quantum theory, light travels in packages called photons and each of them has an energy equal to the product of its frequency by Plank's constant *h*.

$$E = h\upsilon \qquad 1\text{-I}$$

where $h = 6.626 \times 10^{-34}$ J s.

Since energy is inversely related to wavelengths, a blue light photon (about 400 nm) is more energetic than a red light one (around 700 nm). Photosynthetic pigments absorb the energy of the light and transfer it to the photochemical complexes, where it is transformed in chemical energy and used for the overall photosynthetic process. Light energy is measured in several ways and by using several units. Here we discuss about irradiance, as the flux of photons that hits a surface in the unit of time, measured in μmol quanta m^{-2} s^{-1} or μE m^{-2} s^{-1}. An alternative units is W m^{-2}.

1.2.4. Harvesting light: Light Reactions

The light reactions of photosynthesis take place in Photosystems II and I (PSII and PSI), contained in the chloroplast. The chloroplast is constituted by an outer membrane and an inner one that surround the stroma. Embedded in the stroma, there are grana, stacks of membranes called thylacoids. Between one grana and another there are connections of membranes called stromal lamellae, as shown in Figure 1.6.

Antenna systems are molecular complexes with the primary function of light harvesting and energy transfer to the photosynthetic reaction centres PSII and PSI. A group of complexes Light Harvesting Complex II (LHC II) serves PS II, and a genetically and biochemically different group called Light Harvesting Complex I (LHC I) is associated with PS I.

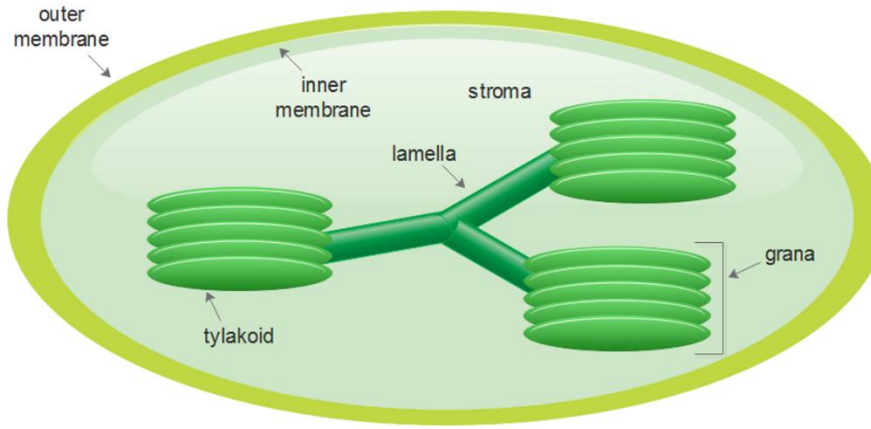

Figure 1.6: Chloroplast structure.

PSII is a macro-complex of subunits embedded in the grana, while PSI and ATPase are located in stromal lamellae. As all cellular organelles, this structure can vary; in fact, the thylakoid membrane is flexible and can reorganise PSII in order to respond to environmental stresses. PSII is a multisubunit complex contained in the chloroplast of cyanobacteria, algae and higher plants. It harvests light and converts it in chemical energy employed to oxidize water and reduce Plastoquinone (PQ) (Drop et al., 2014). The PSII is composed by a Reaction Centre (RC) that is conserved, plus some LHCs or Antenna. These are variable in number and quality depending on the organism and on the environmental condition. The RC always contains 6 Chl *a* and 2 Pheophytin (Pheophytins are first electron carrier intermediate in the electron transfer pathway of PS II in plants) and it is contained into a core complex, which includes as well two antenna complexes: CP43 and CP47. They carry other 13 and 16 Chl *a* and several β-carotene molecules. The antenna complexes are not too much close to the reaction centre because here, during charge separation, pigments are oxidated, but they need to be close enough to transmit the energy from the photosynthetic pigments of the antennas to the reaction centre, where

the energy is processed. In the core there are about 20 subunits but the ratio between pigments and protein is quite low. This is why, during the evolution, other light-harvesting complexes developed with a higher ratio (Van Amerongen and Croce, 2013). The LHC complexes usually contain Chl *a* and *b* pigments together with xanthophylls lutein, violaxanthin and neoxanthin, responsible for light absorption and Photosynthetic Electron Energy Transfer (PET). In the context of overall photosynthesis, PSII is where separation of charges begins; the primary donor is P680 and then electron flows through pheophytin to plastoquinone QA and then to QB, as shown in Figure 1.3.

Between PSII and PSI there is an intermediate cytochrome b6/f complex; the electron flow through them is assisted by two mobile carriers: plastoquinone (Q) from PSII to cytochrome b6/f complex and plastocyanin (PC) from cytochrome b6/f complex to PSI. Plastoquinone also translocate two protons from the stroma to the lumen.

PSI is the second complex responsible for light absorption in the photosynthetic process. It has the main role of reducing ferrodoxin (Fe) and oxidating plastocyanin (PC). It contains a core with about 100 Chl *a* and usually there are, as in PSII, outer antennas of the LHCI multigenic family. The PSI is the highest efficiency quantum converter in nature (Nelson, 2009): the ratio between the number of generated electrons and the absorbed photons is almost 1. Again, the peculiarity of these high efficient photosystems consists in the presence of proteins that keep the pigments at the right distance to the reaction centre. The core complex contains about 11-14 subunits and, in cyanobacteria, includes 96 Chl *a* and 22 β carotenes. Pigments are mainly associated to the two largest subunits, PsaA and PsaB. The primary PSI donor is P700, absorbing at 700 nm. PET in the PSI core is very fast (20-40 ps), despite the presence of chlorophyll red forms that absorb at lower energies and are slower. These chlorophylls, at the same time, broaden the absorption spectrum. In higher plants, antenna complex is made of four LHCa complexes (LHCa 1-4), organised in two dimers. All the members of LHC multigenic family are able to switch from a "light-harvesting" state to a "quenched" state, involved in photoprotection in the case in which excess energy needs to be dissipated (Croce and van Amerongen, 2013). In plants, the super complex PSI-LHCI traps the light in about 50 ps; the most red-forms are associated with the outer antenna. When PSI is excited, part of the LHCII population moves to PSI in order to form a PSI-LHCI-LHCII super complex. This is a short-term acclimation mechanism to keep the excitation balance between the two photosystems in case of rapid changes in light.

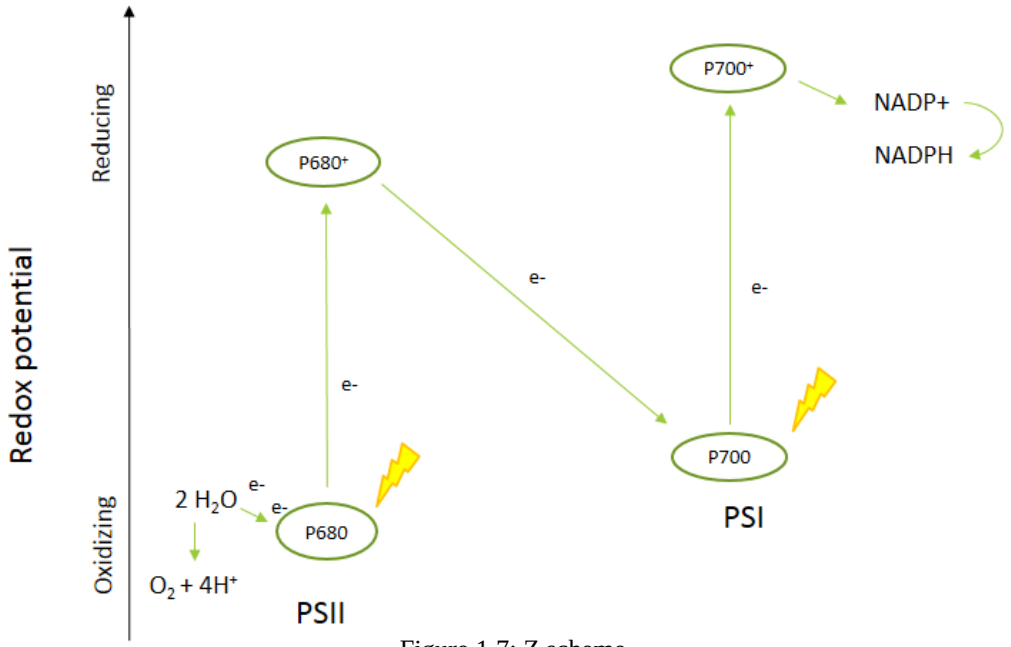

Figure 1.7: Z scheme.

Under an energetic point of view, redox reactions of the light reactions of photosynthesis are described by a model called Z scheme, first proposed by Hill and Bendall (Hill and Bendall, 1960) and depicted in Figure 1.7. This shows the pathway of electron transport from water to NADP+, that, as already mentioned, leads to the release of oxygen, the "reduction" of NADP+ to NADPH (by adding two electrons and one proton), and the building-up of a high concentration of hydrogen ions inside the thylakoid lumen (needed for ATP production). The scheme shows the energetic levels of the participants to all these reactions. According to this scheme, electron transport from PSII to PS I is realized by intermediate charge carriers and electron need of P680+ (strong oxidant with E0 = 1.1 eV) in PSII is compensated by water molecules (water oxidation). Electron transport through thylakoid membrane and water oxidation reactions results in a proton concentration gradient across the thylakoid membrane. Energy created by proton electrochemical potential resulting from this proton gradient is used by ATP synthase to produce ATP from adenosine diphosphate (ADP) and pyrophosphate (Pi). The net reaction, in light dependent reaction system, is the electron transport form a water molecule to a NADP+ molecule with the production of ATP molecules (Ipek and Uner, 2012). This is realized by ATP synthase or ATPase, regulate by pH level in the lumen and composed of two multisubunit subcomplexes, CF0 and CF1. The complex catalyses the synthesis of ATP from ADP and Pi. The subunit CF0 act as a proton channel and the flux of protons drives the subunit CF1, which forms a ring structure with catalytic sites for ATP synthesis. The passage of about four protons is required for the synthesis of one ATP molecule (Richmond and Hu, 2013).

The reaction conducted by ATPase is called photophosphorylation and can be expressed as:

$$2NADP + 2H_2O + 3ADP + 3Pi \xrightarrow{\text{light energy, chlorophyll}} 2NADPH_2 + 3ATP + O_2 \qquad \text{1-II}$$

1.2.5. Dark reactions

Carbon assimilation, also called Benson-Calvin Cycle is one of the dark reactions of photosynthesis. In order to fix one CO_2 molecule, two $NADPH_2$ molecules and three of ATP are required, as expressed in the following equation:

$$CO_2 + 2H^+ + 4e^- \xrightarrow{2\ NADPH2, 3\ ATP, enzymes} (CH_2O) + H_2O \qquad \text{1-III}$$

The fixation of CO_2 occurs in four phases:

- Carboxilation phase, where CO_2 is added to the 5-carbon sugar ribulose bisphosphate (Ribulose-bis-P) to form phosphoglycerate (glycerate-P). This reaction is calatalysed by the enzyme ribulose bisphosphate carboxylase/oxygenase (Rubisco);
- Reduction phase, where the phosphoglycerate is converted to 3-carbon products by its phosphorylation (involving ATP) and the subsequent reduction (involving $NADPH_2$);
- Rigeneration phase, where Ribulose phosphate is regenerated for further CO_2 fixation,
- Production phase, in which carbohydrates but also fatty acids, amino acids and organic acids are synthesized.

The process is shown in Figure 1.8.

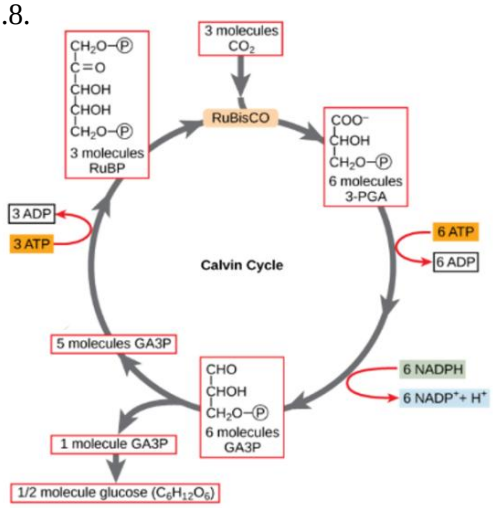

Figure 1.8: Calvin cycle. The process is divided in four phases: Carboxilation phase, catalyzed from the enzyme Rubisco, Reduction phase, Rigeneration phase and Production phase (Richmond and Hu, 2013).

The other dark reaction representing a competing reaction to carboxylation is the photorespiration. In it, organic carbon is converted into CO_2 without any metabolic gain. Photorespiration depends on the relative concentrations of oxygen and CO_2: if the O_2/CO_2 ratio is high, this process is favored while a low ratio favors carboxylation.

1.2.6. Regulation of photosynthesis

1.2.6.1. Alternative sinks for electrons

Several other electron sinks, diverse from Benson-Calvin cycle, are present in the chloroplast. They are metabolic pathways and/or signaling networks that requires energy and may apparently act in opposition to carbon assimilation. Besides the already described Linear Electron Transfer mode (LEF), in which the ferrodoxin transfer electrons to FNR (Ferrodoxin NADP+ Reductase) to produce NADPH, the photosynthetic apparatus can also a Cyclic Electron Transport (CEF) in which ferrodoxin transfers electrons back to the plastoquinone pool, causing a cyclic electron flow around PSI. This causes proton translocations, so acidification of the lumen and consequently ATP formation. These two processes are modulated together in order to match the photochemical reactions to Calvin-Benson cycle; in fact, the assimilation of CO_2 in the Benson-Calvin cycle requires ATP and NADPH in a 3:2 ratio. This ratio cannot be completely satisfied by LEF, which generates a pH gradient insufficient for the required ATP generation. Furthermore, CEF is adopted also in other cases such as low CO_2, high light or drought (Rochaix, 2010).

In case of an over reduction of electron transport, in order to prevent electrons to stall, another alternative cycle operates, called Mehler reaction. This is a pseudo-cyclic electron flow from water to PSI with molecular oxygen as alternative electron acceptor. This process leads to the formation of a superoxide converted by superoxide dismutase and catalase to water and oxygen. This water-water cycles restores the redox levels into the photosynthetic membranes.

Another pathway consists in the chlororespiratory chain, which is involved in electron transfer reactions from stromal reductants to dioxygen through the PQ pool. It involves a NADP dehydrogenase complex and a plastid quinol terminal oxidase called PTOX.

Photorespiration acts as an alternative sink for excess electrons due to consumption of NADPH and ATP. In it, organic carbon is converted into CO_2 without any metabolic gain. More than 20% of total electron flux through RuBisCo may fuel O_2 reduction and, for this reason, it has been for long time seen as a wasteful side product of carbon assimilation. Actually, since this process competes with CO_2 assimilation, modulation of the relative rate of O_2 and CO_2 reduction may contribute to maintaining a redox homeostasis with respect to electron transport and ATP synthesis, especially when CO_2 availability is restricted (Eberhard et al., 2008). It has also been demonstrated that the

photorespiratory pathway may play an indicative role in protection of plants against photoinhibition (Rumeau et al., 2007).

1.2.6.2. Plastoquinone oxidation state as a regulation of photosynthesis

PSI and PSII have a slightly different pigment composition and they can be differently excited depending on the nature of light. The difference in electron transport chains is balanced by state transitions; in fact, the plastoquinone pool can be reduced or oxidated depending which photosystem is more exited between PSI and PSII. If plastoquinone is reduced, a kinase is activated which phosphorylates LHCII and this causes the migration of LHCII to PSI rebalancing the excitation energy between PSI and PSII. The redox state of plastoquinone is therefore in a central point in the electron transfer regulationand can be affected by factors as wavelength shifts, light intensity, ATP/ADP ratio, CO_2 concentration, level of PTOX and operation of the Benson-Calvin cycle. Changes in plastoquinone pool redox state can also induce a change in chloroplast and nuclear gene expression. Furthermore, plastoquinone is, as already mentioned, a mobile electron carrier from PSII to cytochrome b6/f complex. Its diffusion can act as a regulatory limiting step in the electron flow. It was proposed that it moves quickly in some microdomains located in the vicinity of PSII active centers and diffuses slowly if it migrates through long distances. The creation of these microdomains is therefore a regulative factor and it was also suggested that phosphorylation/dephosphorylation of LHCII and PSII plays a role in this regulation (Rochaix, 2011).

The plastoquinone pool oxydation state can be affected also by the trans-thylacoid lumen pH. In fact, most of the electron transfer downregulation pathways consists in a feedback mechanism involving the two main products of photosynthesis: NADPH and the ΔpH in the lumen. The latter has a direct effect on PQ oxidation at the lumenal site of the cytochrome b6/f complex. This control has the role of tight coupling between electron and proton transfer during PQH2oxidation.

1.3. High-value compounds: pathways and production

1.3.1. Fatty acid synthesis and transport

In plants, the *de novo* fatty acids synthesis occurs inside the plastid. The first enzyme involved in this process is the plastidial pyruvate dehydrogenase complex (PDHC), that catalyzes the oxidative decarboxylation of pyruvate to produce acetyl-CoA, CO_2 and NADH (Johnston et al., 1997). The PDHC is made of three components: E1 (pyruvate dehydrogenase, PDH, composed of E1α and E1b subunits), E2 (dihydrolipoyl acyltransferase, DHLAT), and E3 (dihydrolipoamide dehydrogenase, LPD) (Figure 1.9). The E2 protein is covalently bound to lipoic acid (6,8-thioctic acid or 1,2-dithiolane- 3-pentanoic acid), that is needed as coenzyme for E1. In order to complete the catalytic cycle, E3 re-oxidases the lipoamide cofactor. Lipoic acid involved in this process is

synthesized from octanoic acid (Figure 1.9) by the addition of two sulphur atoms into the octanoyl group bound to acyl carrier protein (ACP). This reaction is catalyzed by lipoic acid synthase (LS; Yasuno and Wada, 2002). A lipoyltransferase (LT) then transfers the lipoyl group from lipoyl-ACP to apoproteins such as E2 (Wada et al., 2001).

The first step of the de novo lipid synthesis is realized by ACCase (acetyl-CoA carboxylase), located in the chloroplast of *Nannochloropsis* and responsible for the carboxylation of acetyl-CoA to produce malonyl-CoA (Li-Beisson et al., 2019; Mühlroth et al., 2013). ACCase catalyses this ATP-dependent reaction in two steps: in the first one, BC, biotin carboxylase, transfers CO_2 from bicarbonate to a biotin prosthetic group attached to the second domain of ACCase, the biotin carboxyl carrier protein (BCCP). Then, the other domain of ACCase, the carboxyltransferase (CT), transfers the carboxyl group from carboxy-biotin to acetyl-CoA to produce malonyl-CoA. Then, malonyl-CoA ACP malonyltransferase (MCT) converts malonyl-CoA to malonyl-acyl carrier protein (ACP) (Li-Beisson et al., 2019).

The production of 16- or 18-carbon fatty acid is performed by the Fatty Acid Synthase (FAS) complex. It is composed by the *3*-ketoacyl-ACP synthase (KAS), the hydroxyacyl-ACP dehydrase (HAD), the ketoacyl-ACP reductase (KAR) and the enoyl-ACP reductase (ENR) (Li-Beisson et al., 2013). The complex ligates Malonyl-ACP to an acetyl-CoA molecule to form a 3- ketoacyl-ACP by ketoacyl-ACP synthase, while releasing a molecule of CO_2. The 4-carbon 3-ketoacyl-ACP is subsequently reduced (by ke- toacyl-ACP reductase, KAR), dehydrated (by hydoxyacyl-ACP dehy- drase, HAD), reduced again (by enoyl-ACP reductase, ENR) until finally a 6-carbon-ACP is formed (Figure 1.9). This substrate undergoes to this process again from the beginning until a chain of 16 or 18 carbons is made. Each cycle leads to the extension of the chain of two carbons. ACP desaturase (SAD) acts as well in the plastid and is responsible for the conversion of 18:0-ACP to 18:1-ACP. In this way, 16:0-ACP, 18:0-ACP and 18:1-ACP are produced and exported in the cytosol in the acyl-CoA and acyl-lipids pool.

Long-chain acyl groups are then hydrolyzed by acyl-ACP thioesterases that release fatty acids and complete the fatty acid elongation. Two main thioesterase types have been described: the FatA class, which preferentially removes oleate from ACP, and FatB thioesterases that are active with saturated and unsaturated acyl ACPs, and, in some species, with shorter-chain-length acyl ACPs. The combination of the actions of the fatty acid synthase complex, desaturase, and the two thioesterases generates the kind of acyl chains produced in the plastid for TAG formation. These fatty acids are ultimately activated to CoA esters by a long-chain acyl-CoA synthetase (LCS) and exported to the endoplasmic reticulum.

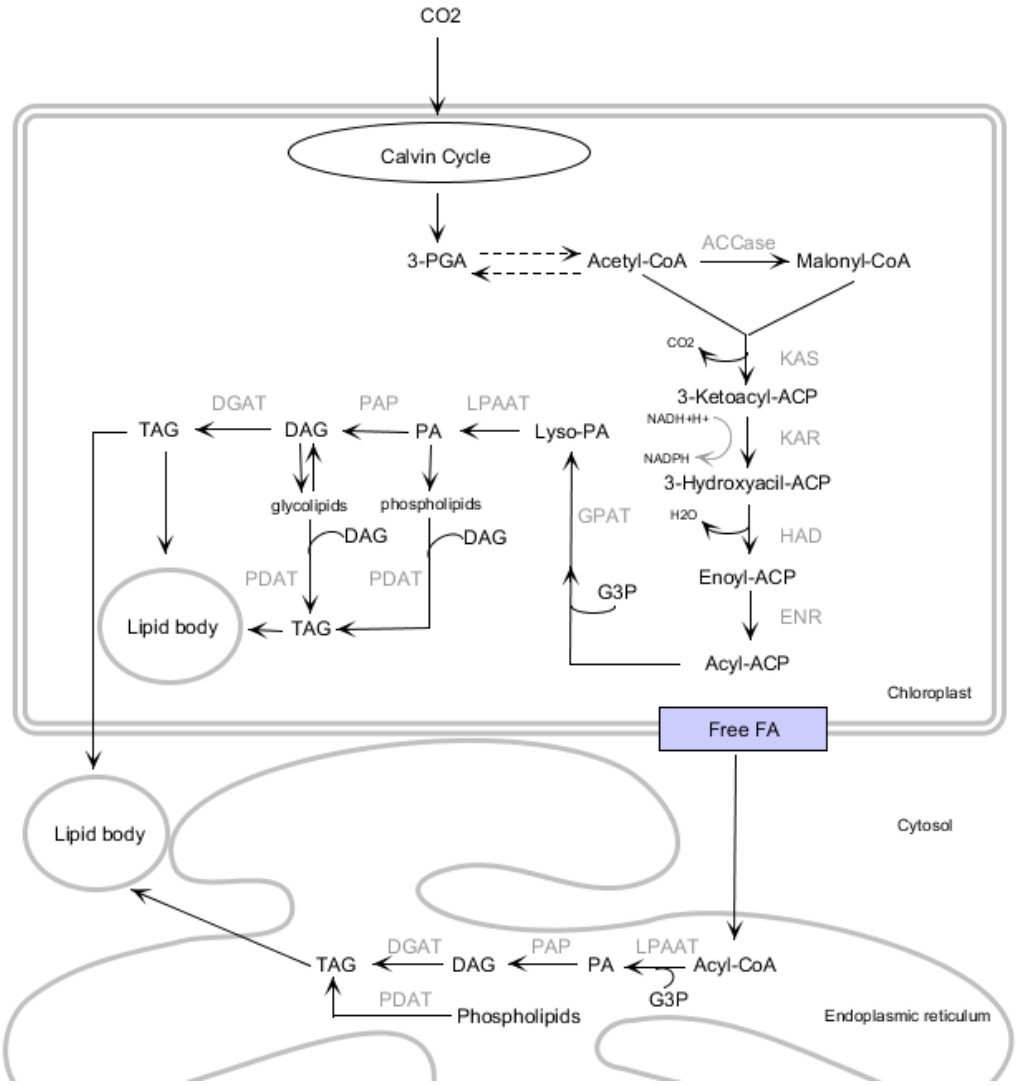

Figure 1.9: Pathways involved in the *de novo* fatty acid synthesis, their integration in TAGs and sequestration into Lipid bodies.

The majority of fatty acid synthesized in algae and plants are esterified to glycerol in order to make tryacilgrlycerols (TAGs). Glycerolipids are synthetized through an ensemble of reactions known as Kennedy pathway, consisting in three sequential acylation steps of Glycerol 3 phosphate (G3P). This pathway involves GPAT (acylCoA:glycerol-3-phosphate acyltransferase), LPAT (acyl-CoA:lysophosphatidic acyltransferase), DGAT (diacylglycerol acyltransferase) and PAP (phosphatidic acid phosphatase). The pathway starts with the acylation of G3P by GPAT. Then, there is another acyl-CoA dependent acylation catalysed by LPAT that forms the phosphatidic acid (PA). PAP catalyses the release of phosphate to produce diacylglycerol (DAG). The final step is the acylation of DAG to produce TAG, driven by DGAT (Cagliari et al., 2011) (Figure 1.9). TAGs are sequestered into Lipid bodies (LB), subcellular organelles

that develops in microalgae in particular under stress such as high light or nitrogen starvation. They may range in size (0.2-8 μm) (Murphy, 2001) and are encircled by a monolayer membrane containing proteins. In general, they contain 1-5% (w/w) proteins, over 80% (w/w) neutral lipids and 1-5% (w/w) polar lipids. More than 90% of LB lipids are TAGs (Zweytick et al., 2000) and the major fatty acids are C16:0, C18:1 and C18:2 (Richmond and Hu, 2013). Even if LBs have been for long believed to have only a lipid accumulation function, nowadays a common opinion is that they are involved in lipid metabolism. In fact, proteins that take part to the LBs are associated to other organelles, such as endoplasmic reticulum (ER), chloroplasts and mitochondria.

Of increasing interest is a particular lipid class, the PUFAs, whose industrial value is increasing because of the several and fundamental proprieties and function they carry out in the animal body (Wiktorowska-Owczarek et al., 2015). In particular, the omega-3 series has a great industrial interest. For this reason, the biotechnological accumulation of this lipid class in microalgae have been addressed in the last years (Yu et al., 2011). One interesting genus is *Nannochloropsis*, in which the omega-3 EPA has been found in large amounts (Rebolloso-Fuentes et al., 2001).

1.3.2. Carotenoids synthesis

Isoprenoids are compounds produced by all photosynthetic organisms but also from other bacteria and microorganisms. On the base of their composition, they are divided in carotenes, pure hydrocarbons and xanthophylls, containing also oxygen in their structure (Mulders et al., 2014). They are also distinguished as primary, when their function is essential for the cell and the photosynthesis, and secondary, when their function is accessory, and they are produced after a precise stimulus, as nutrient starvation or excess light. In fact, the carotenoid function can be structural, as some of them are bound to photosynthetic proteins and are responsible for the light harvesting in the LCH (see paragraph 1.2.4). They can also have a protection function because of the double bond conjugated system that allows the excess energy dissipation and the protection against oxidative damage (Henríquez et al., 2016). Furthermore, carotenoids can be accumulated in the thylacoids or, in some cases, in lipid vesicles, as in the case of astaxanthin in

Haematococcus pluvialis (Jin et al., 2003). The production of all isoprenoids starts from isopentenyl pyrophosphate (IPP) and from its isomer, dimathylallyl pyrophosphate (DMAPP). The enzyme responsible for the isomerization is the isopentenyl pyrophosphate isomerase (IPP isomerase). The production of these milestones for the terpene production is obtained through two alternative pathways, the mevalonate (MVA) pathway, and the relatively new 2- C -methyl- D -erythritol 4-phosphate (MEP) pathway (Lichtenthaler, 2004). The first one is adopted in the cytoplasm of archeabacteria, fungi and animals, while the second one is found in the plastid of cyanobacteria, plants and algae (Paniaqua-Michel et al., 2012). They are shown in Figure 1.10.

IPP is then used as base for the production of phytoene, the firs uncoloured carotenoid. The process goes through consecutive condensation of 5C units catalysed by the prenyl transferase and leads to the production of geranylpyrophosphate (GPP, C10), farnesylpyrophosphate (FPP, C15) and geranylgeranylpyrophosphate (GGPP, C20). The condensation of two molecules of GGPP, catalysed by the phytoene synthase, produces the phytoene (C40) (Figure 1.10). The phytoene is then used as a base for the production of all the other carotenoids. Some of them are specie-specific, while others are universal. For example, in Figure 1.11 the production pathway of green microalgae is shown.

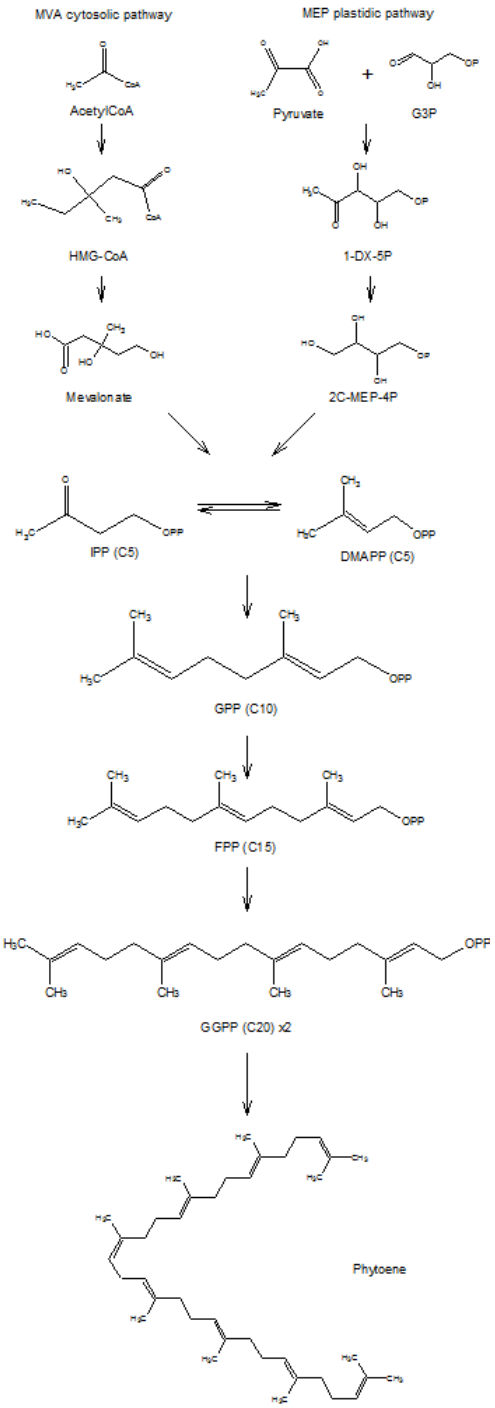

Figure 1.10: First step of production of carotenoids: two alternative pathways lead to the production of IPP that is transformed in phytoene, the firs uncoloured carotenoid.

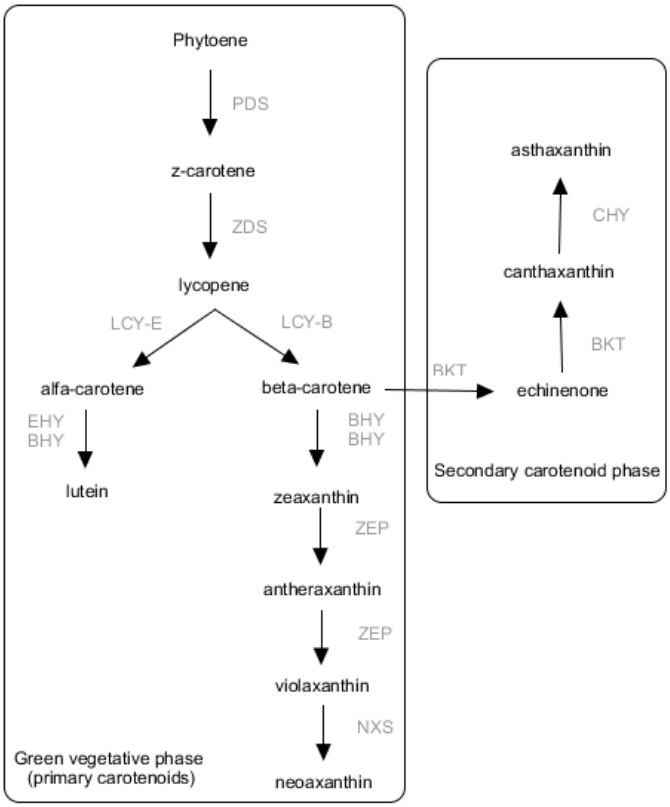

Figure 1.11: Pathway of production of primary and secondary carotenoids in green algae.

The phytoene is first desaturated by a phytoene desaturase (PDS) to produce the z-carotene, that undergoes to another step of desaturation catalysed from a z-carotene desaturase (ZDS) to produce the lycopene. It undergoes to a double cyclization to both ends catalysed by lycopene beta-cyclase (LCY-b) or lycopene e-cyclase (LCY-e) to produce beta- or alfa-carotene. The two beta rings of beta-carotene are subjected to hydroxylation to yield zeaxanthin, which in turn is epoxidated once to form antheraxanthin and twice to form violaxanthin. Neoxanthin is obtained from violaxanthin by an additional modification. Astaxanthin is produced from the base of beta-carotene, with the introduction of two hydroxyl groups at C3 and C30 by the beta-carotene ketolase, BKT (Ambati et al., 2019; Cezare-Gomes et al., 2019; Henríquez et al., 2016).

1.3.3. Starch

Accumulating starch is a distinctive trait of plant cells, which employ it as energy storage. In higher green plant and algae it is accumulated in the plastids, while in red algae in the cytosol (Busi et al., 2014). Starch is made out of two macromolecules: amylopectine and amylose. Both of them are polymers of glucose; the first one is branched while the second one is linear or helicoidal (Buléon et al., 1998). Amylopectine accounts for the 75% of the starch composition, while amylose for the remaining part. Amylopectine is also responsible for the peculiar starch structure, which accumulates in cells under form of granules. In particular, granules have a lamellar structure, made of crystalline insoluble layers alternated with amorphous ones (Zeeman et al., 2010). The combination of chain length, branching frequency and pattern origins the branched and regular structure of starch granules. The starch granules particular structure makes them insoluble, thus not easily degradable in the aqueous matrix in which they are embedded.

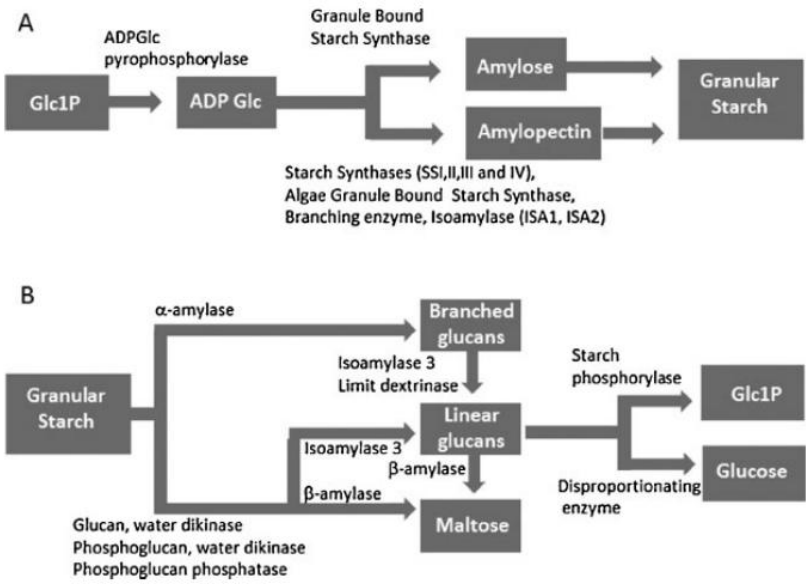

Figure 1.12: Simplified pathways for synthesis and degradation of starch (Busi et al., 2014).

The mechanism for starch synthesis and degradation is showed in Figure 1.12 (Busi et al., 2014). The synthesis of starch, in Figure 1.12A, starts with the Glucose 1 phosphate (Gcl1P) that is converted in ADP glucose (ADP Glc) by the action of ADP Glc pyrophosphorilase. ADP Glc is then exposed to the action of Starch synthases (SSs) that catalyze the elongation of a-1,4-glucans by the transfer of the glucosyl moiety from the sugar nucleotide to the non-reducing end of the growing polyglucan chain. The soluble SSs are involved in the synthesis of amylopectin, while Granule bound starch synthase (GBSS) participates in amylose synthesis. Also branching enzymes (BE) are involved in the starch synthesis as they cleave a linear glucose chain and transfer it to a glucose

residue within an acceptor chain via an a-1,6 linkage to form a branch and ISA 1 and 2 (Isoamylase 1 and 2) facilitates granule crystallization by removing wrongly positioned branches. Isoamylases are also involved in the starch degradation, even if their contribute is essential for its synthesis. It is to point out that the enzymes responsible for starch synthesis are physically associated in complexes (Busi et al., 2014).

The starch granules degradation, in Figure 1.12B, starts from the granule surface phosphorylation. This makes it soluble and accessible to hydrolases. The transient amylopectin phosphorylation proceeds together with glucan hydrolysis and the procedure is repeated for each crystalline layer of the starch granule (Zeeman et al., 2010). Glucan, water dikinases (GWD), which add phosphate groups using the β-phosphate of ATP, and phosphoglucan,water phosphatases (PWD), which remove these phosphate groups are responsible for the granule phosphorylation. Then, β-amilases intercourses for hydrolysing starch chains. For the complete degradation, also de-branching activity is required in order to release the branching points; for this reason, other enzymes such as α-amylase ISA3 and pullulanase may intervene in the process. The obtained linear glucans are metabolized to maltose, to glucose or through starch phosphorylase. Maltose and glucose are then transported from chloroplast to cytosol (Zeeman et al., 2010).

An interesting fact is that starch synthesis has common precursors with lipid synthesis and their pathways are interconnected (Richmond and Hu, 2013). This is linked to the fact that some microalgae tend to accumulate lipids (such as the genus *Nannochloropsis*) while others prefer accumulating starch (*e.g.* genus *Tetraselmis*).

1.4. Growth kinetics

1.4.1. Batch growth and specific growth rate μ

For the sake of completeness, basic concepts concerning cells growth kinetics are shoertly summarised in this paragraph, as these will be employed later on in this thesis. Most of this paragraph content is adapted from Doran, 2013 (Doran, 2013).
When cells are cultured in batch cultures, a typical growth curve is observed. This model growth is applied to several kinds of cells, comprising microalgae. In particular, by plotting the natural logarithm of the concentration of cells *vs* time of cultivation, the characteristic curve of Figure 1.13 is typically observed.

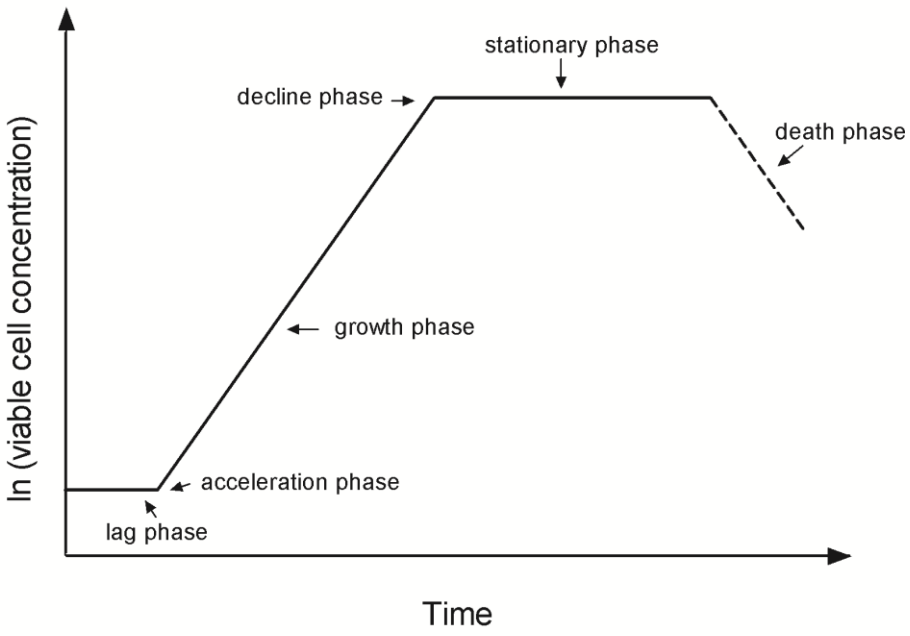

Figure 1.13: Typical batch growth curve.

Different phases are observed on the base for growth rate and for the relevant *specific growth rate* (μ). The observed growth phases are:

- Lag: cells are adapting to the new growth condition, new enzymes and proteins are produced in order to sustain the growth; μ is equal to zero.
- Acceleration: growth starts; μ increases but is still smaller than the *maximum specific growth rate* (μ_{max}).
- Growth: the growth is exponential, cells are consuming the nutrients; μ is constant and equal to μ_{max}.
- Decline: nutrients become limiting and growth slows down; μ is lower than μ_{max}.
- Stationary: growth stops; μ is equal to zero.

- Death: some cultures exhibit a death as the cells lose viability, the curve has a negative slope; in this case μ is less than zero.

When death rate is negligible, the rate of cell growth is described by the simple equation:

$$\boldsymbol{r_x = \mu x} \qquad \text{1-IV}$$

where r_x is the volumetric rate of biomass production [kg m^{-3} h^{-1}] while x is the viable cell concentration [kg m^{-3}] and μ is the *specific growth rate*. It has the dimension of [T^{-1}] and the unit of, for example, h^{-1}.

In a system where the growth is the only factor affecting the cell concentration, the rate of growth is equal to the rate of cell concentration change:

$$\boldsymbol{r_x = \frac{dx}{dt}} \qquad \text{1-V}$$

From equations 1.IV and 1.V one obtains:

$$\boldsymbol{\frac{dx}{dt} = \mu x} \qquad \text{1-VI}$$

If μ doesn't change on time, it is possible to integrate.

$$\int \frac{\mathbf{dx}}{\mathbf{x}} = \int \mu \, \mathbf{dt} \qquad \text{1-VII}$$

or

$$\boldsymbol{ln\, x = ln\, x_0 + \mu t} \qquad \text{1-VIII}$$

Where x_0 is the viable cell concentration at time zero. The following equation:

$$\boldsymbol{x = x_0\, e^{\mu t}} \qquad \text{1-IX}$$

represents therefore the growth during the exponential phase, where the *specific growth rate* is the maximum possible and the cell concentration x is a function of time.

The *specific growth rate* μ can be assessed by arranging equation 1-VIII as:

$$\boldsymbol{\mu = \frac{ln\, X - ln\, X_0}{t - t_0}} \qquad \text{1-X}$$

During the stationary and the decline phases, growth is limited by nutrient concentration. The dependence of μ on each substrate is given by the Monod model (Monod, 1949), the kinetic model most commonly employed to describe microbic growth.

When growth rate is affected by several nutrients (S_1,S_2,…S_n), the growth is regulated by the following equation:

$$\boldsymbol{\mu} = \mu_{max}\left[\frac{S_1}{S_1+K_{s1}}\,\frac{S_2}{S_2+K_{s2}}\,\frac{S_3}{S_3+K_{s3}}\ldots\ldots\frac{S_n}{S_n+K_{sn}}\right] \qquad \text{1-XI}$$

where

- S [g lt^{-1}] is the concentration of nutrient;
- μ_{max} [h^{-1}] is the maximum value of *specific growth rate* μ ;
- K_s [g l^{-1}] is the *substrate constant*.

A single substrate is often the one limiting growth and the equation becomes:

$$\boldsymbol{\mu} = \frac{\mu_{max}\,S}{S+K_s} \qquad \text{1-XII}$$

The form of equation 1-XII is depicted in Figure 1.14.

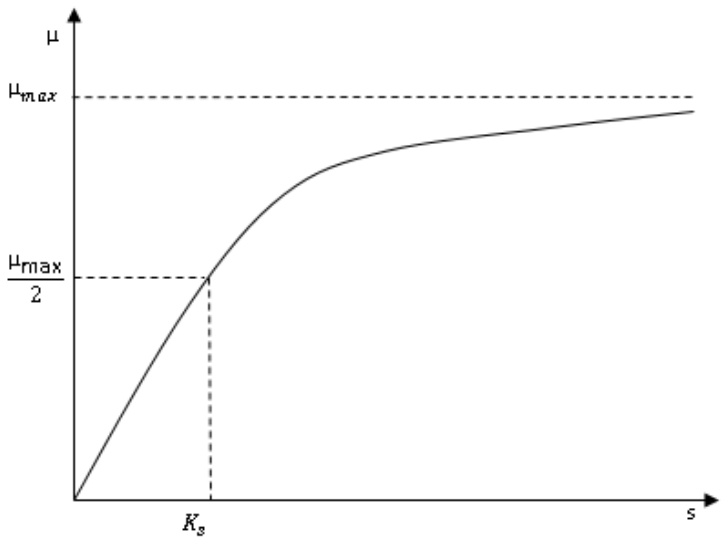

Figure 1.14: Kinetic representation of the relation between specific growth rate and concentration of limiting substrate.

In this graph, μ_{max} is the asymptotic value of μ when S increases. The constant K_s represents the value of S for which $\mu = \frac{\mu_{max}}{2}$.

Typically, *susbtrate constant* K_s is very small, in the order of μg/l, and nutrients are in saturating concentration (S >> K_s). In this condition, the term K_s of the equation 1-XII is negligible and the μ practically equals μ_{max}. This is the condition in which cells give rise to the exponential phase, when the concentration of nutrients is abundant.

Once substrate concentration decreases below $10K_s$, the term K_s of the equation 1-XII cannot be neglected anymore and growth rate depends on substrate concentration S, until growth stops because of lack of nutrients. This is what happens in the decline and stationary phases.
It's important to notice that values of μ_{max} e K_s depends on the type of microorganism, substrate, culture medium and other factors such as pH and temperature (Merchuk and Asenjo, 1994).

1.4.2. Growth kinetics in microalgae

Part of the contents of this paragraph is adapted from Lee et al. (Lee et al., 2013).
Being microalgae photosynthetic microrganisms, in autotrophic cultivation of algae the main limiting substrate for their growth is light. Figure 1.15 shows the phases of a microalgal culture when limited by light. It is worth noticing that the viable biomass dynamics in Figure 1.15 takes into consideration also cell death rate experienced by all microbial cultures.

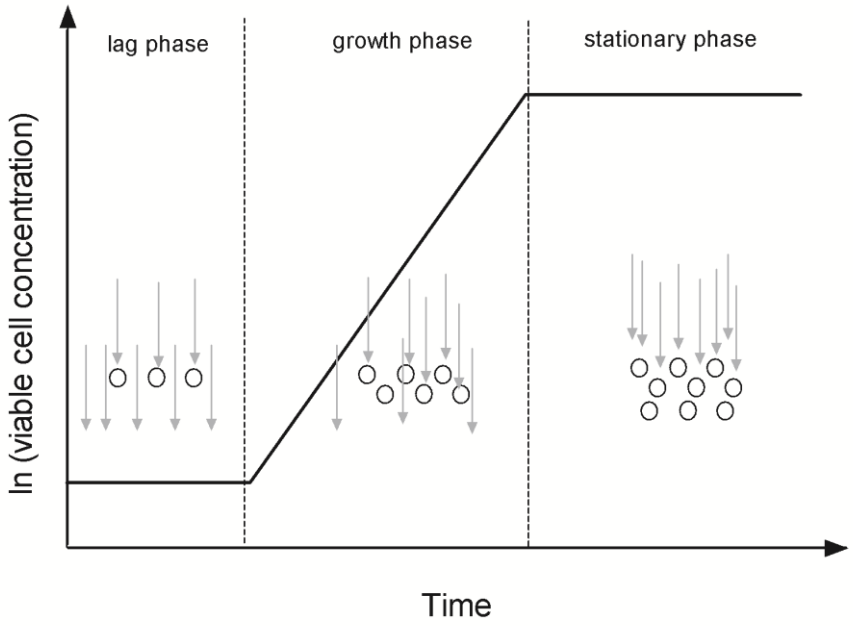

Figure 1.15: The growth phase in a photosynthetic microalgal culture.

Cells harvest light and use it to perform photosynthetic reactions, so virtually when light hits a cell it is absorbed and no more available for other reactions. This is called self-shadowing effect and is one of the main troubles when cultivating microalgae. In the lag phase light is not limiting and microalgal cells go through a phase of adaption to the new growth conditions. This phase is identical to the one observed in Figure 1.13.

In the exponential phase cells grow and divide as an exponential function of time, as long as the following inequality is satisfied at all points inside the photobioreactor:

$$\boldsymbol{IA} > \mu_{\boldsymbol{max}}\boldsymbol{x} \cdot \boldsymbol{V}/\boldsymbol{Y} \qquad \text{1-XIII}$$

where

- $\boldsymbol{I}$ [J m^{-2} h^{-1}] is the photon flux density in the photosynthetically available range;
- $\boldsymbol{A}$ [m^2] is the illuminated surface area;
- $\boldsymbol{V}$ [m^3] is culture volume;
- $\boldsymbol{Y}$ [g J^{-1}] is the *photosynthetic yield*.

Under these conditions, $rx=\mu_{max}\, x$ and the steepest exponential growth occurs.
In the growth phase cell concentration exponentially increases until all photosynthetically active photons impinging on the culture are absorbed. After that, a light-limited growth phase occurs, where the relationship between the biomass output rate and the light energy absorbed may be expressed as (Pirt et al., 1980):

$$\boldsymbol{IA} = \mu\boldsymbol{x} \cdot \boldsymbol{V}/\boldsymbol{Y} \qquad \text{1-XIV}$$

This equation implies that, for I and Y constant, μ varies when cell concentration x varies.
The relationship between *photon flux density I* and *specific growth rate* μ may be put in a form similar to a Monod relation (Lee et al., 2013):

$$\boldsymbol{\mu} = \frac{\mu_{\boldsymbol{max}}\ \boldsymbol{I}}{\mathbf{I}+\boldsymbol{K_i}} \qquad \text{1-XV}$$

where K_i is the *light saturation constant*, i.e. the photon flux density required to achieve half of the maximum specific growth rate.
In the stationary phase, a soluble substrate is eventually exhausted. In this phase, photosynthesis still is performed and cells store products such as lipids and carbohydrates.

1.5. Cultivation of microalgae

1.5.1. Metabolic modes

Microalgae can grow in a quite broad range of metabolic modes, all centered around two main kinds: autotrophy and heterotrophy. Autotrophic algae are photoautotrophic, which means they obtain their energy from light and require only inorganic mineral ions to live; they are also referred as photolithotrops (Lee, 2008). They could be chemoautotrophic

(chemolithotrophic) if they oxidize inorganic compounds for energy. Heterotrophic organisms obtain both energy and nutrients from organic compounds produced by other organisms. Photoheterotrophic is something between the two main categories: they obtain energy from light and nutrients from organic compounds. Mixotrophy is the state in which heterotrophy and autotrophy coexist; there is not a definite prevalence of one of them, except in total darkness where the heterotrophy prevails. It is important to highlight that there is not net distinction between one state and another, and that there are some species forced to adopt one of the metabolic modes and others that can switch amongst them. All the distinctions are found in Table 1.1.

Table 1.1: Description of the microalgal metabolic modes. They are distinguished on the base of the energy and of the nutrient source.

Cultivation condition	Energy source	Nutrient source
Photoautotrophic Or photolithotrops	Light	Inorganic compounds
Chemoautotrophic	Organic compounds	Inorganic compounds
Heterotrophic	Organic compounds	Organic compounds
Photoheterotrophic	Light	Organic compounds
Mixotrophic	Light and organic carbon	Inorganic and organic compounds

1.5.2. Nutrient requirements

The main elements needed for algal growth are C, N and P. Carbon is required as CO_2 or as HCO_3^- and their supply is necessary in autotrophy for reaching high biomass yields. The bicarbonate-carbonate buffer system is the most important mean present in freshwater to control the pH. It follows the equations:

$$\boldsymbol{2HCO_3^- \leftrightarrow CO_3^{2-} + H_2O + CO_2} \quad \text{1-XVI}$$

$$\boldsymbol{HCO_3^- \leftrightarrow CO_2 + OH^-} \quad \text{1-XVII}$$

$$\boldsymbol{CO_3^{2-} + H_2O \leftrightarrow CO_2 + 2OH^-} \quad \text{1-XVIII}$$

The CO_2 used for photosynthesis makes OH^- accumulate in the culture, so a consequence of photosynthesis is the increase of pH. Adding CO_2 directly to the culture is aimed also at reducing the pH.

Nitrogen is the second most important nutrient as it contributes to the formation of proteins. Typical responses to nitrogen limitation are discoloration and accumulation of organic carbon compounds. It is usually supplied as nitrate (NO_3^-) but often ammonia (NH_4^+) and urea are used. Phosphorus is essential in many cellular processes, such as energy transfer and biosynthesis of nucleic acids. It is usually supplied as orthophosphate (PO_4^{2-}).

As summarized by Lin, 2005 (Lin, 2005), developing nutrient recipes for algal cultivation requires attention in:

- Total salt content;
- Composition of macronutrients (K^+, Mg^{2+}, Na^+, Ca^{2+}, SO_4^-, Cl^-);
- Nitrogen source;
- Carbon source;
- pH;
- Trace elements and chelating agents;
- Vitamins.

1.5.3. Commercial cultivation of microalgae

Microalgae can be cultured using several systems. The major difference is between *open pond systems* and *closed photobioreactors*. Both of them have their own advantages and disadvantages.

1.5.3.1. Open ponds

They are categorized into natural waters (lakes, lagoons, ponds) and artificial ponds or containers. The open ponds can be circular or raceway, as shown in Figure 1.16. Cultures in these systems are more exposed to climate conditions and to contaminations; it is therefore impossible to control temperature and pH.

Figure 1.16: Circular and raceway open ponds. A) *Chlorella* Industries, Japan, circular ponds, each ~500 m2, with central pivot mixing B) Cyanotech Co., Hawaii, producing Spirulina (Benemann, 2013).

Major limitations in open ponds include the possibility of biological and chemical contaminations, evaporative losses, loss of insufflated CO_2 to the atmosphere and requirement of flat land areas possibly employable for crop cultivation. In practice, only very robust strains, able to survive to these conditions and to successfully compete with predators or other species can be cultured (Kumar et al., 2015). During the last years, several modifications were proposed in order to optimize biomass yields in open ponds. These ones focused on improving the mixing, in order to optimize the exchange of nutrients and of CO_2 from the atmosphere. In fact, oxygen removal is one of the main problems in open pond cultivations and it overcomes also the carbon need. For this reason it may be necessary to supply CO_2 also when it is not strictly necessary (Mendoza et al., 2013). In other cases, large scale biomass production relies upon manual mixing or upon employment of paddlewheels (Moazami et al., 2012). Ponds with paddlewheels are better mixed than the one without them, so they are more efficient with a better CO_2 absorption but also more expansive. Also the design of bend and floor surface geometries affects the performance of these systems (Kumar et al., 2015).

1.5.3.2. Photobioreactors

Apart from the great advantage of avoiding contaminations, they also offer significantly higher volumetric algal productivities (0.05–0.32 g $L^{-1}d^{-1}$) compared to those of ponds (0.12–0.48 g $L^{-1}d^{-1}$) (Brennan and Owende, 2010; Ketheesan and Nirmalakhandan, 2012). Closed PBRs prolong the gas retention time and improve the mass transfer efficiency. Furthermore, airlift reactors have advantages such as high volumetric mass transfer rate of CO_2, efficient mixing, and possibility to perform light/dark cycle. On the other hand, closed PBRs several disadvantages, which limit their use for commercial scale. For example, a commercial PBR may cost up to 100 times more than open ponds. Operation and cleaning may also become laborious, costly, and time consuming in the case of several individual PBRs. For these reasons, the majority of commercial cultivations employs open ponds, although the final quality of microalgal biomass is superior in PBR cultivation systems and there are companies successfully employing them.

1.5.3.3. Vertical-column photobioreactors

An example of vertical-column or bubble column is shown in Figure 1.17. This kind of reactors shows a variety of designs and scales and is often used for indoor cultivation of microalgae. Usually there is an inner compartment suitable for inserting a light source and mixing occurs thanks to rising gas bubbles, injected through porous tubes at the bottom of the reactor, that also provide the needed gas

Figure 1.17: Microalgae cultivation in bubble column reactors at Sea & Sun Technology GmbH. https://www.abire.org/consortium/s

exchanges. They are normally used in lab-scale and not in commercial plants (Sánchez Mirón et al., 2000). They have several advantages, such as the simplicity in design, ease of operation, small occupied area and good gas exchange with low energy requirements (López-Rosales et al., 2019).

1.5.3.4. Air-lift photobioreactors

An air-lift system is composed by two vertical compartments, the riser and the downcamer. A gas is insufflated at the bottom of the riser through a sparger. The degasser is the horizontal compartment which allows the separation of the liquid and gas phases; if the degasser is properly designed, there is no gas in the downcamer section and the circulation is optimized. The density difference in the two compartments (riser and downcamer) generates a pressure difference at the base of the system which allows the fluid circulation inside the PBR (Sánchez Mirón et al., 2000). The biomass circulation in a photobioreactor can be led by an air-lift system, if it is well-dimensioned, as shown in Figure 1.18 (Molina et al., 2001). In this case, the air-lift has also role of efficient oxygen stripping; the length of the tubular photobioreactor is furthermore linked to the degassing capability of the airlift, that depends on its height (Acién Fernández et al., 2001; Molina et al., 2001).

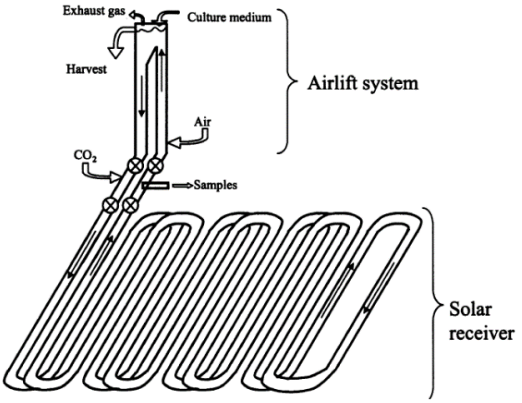

Figure 1.18: Photobioreactor plant with air-lift system (Molina et al., 2001).

1.5.3.5. Tubular photobioreactors

Figure 1.19: Horizontal and vertical orientation of coil tubular PBR.

Among the proposed photobioreactors, tubular photobioreactors are quite well suited for outdoor mass cultures. Most outdoor tubular photobioreactors are usually constructed with either glass or plastic pipes and their cultures are re-circulated either with pumps or

with airlift systems. They consist of a solar collector tubing through which the culture flows, recirculated by aeration or mechanical pumps. The coil tubular PBR usually have diameters between 0.01 and 0.06 m and variable length. These plastic plants can be exploited in lab-scale and for the scale-up to the commercial plant, allowing a good illumination. The main disadvantages are the low ratio section/lenght which sometimes generates pH gradients and high O_2 concentration which can accumulate in bubbles toxic for the algae (Acién Fernández et al., 2013; Molina et al., 2001). Examples of horizontal and vertical coil tubular PBR are depicted in Figure 1.19.

1.5.3.6. Flat-plate photobioreactors

The first proposed flat culture vessels as photobioreactor dates back to 1953 (Burlew, 1953) and following this work, a flat reactor equipped with fluorescence lamps was proposed (Samson and Leduy, 1985). Later on, this kind of reactors was extensively studied by several authors (Hu et al., 1996; Tredici and Materassi, 1992; Zhang et al., 2002). These systems have a bigger surface/volume ratio compared to other kind of photobioreactors. In this way, the light energy is better used and major amounts of biomasses are obtained. They are made of PVC or PC panels and the space between them varies from few millimeters to 0.05-0.07 m. Surfaces are comprised between 0.5 and 2 m^2 (Posten, 2009). This kind of photobioreactor is flexible and can be connected in series or in parallel. It can adopt several inclinations in order to maximize the illumination. The movement of biomass is obtained by insufflating gases from the bottom and oxygen accumulation is generally lower than in tubular photobioreactors (Ugwu et al., 2008). This system has anyway several disadvantages: the costs are higher than the other systems and it is often necessary to regulate the temperature, introducing refrigerating system. For this reason, they are not frequently employed in commercial plants. Flat-plate photobioreactor from Arizona University are depicted in Figure 1.20.

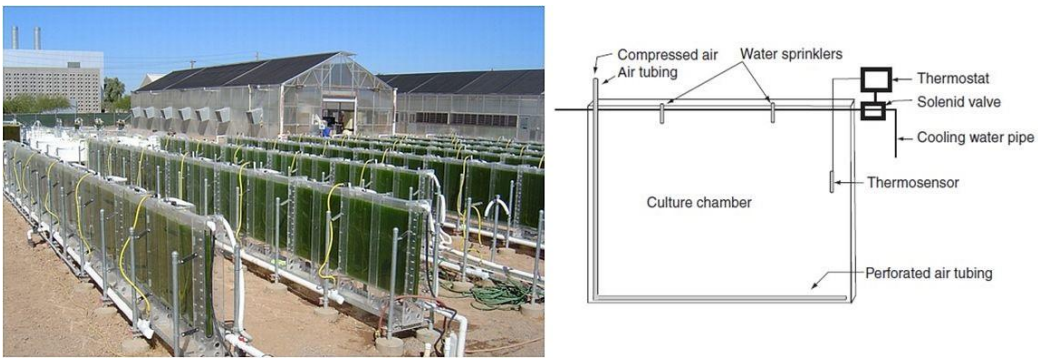

Figure 1.20: Flat plate photobioreactors from Arizona University

1.6. Applications: the industrial world of microalgae

1.6.1. Historical use of microalgae

Consuming algae as food is a trend of the last years but it isn't actually an innovation. The first known use of microalgae in humane culture was approximately 2000 years ago, when the cyanobacterium *Nostoc sp*. was consumed in China as a food, due to its nutritional proprieties (Gao, 1998). One of the most famous historically consumed microalgae is *Arthrospira platensis*, known as *Spirulina*, is consumed as a food since a long time; there is a history of its consumption in Mexico and in Africa (Ciferri, 1983). Some works describe the methodology by which natives harvest this microalga from Lake Kossorom (Chad) and estimate the annual value of the *dihé*, traditional name of the dry biomass, to more than US $100,000 (Abdulqader et al., 2000). Algae are daily harvested by women and subsequently filtered and sun-dried on the shores of the lake. The semi-dried biomass is cut and taken to villages where it is consumed or sold. More recently, attempts to cultivate microalgae were done by Germans during world war II. Between early 1970s and late 1970s, commercial production of algae was initiated in East Europe, Israel and Japan (Ugwu et al., 2008).

1.6.2. Modern applications of microalgae

1.6.2.1. Microalgae as Food and in Health

According to a recent review, algae are an under-exploited crop for production of dietary foods (Koyande et al., 2019) due to the height nutritional power they have. Several species of microalgae are characterized by a high value in proteins; examples are *Spirulina*, with 55.8% of crude protein compared to the dry biomass, *Chlorella* with 55.3%, *Pheodactylum tricornutum* with 39.6 % and *Nannochloropsis granulata* with 33.5 % (Tibbetts et al., 2015). This feature makes algae eligible for the group of *functional foods*, i.e. food able to protect consumer's health (Plaza et al., 2008). A food is ''functional'' if, besides its nutritious effects, it has a demonstrated benefit for one or more functions of the human organism, improving the state of health or well-being or reducing the risk of disease. Microalgae are also often inserted into the group of "nutraceutic" food. The word "nutraceutic" derives from nutrition and pharmaceutics. It is a new branch of knowledge that is attracting interests from all over the World. It studies the extracts of plants, animals, minerals and microorganisms in order to use them as isolated nutrients, supplements o specific diets. Microalgae are rich of health-valuable compounds such as carotenoids (antioxidants), vitamins, vegetal omega- 3 (Koyande et al., 2019). Furthermore, algal composition can be modified and enriched by adding components, such as vitamins. They have the potential to become the solution to malnutrition because the high possibility that they offer in terms of enrichment and added-value. Compared to traditional crops, algae have several advantages. For instance,

they grow fast and can be grown in lands not suitable for other cultivations. In order to fight malnutrition and food scarcity, there is a need for nutritious food, rich in vitamins and micronutrients (vit A, vit B2, B6, B12, iron, selenium, iodine, zinc). Microalgae offer a good alternative as a source of quality food able to play a crucially in view of the growing food crisis in the world considering the predicted growth of human population in the next years (FAO, 2017).

1.6.2.2. Microalgae in the Cosmetic and Health

The benefits of microalgae as a cosmetic are mainly related to their high content in fatty acids, often reaching 50% of the dry weight. In particular, they contain a high amount of linoleic acid (ω-6), which is the essential fatty acid most frequently employed in cosmetic products (Lautenschläger, 2003). It helps in prevention of disorders of the skin such as barrier and cornification, reduces the transepidermal water loss and increases skin moistness. Linoleic acid is part of the ceramide I, which is the most important compound in external layers of the skin. Vegetable oils are a rich source of fatty acids and are successfully employed in cosmetic products. Because of their oiling, softening, smoothing and protective properties they are classified in the group of emollients. They are often used to produce cosmetic masks, protective lipstick, bath fluids, nail varnish and nail cleaners. In cosmetics they are used both as a base as well as active ingredients; in fact many natural substances of high biological activity such as vitamins A, D, E, provitamin A and phospholipids, hormones, steroids and natural dyes, dissolve in fatty acids [1÷7] (Lautenschläger, 2003; Zielińska and Nowak, 2014). Furthermore, algae produce secondary-metabolites known for their skin benefits, such as protection from UV radiations and prevention of rough texture, wrinkles, and skin flaccidity (Ariede et al., 2017). Another important characteristic of microalgae biomass is the strong antioxidant potential they have that derives mainly from their carotenoid content but also for the phenolic substances they contain (Goiris et al., 2012). Furthermore, the carotenoid content of some algae can be increased by manipulating environmental conditions (Priyadarshani and Rath, 2012). For example, it is well know that growing microalgae under nitrogen starvation increases the percent of carotenoids they contain (Lamers et al., 2012). One of the carotenoid most studied for its antioxidant power is the astaxantin, produced from *Haematococcus Pluvialis* or from *Chlorella zofingiensis*. It has been demonstrated that it has a strong antioxidant function and a role of prevention for certain cancers (Nishino et al., 2009; Tanaka et al., 1995). In this respect, microalgae could also be used as a natural drug in the field of health. Astaxanthin for example, as one of the most famous microalgal carotenoid, is much more effective in scavenging free radicals than other carotenoids and Vitamin E (Kurashige et al., 1990; Naguib, 2000; Palozza and Krinsky, 1992). It can reduce DNA damage (Santocono et al., 2007), protect cells of eyes and skin from UV-light mediated photo-oxidation (Lyons and O'Brien, 2002), attenuate inflammation by quenching ROS (Pashkow et al., 2008), boosting immune system by

enhancing the production of antibodies and increasing the total number of T-cells (Jyonouchi et al., 1995, 1993), and benefiting heart health by modifying blood levels of LDL and HDL cholesterol (Yoshida et al., 2010).

1.6.2.3. Microalgae as feed

Astaxanthin has been used as a feed supplement in aquaculture, in order to reinforce the pinkish-red colour of the flesh of aquatic animals, and for improving their growth and survival (Ip and Chen, 2005), so it is strongly required as feed, especially in aquaculture. Animals cannot synthesize carotenoids *de novo* but they have to obtain carotenoids through their food chain or feeds. It is the dietary carotenoids that give salmonids and crustaceans the reddish-orange color that is regarded by consumers as one of the key quality attributes. Astaxanthin is the major carotenoid found in certain marine animals; for example, in crabs, the red pigment accounts for more than 80% of total carotenoids. Astaxanthin is also used in the tropical marine industry aiming at pigmenting ornamental fish. It is possible to find in the market astaxanthin at various prices, depending on the concentration in microalgal biomass, but generally the price of 5% astaxanthin is about US \$1900 kg^{-1} (http://www.herbridge.com/bencandy.php? fid-55-id-23446-page-1.htm) (Rastogi et al., 2017). It can be accumulated in several microalgae such as *Haematococcus pluvialis* (Yuan and Chen, 2000), *Chlorella zofingiensis* (Del Campo et al., 2004) and *Scenedesmus obliquus* (Qin et al., 2008) amongst others. There are also other classes of high value compounds in the microalgal biomass such as lutein, beta-carotene and chlorophyll employed in the sector (Yaakob et al., 2014). Lutein is another carotenoid used for the pigmentation of foods, drugs and cosmetics. It has been demonstrated to have some roles in improving the health, such as delaying chronic diseases or stimulating the immune response. It is accumulated in several algae such as *Chlorella zofingiensis* (Del Campo et al., 2004) and *Chlamydomonas reinhardtii* (Ma et al., 2019). Beta carotene is a pigment demanded for applications in several categories: as food coloring agent, pro-vitamin A (retinol), as food and feed and as antioxidant drug. It is massively produced by the algae *Dunaliella salina* (Morowvat and Ghasemi, 2016). Chlorophyll has been investigated as ingredient in the cosmetic industry and as a natural pigment source in the food market, to be preferred to artificial pigments. Other high-value compounds present in microalgae are phycobiliproteins, that can be used as a source of natural pigments in food market and for labeling bioactive molecules in clinical tests, and Polyunsaturated fatty acids (PUFAs), such as docosahexaenoic (DHA) and eicosapentaenoic (EPA) acids. PUFAs are usually obtained from fish or extracted from fish oil, but the PUFAs in fish are derived from microalgae, so it seems more convenient to extract them directly from microalgae as this allows complete control of the growth environment and therefore ensures the absence of undesired contaminations. All these characteristics ensure the use of microalgal biomass as poultry feed and aquaculture feed.

1.6.2.4. Microalgae as fuel

Biofuels are fuels generated from biological material, a concept that has recently been restricted to renewable sources of carbon. With the growing concerns about the greenhouse gas emissions, the use of biofuels is often a more environmentally friendly option because the carbon balance of biofuel is close to neutral when compared with petroleum-derived fuels such as gasoline, diesel, or kerosene (DeCicco et al., 2016).

One can distinguish three generations of biofuels:

- first-generation biofuel, derived from biomass that is generally edible, as grains, oilseeds, animal fats, and waste vegetable oils;
- second-generation biofuel, that is produced by non-traditional biochemical and thermochemical conversion processes and feedstock mostly derived from not-edible feedstocks, as lignocellulosic fractions of agricultural and forestry residues;
- third-generation biofuel, derived from feedstocks such as algae and energy crops (they are linked to utilization of CO_2 as feedstock).

There are several advantages of using microalgae as biofuel for example: they can be cultured all year round; they grow in aqueous media but need less water than terrestrial crops as the major part of water used for growing algae can be recycled; they can be cultured in brackish water on non-arable land, so they do not compromise the production of food; microalgae biomass production can effect biofixation of waste CO_2 (Brennan and Owende, 2010). Despite its inherent potential as a biofuel resource, many challenges prevented the development of algal biofuel technology to commercial viability that could allow for sustainable production and utilization. The main problems regard the economic balance: obtaining biofuels from other crops is, at the moment, cheaper than from microalgae.

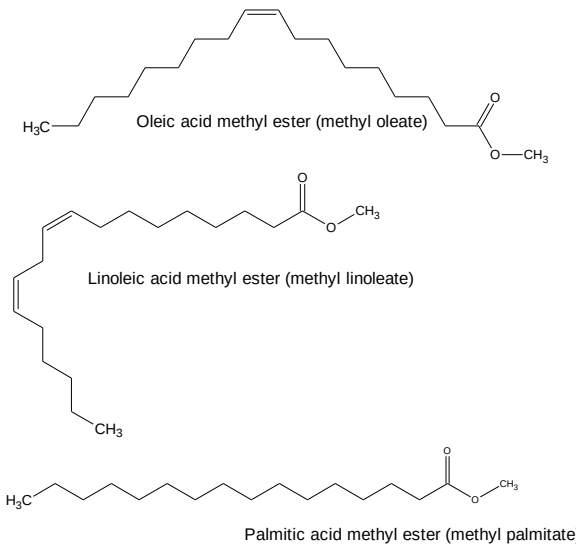

Figure 1.21: Examples of FAMEs.

A strategy for overtaking the problem could be looking for a species that balances requirements for biofuel production and extraction of valuable co-products (Ono and Cuello, 2006). Another problem is the shortage of plants in operation, therefore, there is a lack of data for large scale plants (Pulz, 2001).

The fuels that can be obtained from microalgal biomass are biodiesel and bioethanol. Biodiesel is defined as the mono alkyl esters of long chain fatty acids derived from vegetable oils or animal fats, for use in compression–ignition (diesel) engines (Robles-Medina et al., 2009). Fatty Acid Methyl Esters (FAMEs) (Figure 1.21) are currently employed as a biofuel to be mixed with carbon derived diesel fuel, to comply with environmental regulation. Biodiesel has an energy content and physical and chemical properties similar to conventional diesel fuel, which allows it to function efficiently in conventional diesel engines without any modification. Furthermore, it does not produce explosive vapors and has a quite high flash point (close to 150 °C), so transportation, handling and storage are safer than with conventional diesel (Sulaiman Al-Zuhair, 2007). It is formed by transesterification of vegetable oils with methanol or ethanol (Figure 1.22).

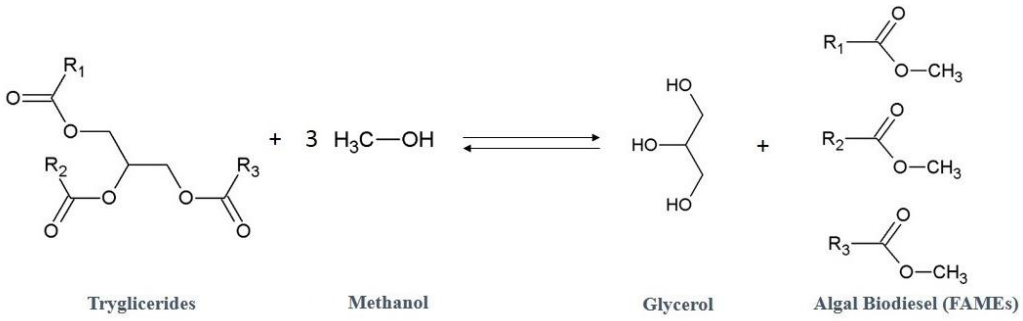

Figure 1.22: Reaction of transesterification.

Bioethanol is another major commercialized biofuel at present and is primarily produced from sugar and starch-based food crops (e.g., corn and sugarcane) via biological fermentation processes. In contrast to lignocellulosic biomass, some microalgae can accumulate large amounts of carbohydrates in the form of starch or cellulose during periods of extreme environmental stress. For these reasons there is currently considerable interest in the use of microalgae as an alternative feedstock for bioethanol fermentation (Ho et al., 2014).

Although the interesting applications of this field, at the moment technologies are not enough developed to guarantee an optimal cost of microalgal cultivation, so the energetic applications are still far away to be employed.

1.6.2.5. Microalgae for the environment

Microalgae can be used in several ways to mitigate atmospheric CO_2 or treat wastewaters. They can be used for the biological CO_2 mitigation, which has the advantage, compared to other kinds of CO_2 mitigation, to produce biomass in the process of CO_2 fixation through photosynthesis (Rasoul-Amini et al., 2014). A part from atmospheric CO_2

fixation, valuable biomass and biocompounds are produced, possibly making microalgae CO_2 bio-mitigation also profitable. Microalgae can fix carbon dioxide from different sources such as from the atmosphere, from industrial exhaust gases and from fixed CO_2 in the form of soluble carbonates. Carbon dioxide in flue gas is available at little or no cost. The CO_2 concentration of flue gas is up to 15%. There are several microalgal species which tolerate this amount of CO_2, such as *Chlorococcum littorale*, *Scenedesmus obliquus* and *Chlorella kessleri* (Rasoul-Amini et al., 2014). Microalgae may be used as well for the treatment of wastewater (Abdel-Raouf et al., 2012; Delrue et al., 2016; Rasoul-Amini et al., 2014). They are able of incorporating nutrients such as nitrogen and phosphorus causing eutrophication. The algal systems can treat human sewage, livestock, agro-industrial wastes and industrial wastes. They are studied for the treatment of other wastes such as piggery effluent, the effluent from food processing factories and other agricultural wastes. The biotreatment of wastewater consists of removing nutrients such as nitrogen and phosphorus. Microalgae can provide at the same time oxygen for aerobic bacteria. This mechanism was proposed in 1955 (Oswald et al., 1985) and is based on the need of oxygen for the stabilization of organic matter. The algae, as photosynthetic organisms, have the double role of producing oxygen and fixing the nutrients in sewage in reclaimable material. Microalgae have as well the capacity to remove heavy metals and toxic organic compounds, so they can be used also to bioremediation purposes (Zeraatkar et al., 2016). The process used by algae to bioremediate heavy metals is called biosorption, but it is far more effective using dead biomass than living microalgae. In fact, absorption mechanisms in living algae are more complex than in non-living algae. Non-living algae cells absorb metal ions on the surface of the cell membrane and it is considered an extracellular process. Non-living algal biomass can be regarded as an assemblage of polymers (such as sugars, cellulose, pectins, glycoproteins, etc.) that are capable of binding to heavy metal cations as adsorbents with the potential of cost-effective wastewater treatment.

1.6.2.6. Microalgae as biotechnological platform

There is a growing demand for transgenic proteins because of their applications in fields like industry, diagnosis and therapy. Currently, transgenic proteins are produced in several hosts: bacteria, yeasts, eukaryotic cells and plants. Each of them has its own advantages and disadvantages and is employed in specific applications. Bacteria have no post-traductional and post-translational modifications, such as intron splicing, multimeric protein assembly, glycosylation and disulfide bond formation, and processes that are essential for generating functional eukaryotic proteins (Cereghino and Cregg, 1999). Mammalian lines are usually employed for producing proteins for therapeutics, although there are often problems such as oxygen deficiency, the accumulation of waste products or sensitivity to stirring forces which can result in instability of mammalian cells, making it difficult to culture them in large volumes (Chu and Robinson, 2001). Microalgae have

several advantages compared to other biotechnological platforms: they have a similar glycosylation pattern compared to human cells, the accuracy of protein folding is high, they are grown easily and on cheap substrates, the production time is short and the contamination risk is low. For these reasons, microalgae are a good host for producing transgenic proteins (Yan et al., 2016). Genetic manipulation is reported in literature for at least 40 different species; among them the most studied are *Chlamydomonas reinhardtii* and *Pheodactylum tricornutum*, respectively a green algae and a diatom (Hempel et al., 2011). There are genetic tools for both for nuclear and chloroplastic genomes, even if nuclear transformation has some disadvantages compared to chloroplastic one. In fact, there is poor transgene integration, codon bias, positional effects and gene silencing which can lead to poor or unstable transgene expression. The available delivery methods are biolistic, agitation in presence of glass beads, electroporation or agrobacterium-mediated transformation. On the other way, chloroplast genome engineering is particularly attractive given the ability to target transgenes into specific, predetermined loci via homologous recombination, and the high levels of expression that can be achieved. To date, several different kinds of high-value molecules have been expressed in microalgae. Monoclonal antibodies, immunotoxins, vaccine antigens, several enzymes have been successfully expressed (Hempel et al., 2011; Tran et al., 2013; Zedler et al., 2015). Despite the high number of reports on producing transgenic proteins in microalgae, it's hard to find literature on the scale-up of these productions. This is caused by a lack of knowledge on these topics and proves that much work still needs to be done in this field in order to boost genetic manipulation of microalgae for the future expansion of microalgal industry.

Section 2: Microalgae as Biotechnology Platform: production of Human Intrinsic Factor in *Chlamydomonas reinhardtii*

Part of the content of this section was published as:

- S. Lima, C. Webb, E. Deery, C. Robinson, J. Zedler, Human Intrinsic Factor Expression for Bioavailable Vitamin B12 Enrichment in Microalgae, Biology (Basel). 7 (2018) 19. doi:10.3390/biology7010019

2.1. The market of nutraceutical and supplements: current state and perspectives

There is an increasing awareness of the effect of diet on human health and, in particular, on the development of illness and chronic diseases. This has led to an upward trend in consumer demand for naturally occurring bioactives that can be delivered in the form of dietary supplements or incorporated into functional foods. This interest is reflected also by the scientific community, as shown by the increasing number of the word "nutraceuticals" search counts in Pubmed, shown in Figure 2.1.

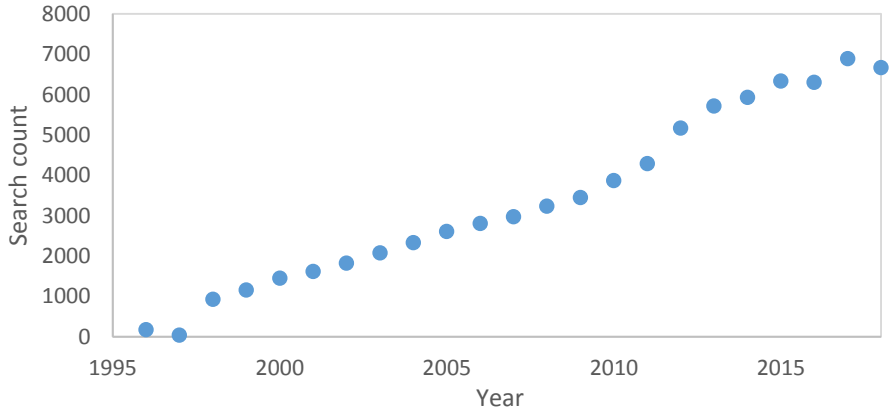

Figure 2.1: Timeline of the Pubmed search of the word "nutraceutical" over years.

This growing awareness about the effects that food has on health has led to the development of products with the aim of supplementing healthy substances that can help the human (or animal) body. There are several kind of products and usually the categories are confused by the consumers. The "physiologically functional foods" have been defined in Japan in 1980s as "any food or ingredient that has a positive impact on an individual's health, physical performance, or state of mind, in addition to its nutritive value" (Hardy, 2000). A "medical food", instead, is defined by the U.S. Food and Drug Administration (FDA) as "formulated to be consumed or administered entirely under the supervision of a physician and which is intended for the specific dietary management of a disease or condition for which distinctive nutritional requirements, on the basis of recognized scientific principles, are

established by medical evaluation" (Hardy, 2000). In 1989, a new word, *nutraucetical*, was created by the Foundation for Innovation in Medicine to indicate "any substance that may be considered a food or part of a food, and provides medical or health benefits, including the prevention and treatment of disease." (Hardy, 2000; Nasri et al., 2014). Although not all the commercialised nutraceuticals have been proved to work as they are supposed to, and to have real positive effects on health (Espín et al., 2007), their market gained a major importance in the last decades. In fact, it is expected to reach $302,306 million by 2022 from $184,092 million in 2015 with a Compounded Average Growth Rate (CAGR) of 7.04% from 2016 to 2022 ("Nutraceuticals Market Size, Share & Trends | Industry Analysis, 2022," n.d.). For what concerns in particular vitamin B12, one of the most supplemented vitamins, in 2017, the global Vitamin B12 market size was 310 million US$ and is forecast to hit 400 US million in 2025, growing at a CAGR of 3.1% from 2018 ("Vitamin B12 Market Value to boost by 400 million US in 2025").

The exponential growth of this sector has been caused by companies eager to invest in easy financial returns also because of the simpler regulations on nutraceuticals compared for example to novel foods (Brower, 1998). Furthermore, nutraceuticals and supplements are object of multi-level marketing companies (such as Herbalife and Usana), leading to ethical constraints because of the doubted quality of the sold products (Cardenas and Fuchs-Tarlovsky, 2018). On the other side, a specialised market of nutraceuticals from microalgae has expanded in the last decades (Borowitzka, 2013). The scientifically demonstrated healthy proprieties of several molecules produced by microalgae was already discussed in Section 1. As microalgae are seen as food of the future (Caporgno and Mathys, 2018), the genetic engineering of them could be a tool for increasing the beneficial value for health of this food, creating a new frontier of food supplement. This has, of course, a great relevance for future industrial developments in the field.

2.2. *Chlamydomonas* as model organism

Chlamydomonas reinhardtii is a model organism in the world of microalgae. As a matter of fact, it started to be considered a model organism many decades ago and most of the commonly used strains are originated from isolates back in 1945 (Harris, 2001). This alga is a biflagellate and unicellular Chlorophyte, and was referred in the past as "planimal" because of the mixture of traits from the animal and plant kindoms (Redding and Cole, 2008). This trait gives *Chlamydomonas* a special importance for biotechnological industry. It has also a fast doubling time, grows easily and has the capacity of reproducing sexually or asexually. These characteristics make it an ideal model organism, also because of the knowledge about its metabolic pathways that has helped in its genetic manipulation for the production of heterologous proteins of

other high-value compounds. Another characteristic of eukaryotic microalgae is their compartmentalization (presence of chloroplast and mitochondria, with an own genome) that allows the targeting of produced proteins in the preferred district, making the subsequent purification step easier. The three genomes are sequenced and can be genetically manipulated (Maul et al., 2002; Merchant et al., 2007; Vahrenholz et al., 1993); furthermore, several mutants are available (Neupert et al., 2009). The ability of posttranslational modifications is furthermore desired in order to produce complex proteins, together with the possibility of glycosylate them in the cytosol but not in the chloroplast (Mayfield and Franklin, 2005). *Chlamydomonas* is preferred as organism choice for genetic modification also because of the several established tools available but also because stable transformations lines can ideally be generated in short times (Mayfield et al., 2007). As shown in paragraph 1.5.5.6, the usage of microalgae as biotechnological platform may have an increasingly bigger importance in industry, leading to a brighter future for microalgae exploitation.

2.3. Genetic modification techniques in microalgae

To date, the transformation of more than 40 species has been reported (Gangl et al., 2015b). Most of the successful transformations have been found in *C. reinhardtii*, but also species such as the diatom *Pheodactylum tricornutum*, *Chlorella*, *Volvox carteri* have been transformed (Walker et al., 2005). Also some efforts have been done with *Haematococcus pluvialis* (Steinbrenner and Sandmann, 2006; Yuan et al., 2018), *Nannochloropsis* (Kang et al., 2015; Li et al., 2020) and *Schizochytrium* (Cheng et al., 2012). A fundamental step of microorganism's transformation is the DNA delivery. Several methods have been developed; one of the first ones is the biolistic, optimised 30 years ago for chloroplast and nuclear genome (Boynton et al., 1988; Debuchy et al., 1989). It consists in shooting the target cells with high-velocity projectiles coated with DNA. An alternative method is the agitation of cells with DNA and glass beads (Kindle, 1990). The method consists in creating transient holes in the cell membrane that allow the DNA to enter in it. For these methods usually cell deficient strains are employed. Another alternative is the electroporation, used both for nuclear and for chloroplastic genome (Kindle, 1990), that creates an electric field capable of targeting the DNA in the cells. A very used method in plant transformation, that has been employed also for microalgae, is DNA transfer mediated by *Agrobacterium tumefaciens* (Kumar et al., 2004).

For what regards the best district to transform, both the chloroplast than the nuclear genome of *Chlamydomonas* have been targeted for genetic manipulation and both of them have pro and cons. In the nuclear genome the DNA can be inserted through homologous recombination, that is not very efficient and occurs essentially random. Therefore, often an epigenetic silencing is observed. The chloroplast genome, on the

other side, is easier to transform, but its polyploidy makes the transformants not stable. Furthermore, not all the post translational modifications are performed (for example glycosylation does not occur in the chloroplast), making the expression of complex proteins not possible.

Anyway, a complete toolkit of molecular instruments, such as promotors, selectable markers and reporter genes, are available for both the genomes (Mussgnug, 2015).

2.4. Vitamin B12: biological roles and deficiency

Vitamin B12 or cobalamin (B12), is an essential cofactor produced by certain prokaryotes via two main complex biosynthetic pathways (Warren et al., 2002). In humans, B12 is an essential cofactor required for a range of cellular metabolism functions (e.g., DNA synthesis and methylation, mitochondrial metabolism) (Green et al., 2017). B12 uptake and transport from ingestion to the blood stream is a multi-step complex pathway, described in Figure 2.2 (Nielsen et al., 2012). One of the proteins playing a key role in this process is the human protein *intrinsic factor* (IF). The glycoprotein binds free B12 in the ileum and the IF-B12 complex is then recognized by the cubam receptor complex facilitating receptor-mediated endocytosis (Alpers and Russell-Jones, 2013). The lack of a functional IF protein leads to the severe autoimmune disease *pernicious anaemia* (Nielsen et al., 2012). Less severe but rather common cases of B12 deficiency are typically found in children, pregnant women and the elderly. Vegetarians and vegans are also at a higher risk for B12 deficiency, as higher plants do not produce or uptake B12 and are, therefore, not a dietary source of B12 (Pawlak et al., 2013). To counteract the lack of dietary B12 intake, a wide range of supplements are commercially available. For instance, microalgal *Chlorella* supplements were found to contain amounts of B12 varying from trace amounts up to 415 µg per 100 g dry weight (Bito et al., 2016).

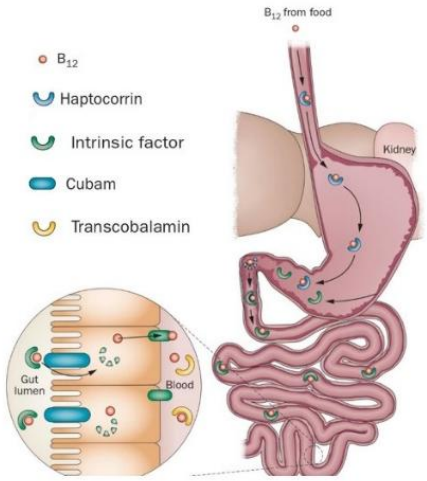

Figure 2.2: Multistep pathway of uptake and transport of vitamin B12 in the gut lumen. (Nielsen et al., 2012)

2.5. Aim of this section

In the context of this study, three main applications of microalgae are taken in consideration: (I) microalgae for functional foods (due to their high protein content, anti-oxidative properties and other potential health benefits) and as a vegetarian source of bioactive supplements (Borowitzka, 2013; Plaza et al., 2009; Wells et al., 2017); (II) microalgae as a novel recombinant biotechnological host (Gangl et al., 2015a; Nielsen et al., 2016; Rasala and Mayfield, 2015; Scaife et al., 2015); and (III) microalgae as a source of natural high-value compounds (Gangl et al., 2015a; O'Neill and Kelly, 2017).

These themes of microalgal applications are brought together in this proof-of-concept study by testing the possibility of enriching B12 in microalgae using the human IF protein. To this end, nuclear transformants of the green model alga *Chlamydomonas reinhardtii* expressing IF were generated. The IF protein was successfully expressed and the addition of a signal peptide from arsylsulfatase (ARS) resulted in the efficient secretion of IF to the medium. The supplementation of the culture medium with B12 led to a higher IF abundance in the generated microalgal strains. Figure 2.3 shows the two strains of *Chlamydomonas* able to produce a cytosolic and a secreted version of IF, both able to bind B12. This proof-of-concept shows microalgae are a viable host for the production of a vegetarian IF source for B12 enrichment. This could pave the way for developing a vegetarian source of bioavailable B12 for dietary supplements and the enrichment of functional foods.

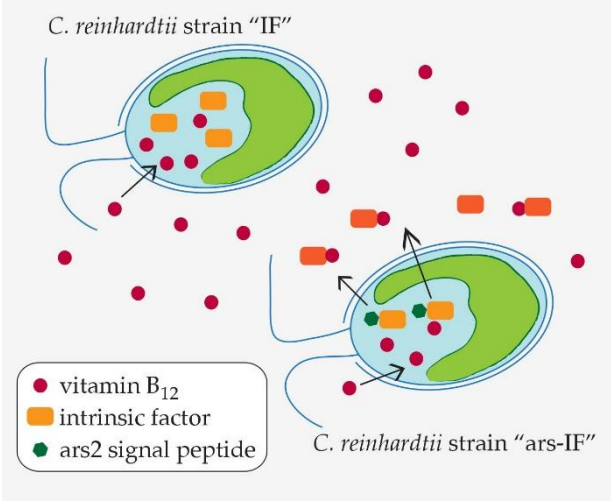

Figure 2.3: "IF" strain of *Chlamydomonas reinhardtii* producing the human protein Intrinsic Factor (IF) in the cytosol and "ars-IF" strain secreting it in the growth medium thanks to the signal peptide from arsylsulfatase. Both the versions of intrinsic factor are able to bind vitamin B12.

2.6. Materials and Methods

2.6.1. Construct design and Plasmid Construction

The amino acid sequence of the human intrinsic factor (Uniprot KB: P27352) was codon-optimized for nuclear expression in the green alga *C. reinhardtii* using the software GeneDesigner 2.0 (Villalobos et al., 2006). The N-terminal native signal peptide (amino acid sequence (AA) 1–18) was removed and a C-terminal hemagglutinin (HA) epitope tag (YPYDVPDYA) was added for detection of the protein. Additionally, a second construct was made with an N-terminal secretion signal peptide of the *C. reinhardtii* native arsylsulfatase ARS2 (AA 1–21, Uniprot KB: Q9ATG5) (Eichler-Stahlberg et al., 2009). The synthetic genes were custom synthesized by Genscript (USA) and cloned into the pCrEX1 nuclear expression vector, based on pSR108 (Stevens et al., 1996), using the restriction sites SapI (LguI) and BglII. Figure 2.4 gives an overview of the expression cassettes. The correct construct assembly has been verified by sequencing. All plasmids were amplified in *Escherichia coli* DH5α and purified for transformation of *C. reinhardtii*.

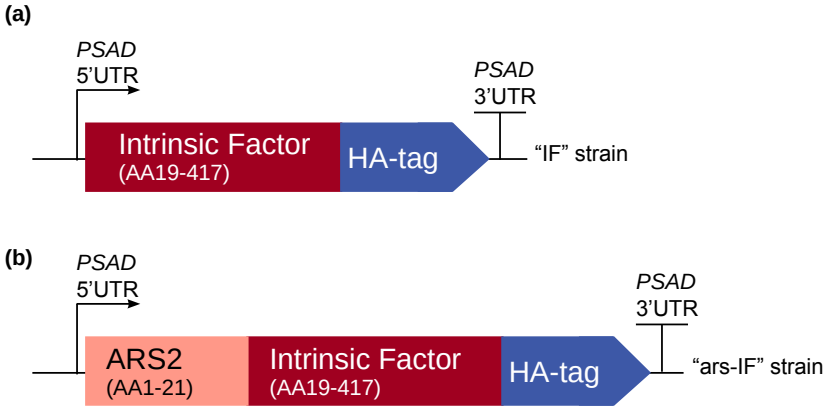

Figure 2.4: Overview of the intrinsic factor (IF) expression cassettes used for *C. reinhardtii* transformation. The strains expressing the constructs have been named "IF" and "arsIF" respectively. The 3′ and 5′ untranslated regions of the *C. reinhardtii* PSAD gene are used for gene expression. (a) The N-terminal native signal peptide of the human IF protein was removed and the full length protein was codon-optimized for *C. reinhardtii* nuclear expression. A C-terminal HA epitope tag was added to the protein for detection purposes. (b) Additionally, a second version of IF was constructed with the secretion signal peptide of arsylsulfatase ARS2.

2.6.2. Strains and cultivation conditions

The *C. reinhardtii* strain CC-849 (cw10, mt−) was obtained from the *Chlamydomonas* Resource Center (University of Minnesota, Minneapolis, MN, USA). All strains were maintained at 25 °C and approximately 50 μE m^{-2} s^{-1} continuous illumination on 2% Tris Acetate Phosphate (TAP) (Gorman and Levine, 1965) agar plates with a modified trace element recipe (Kropat et al., 2011). Liquid cultures were grown in TAP medium at 25 °C, 110 rpm shaking and approximately 100 μE m^{-2} s^{-1} continuous illumination. When TAP medium was supplemented with vitamin B12 (20–100 μg L^{-1}), commercially obtained cobalamin (Sigma-Aldrich, US) was added from a 0.1 g L^{-1} stock solution.

Initial screens for positive transformants were performed in 24 well plates. The wells were inoculated with single colonies and grown for 5 days before analysis. For protein expression analysis, 100 mL pre-cultures were inoculated from a plate. After 6 days, 100 mL cultures were re-inoculated to an OD750 of 0.01. Cells were subsequently harvested at mid to late log phase. For protein concentration and B12 assays, 1 L cultures were inoculated to an OD750 = 0.02 from a 1 week-old 100 mL pre-culture and grown to a mid-log phase stage before processing.

2.6.3. Nuclear transformation

For nuclear transformation, 1 μg of the respective plasmid was linearized by cutting with EcoRI. A nuclear glass-bead transformation protocol was used based on a previously described method (Kindle, 1990; Lumbreras et al., 1998). In brief, a 200 mL culture of CC-849 was grown to early log-phase and resuspended in 2 mL fresh TAP medium. Per transformation, 300 μL concentrated cells and 1 μg of linearized plasmid were used. The cell-DNA mixture was added to approximately 300 mg 400–600 μm acid-washed glass beads (Sigma-Aldrich, US) and agitated on a vortex for 15 s on maximum speed. The cells were diluted with TAP medium to a final volume of 10 mL and grown for approximately 18 h. After resuspension of the cell pellets in 500 μL TAP medium, soft agar (0.5%) was added and the mixture spread on TAP plates containing 10 μg mL^{-1} Zeocin (InvivoGen, US) for selection of transformants that incorporated the construct containing the ble marker (Stevens et al., 1996). After approximately 8 days, colonies were re-streaked and subsequently analyzed for the presence of the gene of interest.

2.6.4. PCR analysis

Transformant colonies were screened for the presence of the gene of interest using Polymerase Chain Reaction (PCR). A gene fragment was amplified from genomic DNA using a standard protocol with Phire Plant Direct Master Mix (Thermo Fisher

Scientific, US). The following primers were used to amplify a 600 base pair fragment confirming the presence of the IF/ars-IF expression cassette: IF-fragF (5′-3′) CAGCATGAAGATTAAGGACA and IF-fragR (5′-3′) GTAGTACTGCGTGAAGTTG.

2.6.5. Preparation of cellular lysates and medium samples for protein expression analysis

For protein expression analysis, cultures were grown as indicated in paragraph 0. Cellular lysates were prepared by resuspending an equivalent of OD_{750} = 1 cells in mid to late log phase in 100 µL 10 mM tris(hydroxymethyl)aminomethane (tris) -HCl (pH 8.0). To analyze the medium, 1 mL of culture was spun down at 20,000× g for 5 min and the cleared supernatant transferred to a separate tube.

2.6.6. Protein concentration and Ion Exchange Chromatography

1 L mid-log phase cultures were harvested at 4000× *g* for 20 min at 4 °C. For protein concentration from the medium, the culture supernatant was filtered through Whatman filter paper to remove any debris and subsequently through a 0.2 µm membrane to remove any residual cells. The pre-purified medium fraction was subsequently loaded on the column.

For concentration of cellular proteins, the harvested cells were resuspended in lysis buffer (20 mM Tris-HCl (pH 7.2), 5% glycerol, 20 $\mu g \cdot mL^{-1}$ DNaseI (Roche, CH), EDTA-free protease inhibitor (Roche, CH)) and sonicated (3 cycles of 30 s sonication and 30 s on ice). The lysate was cleared by ultracentrifugation at 70,000 rpm, 30 min (TLA-100.3 rotor, Beckmann, US) and the soluble supernatant loaded on the column.

For ion exchange chromatography (IEC), 10 mL columns (Q Sepharose Fast Flow, GE Healthcare, US) were freshly prepared for each purification. A vacuum pump was used to pass the medium samples through the column. After loading of the sample (medium or cellular lysate), the column was washed with a Tris based buffer (20 mM Tris-HCl -pH 7.2), 5% glycerol, 1 mM $MgCl_2$, 5 mM dithiothreitol) containing 50 mM NaCl. Protein fractions were then eluted with buffer containing rising concentrations of NaCl (100 mM, 150 mM, 200 mM, 300 mM, 400 mM and 1 M NaCl). The process is shown in Figure 2.5.

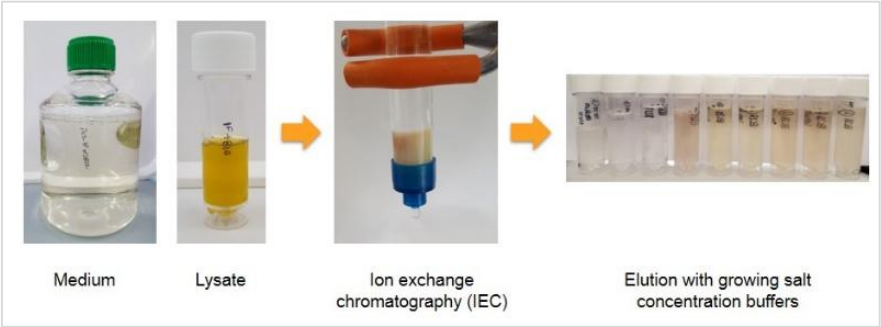

Figure 2.5: Loading of medium or lysate inside a freshly prepared columns for Ion Exchange Cromatography (IEC). Protein fractions were eluted with buffer containing increasing concentrations of NaCl.

2.6.7. Vitamin B_{12} assay

The bioassay for the detection of B12 content in the protein fractions from ion exchange chromatography is based on the *Salmonella enterica Typhimurium* LT2 strain AR2680 (metE–, cbiB–). Details of the assay are described elsewhere (Raux et al., 1996). In very brief, this *Salmonella* strain cannot synthesize B12 de novo (CbiB–) and has no B12-independent methionine synthase (MetE–). Thus, growth of this strain is dependent on an external source of vitamin B12 as a co-factor for the vitamin B12-dependent methionine synthase MetH. The plaque size (growth) is dependent on the amount of externally supplemented vitamin B12, and can thus be used to semi-quantify Vitamin B12 levels in the sample. Plaques appearance is shown in Figure 2.6. A calibration curve using 10 µL of 0.001 µM, 0.01 µM, 0.1 µM and 1 µM B12 solutions led to the equation used to calculate the B12 content in the analyzed samples:

$$\text{vitamin B12 concentration } (\mu M) = 0.0029 \times (\text{plaque diameter in cm})^{5.4616}$$

Unpaired Student's t-tests were performed using the software Graph Pad Prism (version 7.0, US). Values were considered statistically significant for $p < 0.05$.

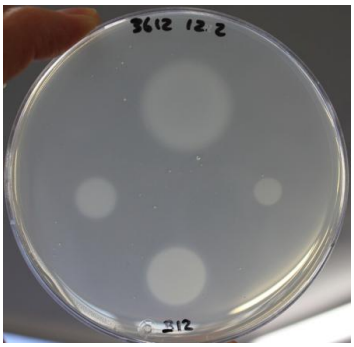

Figure 2.6: Plaques of *Salmonella enterica Typhimurium* auxotroph for B12 grown thanks to the supplementation of the vitamin. The size of the plaque is correlated with the concentration of B12.

2.6.8. Reducing SDS-PAGE, Native PAGE and Western Blotting

Samples were separated by electrophoresis on 12% polyacrylamide gels using a Mini Protean Gel system (Bio-Rad, US). For reducing, denaturing SDS-PAGE, samples were boiled with Laemmli buffer containing β-mercaptoethanol at 95 °C for 5 min (crude cellular lysates and medium samples) or 10 min at 50 °C (fractions from ion exchange chromatography). For native analysis, samples were not boiled and no sodium dodecyl sulfate nor β-mercaptoethanol was used in samples, gels or running buffer. The polyacrylamide gels were subsequently immunoblotted using antibodies against the C-terminal HA-tag (Sigma-Aldrich, US) and against the C-terminus of the IF protein (abcam) to detect the protein of interest.

2.6.9. Densitometric Analysis

Densitometry analysis of immunoblots was performed using ImageLab Software Version 4.1 (Bio-Rad, US). The relative abundance of the IF protein was calculated in relation to the protein band found without supplementation of B12 to the medium. For the ars-IF strains, the calculated abundance was normalized to the OD750 of the cultures measured at harvesting to account for growth differences. This correction was not performed for the IF strains as equal amounts of cellular lysate standardized to OD750 were loaded on the gel.

2.7. Results

2.7.1. Generation of *C. reinhardtii* nuclear transformants "IF" and "ars-IF"

For this study, constructs for nuclear transformation of a wall-deficient *C. reinhardtii* strain (CC-849) were assembled with the human gene encoding the mature sequence of the B12-binding protein IF flanked by 5′ and 3′ Untranslated regions (UTRs) of the PSAD gene. Two constructs were generated—one for cytoplasmic expression

(Figure 2.4a) encoding IF and a second version with the addition of an N-terminal signal peptide from ARS2 (Figure 2.4b). This signal peptide has previously been shown to enable secretion to the medium in *C. reinhardtii* of recombinant proteins (Eichler-Stahlberg et al., 2009). Additionally, a C-terminal HA epitope tag was added to both proteins for detection purposes. The ble marker downstream of the gene of interest on the pCrEX1 plasmid was used to select for positive transformants after transformation by agitation of a DNA-cell mixture with glass beads (modified from previously described methods (Economou et al., 2014; Kindle, 1990), see Paragraph 2.6.3). The presence of the IF cassette was verified by PCR (Figure 2.7) in colonies that grew on Zeocin after transformation. Positive candidates based on PCR results were then subjected to immunoblot analysis to screen for expression of the IF protein. Two strains with the respective constructs were found to express detectable levels of IF (Figure 2.8). The strains were named "IF" and "ars-IF" (Figure 2.4) and subjected to further analysis.

Figure 2.7: PCR analysis of *Chlamydomonas reinhardtii* strains IF and ars-IF. A 0.6 kilo base pair (kb) DNA-fragment of the intrinsic factor gene has been amplified from genomic DNA. Lanes show the transformant strains IF and ars-IF, CC-849 (N, negative control) and a positive control (P, plasmid DNA used for transformation mixed with CC-849 cells).

2.7.2. Expression of Human Intrinsic factor in *C. reinhardtii*

The expected size of the mature size IF based on its amino acid sequence is 44.6 kDa. The IF protein expressed in the IF strain has a similar size migrating on an SDS-PAGE slightly faster than the 46 kDa molecular weight standard (Figure 2.8a). Additionally, a second non-specific band cross-reacting with the HA antiserum was detected in cellular lysates of both, the IF and the control strain around 32 kDa that was previously observed in *C. reinhardtii* cellular lysates (Zedler et al., 2015). The IF protein was expressed with an N-terminal ARS2 signal peptide in the ars-IF strain. The signal peptide and the mature IF protein have a combined predicted molecular weight of 46.3 kDa, however, the expected size of the mature protein after cleavage of the ARS2 signal peptide is the same molecular weight as the cytoplasmic IF protein with 44.6 kDa (this observation is discussed in more detail in Paragraph 2.8.2). Immunoblot analysis of the ars-IF culture medium shows the protein migrating at a

size around 50 kDa which is slightly bigger than expected. To further verify the band, which is not present in the CC-849 control strain (Figure 2.8b), the protein was also immunoblotted using an IF-specific antibody. With both antibodies, the same band was detected.

To determine the localization of the protein, culture supernatant (medium) and pelleted cells (cellular lysate) were immunoblotted separately. In the IF strain, the IF protein was only detected in cellular lysates (Figure 2.8a,d). In contrast to this, the IF protein expressed in the ars-IF strain with the ARS2 signal peptide was only found in the culture supernatant (Figure 2.8b), no protein was detected in cellular lysates (Figure 2.8c).

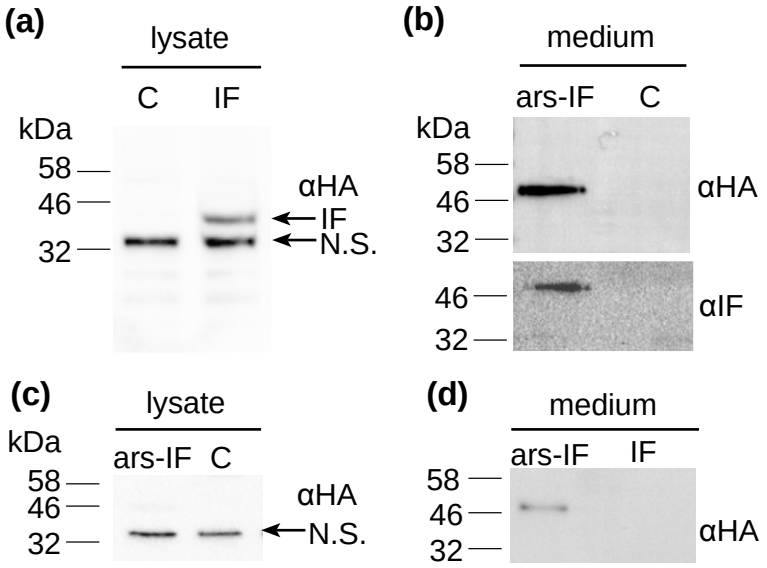

Figure 2.8: Expression of human intrinsic factor (IF) protein and ars-IF in *C. reinhardtii* CC-849 detected by immunoblot analysis using HA (αHA) and intrinsic factor (αIF) antibodies respectively in the culture medium and cellular lysates. (a) Cellular lysates of IF strain expressing protein. The protein band is indicated with an arrow (IF). A second, non-specific band cross-reacting with the HA antiserum is indicated (N.S.). (b) Culture supernatant (medium) of transformed CC-849 strain expressing ars-IF. 'C' indicates a negative control (cellular lysate and supernatant of the untransformed CC-849 strain). (c) Cellular lysates of ars-IF strain and CC-849. (d) Culture medium of ars-IF and IF strain.

2.7.3. *C. reinhardtii*-produced IF stability increases with external vitamin B_{12} supplementation

To test the B_{12} binding capacities of the microalgal IF produced protein, the IF and ars-IF strains were grown in TAP medium supplemented with vitamin B_{12} at a concentration of 0, 20, 50 and 100 $\mu g \cdot L^{-1}$. As shown by immunoblotting, a correlation between higher B_{12} levels and the IF protein (ars-IF strain) in the medium is observed (Figure 2.9a). The protein abundance increases approximately 2.1 fold (±0.50) with the addition of 100 $\mu g \cdot L^{-1}$ B_{12} in the culture medium (Table 2.1). Similarly, based on densitometric analysis of relative protein abundance, the cytoplasmic IF protein in the IF strain is also estimated to be more abundant with B_{12} supplemented in the medium. However, here the highest abundance of IF is estimated to be at 50 $\mu g \cdot L^{-1}$ B_{12} (Figure 2.9b and Table 2.1).

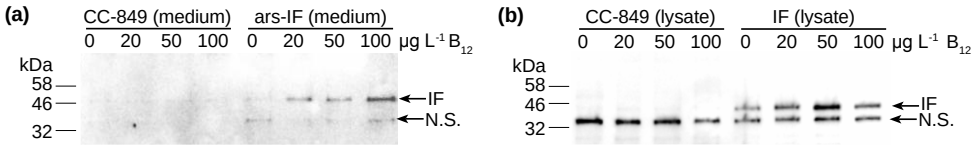

Figure 2.9: Accumulation of human intrinsic factor (IF) protein in *C. reinhardtii* ars-IF and IF cultures with increasing concentrations of vitamin B_{12} (cobalamin) supplemented TAP medium. (**a**) HA-immunoblot of medium harvested from CC-849 and ars-IF cultures grown to late log phase containing 0, 20, 50 and 100 $\mu g \cdot L^{-1}$ Vitamin B_{12}. Equal amounts of culture supernatant (20 µL) loaded per lane. (**b**) HA-immunoblot of cellular lysates from CC-849 and IF cultures grown to late log phase with 0, 20, 50 and 100 $\mu g \cdot L^{-1}$ Vitamin B_{12} supplemented. Equal amounts of cellular lysate standardized by OD_{750} loaded. Mobility of IF protein indicated by arrow, N.S. denotes a non-specific protein cross-reacting with the HA-serum. In the Supplemental Information a Coomassie stained SDS-polyacrylamide gels with total protein loaded for respective western blot samples is shown.

Table 2.1: Relative human intrinsic factor (IF) protein expression levels in IF and ars-IF strains for different B_{12} concentration supplemented to growth medium (n = 3 ± standard error).

Vitamin B_{12} in Medium ($\mu g \cdot L^{-1}$)	ars-IF Strain (Medium)[1]	IF Strain (Cytoplasmic)[2]
0	1.0	1.0
20	1.1 ± 0.01	1.4 ± 0.15
50	1.6 ± 0.17	2.3 ± 0.17
100	2.1 ± 0.50	1.4 ± 0.11

[1] Densitometric relative quantity of IF was normalized to the OD_{750} of the respective cultures measured when samples were harvested. [2] Equal amounts of cells, normalized to OD_{750}, for all cultures were loaded on gel for immunoblotting.

2.7.4. Correlation of Vitamin B_{12} and IF protein levels

To further investigate if the IF protein was binding B_{12}, the protein was concentrated from cellular lysates (IF strain, CC-849 control) and the medium (ars-IF strain, CC-849 control). Ion exchange chromatography was used to concentrate and separate protein fractions from the total cellular (IF strain) or secreted protein (ars-IF) mixture. Protein fractions were eluted with rising NaCl concentrations from 100 mM to 1 M NaCl. Both IF expressing strains and the negative control strain CC-849 were grown with either no B_{12} or 20 $\mu g \cdot L^{-1}$ B_{12} supplemented to the medium. The majority of the IF protein was eluted with 100–150 mM NaCl in both cases, the medium and the cytoplasmic IF version, as shown by immunoblot analysis of the individual protein fractions (Figure 2.10). Immunoblots of IF concentrated from cellular lysates of the IF-strain showed one prominent band of the protein with both reducing SDS-PAGE and native PAGE (Figure 2.10a). In the medium version, bands migrating differently in native PAGE than with reducing SDS-PAGE were observed (Figure 2.10b).

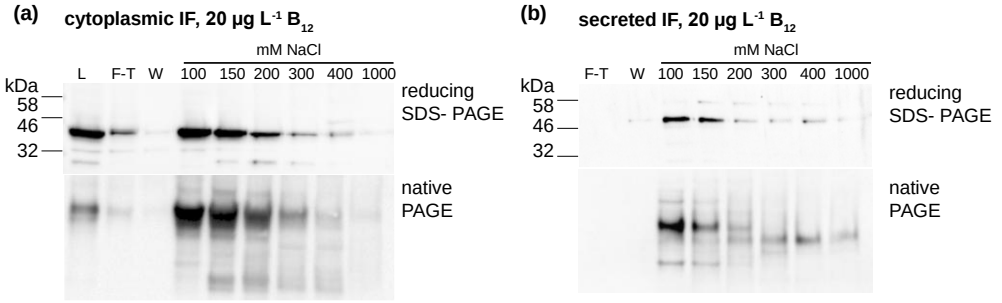

Figure 2.10: Protein fractions purified from (**a**) cellular lysates (human intrinsic factor (IF) strain) and (**b**) medium (ars-IF strain) HA-Immunoblots of reducing SDS- and native-PAGE show the presence of the IF protein in the separate fractions. L-lysate; F-T—flow-through; W-wash fractions (wash 1 and wash 2 as shown in Figure 2.11 were pooled); 100 mM–1000 mM: NaCl concentrations of eluted fractions.

All fractions, the lysates and medium samples were subsequently used in a B_{12} bioassay to quantify their B_{12} content. This bioassay is based on the growth dependency of a *Salmonella typhimurium metE*$^{-}$ strain on external B_{12} supplementation. All experiments were performed in triplicate and the B_{12} content found in the individual fractions is shown in Figure 2.10a for the IF-strain and Figure 2.10b for the ars-IF strain when cultures were supplemented with 20 $\mu g \cdot L^{-1}$ B_{12}. The table with results and the pictures of the plates are shown in Supplemental information. In both cases, the highest B_{12} content was found in the lysate (medium), flow-through and wash fractions. Significant differences in B_{12} content between the control strain and the IF strain were only found in the cellular lysate (p = 0.01) however this observation was not supported by the eluted protein fractions (Figure

2.11a). In case of the ars-IF strain, significant differences were only found in the 100 and 150 mM NaCl eluted protein fractions ($p = 0.02$) (Figure 2.11b). All purifications from cultures grown without B_{12} supplemented in the medium did not contain B_{12} levels detectable with the bioassay. The elution pattern of the IF protein in these samples was, however, found to be overall the same as from cultures supplemented with B_{12}. The majority of secreted IF protein was found to be cleaved or degraded without B_{12} supplementation as seen by SDS-PAGE analysis during the purification process (Figure 2.12b). Whereas a similar pattern, with and without B12 supplementation of the medium, was found for the cytoplasmic IF protein (Figure 2.12a).

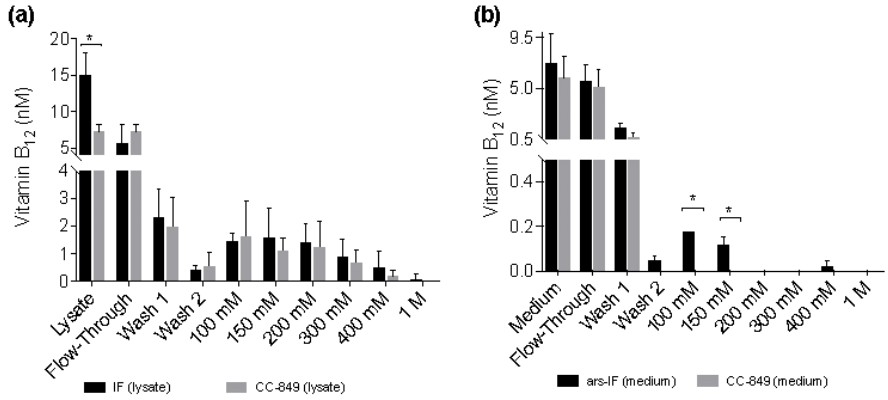

Figure 2.11: Vitamin B_{12} content of protein fractions purified from human intrinsic factor (IF) and ars-IF strains grown with 20 $\mu g \cdot L^{-1}$ supplemented TAP medium determined using a plaque assay of *Salmonella typhimurium* metE⁻. Fractions were eluted with increasing concentrations of NaCl (100 mM to 1 M). Data show average values, error bars: standard error ($n = 3$). Statistically significant differences between the control and the respective strain for each fraction are indicated with an asterisk (Student's *t*-test, $p < 0.05$). (**a**) B_{12} amounts detected in fractions of 1 L cellular lysates from IF and CC-849 strains. (**b**) B_{12} amounts detected in protein fractions purified from 1 L medium of ars-IF or CC-849 cultures.

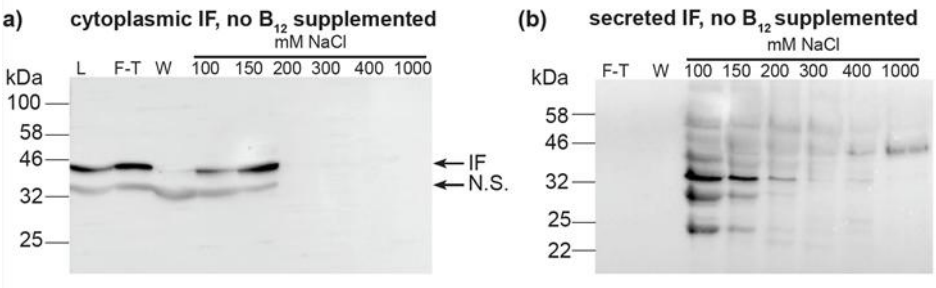

Figure 2.12: IF purified from cultures without B12 supplementation. (a) Cytoplasmic IF purified from IF cellular lysates. (b) Secreted IF purified from ars-IF cultures. Anti-HA immunoblots of fractions shown . L- lysate, FT – flow-through; W-wash fractions (wash 1 and wash 2 as shown in Figure 2.11 were pooled); 100 mM – 1000 mM: NaCl concentrations of eluted fractions. N.S. denotes non-specific protein band.

2.8. Discussion

2.8.1. Expression and efficient secretion of a human glycoprotein intrinsic factor in microalgae

In this study the human B12 receptor protein IF was successfully expressed in *C. reinhardtii*. The protein was expressed from the nuclear genome as this allowed for secretion of the protein to the medium and potential glycosylation of the protein. Two different strains were generated for this study—one strain expressing the 44.6 kDa IF protein in the cytoplasm (IF-strain) and a second strain that secretes the protein to the medium (ars-IF). The ars-IF expressed IF protein has been found to be efficiently secreted to the medium by means of an ARS2 signal peptide that has previously been used to secrete a recombinant enzyme (Eichler-Stahlberg et al., 2009). No protein was detected in the cellular lysate in the ars-IF strain (Figure 2.8c). This suggests more efficient secretion of the ars-IF than what has been reported for secretion of a luciferase using the same ARS2 signal peptide (Eichler-Stahlberg et al., 2009). To date, only few studies on the secretion of recombinant proteins in microalgae are available. Most reports are from the green alga *C. reinhardtii* (Eichler-Stahlberg et al., 2009; Lauersen et al., 2013a, 2013b; Ramos-Martinez et al., 2017; Rasala et al., 2012), or the diatom *Phaeodactylum tricornutum* (Hempel and Maier, 2012; Vanier et al., 2015).

2.8.2. Posttranslational-modification of the secreted IF protein

Based on migration on SDS-PAGE gels, the secreted microalgal IF protein showed a consistently larger molecular size compared to the cytoplasmic protein (Figure 2.9, Figure 2.10, Figure 2.11b,c). There are several reasons that could explain this. One possibility is the failure to cleave the signal peptide. However, the ARS2 signal peptide only adds approximately 1.7 kDa to the mature protein which seems unlikely to cause the observed shift of around 5 to 10 kDa. A previous study has used an ARS1 signal peptide for secretion of a protein to the medium and observed a similar pattern. In this study, the signal peptide was not found with mass fingerprint analysis suggesting that the non-cleavage of the signal peptide was unlikely (Eichler-Stahlberg et al., 2009).

Another possibility that could explain the size difference is the post-translational modification of the IF protein. This is likely as the human IF protein contains an N-glycosylation site (Mathews et al., 2007) and is known to be highly glycosylated. When previously expressed in higher plants (Arabidopsis thaliana) glycosylation was observed and the protein detected had a similar size of 50 kDa to the algal expressed IF (Fedosov et al., 2003). The glycosylation of IF seems to be non-essential for B12

and receptor binding (Gordon et al., 1991), however, it may stabilize and protect the protein from degradation in the low pH and proteolytic conditions in the intestine. Not much is known about N-glycosylation in *Chlamydomonas* (Mathieu-Rivet et al., 2014, 2013; Ramos-Martinez et al., 2017) and efforts to characterize the secreted IF protein in more detail were prevented by low expression levels. Treatment of the protein with a commercial deglycosylation enzyme cocktail (Protein Deglycosylation Mix II, New England Biolabs, UK) was inconclusive and not sufficient amounts of pure protein were obtained for mass spectrometry (data not shown) from 1 L cultures (OD750nm between 0.6 and 0.8). Low expression levels of recombinant proteins are to date a common problem seen in *Chlamydomonas* (previous studies have reported 0.25% of total cellular protein (Barahimipour et al., 2016) or 0.25% of total soluble protein (Rasala et al., 2012) for example). This is likely due to various factors such as random insertion of the construct in the nuclear genome and efficient silencing mechanisms (Cerutti et al., 1997). Recent efforts to establish targeted DNA approaches (see (Cerutti et al., 1997; Jinkerson and Jonikas, 2015), for recent reviews) such as CRISPR/Cas9 technology (Greiner et al., 2017; Jiang et al., 2014) for nuclear transformation in *C. reinhardtii* could be promising tools to increase recombinant protein yields allowing for a more detailed characterization of the algae-produced IF protein.

2.8.3. Vitamin B_{12} enrichment in IF expressing *C. reinhardtii* strains

Eukaryotic microalgae do not produce B12 and more than half of microalgal species are thought to be B12 auxotrophs relying on B12 obtained from symbiotic relationships with bacteria (Croft et al., 2005; Helliwell et al., 2011). The model alga *C. reinhardtii* used in this study has been shown to be B12 independent as it contains METE (B12-independent methionine synthase gene). However, the alga also contains the B12-dependent B12 methionine synthase MetH which is preferably used in the presence of B12 (Croft et al., 2005).

No B12 was detected in any protein fractions concentrated from cultures grown without B12 supplementation (Table and pictures in Supplemental Information) which is expected as the algae were grown axenically. When supplementing the medium with B12, increased amounts of the IF protein were detected in both strains, IF and ars-IF (Figure 2.9 and Table 2.1). This indicates that the IF protein is stabilized due to B12 binding. IF is a known B12 binding protein and formation of the holo-IF form stabilizes the protein (Mathews et al., 2007). Binding of B12 to the cytoplasmic IF protein presumes the cellular uptake of B12 from the medium into the cell. B12 transport into the cell in *Chlamydomonas* is existent, evident by their ability to utilize B12 (Croft et al., 2005; Fumio Watanabe et al., 1991) but molecular mechanisms of B12 uptake in microalgae have hardly been described (Bertrand et al., 2012). The

semi-quantitative B12 assay shows a significant difference of the total B12 amount accumulated in the IF strain lysates compared to a negative control strain (Figure 2.10a). However, this observation was not supported by the individual elution fractions. If the increased amount of B12 found in the IF lysates was directly due to binding to the IF protein, one would expect to see a significant difference in the elutions containing the majority of the IF protein (100 mM, 150 mM NaCl, Figure 2.10). However, no significant differences of any of the elution fractions were found for the IF and CC-849 control strain. Consequently, it is possible that the expression of IF in the algae does lead to an enrichment of intracellular vitamin B12, but further work is needed to support this hypothesis.

With the ars-IF strain, the IF protein was purified from the medium where the background from other co-purified proteins is significantly lower than in the cellular lysates. Here, the fractions that contain the highest amount of IF protein show a significantly higher B12 content when compared with the control strain CC-849 (Figure 2.10b).

In the flow-through and the wash fractions (Figure 2.10b), no significant differences between the ars-IF and the control strain is seen. This is likely to be due to the unbound B12 washing off and the B12 detected in subsequent elution fractions most likely being bound to protein. However, the B12 bioassay used in this study does not allow distinguishing between protein bound B12 and free B12. Therefore, it is impossible to conclude if the B12 was bound to the secreted IF protein.

In the case of the cytoplasmic IF protein, there is a statistically significant difference between B12 concentrations measured in cellular lysates expressing IF and the control strain (Figure 2.10a). However, there was no significant difference observed in the elution fractions. One reason for this might be that the assay does not distinguish between B12 bound to the IF protein or other cellular proteins. Other enzymes already known to be associated with intracellular B12 metabolism in algae will most likely interact with internalized B12 (Helliwell et al., 2011). This could explain the high background found in the protein elutions from both cellular lysates, CC-849 and IF strain (Figure 2.10a). Additionally, a relative decrease of cytoplasmic IF was observed from cultures supplemented with 50 μg•L–1 B12 to cultures supplemented with 100 μg•L–1 B12 (Figure 2.8b and Table 2.1). Although one can only hypothesize, this decrease could be due to concentration-dependent toxicity of the protein and therewith associated cellular regulatory processes. Additionally, due to the random insertion of the expression cassette in the nuclear genome, there is the possibility that other cellular functions may be affected.

2.8.4. Intrinsic Factor for Developing B_{12}-Enriched Microalgae

In this study IF was expressed in the eukaryotic microalgae *Chlamydomonas* exploring the potential of enriching bioavailable B12 using a microalgal host. One proposes that this model alga could be a good chassis for future production of microalgal functional foods and dietary B12 containing supplements. For example, recently it has been shown that cyanobacteria produce a different chemical variant of B12 (Helliwell et al., 2016). This chemical variant of B12 (also known as pseudocobalamin) binds with a much lower affinity to B12 receptor proteins such as IF making it less bioavailable for humans (Helliwell et al., 2016). Eukaryotic microalgae, on the other way, utilize the same B12 variants as humans, therefore, making them a better source of B12 supplementation.

As shown recently for *Chlorella* supplements (Bito et al., 2016), currently available eukaryotic microalgal supplements can contain varying amounts of B12. This is most likely due to different cultivation conditions altering the composition of the associated bacterial biofilms that are the original source of B12 found in the supplements. In this respect, the establishment of closed, standardized growth systems, as previously shown for *Chlamydomonas* (Gimpel et al., 2015; Zedler et al., 2016), allows for much more control over contamination compared to open systems and hereby also of the B12 content in the final product. In addition, efforts to engineer microalgal communities (Gangl et al., 2015a; Kazamia et al., 2014) with symbiotic relationships, as found between *Mesorhizobium loti* and *Lobomonas rostrata* (Helliwell et al., 2018; Kazamia et al., 2012), could allow for a more controlled interaction, and thus flux of B12, of the microalga and associated bacteria. Finally, looking at the current market, IF, of animal (porcine) origin, is commercially available in some B12 supplements. This proof-of-concept study shows that microalgae are a potential vegetarian-friendly alternative to IF-B12 co-formulation in functional foods and dietary supplements.

2.9. Conclusions

The human glycoprotein Intrinsic Factor can be expressed in *Chlamydomonas reinhardtii* from the nuclear genome. The addition of an *ARS2* signal peptide leads to efficient secretion to the medium. Our data suggest that the secreted IF protein directly binds B_{12}, however, it is less clear if the cytoplasmic IF binds the cofactor or has an indirect effect on B_{12} enrichment in the IF strain. Our data also show a correlation of higher protein levels with higher B_{12} concentrations suggesting a potential stabilizing effect on the protein. This study is a first proof-of-concept utilizing a human B_{12} binding protein as a tool for enriching B_{12} in microalgae and can contribute to the future development of microalgal functional foods.

2.10. Perspectives and applications

In order to make algae cultivation profitable, some advances need to be achieved regarding productivity of biomass and of valuable products such as lipids and other high-value biomolecules. Genetic engineering could be useful for overcoming limitations associated with production of these significant compounds (Ng et al., 2017). Thus, it has an important role for the future development of microalgal industry. Furthermore, new and powerful tools are now available for genetic manipulation of algae, such as the sequencing of several algae genomes. These conditions allowed in the past and will allow in the future to achieve important results in the field of microalgal genetic engineering, making some applications very impressive and promising. The other side of the coin is, however, that there is still a clear gap between the potential shown in proof-of-concept studies and the transition to an industrial scale. In particular, species like *Chlamydomonas* are very sensitive to several stresses, such as temperature and shear stress, so they are not ideal strains for industrial cultivation. Another issue of genetic engineering is the actual impossibility of coordinate the expression of more than one gene, making impossible to introduce, for example, a new pathway in a host. This application will be achievable in the future in the context of an approach referable as synthetic biology or metabolic engineering. Furthermore, the employment of genetic modified (GM) organisms in nutrition generates several problems about public concerns, although the consumption of GM food has been declared safe by more than 100 Nobel prize winners (Ng et al., 2017). Issues are linked also to the possible escape and spread of GM, which remains a possible problem. Furthermore, the huge genetic unexplored diversity in the microalgae category may indicate that genetic manipulation is premature and not necessary. Although genetic manipulation will lead to big achievements in microalgae industry in the future, what is needed now are strategies to improve the economy of microalgae cultivation. Two possible ways, explored in next sections, are the exploitation of photosynthesis in order to force the production of high-value compounds or the utilisation of indigenous strains, selected by centuries of natural selection, for obtaining biomass using as substrate wastewaters.

Section 3: Strategies for enhancing growth and accumulating high-value compounds: the role of flashing light

Part of the content of this section was published or submitted for publication as:

- S. Lima, F. Grisafi, F. Scargiali, G. Caputo, A. Brucato, Growing Microalgae in a "Quasi-isoactinic" Photobioreactor, in: Chem. Eng. Trans., 2018: pp. 673–678. doi:10.3303/CET1864113.
- S. Lima, P. S. C. Schulze, L. M. Schüler, R. Rautenberger, D. Morales-Sánchez, T. F. Santos, H. Pereira, J. C. S. Varela, F. Scargiali, R.H. Wijffels and K. Viswanath. Induction of proteins, polyunsaturated fatty acids and pigments in three microalgae using flashing light. Submitted for publication to *Scientific Reports*.
- D. Morales-Sánchez, L. Jep, S. Lima, P. S. C. Schulze, R.H. Wijffels, and K.Viswanath. Gene expression of *Nannochloropsis gaditana* under different flashing light. Under preparation.
- S. Lima, V. Villanova, F. Grisafi, A. Brucato, F. Scargiali. Combined effect of nutrient and flashing light frequency for a biochemical composition shift in *Nannochloropsis gaditana* grown in a "quasi-isoactinic" reactor. Submitted for publication to *Canadian Journal of Chemical Engineering*.

3.1. Flashing mechanism and definition

Flashing light (FL) consists in providing illumination by dense packs of high-intensity light spaced with relatively short dark periods as a difference from continuous light (CL). It is, in practice, the repetition of light (t_l) and dark (t_d) periods with an approximately rectangular waveform, as shown in Figure 3.1. The sum of one light and one dark period is defined as the flashing cycle (t_c) (Figure 3.1). How often a flashing cycle repeats per second (s^{-1}) is indicated by the flashing light frequency (f). For example, a frequency of 50 Hz means that light and dark periods are repeated 50 times per second. The ratio between the light and the flashing cycle (t_l / t_c) is defined as the *duty cycle* (DC). For example, a duty cycle of 0.05 indicates that the light is on for only 5% of the whole flashing cycle, while 95% of the time the light is turned off. The averaged light intensity (I_a) provided under flashing illumination is the average obtained during one flashing cycle, which is composed by an instantaneous light intensity I_l emitted during the light flash period (t_l) and no light emission (I_d= 0 µmol s^{-1} $m^{)2}$) during the dark phase t_d. For example, an averaged light intensity of I_a= 300 µmol s^{-1} m^{-2} with a duty cycle of 0.05, implies an instantaneous light intensity of I_l=6000 µmol s^{-1} m^{-2}. When comparing continuous and flashing light, the same averaged light intensity is always used in the present study.

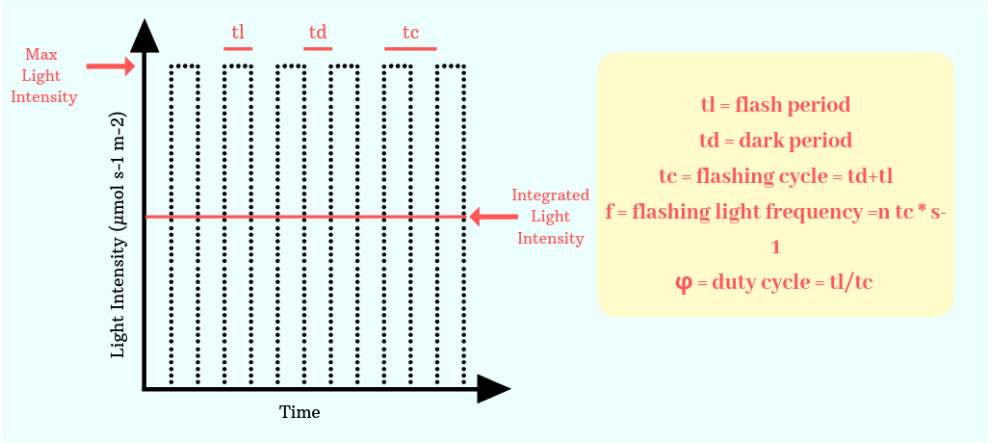

Figure 3.1: Flashing light is the repetition of dark (t_d) and flash (t_l) periods in an approximative rectangular waveform. A flash cycle (tc) is formed by the sum of dark and flash periods and the number of flash cycles per second is the frequency (f) of the flashing light. The enlightened portion of the flashing cycle is the duty cycle (DC).

3.2. State of the art

As it is well known, in the last decades microalgae gained a great interest because of their potential in various biotechnological applications. Besides the importance that they could achieve in industry, current industrial scaled phototrophic microalgal cultivations face low biomass productivities, deriving from inefficient light utilization by cells inside the culture (Ruiz et al., 2016). Strategies to increase their productivity have been therefore addressed by several researches.

In order to optimize a strategy to increase biomass productivity, the lighting of microalgal cultures was firstly analysed. In fact, assuming that nutrients inside a PBR are abundant, the most limiting factor for growing microalgae is light availability; in nature sunlight provides energy supporting the metabolism and the increase in biomass (Simionato et al., 2013a). Microalgae in culture are subject to self-shading effects (Hubble and Harper, 2001), especially when their concentration increases and light cannot reach homogeneously the cells. The distribution of light inside microalgae cultures is in practice typically highly variable (Zou and Richmond, 2000), which makes it difficult to assess the actual effects of illumination features on a culture. In addition, it is to bear in mind that all the photosynthetic cells are prone to light inhibition effects if light intensity is larger than that they can actually use for photosynthesis (Richmond and Hu, 2013). In such cases, excess light triggers acclimation responses (e.g. chloroplast movement or non-photochemical quenching

NPQ). These mechanisms avoid the damages caused by excess light (Li et al., 2009) but at the same time, they waste energy.

Another point to take in to consideration is the light source. A part of sun light, it can also be artificial and can be used for the photoautotrophic production of microalgal biomass (Blanken et al., 2013). Large scale production facilities use sunlight as the cheapest light source, and the systems are therefore commonly located in places with high annual solar irradiances (e.g., countries near the equator). On the other hand, there are places, for example microalgae production facilities at high latitudes, that rely on expensive artificial light due to insufficient year-round natural irradiance (Baliga and Powers, 2010; Kim and Choi, 2014). High costs of these production systems are connected with artificial lighting, as a result of electric energy consumption and replacement of lamps (Blanken et al., 2013).

To cut costs and improve biomass and biocompound productivities of microalgal cultures, light emitting diodes (LEDs) can be conveniently employed to emit flashing or pulsed light. Their use may allow avoiding the effect of excess light (Schulze et al., 2017b) so enhancing the photosynthetic apparatus efficiency. What exactly happens is that chlorophyll enters in an excited state and can transfer the energy to other chlorophyll molecules in photosystems I or II (PSI or PSII), turning them in a closed state. If the reaction centres are closed, they are not able to process further energy and they need some time to get back to their original state (Varela et al., 2015). For this reason, in order to make microalgae capable of using all the supplied light and to minimise the waste of energy employed for repairing themselves from excess light, a possibility is to adjust the flashing cycle by suitably tailoring the lighting time with respect to the dark time. In this way photosynthetic cells may not need to protect themselves from excess light making them able to use most of the energy they receive to increase their biomass. In particular, reducing the flash time in comparison with the dark time and increasing the frequency might well be a successful strategy according to some authors (Schulze et al., 2017b).

Flashing light was also claimed in the past to increase photon penetration-depth into a cell-dense culture because of the higher instantaneous light intensity employed, as described by the Beer–Lambert law (Lee, 1999). Nowadays however researchers attention has significantly shifted towards studying whether flashing illumination may affect the accumulation of biomolecules.

Flashing light can in fact be tailored to improve production of microalgal biomass and accumulation of target biocompounds (De Mooij et al., 2016; Glemser et al., 2016; Phillips and Myers, 1954; Schulze et al., 2017b). Although flashing light irradiation has not always been found to improve microalgal growth over continuous

light irradiation (Vejrazka et al., 2012; Yoshioka et al., 2012), the use of flashing light has the potential to promote the induction of target biomolecules such as pigments (Katsuda et al., 2008; Kim and Choi, 2014; Kim et al., 2006). In Figure 3.2 an example of flashing light application is shown. The effects of high intensity continuous light on triggering the production of certain biomolecules might be triggered by flashing light as well, while spending less energy. It has become clear, however that microalgae respond differently to flashing light, and hence change their protein, carbohydrate, lipid or pigment contents (Park and Lee, 2000; Schulze et al., 2017b; Sforza et al., 2012). Such dissimilarities may be due to different strain-specific genetics, culture systems, unique biotic and abiotic growth conditions, or the analytical and data processing procedures employed in different studies (Moody et al., 2014). In addition, the prevailing culture growth stage at the time of harvesting is a major cause of intracellular changes of the biochemical profile in any microalga (Rebolloso Fuentes, 2000; Su et al., 2013).

The differential composition of microalgae grown under flashing light must depend on a specific molecular regulation able to result in a different production of biomolecules. Molecular techniques in microalgal field gained a growing importance in the last years and several advances have been achieved as reported by some authors (Fu et al., 2019). For instance, *N. gaditana* genome has been assembled and transcriptomic profiles were recorded for nitrogen depletion (Corteggiani Carpinelli et al., 2014). Furthermore, a genome-scale metabolic model was also proposed (Shah et al., 2017).

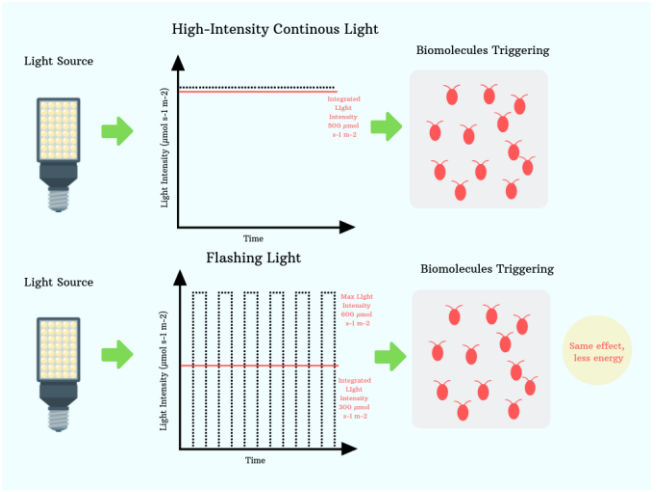

Figure 3.2: An example of application of flashing light in industry. The effect of light stress caused by high-intensity light could be reached by employing flashing light, with a smaller average light intensity and a saving of energy.

Another point to take into consideration is the "temporal dilution of light" that flashing lighting could provide. In fact, according to Tredici (Tredici and Zittelli, 1998), one of the main problems of algal outdoor cultivations is the saturation effect caused by natural sunlight. This could be overcome by diluting light, in a temporal or in a spatial way. In this section we are going to address the first method, consisting in providing light in packages intercut with dark periods, while in Section 5 the spatial dilution of light will be investigated.

In the followings the work done on the study of microalgae illumination by flashing lights is summarised. In the first part, it is proposed to use a flat-bed PBR lit by LED panels on both sides in order to make light distribution more homogenous, so allowing a reliable evaluation of illumination features on algal growth. Starting from previous studies, (Brucato et al., 2007) in which a "quasi-isoactinic" reactor was proposed in the realm of heterogeneous photocatalytic processes, a "quasi-isoactinic" photobioreactor was built. In it, there is an almost homogenous distribution of light so that the local volumetric rate of photon absorption (LVRPA), can be considered uniform to a good extent. An inexpensive set up for accurately controlling the light quality and quantity and setting-up flashing light illumination was also devised.

Successively, the "quasi isoactinic" reactor was employed to grow *N. gaditana* while using flashing light, with the aim of studying its effects on the *specific growth rate* μ, biochemical profile, carotenoids accumulation. The aim was to test two different growth media with different concentrations of nitrate and phosphate and to assess which was the best one to enhance growth. In this part of the work, DC was set at 0.25 and the effect of frequency was assessed (f= 25, 250, 2500 Hz). The average light intensity analysed was 70 μmol m^{-2} s^{-1}.

In the following part of this section the application of flashing light was extended to higher light intensities and to other two species of microalgae. In particular, the work was focused on the effect of flashing light on growth as well as protein, carbohydrate, lipid, fatty acid and pigment contents of the Eustigmatophyte *Nannochloropsis gaditana*, and the Chlorophytes *Koliella antarctica* and *Tetraselmis chui*. Because flashing light conditions able to effectively induce biocompounds often inhibit microalgal growth (Schulze et al., 2017b), a two stage cultivation approach was also employed. In the first stage, enough algal biomass was produced under growth-stimulating light conditions, while the second stage triggered biocompound induction using flashing light. The DC was set at 0.05 and the frequencies analysed were 5, 50 and 500 Hz, while the average light intensity was 300 μmol m^{-2} s^{-1}.

The work continued with the analysis of the molecular response of one of the strains, *N. gaditana*, to the same flashing light conditions of the previous experiment. Also photosynthesis efficiency of the algae grown under these conditions was assessed. The transcriptomic expression of key genes of metabolic pathways leading to the production of high-value biomolecules, such as carotenoids, chlorophyll, lipids, in particular the unsaturated ones, was analysed. The adopted technique allowed to analyze the transcript levels of target genes in a not axenic culture.

PART 1: EXPERIMENTS CARRIED OUT AT PALERMO UNIVERSITY

3.3. "Quasi-isoactinic" reactor: structure and theory

3.3.1. "Quasi-isoactinic" reactor set up

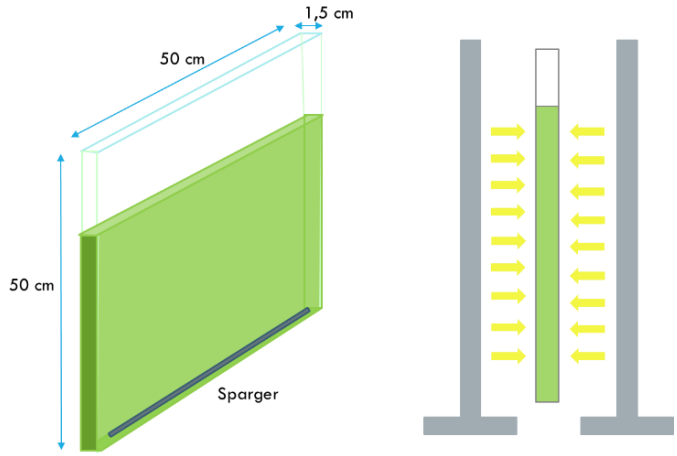

Figure 3.3: Sketch of the "quasi-isoactinic" photobioreactor: a) flat panel reactor irradiated on both sides by LED panels emitting controlled light. b) the glass flat panel has length and height of 50 cm, a width of 1,5 cm and a linear gas sparger is fitted on its bottom.

Figure 3.4: Picture of "quasi-isoactinic" reactor set up. LED panels are positioned at a certain distance from the reactor in order to provide a homogeneous light distribution on reactor's walls.

The reactor is a glass thin-slab (Figure 3.3 and 3.4, 2.5 litres maximum volume) with an internal thickness of 1.5 cm; slab thickness is therefore quite smaller in comparison with the other two dimensions, both equal to 50 cm.

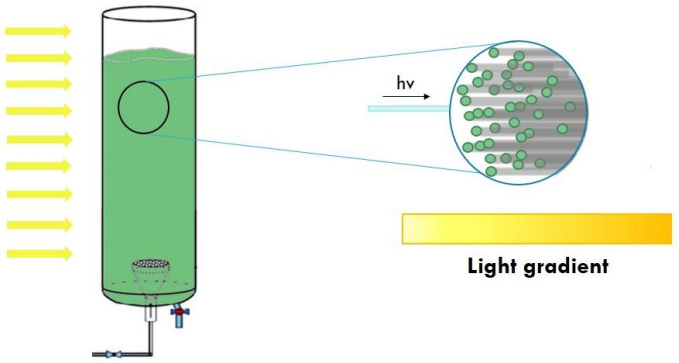

Figure 3.5: Self-shading effect caused by the absorption of part of the light addressed to a culture by the superficial layer of cells. This creates shadows that do not allow an uniformal light distribution inside the culture.

In Figure 3.5, a very common effect observed in microalgae cultivations is shown. It is called Self-shading effect and is caused by the fact that each cell absorbs light and in this way creates a shadows for the cells beside it. This causes the presence light gradients inside the reactor that make light distribution not uniform inside it. Considering that in all microalgal cultivations the biomass concentration and the light penetration are in conflict simply because the self-shading effect, we employed a small thickness PBRs in order to extend the light penetration for the entire depth of the reactor. In fact, as suggested by other studies (Bertucco et al., 2015; Lunka and Bayless, 2013) in small thickness PBRs the light is able to reach all the cells in a quasi uniform way, provided that cells concentration is small enough.

The two-sided LED irradiation of the present photobioreactor allows to extend the quasi-uniform irradiation condition to higher cells concentrations. A picture of the photobioreactor here employed is reported in Figure 3.4. During all experimental runs, the reactor was located in a container darkened by a thick black cloth. Taking into account the light attenuation by irradiating the photobioreactor from one side only, the irradiation from both sides makes a superposition of the effects such as to create a quasi-homogeneous irradiation inside the photobioreactor. As a matter of fact, according to the simplified "zero reflectance" irradiation model (Brucato and Rizzuti, 1997) the irradiation distribution inside a dispersion containing purely absorbing particles (non scattering) can be simply expressed as:

$$\boldsymbol{G = G_0 e^{-x/L_E}} \qquad \text{3-I}$$

$$\boldsymbol{L_E = \frac{1}{n_p a_p}} \qquad \text{3-II}$$

Where G_0 is the inlet irradiation intensity, n_p is the number of particles per unit suspension volume, a_p the capture cross section and L_E the characteristic extinction lenght. This is shown in Figure 3.6 for the particular case in which the ratio between reactor thickness L_r and the characteristic extinction length L_E equals the value of 0.693. In such a case the radiation traveling in one direction is exactly halved within the reactor before exhiting from the back side. As a consequence, the total radiation absorbed inside the photobioreactor exactly equals the radiation that would have been adsorbed had reactor been illuminated from one side only and its optical density were such that light radiation was completely extinguished within the reactor. Notably, with the two-sided irradiation the same amount of light is absorbed (and consequently the same biomass production achieved) in conjunction with a quite small maximum deviation from uniformity of only 5.7%. It is worth noting that had scattering been taken into account, even smaller deviations from uniformity would have been predicted, with respect to the limiting "zero reflectance" case here reported. At the bottom of the photobioreactor, filtered air (0.22 µm) is injected inside the reactor by a gas sparger which also assures the mixing of the culture. The LED panels are hand-made panels obtained by means of two 50 mm aluminium slabs where RGB LED strips (KWB 5m 5050 RGB IP44), 7.5 m long, are applied. The strips were disposed as shown in Figure 3.7 and the installation process is shown in Figure 3.8. The distance amongst the central 6 strips is 5 cm and that of the side strips 4 (on the two sides) is of 3.5 cm.

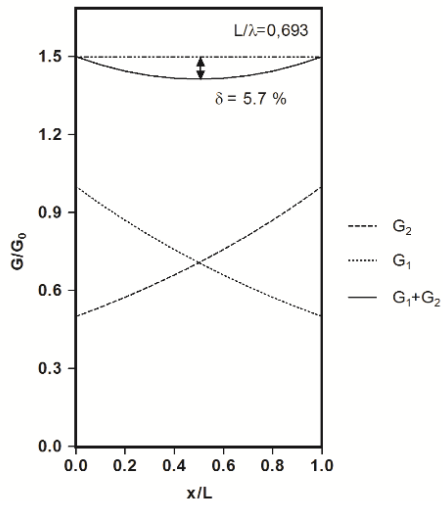

Figure 3.6: Diagram showing the "quasi isoactinic" light distribution set up. The total irradiation, here indicated with G1+G2, is given by the superposition of the irradiations coming from the two panels at the sides of the reactor (G_1 and G_2). This effect produces a fairly homogeneous distribution of light intensity inside the reactor.

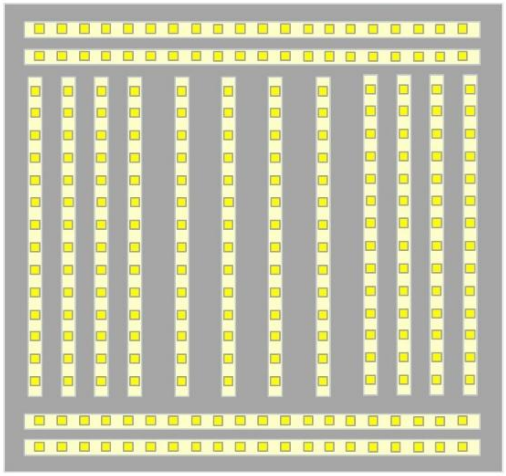

Figure 3.7: Scheme of the LED panel. Distance amongst the central 6 strips is of 5 cm and the one of the lateral 4 is of 3.5. This is done in order to provide an equal light distribution on the central part of the reactor compared to the lateral parts.

Figure 3.8: Installation process of RGB LED strips (KWB 5m 5050 RGB IP44) on aluminium panel in order to make LED panel.

This difference has been inserted in order to reinforce the light distribution on the sides of the reactor to compensate for the lack of further strips and improve homogeneity with respect to the central part. The light distribution was measured on the surface of the reactor in 9 equally-spaced points by means of a Delta Ohm-HD 9021 equipped with photosynthetic active radiation (PAR) probe (Delta Ohm LP 9021 PAR). The light intensity difference between any two points of the reactor was found to differ by a maximum of 10% of the mean value. An Arduino system was employed to control the LED panels in order to regulate (i) light intensity, (ii) wavelength (λ) and (iii) light-dark cycles.

3.3.2. Set-up of an Arduino system for driving LED strips

In order to provide a low cost system to handle light intensity and flashing cycles, an Arduino Uno© was suitably programmed. With the employed program, light intensity could be separately controlled for each of the three components of the RGB LED. This was obtained by the Printed Circuit Board (PCB) depicted in Figure 3.9, made according to the electrical diagram shown in Figure 3.10. Three mosfets 33N10 (Q1, Q2, Q3) were tinplated on the shield together with six resistors, three small LEDs, cables for the power supply (+ and -), cables for the control of the LED panels (out) and cables coming from Arduino. A homemade LED shield showed in Figure 3.11

was in this way obtained. In Figure 3.12 the final system supplied with a power pack is shown.

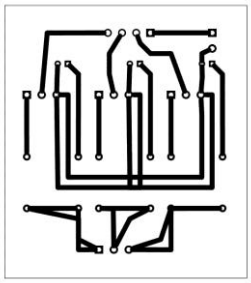

Figure 3.9: Printed Circuit Board (PCB) obtained from the Elecrical diagram and printed on the vetronite slab in order to obtain a circuit.

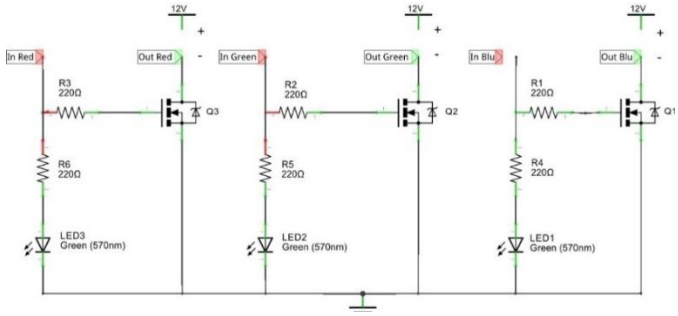

Figure 3.10: Electrical diagram used as model for the PCB. It represents the power source going to the LEDs (12V), three mosfets (Q1, Q2 and Q3), six resistors (R 1 to R6) and three Green LEDs (LED 1 to LED 3). For each component of the RGB LED, there is an in tension (5V) coming from Arduino and an out tension going to the LEDs.

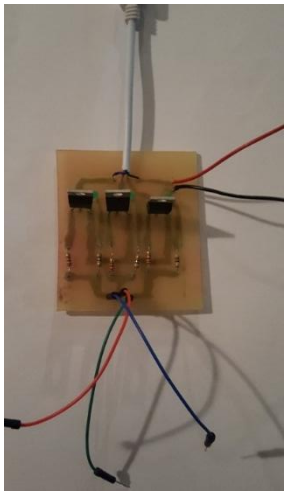

Figure 3.11: Homemade LED shield able to control the LED panels.

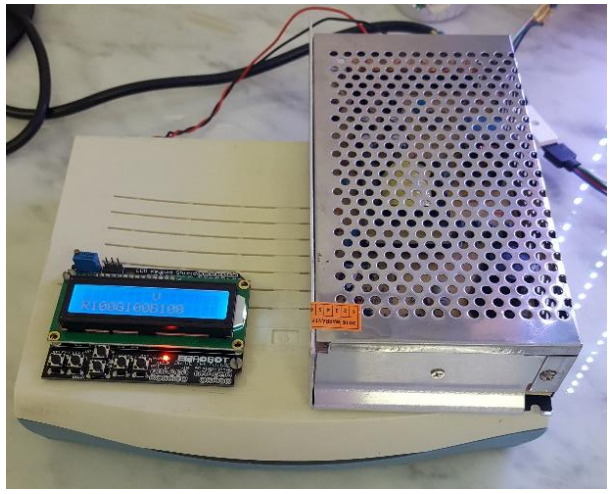

Figure 3.12: Final system supplied with an Arduino, the LED shield (inside the box), a led display with controller and a power pack.

3.4. Experiment in the "quasi-isoactinic" reactor: combined role of nutrient richness and flashing light

3.4.1. Materials and Methods

3.4.1.1. Algal growth

The cultures of *Nannochloropsis gaditana* (CCAP 849/5 Scottish Association for Marine Science, Oban, Scotland), Eustigmatophyceae, were maintained in liquid cultures inside Erlenmeyer flasks with F-medium (Guillard, 1975). For the experiments, two different versions of the same medium were employed: the first one is called "basic medium" and consists of artificial sea water (6.3 mM KCl, 2.0 mM $NaHCO_3$, 7.1 mM KBr, 0.36 mM H_3BO_3, 0.024 M Na_2SO_4, 9 mM $CaCl_2$ $2H_2O$, 0.046 M $MgCl_2$ $6H_2O$, 0.35 M NaCl) supplemented with a modified F- medium (3.5 mM $NaNO_3$, 0.036 mM NaH_2PO_4, 0,12 µM $FeCl_3$ $6H_2O$, 0,12 µM Na_2EDTA, 0.04 µM $CuSO_4$ $5H_2O$, 0.076 µM $ZnSO_4$ $7H_2O$, 0.042 µM $CoCl_2$ $6H_2O$, 0,91 µM $MnCl_2$ $4H_2O$, 0.025 µM Na_2MoO_4 $2H_2O$); the second one is called "enriched medium" and has the same composition as the first one but is supplemented with ten times more $NaNO_3$, and NaH_2PO_4 (35 mM and 0.36 mM, respectively).

A pre-culture was set up by inoculating 10 ml of a back-up culture in 100 ml of the same liquid medium used for the main experiment. When the cells were in late lag phase (around 10 days from culture start), they were used to inoculate the "Quasi-isoactinic" reactor in order to reach an initial concentration of approximately 0.1 AU (λ=750 nm) (Lima et al., 2018).

The cultures inside the reactor were mixed by supplying microfiltered air (0.22 µm) passing through a sparger with micro-holes. When the pH was above 8.0, pure CO_2 was supplied through the same sparger until it reached the value of 7.0. Each experiment was carried out for 13 days. The concentration of the microalgal suspension was checked daily by manually counting the cells in a Burker chamber. The suspension was diluted in order to have between 100 and 200 cells per square. The number was then multiplied by the dilution factor and by a multiplier (10^4) in order to obtain the concentration in cell/ml. Measurements were done in triplicate (n=3) and the average value was retained and reported together with the standard deviation.

3.4.1.2. Light conditions

Three different conditions of flashing light with different frequencies were employed in this work: 25, 250 and 2500 Hz with the same duty cycle (DC) of 0.25. The average light intensity is the same amongst the three conditions and the continuous light

control and correspond to 70 μmol m^{-2} s^{-1}. The maximum light intensity in the three flashing light condition is the same and equal to 280 μmol m^{-2} s^{-1}. The light distribution was measured on the surface of the reactor in 9 equally-spaced points by means of a Delta Ohm-HD 9021 equipped with photosynthetic active radiation (PAR) probe (Delta Ohm LP 9021 PAR).

3.4.1.3. Determination of specific growth rate μ

In order to estimate the specific growth rate (μ), the cell concentration was plotted on a semi-log diagram vs the time of cultivation in days. Then, the point of exponential growth were selected and their slope was assessed. This value returns the amount of increase as viable cells/ml per day.

3.4.1.4. Sample preparation

After 13 days from the cultivation start the cell suspension was centrifuged and the obtained biomass was frozen in liquid nitrogen and freeze-dried for 48 h in a bench lyophilizator (FreeZone 2.5L, LABCONCO, US). The biomass was then stored at -20°C for further analysis.

3.4.1.5. FTIR analysis

Samples of biomass were analyzed by Fourier Transform Infrared Spectroscopy (FTIR) in order to assess the approximate biochemical composition. The method was adapted from Stehfest et al. (Stehfest et al., 2005). About 2 mg of freeze-dried biomass were weighted and transferred in a mortar together with 100 mg of Potassium bromide (KBr) to prepare glassy sample discs. Then the mixture was vigorously crushed and a pellet was made by a hydraulic press (CrushIR, PIKE Technologies, US). Pictures of the kit for making the pellet (Evacuable Pellet Press, PIKE Technologies) and ready pellets are shown in Figure 3.13 and Figure 3.14. The pellet was then scanned in a Cary 630 Spectrometer (Agilent Technologies, US). This technique correlates one or more peaks to the corresponding biochemical macromolecule, thanks to the vibrational frequency of the related functional group. By integrating the area under the curve, a semi-quantitative analysis of the macromolecule is obtained. Here we examine the ratios between different areas in order to make different samples comparable. In Table 3.1 the employed wavelengths to integrate different peaks are shown.

Table 3.1: Reference wavelengths for peaks integration connected to macromolecules by the vibrational frequency of the related functional group.

Wavelenght (cm^{-1})	Assignment	Macromolecule
2799-300	CH of saturated CH	Lipids
1584-1725	Amide I C=O of amides from proteins	Protein
1490-1584	Amide II N-H of amides from proteins	Protein
950-1200	C–O–C of saccharides	Carbohydrates

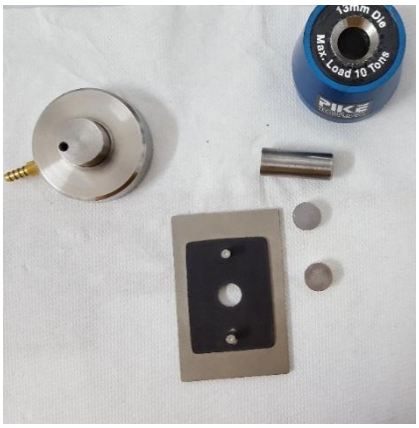

Figure 3.13: PIKE Technologies Evacuable Pellet Press employed for making pellets for FTIR analysis.

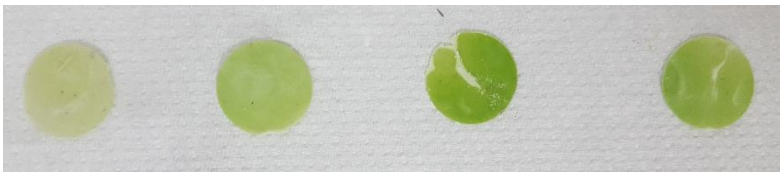

Figure 3.14: Pellets of microalgae biomass ready to be analysed by FTIR spectroscopy.

3.4.1.6. Extraction of lipids and analysis of Fatty Acids

The extraction of lipids was made by crushing 20 mg of dry microalgae biomass in a mortar with 5 ml of chloroform/methanol (2:1, v/v) and 1 ml of NaCl 1%. The mixture was vortexed until the formation of two phases. The lower phase (chloroform phase) was transferred in a pre-weighted tube and the solvent was evaporated under a nitrogen stream. After complete evaporation of the solvent, the total lipids were determined gravimetrically. Then they were transesterificated by adding 1 ml of sodium metoxide (1 g NaOH in 100 ml MeOH) and 1 ml of hexane. The upper phase (hexane phase) was then and analyzed by gas chromatographic analysis using a GC 7890B System (Sigma-Aldrich, US) supplied with a FID detector and a capillary column Omegawax 250 (Sigma-Aldrich, US). Initial temperature was 50 °C, increased to 220°C as working temperature. Total analytic time was 79.5 minutes and argon was used as eluent gas. The quantification of lipid were done comparing samples chromatograms with the standard. *Supelco 37-Component FAME Mix* (Sigma-Aldrich, US) was used as standard.

3.4.1.7. Spectrometric Pigment Analysis

For the chlorophyll and total carotenoid extraction, biomass was disrupted in methanol by crushing in a mortar approximately 20 mg of biomass. The methanol extract was separated from the algae pallet via centrifugation and spectrophotometrically analysed (Cary 630 Uv/Vis spectrophotometer, Agilent) against a methanol blank. All analyses were done under dimmed light. Chlorophyll *a* (C_a) and and total carotenoids (C_{carot}) were determined according to Lichtenthaler and Wellburn (Lichtenthaler and Wellburn, 1983) and Henriques et al. (Henriques et al., 2007) by applying the OD measurements at 666 and 470 nm (A_{666}, A_{470}) from the methanol extracts to equations 3-III and 3-IV:

$$\mathbf{C_a = 15.65\ A_{666}} \qquad \text{3-III}$$

$$\mathbf{C_{carot} = (1000\ A_{470} - 44.76\ A_{666})/221} \qquad \text{3-IV}$$

3.4.1.8. Data analysis

Data from three different experiments were tested for statistical significance of the variations in different strains and treatment. Two-way ANOVA analysis was performed to detect statistical differences among the parameters *treatments* and *strains*. The output F-values together with p-values were used to describe the impact of treatment on the variables. Bonferroni´s correlation (p value) was used to quantify the variability between control and treatments. Data were considered significant for p-values smaller than 0.1. Results are shown as means and

standard deviations and are reported as error bars. All the details about statistical analysis are reported in Supplemental Information.

3.4.2. Results and discussion

3.4.2.1. Growth performance

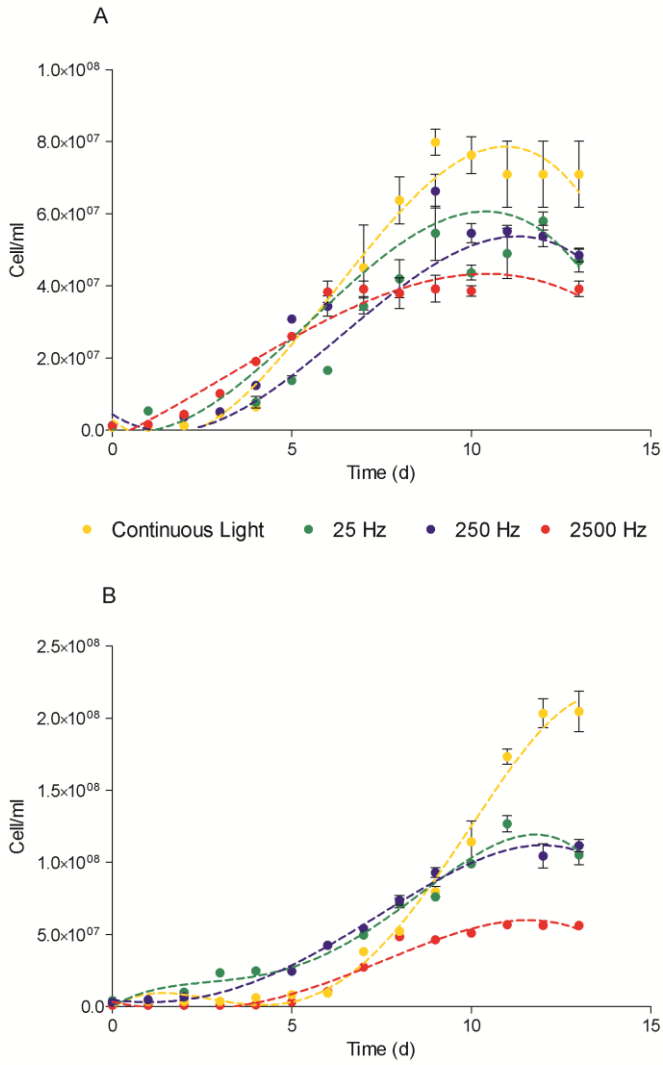

Figure 3.15: Growing curves of *Nannochloropsis gaditana* grown in basic (A) and enriched (B) medium. Three flashing light conditions (25, 250 and 2500 Hz, referred as FL 25, 250 and 2500) are shown in green, blue and red, together with a control of continuous light in yellow. Values are shown as means (n=3) and error bars report the standard deviation.

Figure 3.15 shows the growing curves of *N gaditana* cultivated in two different media, a basic version (Figure 3.15A) and an enriched version with nitrate and phosphate (Figure 3.15B), under the three studied flashing light conditions of 25, 250 and 2500 Hz (FL 25, 250 and 2500) and a control of continuous light (CL). Algal cells grew more in the enriched medium than in the basic one; in fact, the maximum concentration in the enriched medium was 2,05E+08 ± 2,42E+07 cell/ml of the CL control, versus the concentration of 7,09E+07 ±1,59E+07 cell/ml of the CL control in the basic medium. The reached cell concentrations are coherent with other studies in literature (Rocha et al., 2003; Simionato et al., 2013b). Also all the other light conditions showed a stronger growth in the enriched medium than in the basic one, and this is easily explanable by the higher concentration of nutrients. In both the growth media, cells grown under the CL control grew better than in all other conditions. As observed in Figure 3.15 A and B, the growth performance got worse when moving to higher frequencies. In fact, the highest concentration occurred under FL 25 is 4,70E+07±5,57E+06 and 1,05E+08 ±1,17E+07 cells/ml, respectively in basic and enriched media. Under FL 250, the reached concentrations are 4,85E+07±3,23E+06 and 1,12E+08±7,51E+06 cells/ml and under FL 2500 3,92E+07±3,69E+06 and 5,63E+07±2,08E+06 cells/ml respectively in basic and enriched media. Details about microalgae concentration are reported in Supplemental Information. It is worth noting that the low and medium frequency flashing light conditions (25 and 250 Hz) had a similar growth performance in both the media. Growth performance was also measured by assessing the *specific growth rate μ;* its measure is reported in Figure 3.16. In both the media, the *specific growth rate μ*, in day^{-1}, was lower in the flashing light conditions compared to the continuous light control and it progressively increased with the increase of the flashing frequency and reached under FL 2500 a comparable value than in the continuous light control in the basic medium, and a higher value than the control in the enriched medium. The specific growth rate is a measurement of reproduction speed during the exponential phase; thus it means that cells under 25 and 250 FL were slower than the control and in the same time they reached a lower final cell concentration. In the third FL condition, 2500 Hz, cells had the same (or higher, in the enriched medium) rate in reproducing during the exponential phase but they reached the smallest final concentration compared to all the other conditions.

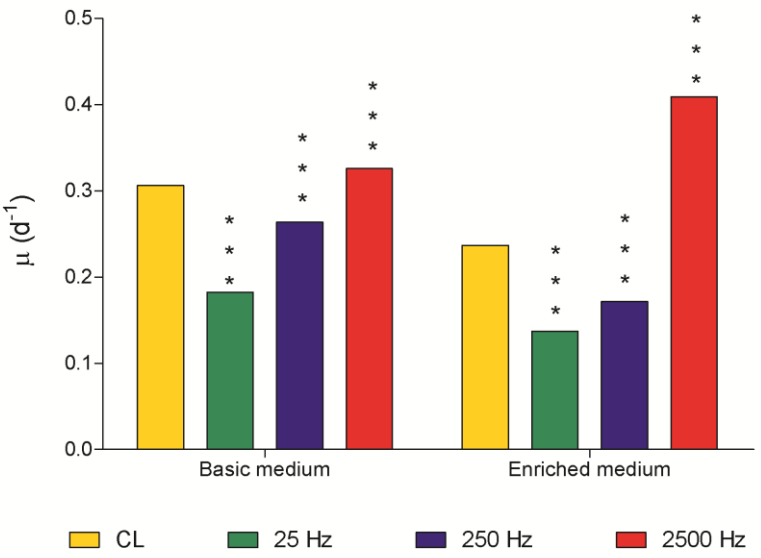

Figure 3.16: Specific growth rate μ of *N. gaditana* grown in basic and enriched medium under three flashing light conditions and a control of continuous light. Values are reported as means (n=3) and error bars report the standard deviations. Asterisks indicate if the treatment is statistically different from the continuous light control. One asterisk indicates a P value <0.1, two asterisks <0.01 and three aterisks < 0.001.

The flashing light effect has been widely studied in literature, as reviewed by some authors (Abu-Ghosh et al., 2016; Schulze et al., 2017b). Several authors found a correlation between the flashing frequency and the growth performance. For example, in a very similar way than in the present work, Verakza et al. observed that *Chlamydomonas reinardtii* specific growth rate decreased from continuous light to flashing light and increased by increasing the flashing frequency (DC= 0.1, f=5-100 Hz) (Vejrazka et al., 2012). Interestingly, at the highest frequency of the work, 100 Hz, the *specific growth rate* μ returned to be similar than the one of continuous light. Other authors found no increased growth and no increased μ in cultures exposed to flashing light compared to continuous light, in a range of duty cycles and frequencies and for several microalgae species (Matthijs et al., 1996; Park and Lee, 2000; Sforza et al., 2012). On the contrary, there are a few works in which authors observed an increase of the growth performance under flashing light compared with continuous light irradiation. For example, Lunka and Bayless, during the cultivation of *Scenedesmus dimorphus*, observed a higher biomass increase under flashing light compared to continuous light control (DC=0.2, f=10 KHz) (Lunka and Bayless, 2013). In another case, Yoshioka et collaborators observed in *Isochrysis galbana* an increased *specific growth rate* μ until the sixth day of cultivation and an increased final cell concentration in FL compared to CL (DC=0.5, f=10KHz) (Yoshioka et al.,

2012). There is, therefore, a significant uncertainty on the effects of the flashing lights on microalgal cultures. This may be due to factors that take part to the phenomenon, such as the duty cycle and the intensity of the flashing light, that were not explored in the present work. On the other hand, Simionato and coworkers hypotized that the lenght of the light pulse is one of the main parameters affecting the biomass productivity and that the optimal is around 10 ms (Simionato et al., 2013a); in this work the duration of light pulses decreases when frequency increases: in FL 25 it lasts 10 ms, in FL 250 1 ms and in FL 2500 condition 0.1 ms. These results, therefore, confirm the theory, that could be adopted as explanation for the different response to flashing light of microalgal cultures.

3.4.2.2. Biochemical characterization

FTIR analysis

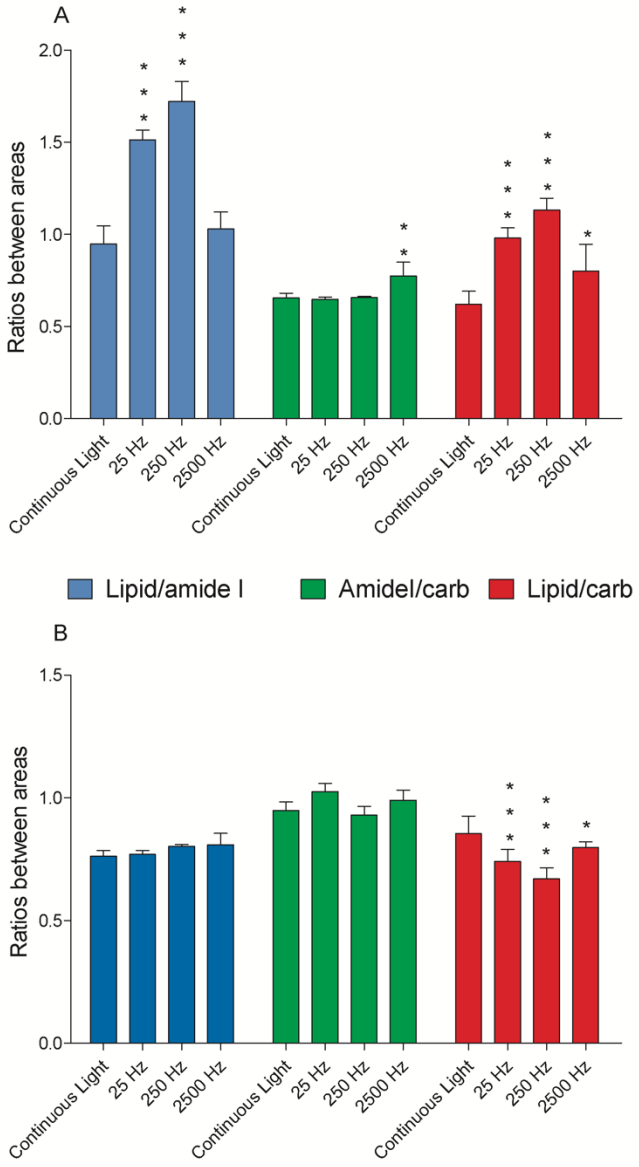

Figure 3.17: FTIR analysis on the microalgal biomass grown in a basic (A) and an enriched (B) version of the same medium and under three different flashing light conditions and a control. Ratios between areas under peaks related to macromolecules are reported. Values are reported as means (n=3) and error bars report the standard deviations. Asterisks indicate if the treatment is statistically different from the continuous light control. One asterisk indicates a P value <0.1, two asterisks <0.01 and three aterisks < 0.001.

Fourier Transform Infrared Spectroscopy was employed in order to obtain a gross analysis of the composition of the biomass harvested at the end of the experiments. This methodology, broadly employed in the characterization of microalgae biomass (Dean et al., 2010; Mayers et al., 2013; Stehfest et al., 2005), connects the presence of vibrationally active functional groups with correspondent macromolecules. The related peaks are integrated and the results are reported as ratios between areas in order to make different samples comparable. By comparing three different ratios it is possible to approximately understand the composition of the biomass. Results are reported in Figure 3.17 and in Supplemental Information together with original spectra. The reported areas are Lipid/amide I (L/A), Amide I/carbohydrates (A/C) and Lipid/carbohydrates (L/C).

Under a statistical point of view, L/A ratio is influenced more by the *medium* ($F=304.0$, $p<0.0001$) than by the *light treatment* ($F=41.26$, $p<0.01$). A/C ratio, in the same way, is affected more by the *medium* ($F=77.13$, $p<0.01$) than by the *light treatment* ($F= 5.829$, $p<0.01$). L/C ratio is influenced in a comparable way by the *medium* ($F=15.30$, $p<0.01$) and by the *light treatment* ($F=8.938$, $p<0.01$). Details of statistical analysis are reported in Supplemental Information. This analysis allows to hypotize that lipids and carbohydrates content is affected both by the richness of nutrients and by the frequency of flashing light. In fact, is well known that a lack of nutrients, in particular nitrate, facilitates an accumulation of lipids (e.g. in *Nannochloropsis oceanica*) (Meng et al., 2015) or carbohydrates (e.g. in *Tetraselmis sp*.) (Kim et al., 2016). Furthermore, several studies showed a correlation between lipids accumulation and flashing lights, for example in *Isochrysis galbana* (Yoshioka et al., 2012) and in *Chlorella vulgaris*, *Acutodesmus obliquus* and *Micractinium reisseri* (Choi et al., 2017).

In the case of *N. gaditana* grown in the basic version of the growth medium (Figure 3.17A), the L/A ratio increased from the continuous light to the FL 25 and 250. Then, it decreased under the FL 2500. The A/C ratio, on the other hand, was constant under all the light treatments except for the FL 2500 one, in which it slightly increased. The L/C ratio, on the other hand, shows a similar trend as the L/A one. In fact, it increased from CL control to FL 25 and 250 and decreased under the FL 2500. Probably the lipid content increased from the control to the 25 and 250 Hz light conditions, and decreased in the 2500 Hz treatment.

For what concerns the biomass cultivated in the enriched version (Figure 3.17B) , the situation is almost opposite compared to the previous one. L/A ratio is stable under all lighting conditions, in the same way than the A/C ratio. The L/C ratio, instead, decreased from continuous light control to 25 and 250 Hz flashing light and returned similar to continuous light under the 2500 Hz condition. In this case, it is possible

that the lipid content decreased from the control to the 25 and 250 Hz light conditions, and inecreased in the 2500 Hz treatment.

These results show that flashing lights have an effect on biomass composition that is affected by the richness of nutrients in the growth medium.

Total lipids quantification

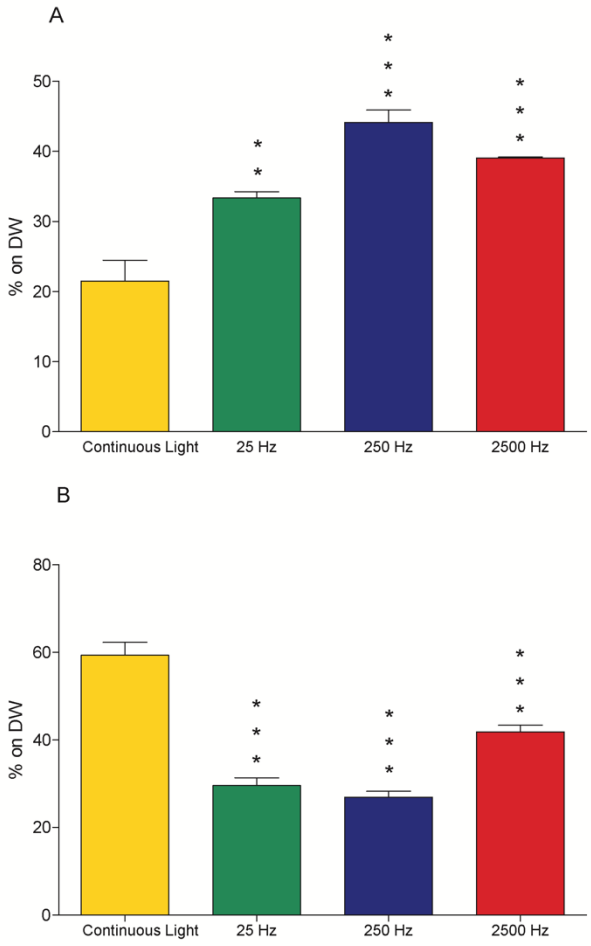

Figure 3.18: Total lipids on Dry Weight (DW) of microalgal biomass grown in a basic (A) and an enriched (B) version of the same medium and under three different flashing light.conditions and a control. Values are reported as means (n=3) and error bars report the standard deviations. Asterisks indicate if the treatment is statistically different from the continuous light control. Two asterisks indicate a P value <00.1 and three aterisks < 0.001.

The dry biomass at the end of the cultivation was analyzed in order to assess the percent of total lipids on Dry Weight (DW). Results are shown in Figure 3.18 and in Supplemental Information.

The detected contents of total lipids in the dry biomass of *N. gaditana* ranged from 21.5±5.1% to 59.3±5.1% and is coherent with literature data (Ma et al., 2016; Rebolloso-Fuentes et al., 2001).

According to ANOVA analysis, both *light treatment* and *medium* affected the lipid quantity in a comparable way (F=9.433, p<0.01; F=11.87, p<0.01). The analysis revealed also that the *interaction* between these two parameters accounted for approximately 79% of the total variance (F=72.44, p<0.01). This means that there is less than the 0.01% chance of randomly observing this interaction in an experiment of this size. In other words, the interaction is extremely significant.

As shown in Figure 3.18A and confirmed by FTIR analysis of Figure 3.17A, when cells were cultivated in the basic medium the lipids quantity gradually increased from the CL control to the FL 25 and 250. FL 2500 had as well a higher lipid content than the control, but slightly lower than in the other light conditions. On the other hand, the effect observed in cells cultured in the enriched medium was the opposite: the lipids content decreased from the continuous light control to the flashing light treatments. In particular, it gradually decreased from FL 25 to 250 and slightly increased in the FL 2500. This double effect of richness of nutrients and light condition is also linked to the fact that in the continuous light control grown in enriched medium the lipid content was higher than in the control grown in the basic medium. This is due to the already quoted phenomenon of lipid accumulation in algae grown in nitrogen starvation, reported by several authors (Corteggiani Carpinelli et al., 2014; Simionato et al., 2013b).

Several studies addressed the correlation between lipid content and flashing light. Some of them did not find any relevant difference in the lipid content under continuous light and under flashing light (Kim et al., 2014; Mouget et al., 1995; Yoshioka et al., 2012). Some others, by the way, found interesting differences. For example, Simionato et al. analyzed the response of *Nannochloropsis salina* under a range of frequencies and duty cycles (DC=0.1, 0.33; f=1-30 Hz). It was assessed that the lipid content is lower or higher than the one of the CL condition depending on frequencies and duty cycles (Simionato et al., 2013a). The algae of this study were grown in 1.5 g/L of $NaNO_3$, versus the 0.22 g/L of the basic medium and 2.17 g/L in the enriched medium of the present study. In a very similar way than in the present work, another study by Combe et al. observed, in *Dunaliella salina* grown in nitrogen excess, a decrease in lipids/cell when increasing frequency (DC=0.33, 0.4, 0.5;

f=0.017- 5)(Combe et al., 2015). These results taken together demonstrate that there are several factors involved in the biochemical composition of the microalgae in response to flashing light treatments, and nutrient richness is one of the parameters to take into consideration. A possible interpretation of the already exposed results is that when grown in starvation of nutrients, the effect of flashing is combined to the effect of the starvation that brings to accumulation of lipids. When grown in richness of nutrients, the light energy provided by flashing lights probably flows along other biochemical routes than to the production of lipids.

Fatty acid composition

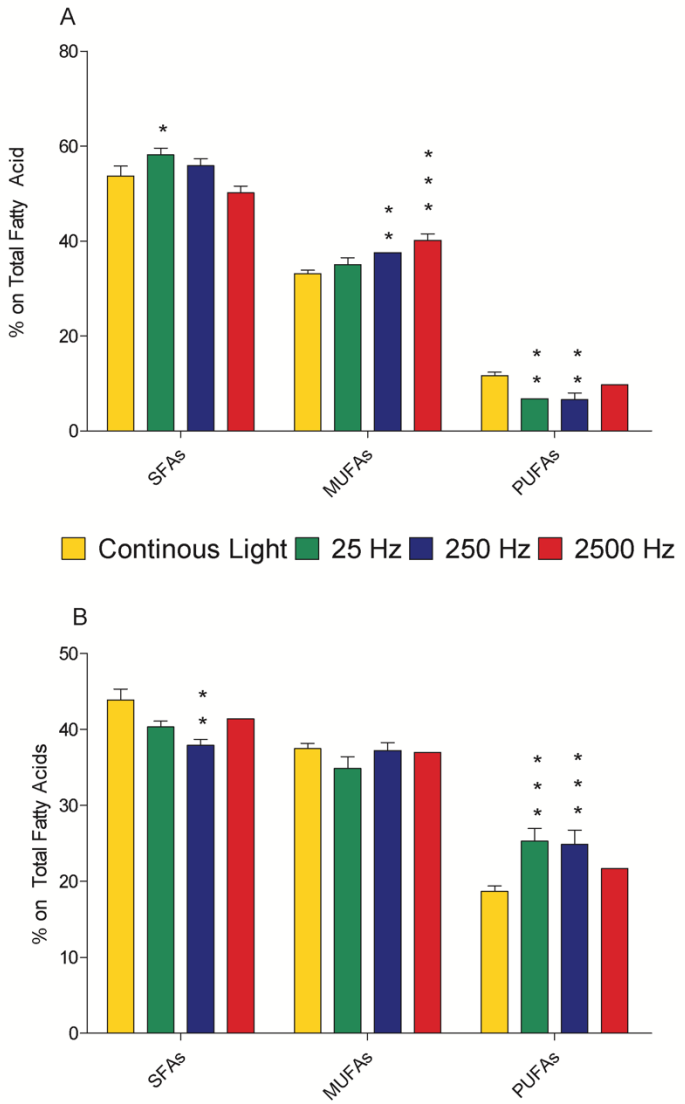

Figure 3.19: Fatty acid composition of microalgal biomass grown in a basic (A) and an enriched (B) version of the same medium and under three different flashing light conditions and a control. The composition is reported as percent of Saturated Fatty Acids (SFAs), Monounsaturated Fatty Acids (MUFAs) and Polyunsaturated Fatty Acids (PUFAs) on total fatty acids. Values are reported as means (n=3) and error bars report the standard deviations. Asterisks indicate if the treatment is statistically different from the continuous light control. One askerist indicates a P value <0.1, two asterisks <0.01 and three aterisks < 0.001.

The fatty acid content of dry microalgal biomass grown in the basic and the enriched version of the medium under three flashing light conditions and a control were assessed and results are reported in Figure 3.19A and B and in Supplemental Information. The analysed fatty acid content of *N. gaditana* is coherent with other literature studies (Ma et al., 2014; Matos et al., 2016; Simionato et al., 2013b).

Under a statistical point of view, the Saturated Fatty Acid percent on total fatty acids is markedly influenced by the *medium* (F=375.7, p<0.01) and much less by the *light treatment* (F=5.356, p<0.01). Oppositely, Monounsaturated Fatty Acid (MUFAs) content is influenced by the *light treatment* (F=10.29, p<0.01) and not by the *medium* (F=0.08047, p<0.01). Polyunsaturated Fatty Acid (PUFAs) content depends on the *medium* (F=641.1, p<0.01) and not on the *light treatment* (F=0.4319, p=0.7359).

By looking at the results of Figure 3.19A and B, the SFAs content did not show big changes between the control and the flashing light conditions, with the exception of the light conditions of 25 Hz in the basic medium and of 250 Hz of the enriched medium. MUFAs content varied in the 250 and 2500 Hz light condition of biomass grown in the basic medium and did not change in algae grown in the enriched medium. In microalgae grown in the basic version, PUFAs content, interestingly, was constant under the CL control and under the FL 2500, while it decreased in the FL 25 and 250. Oppositely, when cultured in the enriched medium, they showed an increase in the 25 and 250 Hz FL conditions compared to the CL control that was again constant compared to the 2500 Hz FL condition.

Several authors studied the effect of flashing light on fatty acid composition of microalgae (Kim et al., 2014; Mouget et al., 1995). Amongst them, Yoshioka et al. observed a similar shift in SFAs, MUFAs aPignd PUFAs than in the present work when *I. galbana* was grown under intermittent light (DC=0.5, f=10 KHz) (Yoshioka et al., 2012).

The increase of PUFAs content can be connected to low-light response (He et al., 2015), as they are included in the thylakoid membranes that multiply with the aim of harvesting as much light as possible (Berner et al., 1989). Low-frequency flashing light conditions may therefore bring to a low-light response, indicating that the cells do not acclimate to the average light intensity, as commonly believed (Nedbal et al., 1996), or to high light intensity (Schulze et al., 2017b), but that the time they spend in darkness conditions more the acclimation. This idea was confirmed also by others (Yarnold et al., 2016) and the effect could be the one observed at low frequencies in the present work when cells are grown in the enriched medium, with no nutrient limitation (Figure 3.19B). The observed effect in the basic medium (Figure 3.19A), instead, is the opposite. This means that, even though the conditions of illumination,

the effect of the nutrient starvation is higher, as confirmed by ANOVA analysis. In fact, other studies demonstrates that in nitrogen depletion PUFAs content decreases (Alonso et al., 2000; Breuer et al., 2012).

Pigment composition

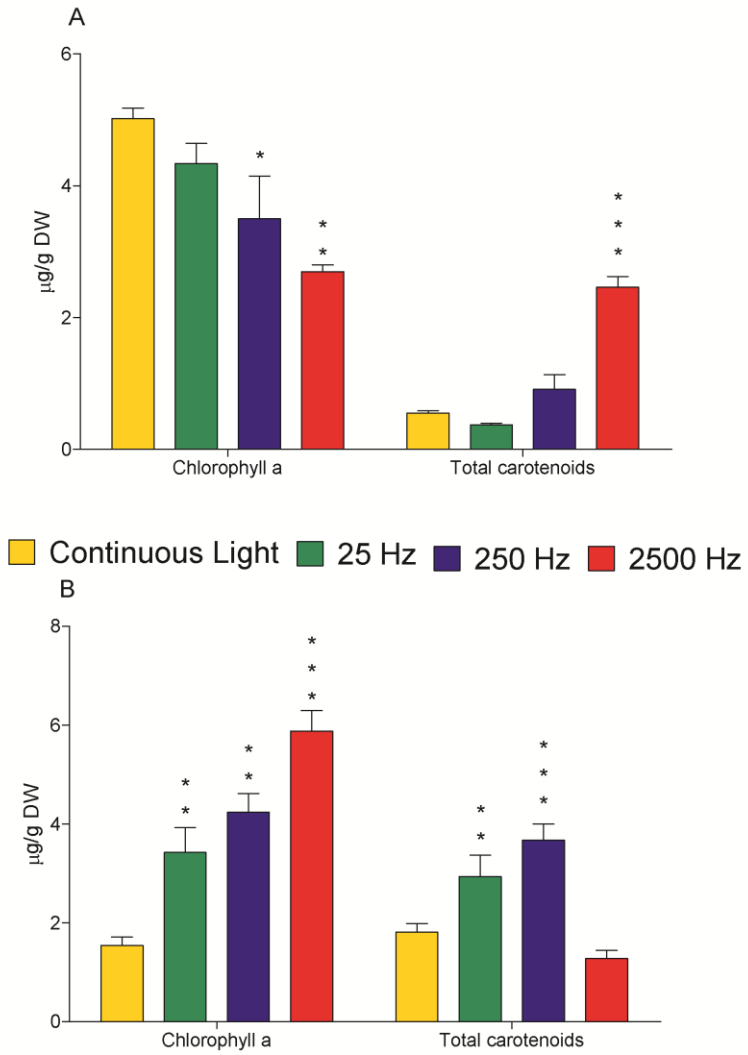

Figure 3.20: Pigment composition of microalgal biomass grown in a basic (A) and an enriched (B) version of the same medium and under three different flashing light conditions and a control. Chlorophyll a and Total carotenoids are reported as µg/g Dry Weight (DW). Values are reported as means (n=3) and error bars report the standard deviations. Asterisks indicate wether the treatment is statistically different from the continuous light control. Two asterisks indicate a P value <00.1 and three aterisks < 0.001.

Microalgal biomass grown in the basic and the enriched version of the medium under three FL conditions and a CL control was spectroscopically analyzed in order to assess the content in Chlorophyll a and Total carotenoids on Dry Weight (DW). Results are reported in Figure 3.20A and B and in Supplemental Information.

The chlorophyll content ranges from 5.88±0.7 to 1.54±0.29 μg/g DW, while total carotenoids from 3.67±0.57 to 0.37±0.05 μg/g DW. These values are in line with the ones found in literature for the same genus (Rebolloso-Fuentes et al., 2001).

Under a statistical point of view, the chlorophyll content is not influenced by the *medium* or by the *light treatment* (F=2.379, p=0.1080; F=0.1907, p=0.6682). It is instead affected by the *interaction* between these two parameters, that accounts the 78% of the total variation (F=27.37, p<0.01). On the other way, total carotenoid content is affected more by the *medium* (F=67.96, p<0.01) than by the *light treatment* (F=7.916, p=<0.01), while the *interaction* accounts for the 46.10% of the total variation (F=30.71, p<0.01).

As observed in Figure 3.20A, the biomass grown in the basic medium showed a quantitative decrease of the content in chlorophyll from the continuous light to the flashing light conditions, while the total carotenoid content, increased. Oppositely, in Figure 3.20B, the biomass grown in the enriched version of the medium showed a different quantitative increase of chlorophyll content from the continuous light to the flashing light conditions and an increase of total carotenoid content in 25 and 250 Hz FL conditions.

As already observed, cells grown in the basic version of the medium increased their amount of lipids under flashing light conditions compared to continuous light; oppositely, their content of chlorophyll decreased when moving from continuous light to flashing light conditions. This may be explained again as a combination of the effect of flashing with the effect of the starvation, that brings to accumulation of lipids instead of pigments. In fact, as observed by Simionato et al. *N. gaditana* grown in nitrogen depletion accumulates less chlorophyll and more carotenoids than in non-limiting conditions (Simionato et al., 2013b). In the same way, also Forján et al. observed an accumulation of carotenoids in nitrate and phosphate limitation in *Nannochloropsis* (Forján et al., 2007), as well as Solovchenko et al. observed a decrease in chlorophyll and an increase in carotenoids in *Parietochloris incisa* in starvation of nitrogen (Solovchenko et al., 2008). Thus, it is possible to hypothesize that by increasing the frequency of flashing light the effect of the scarcity of nutrients is enhanced.

On the other way, when cells are cultured in nutrient abundance, flashing light seemed to lead to carotenoids accumulation instead of lipids, and this is particularly

evident in the 25 and 250 Hz conditions. The effect of flashing light on pigments accumulation has been studied before. For example, similarly to this work, Sforza et al. observed an increase in the quantity of chlorophyll/cell in *N. gaditana* grown with 1.5 g/L $NaNO_3$ under flashing light compared to the continuous light (Sforza et al., 2012). Other studies were addressed to the production of carotenoids, in particular astaxanthin, from *Haematococcus pluvialis*, indicating an increase of the production when the algae were cultivated under flashing lights (Katsuda et al., 2008, 2006; Kim et al., 2006). Another point is that the accumulation of pigments, together with the already cited PUFAs increase, can be interpreted as a low-light acclimation response (Schüler et al., 2017).

In conclusion, the accumulation of pigments from *N. gaditana* is strongly affected by the medium in which the algae were grown and also by the flashing light treatments. In fact, ANOVA analysis indicates a strong interaction between these two parameters in affecting chlorophyll and carotenoids content.

PART 2: EXPERIMENTS CARRIED OUT AT NORD UNIVERSITY, BÖDO, NO

3.5. Exploring the flashing light: effects at low, medium and high frequencies in different algae

3.5.1. Materials and methods

3.5.1.1. Experimental setup

Nannochloropsis gaditana (CCAP 849/5 Scottish Association for Marine Science, Oban, Scotland), *Tetraselmis chui* and *Koliella antarctica* (SAG 1.96, SAG 2030, Culture Collection of Algae at Göttingen University, Germany) were employed and cultivated at 20 °C for *N. gaditana*, while at 15°C for *T. chui* and *K. antarctica*.

As growth medium, seawater from the North Atlantic shoreline of Bodø (Norway, 35 ppt) was enriched with a modified F-medium consisting of 5.3 mM $NaNO_3$, 0.22 mM $NaH_2PO_4H_2O$, 35 µM $FeCl_3\,6H_2O$, 35 µM $Na_2EDTA\,2H_2O$, 0.12 µM $CuSO_4\,5H_2O$, 0.078 µM $Na_2MoO_4\,2H_2O$, 0.23 µM $ZnSO_4\,7H_2O$, 0.126 µM $CoCl_2\,6H_2O$ and 2.73 µM $MnCl_2\,4H_2O$.

Tissue culture flasks (Falcon Scientific, Seaton Delaval, UK) with a total volume of 250 mL and 30 mL (light paths: 3.7 and 2.0 cm, respectively) were filled with 200- and 25-mL cultures for one-stage or two-stage cultivation systems, respectively. A scheme of the flasks is shown in Figure 3.21. They were adopted because they are flat enough to guarantee the full passage of the light, provided that the culture is diluted enough. The cultures were mixed by aeration with humidified and 0.2 µm-filtered air enriched with CO_2 at a flow rate of 160 mL min^{-1}. All algae were cultured during the one-stage batch cultivation for 13 days (n = 3). The two-stage cultivation consisted of a first stage (six days at I_a= 300 µmol s^{-1} m^{-2} under continuous light) and a second stage (five days under the FL treatments). A scheme of the cultivation system is provided in Figure 3.22.

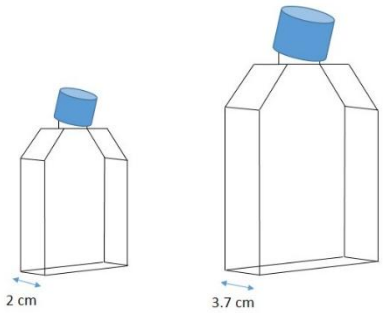

Figure 3.21: Tissue flask employed for this experiment. They were chosen because of the short width, that allowed the passage of light.

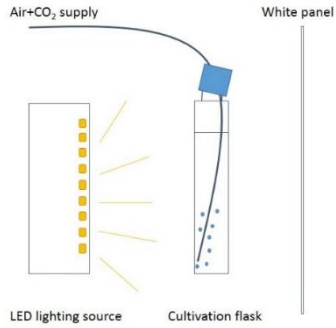

Figure 3.22: Cultivation system employed in the experiment. The flask was placed in front of a white panel and enlightened by the LED light source.

Continuous light was used as a control treatment employing the same average light intensity used under flashing light. A picture of the cultivation system is shown in Figure 3.23.

Optical density at 540 nm (OD_{540}) was measured daily (n = 4) for each algal culture using a 96-well plates (Tecan Sunrise A-5082, Männedorf, Switzerland). To determine the biomass concentration in the culture in grams of dry weight (DW) per litre, a known volume of algal suspension was filtered using glass fibre filters (pore size ø = 0.7 µm), washed twice with 10 mL ammonium bicarbonate (0.5 M) and dried at 105°C for 24 h. The dry weight was determined gravimetrically. Significant linear correlations between OD_{540} and dry weight were obtained for each microalga ($r^2 \geq 0.9$, $p < 0.05$).

Culture samples for biochemical analysis were taken at the end of experiments. The harvested cultures were centrifuged (5000 *g*, 5 min), washed (0.5 M ammonium bicarbonate), freeze-dried and stored at -80 °C until further analysis. Furthermore, part of samples was diluted to approximately 1g DW L^{-1} and the pellet was stored at -20 °C for spectroscopic quantification of total carotenoids and chlorophylls.

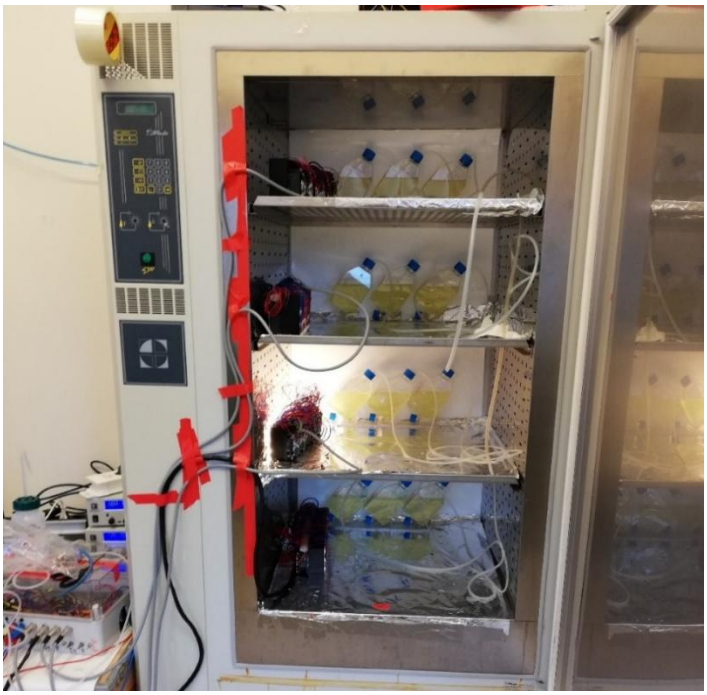

Figure 3.23: Culture system used for the experiment. The tissue flasks were placed in a cultivation chamber with regulated temperature. Each shelf contained a biological triplicate exposed to a different light condition. Led light source are showed.

3.5.1.2. Light source

An array of 36 warm-white LEDs (2700 K, 13 W, MHDGWT-0000-000N0HK427G-SB01, emission spectrum provided in Figure 3.24), mounted on an actively cooled aluminium heat sink, with a total length, height and width of 300, 75 and 40 cm, respectively, was used as an artificial light source. The applied flashing light conditions were: continuous light and flashing light with a duty cycle of 0.05 with the frequencies of 5, 50 and 500 Hz. The time-averaged light intensity was I_a= 300 µmol s^{-1} m^{-2} in all conditions, which corresponded to an instantaneous flash intensity of I_l= 6000 µmol s^{-1} m^{-2}. Flashing lights were adjusted by PWM-OCX (RMCybernetics Ltd, Alsager, UK) pulse width modulators (PWMs) powered by bench EA-PS 2084-05B (EA Elektro-Automatik) power supply units. The pulse signal was provided by a TG4001 (TTi, Huntingdon, UK) function generator or directly through the PWMs. For the continuous light control, the LEDs were directly connected to the power supply units. The voltages and currents supplied to the LEDs were regulated to adjust I_a to 300 µmol s^{-1} m^{-2} and compensate switching and working losses at the LEDs and PWMs. The supplied light intensity (i.e., photosynthetically active radiation) was measured for 1 min at the same position as the flasks (SPQA

5234 connected to a data logger LI-1500, Li-Cor, Lincoln, USA) and averaged over time.

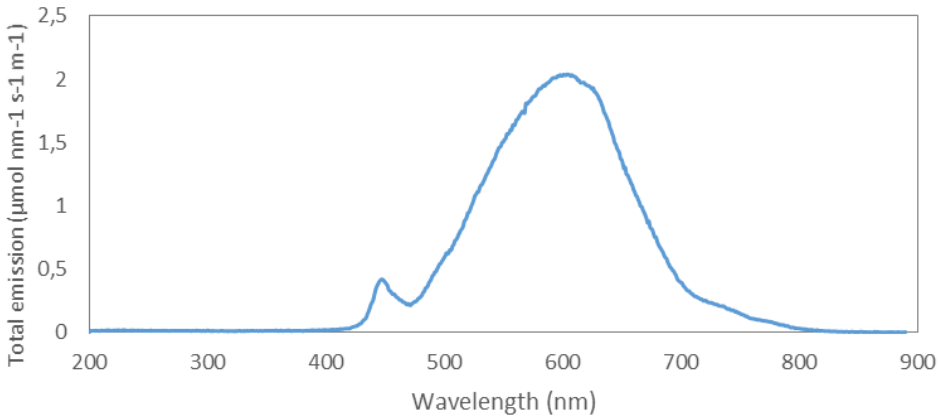

Figure 3.24: Emission spectra of the used LEDs, MHDGWT-0000-000N0HK427G-SB01, Opulent Americas, Raleigh, US

3.5.1.3. Analytical methods

Total lipids, proteins and carbohydrates

Total lipids were determined gravimetrically using a modified Bligh and Dyer method (Bligh and Dyer, 1959) described by Pereira et al. (Pereira et al., 2011). Briefly, 10 to 30 mg of freeze-dried microalga samples were weighed and transferred to glass tubes. Afterwards, 0.8 mL of distilled water was added to soften the samples and kept for 20 minutes. Subsequently, 2 mL methanol and 1 mL chloroform were added and homogenized with an IKA T18 Ultra-Turrax disperser (IKA-Werke GmbH & Co. KG, Staufen, Germany) in an ice bath for 60 seconds. A 1-mL aliquot of chloroform was added and samples were homogenized for 30 seconds, followed by the addition of 1 mL of distilled water and further homogenized for 30 s. Phase separation was performed by centrifugation (2000 *g* for 10 min). Subsequently, 1 mL of the organic phase was transferred into a new pre-weighed tube, and the chloroform was evaporated at 60 °C in a dry bath overnight and cooled down to room temperature in a desiccator. Finally, the remaining lipids in the tube were determined gravimetrically.

Protein contents of the algal biomass was determined with a Bio-Rad DC™ Protein Assay (Bio-Rad Ltd., Hemel Hempstead, UK). Water-soluble proteins from freeze-dried biomass were extracted by re-suspending ~7 mg freeze-dried biomass in 4 mL NaOH (1 M) and bead milled using three cycles of 60 s (6500 rpm, 120 s break

between bead milling; Precellys Evolution, Bertin technologies, Montigny-le-Bretonneux, France). The samples along with glass beads were centrifuged (2000 *g*, 10 min, 20°C) and the supernatant was recovered into clean vials. The water-soluble proteins contained in the supernatant was measured according to Bio-Rad DC Protein Assay manual, at a wavelength of 750 nm (Dr3900, Hach Lange, Salford Quays, UK).

An elemental analysis of the harvested biomass for carbon (C), hydrogen (H) and nitrogen (N) was conducted (Vario EL iii, Elementar Analysensysteme GmbH, Langenselbold, Germany). Thereafter, the protein contents obtained by the Bio-Rad DCTM Protein Assay were confirmed by multiplying the nitrogen content in the biomass (%N) by 4.78 (Lourenço et al., 2004).

Total carbohydrate content was determined according to Trevelyan et al. (Trevelyan et al., 1952). Briefly, 10 mg of freeze-dried biomass were suspended in 3 mL HCl 37% (v/v) and hydrolysed in a water bath for 1 h at 100°C. Subsequently, 4 mL of a fresh anthrone solution (Sigma-Aldrich, Oslo, Norway, 2 mg mL^{-1} in 99% H_2SO_4) were added to 1 mL of sample extract. The absorbance of each sample was read at 620 nm (Dr3900, Hach Lange, Salford Quays, UK). Aliquots of different glucose concentrations (0.02-0.1 mg L^{-1}) were prepared and processed in the same way as microalgal extracts, to obtain a calibration curve.

The contents of protein, carbohydrates and total lipids in microalgal biomass were expressed as % of DW.

Fatty Acid Analysis

For fatty acid analysis, 4 mL of a chloroform:methanol solution (2:2.5 v/v) containing an internal standard (Tripentadecanoin, C15:0 Triacylglycerol, Sigma-Aldrich, Oslo, Norway) were added to ~6 mg of freeze-dried microalgal biomass. Cells were disrupted by bead milling using 0.1 mm glass beads (Precellys Evolution, Bertin technologies, Montigny-le-Bretonneux, France). Thereafter, 2.5 mL tris-buffer (6 g L^{-1} Tris, 58 g L^{-1} NaCl) were added, mixed with a vortex mixer and centrifuged (2000 *g*) to separate the phases. The lower chloroform-phase containing the lipids was transferred into a new glass tube and evaporated under a gentle nitrogen flow to prevent fatty acid oxidation. Subsequently, 3 mL of a methanol solution containing 5% H_2SO_4 were added and kept for 3 h at 70 °C, to convert the fatty acids into the corresponding methyl esters. After the reaction, 3 mL of hexane were added and mixture was shacked for 15 min in an orbital shaker. Finally, the fatty acid methyl esters (FAMEs) in the hexane phase were quantified using gas chromatography equipped with a Flame Ionisation Detector (SCION 436m Bruker, Massachusetts, US) and a CP-Wax 52 CB column (Agilent, Santa Clara, US) using split-less mode.

To identify and quantify the most common FAMEs, an external 37-component standard (Supelco, Bellefonte, US) was used.

Spectrometric Pigment Analysis

For the chlorophyll and total carotenoid extraction, biomass was disrupted in methanol with bead milling (Bertin technologies, Precellys Evolution, Montigny-le-Bretonneux, France) and subsequently kept in ice and darkness for 2 h. The methanol extract was separated from the algae pallet via centrifugation and spectrophotometrically analysed (Uviline 9400, Schott, Mainz, Germany). All analyses were done under dimmed light. Chlorophyll *a* (C_a) and *b* (C_b) and total carotenoids (C_{carot}) were determined according to *Lichtenthaler and Wellburn* (Lichtenthaler and Wellburn, 1983) by applying the OD measurements at 666, 653 and 470 nm (A_{666}, A_{653}, A_{470}) from the methanol extracts to equations 3.V, 3.VI, 3.VII:

$$C_a = 15.65\ A666 - 7.34\ A653 \quad \text{3-V}$$

$$C_b = 27.05\ A653 - 11.21\ A666 \quad \text{3-VI}$$

$$C_{carot} = (1000\ A470 - 2.86\ Ca - 129.2\ Cb)/221 \quad \text{3-VII}$$

Because *Nannochloropsis* microalgae do not contain chlorophyll *b*, a modified formula according to Henriques et al. (Henriques et al., 2007) was used (equations 3.IX and 3.X):

$$C_a = 15.65\ A666 \quad \text{3-VIII}$$

$$C_{carot} = (1000\ A470 - 44.76\ A666)/221 \quad \text{3-IX}$$

HPLC Pigment Analysis

For extraction of single carotenoids (lutein, *β*-carotene, violaxanthin and neoxanthin), ~3 mg of freeze-dried biomass were transferred into a tube together with 50 µL deionized water. Afterwards, 3 mL acetone and 0.7 g of glass beads were added; the samples were then vortexed for 2 minutes (Vortex Mixer, Stuart, UK) and centrifuged (5000 *g*, 5 min). Subsequently, the supernatant was transferred into a clean and light-proof tube and the extraction was repeated sequentially thrice. Acetone was evaporated under a gentle nitrogen stream and resuspended in methanol prior to HPLC injection. Carotenoid extracts were analysed with a Dionex 580 HPLC System (DIONEX Corporation, Sunnyvale, United States) equipped with a PDA 100 Photodiode-array detector and STH 585 column oven set to 20°C. Separation of the compounds was achieved using a LiChroCART RP-18 (5 µm, 250x4 mm, LiChrospher, Merck KGaA, Germany, column with a mobile phase consisting of acetonitrile:water (9:1; v/v) as solvent A and ethyl acetate as solvent B and a constant

flow of 1 mL min-1. The gradient program applied was: (i) 0–16 min, 0–60% B; (ii) 16–30 min, 60% B; (iii) 30–32 min 100% B and (iv) 32-35 min 100%. Adapted from Couso et al.(Couso et al., 2012). The injection volume of the samples was 100 µL, chromatograms were recorded at 450 nm and analysed by Chromeleon Chromatography Data System software (Version 6.3, ThermoFisher Scientific, Massachusetts, US). For the quantification of individual carotenoids, calibration curves for lutein, *β*-carotene, violaxanthin and neoxanthin were used. All pigment standards were supplied by Sigma-Aldrich (Sintra, Portugal). All HPLC grade solvents were purchased from Fisher Scientific (Porto Salvo, Portugal).

3.5.1.4. Data analysis

Growth parameters were estimated according to Ruiz et al.(Ruiz et al., 2013) and are detailed in Supplemental Information at the end of the section.

ANCOVA analysis were performed to detect differences in intracellular biochemical contents among *treatments, strains* and *cultivation approaches* (one- or two stage) while considering the co-variate *biomass concentration* at the time point of harvesting (X_t in g DW L^{-1}) as indicator for the prevailing growth stage (Schulze et al. 2019). Pearson´s correlations (*r*) were used to quantify its effect. A significance level (α) of 0.05 was used for all tests. Normality of the response variables was tested using the Shapiro-Wilk test. ANOVA was used to detect differences in productivity data using the explanatory variables *strains* and *treatment*.

Biomass productivities or biochemical contents data were normalised with the control treatment (continuous light).

Biomass concentration data were log10-transformed to meet the assumption of linearity and homogeneity of variance. The Type III sum of squares analysis was considered and the output *F*-values together with *p*-values were used to describe the impact of treatment, biomass concentration, strain or cultivation approach on the response variables (biomass productivity, protein, carbohydrates, lipids, fatty acids or pigments). The adjusted means with 95% confidence interval from Tukey´s post hoc tests were used to illustrate the results of the ANCOVA and ANOVA analysis in the figures.

3.5.2. Results and discussion

3.5.2.1. Growth performance

The growth curves of *N. gaditana*, *K. antarctica* and *T. chui* were obtained for three flashing light conditions (5, 50 and 500 Hz, referred as FL 5, FL 50 and FL 500) and a control grown under continuous light (CL), for one-stage (Figure 3.25 a, c, e) and two-stage (Figure 3.25 b, d, f) cultivation-systems. Details of the results are reported in Supplemental Information. The results obtained revealed that the microalgal cultures growing under the highest flashing light (FL) frequency tested (f = 500 Hz) reached similar growth than those under CL. Conversely, microalgae under low frequency FL (f = 5 and 50 Hz) often showed less growth (Figure 3.25, Table 3.2). Using the one-stage cultivation approach, all tested strains exposed to FL 5 and FL 50 showed lower biomass productivity and a longer lag phase as compared to FL 500 and CL. Notably, *T. chui* cultures performed better at FL 50 when compared to *N. gaditana* and *K. antarctica* (Figure 3.25, Table 3.2). For example, under FL 50 treatments, biomass productivity of *T. chui* was only about 30% lower compared to cultures exposed to CL, whereas *N. gaditana* and *K. antarctica* cultures displayed a 70% decline.

In the two-stage cultivation approach, all strains treated with the lowest frequency (FL 5) displayed lower biomass productivities when compared to cultures grown under CL. On the other hand, only *K. antarctica* exposed to the FL 50 treatment showed lower biomass productivity, while *N. gaditana* and *T. chui* showed similar values as obtained under CL (Table 3.2). It is worth noting that all strains cultured in the two stage approach and exposed to FL 5 reached higher biomass productivities (0.34-0.43 g DW L^{-1} d^{-1}) as compared to cultures grown in a the one-stage set-up (<0.05 g DW L^{-1} d^{-1}).

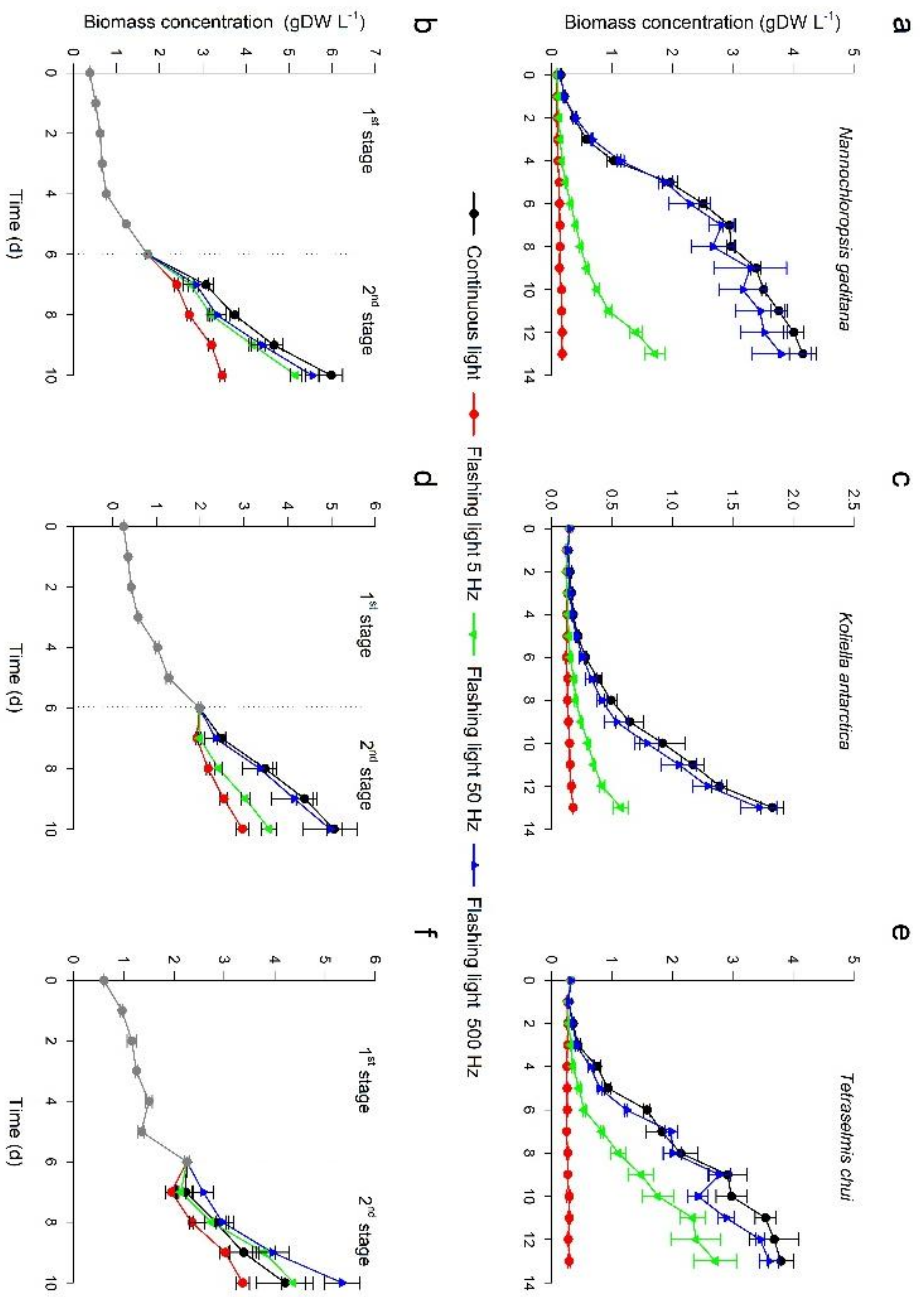

Figure 3.25: Growth curves of algae grown in a one- and two-stage batch culture under different flashing light conditions. *Nannochloropsis gaditana* (a, b), *Koliella antarctica* (c, d) and *Tetraselmis chui* (e, f) were cultivated under continuous light or flashing light with a duty cycle of 0.05 and frequencies of 5, 50, 500 Hz at an average light intensity of I_a= 300 µmol s^{-1} m^{-2}. Data points with error bars at each day are shown as mean ±SD (n=3).

Literature studies concerning several algae and plants, e.g., *Dunaliella salina*, *Nannochloropsis salina*, *Lactuca sativa* (Combe et al., 2015; Jishi et al., 2015; Simionato et al., 2013a), indicated that if the FL frequency is high enough, the photosynthetic system is not able to see a difference between single pulses and CL (Grobbelaar et al., 1996). Other studies (Abu-Ghosh et al., 2015; Grobbelaar et al., 1996; Lunka and Bayless, 2013; Park and Lee, 2000) proposed that microalgal cultures could benefit from high light flashes because they penetrate deeper into the culture. During this work, it was impossible to identify a significant growth enhancement among the strains tested, but only comparable productivities between FL 500 and CL treatments. The levels of flashing light parameters (e.g., frequency and duty cycle) that make microalgal growth performance similar to CL rely on different factors, along with the average light intensity of flashing light, morphological or photoprotective strategies of phototrophs or culture concentration. In the present study, strain-specific responses were observed; *T. chui* coped better with low-frequency FL (e.g., FL 50) as compared to *K. antarctica* or *N. gaditana* (Figure 3.25, Table 3.2). Similarly, Nedbal (1996). identified strain-specific threshold frequencies while testing growth response of cyanobacteria and microalgae under various flashing light conditions (Nedbal et al., 1996). In microalgae, cell architecture and size determine the amount of light that gets absorbed and that is used for photosynthesis inside the cell (Dubinsky et al., 1986). As regards the cell size, *T. chui* cells that have an oval-shape with dimensions of 13 × 5 × 4 μm (Bottino et al., 1978), and an estimated volume of about 260 μm^3, are larger than those of other tested strains: *N. gaditana*, round-shaped, with a diameter of 2-4 μm (Rocha et al., 2003) and a volume of 40 μm^3, or *K. antarctica*, cylindrically shaped, 7.5 × 2.5 μm (La Rocca et al., 2009) with a volume of 60 μm^3. Since cell light absorbing characteristics define the light usable for photosynthesis (Dubinsky et al., 1986), larger cells may cope in a better way with low-frequency FL conditions than smaller cells, because they are less susceptible to photoinhibition (Key et al., 2010), and resist to long-lasting high-light intensities applied at low FL frequencies (e.g., FL 5).

Table 3.2: Biomass productivities (in g DW L^{-1} d^{-1}) of *Nannochloropsis gaditana*, *Koliella antarctica and Tetraselmis chui* under continuous light (CL) and flashing light at frequencies of 5 (FL 5), 50 (FL 50) and 500 (FL 500) Hz and a duty cycle of 0.05 using a one- or two-stage cultivation approach. Productivities that do not share the same letter for a given alga in a particular cultivation approach are significantly different from each other.

		Nannochloropsis gaditana	***Koliella antarctica***	***Tetraselmis chui***
One-stage cultivation	CL	0.361 ± 0.003 a	0.117 ± 0.021 a	0.255 ± 0.022 a
	FL 5	0.008 ± 0.000 c	0.042 ± 0.025 b	0.000 ± 0.000 c
	FL 50	0.085 ± 0.009 b	0.032 ± 0.004 b	0.183 ± 0.031 b
	FL 500	0.329 ± 0.046 a	0.106 ± 0.013 a	0.246 ± 0.024 a
Two-stage cultivation	CL	0.686 ± 0.056 a	0.588 ± 0.024 a	0.510 ± 0.029 a
	FL 5	0.431 ± 0.012 b	0.340 ± 0.012 b	0.393 ± 0.002 b
	FL 50	0.602 ± 0.016 a	0.407 ± 0.023 b	0.531 ± 0.029 a
	FL 500	0.653 ± 0.035 a	0.636 ± 0.069 a	0.523 ± 0.032 a

In the two-stage cultivation set up, low-frequency FL inhibited culture´s growth less in comparison with the one-stage approach (Figure 3.25, Table 3.2). This might be due to a higher biomass concentration prior to the application of the FL regime in the two-stage approach (≈2 g DW L^{-1}), allowing for the distribution of the total supplied photons dose to many cells. On the other hand, the one-stage cultures started at a low biomass concentration (0.1 g DW L^{-1}) and all cells received the full light intensity (e.g., I_a= 300 µmol s^{-1} m^{-2}, I_l=6000 µmol s^{-1} m^{-2}). As mentioned by Xue (2011). (Xue et al., 2011) and made evident by the model developed by Jishi et al. (Jishi et al., 2015), the lower the average light intensity, the better the light-use efficiency under low-frequency FL.

3.5.2.2. Biochemical composition

Proteins, carbohydrates and lipids

The effects of FL on proteins, carbohydrates and total lipids were strain dependent. As shown in Supplemental Information, the protein content in *N. gaditana* was mostly affected by the growth stage (F=175.7, $r_{biomass}$=-0.96, p< 0.01) but not by the treatment (F= 1.9, p> 0.05). On the contrary, protein contents in *K. antarctica* were not affected by the growth stage (F=0.9, p>0.05), but by the treatment (F=9.1, p< 0.01), while *T. chui* was affected by both factors (F=84.5 and 13.3, respectively; $r_{biomass}$=-0.84, p<0.01). In *N. gaditana* and *K. antarctica* carbohydrates levels (Figure 3.26b) were affected by the growth stage (F=5.3 and 6.1, $r_{biomass}$ =-0.61 and 0.82, respectively; p<0.05) but not by the treatment (F<1, p>0.05). Contrarily, carbohydrates in *T. chui* were not influenced by the growth stage but by the treatments, with statistically higher values under CL compared to FL 5 treated cultures (p<0.05). The total lipids in *N. gaditana* were affected by the growth stage (F=21.5, $r_{biomass}$= 0.78, p< 0.01) and to a lesser extent by the treatments (F=3.7, p<0.05), where low frequency FL displayed the lowest values. Lipids in *K. antarctica* and *T. chui* were not influenced by the growth stage nor by the treatment (p> 0.05).

Among strains, the protein contents (Figure 3.26a) were on average highest in *N. gaditana* (20.5±1.8%) and *K. antarctica* (23.8±1.9%) cultures, while *T. chui* showed significantly lower contents (14.6±1.9%). Total carbohydrates (Figure 3.26b) were lowest in *N. gaditana* (9.6±2.7%, p< 0.01) compared to *K. antarctica* (28.3±2.9%) and *T. chui* (26.7±2.8%). Total lipids (Figure3.26c) were highest in *N. gaditana* (36.8±2.3%), followed by *K. antarctica* (15.7±2.4%) and *T. chui* (11.6±2.4%, p< 0.05). The overall protein, carbohydrate and total lipid composition matched those previously reported for *Nannochloropsis*, *Koliella* and *Tetraselmis* strains (Camacho-Rodríguez et al., 2015; Dinesh Kumar et al., 2018; Fogliano et al., 2010; Hulatt et al., 2017; Khatoon et al., 2018; Schulze et al., 2017a; Suzuki et al., 2019).

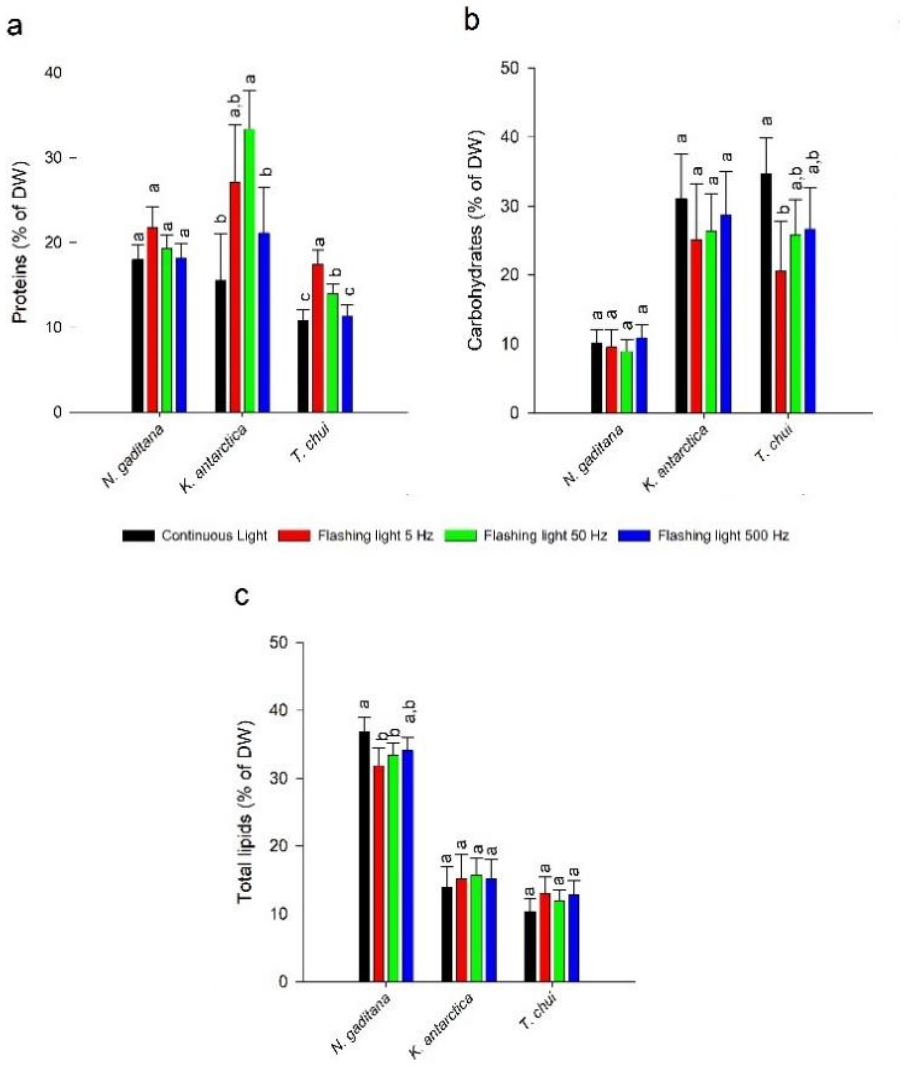

Figure 3.26. Biochemical composition of *Nannochloropsis gaditana*, *Koliella antarctica* and *Tetraselmis chui* exposed to flashing light with a duty cycle of 0.05 and frequencies of 5, 50, 500 Hz at an average light intensity of I_a= 300 µmol s^{-1} m^{-2}. Total proteins (a), carbohydrates (b) and lipids (c) expressed as % in dry weight (DW) are shown by the adjusted means ±95% confidence interval obtained from Tukey´s post hoc test (ANCOVA) for one- and two stage cultivation (n= 3). Treatments that do not share the same letter are significantly different from each other.

Among few published studies testing flashing light on the protein, carbohydrate and lipid contents in microalgae, only minor effects were found for low frequencies (e.g., for *Chlamydomonas reinhardtii*, *f*= 0.5–5 Hz, DC=0.5, or *Scenedesmus obliquus*, f= 5,10,15 Hz, DC= 0.5) (Gris et al., 2014; Kim et al., 2014). In this study, effects of flashing light on proteins, carbohydrates and lipids appeared species-dependent. *K. antarctica* exposed to FL 50, in fact, duplicated its protein content (from 15 to > 30%) when compared to microalgae grown under CL (Figure 3.26a). This may be connected to the fact that low solar irradiance at extreme latitudes makes polar strains more prone to low-light adaption, resulting also to high concentrations of pigments and binding proteins. Polar microalgae may have a higher number of ribosomal proteins to resist cold stress (Lyon and Mock, 2014; Toseland et al., 2013). The high protein levels found in *K. antarctica* cells exposed to low-frequency FL may be thus explained by its natural cold-adaptation and a response to low-light. Unlike *K. antarctica*, the tested *T. chui* strain seemed not to be a true psychrotroph (Schulze et al. 2019) and naturally only contained low amounts of proteins, which could explain the smaller effects of FL 5 and 50 treatments on protein contents. However, future work should be carried out to investigate if similar trends are also observed in other polar strains.

The genus *Nannochloropsis* and *Tetraselmis* are known for their high lipid and carbohydrate contents, respectively, which decrease with increasing protein contents under low-light conditions (Michels et al., 2014; Packer et al., 2011; Solovchenko et al., 2011). Similar responses were also found for *N. gaditana* and *T. chui* cultures exposed to FL 5 and FL 50 (Figure 3.26, Supplemental Information) pointing to a low-light adaption of these cultures as reported for other microalgae exposed to low-frequency flashing light (Grobbelaar et al., 1996). Towards higher frequencies, no differences were found in protein, carbohydrate and lipid levels of the strains compared to CL, indicating no inhibition by high frequency flashing light, as previously reported; e.g., *f*> 100Hz (Yoshioka et al., 2012). In terms of productivity in the two-stage cultivation system, the most promising species for protein production were *N. gaditana* and *K. antarctica* (average: 75.4±4.3 and 77.8±17.1 mg L^{-1} d^{-1}, respectively). *T. chui* and *K. antarctica* were most promising for carbohydrate production (average: 119.8±49.1 and 137.7±14.2 mg L^{-1} d^{-1}, respectively), while lipids (average: 136.7±46.2 mg L^{-1} d^{-1}) were most efficiently produced by *N. gaditana*. Notably, protein productivities were on average 1.1-1.3 times higher for all the tested strains when cultured under flashing light (FL 5 and FL 50) compared to CL, while carbohydrate and lipid productivity decreased by 20-50% (Supplemental Information).

Besides effects of flashing light, growth stage effects were also considered. Protein levels correlated negatively with biomass concentration in *N. gaditana* and *T. chui* (r= -0.96 and 0.85, p< 0.01).This trend can also be described as growth stage-dependent protein drop and a strain-specific accumulation of intracellular carbohydrates or lipids at late growth stages (Brown et al., 1996; Lv et al., 2010; Zhu et al., 1997). A lipid-accumulating trait could be confirmed for *N. gaditana* from a positive correlation between biomass concentrations and lipid contents (r= 0.78, p< 0.01) but a negative correlation with carbohydrate contents (r=-0.61, p< 0.05). On the other hand, the carbohydrate accumulating trait can be confirmed for K. *antarctica* cultures from the positive correlation between biomass in the medium and total carbohydrates (r= 0.8; p< 0.05) but the insignificant correlation with lipids (r= -0.2, p> 0.05) points also to a potential lipid increase of this strain at late growth stages or nutrient deprivation as suggested by Suzuki et al. (Suzuki et al., 2019). Neither a carbohydrate nor lipid accumulating trait could be assessed for *T. chui* as no significant correlation was found for both carbon-binding biocompounds (p >0.05). Nevertheless, a carbohydrate accumulating trait was previously reported for *Tetraselmis* at the late growth stages (Gifuni et al., 2018).

Taken together, our results suggest that processes regulating the biosynthesis of proteins, carbohydrates and lipids depend on the growth stage and the flashing light conditions. The biochemical response to low frequency flashing light suggests a low-light adaption in the tested species, indicated by lower content of carbon-bound compounds (species-specific carbohydrate or lipids) or higher proteins compared to CL. These results confirm the hypothesis of previous experiments with *N. gaditana* in the "quasi-isoactinic" reactor.

Fatty acids

The TFA (Figure 3.27. Supplemental Information) content did not differ under any flashing light treatment compared to CL in all tested strains. Concerning SFA (Figure 3.27b), *N. gaditana* and *K. antarctica* did not show any difference amongst treatments, whereas *T. chui* contained less SFA under the FL 50 treatment. Interestingly, across all algae, the MUFA (Figure 3.27c) fraction tended to be lower in microalgae under FL 5 and FL 50 compared to those under FL 500 and CL. On the other hand, higher PUFA contents (Figure 3.27d) were obtained in all species tested under FL 5 and FL 50 compared to those grown under FL 500 and CL. Among all strains, *N. gaditana* showed the highest productivities of fatty acids (104.3 mg TFA, 16.5 mg SFA, 66.1mg MUFA and 19.7 mg PUFA L^{-1} d^{-1}), confirming that this oleaginous species presented the highest lipid contents among the microalgae tested (Figure 3.26c).

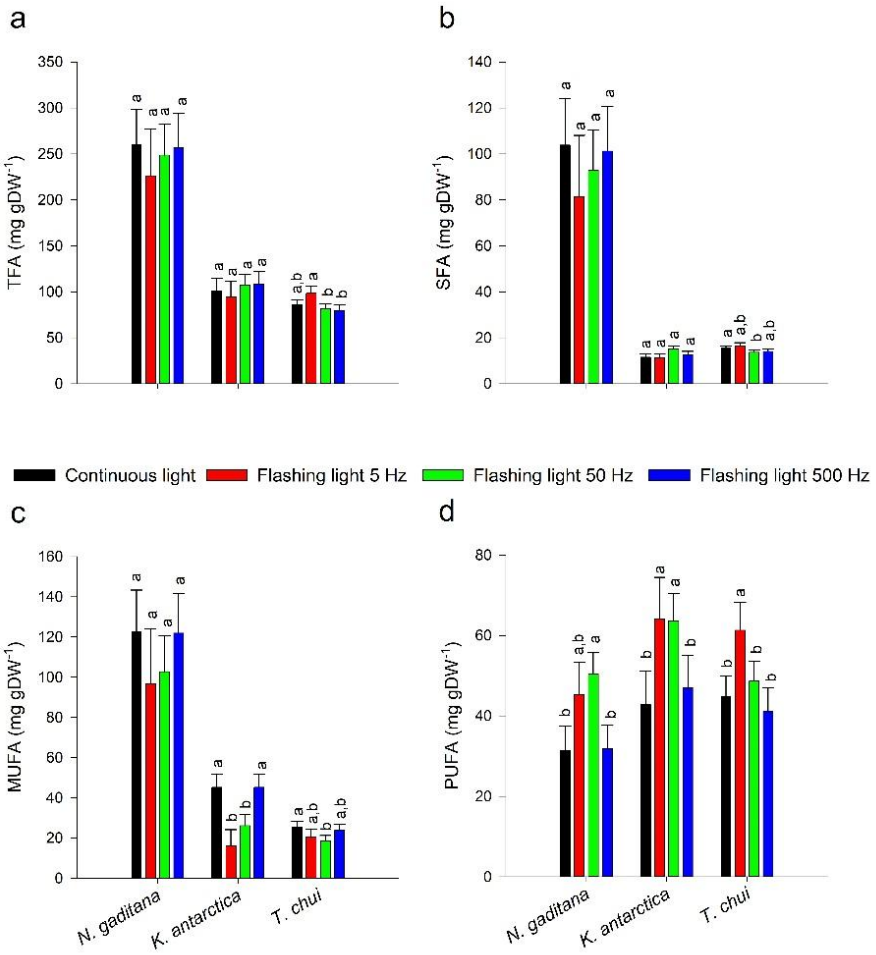

Figure 3.27. Major fatty acid classes for *Nannochloropsis gaditana*, *Koliella antarctica* and *Tetraselmis chui* exposed to flashing light. Contents of total fatty acids, TFA (a), saturated fatty acids, SFA (b), monounsaturated fatty acids, MUFA (c) and polyunsaturated fatty acids, PUFA (d) in dry weight (mg g DW^{-1}) are given as adjusted means ± 95% confidence interval obtained from Tukey´s post hoc test (ANCOVA) for one- and two stage cultivation (n= 3). Treatments that do not share the same letter are significantly different to each other.

The fatty acid profile (given in % of total fatty acids; TFA) differed among species and treatments (Supplemental Information and Figure 3.27). The major fatty acids in *N. gaditana* were C16:0 (palmitic acid, 9-40%), C16:1*n*-7 (23-40%) and C20:5*n*-3 (eicosapentaenoic acid; EPA, 6-41%). In *K. antarctica*, C16:0 (8-13%), C18:1*n*-9 (oleic acid; 9-43%), C18:2*n*-6 (linoleic acid; 3-13%), C18:3*n*-3 (α-linolenic acid; ALA, 10-34%) and C20:5*n*-3 (4-14%) were the most abundant fatty acids. Regarding the fatty acid profile of *T. chui*, mostly C16:0 (6-16%), C16:4*n*-3 (hexadecatetraenoic

acid; 9-16%), C18:1*n*-9 (10-23%), C18:3*n*-3 (11-20%) and C20:5*n*-3 (9-13%) were found. The fatty acid profiles obtained are in accordance with those previously reported for the genera *Nannochloropsis* (Hulatt et al., 2017), *Koliella* (Fogliano et al., 2010; Suzuki et al., 2019) and *Tetraselmis* (Lang et al., 2011; Mohammadi et al., 2015). The strain specific major PUFA usually increased under low frequency flashing light at the expenses of MUFA (Figure 3.27). For example, *N. gaditana* accumulated more C20:5*n*-3 under FL 5 and FL 50, whereas the MUFA, C16:1*n*-4 and 18:1*n*-9, tended to decrease (Figure 3.27 a). Conversely, when exposed to FL 500, this microalga showed a fatty acid profile comparable to cells under CL. Similarly, *K. antarctica* increased the major PUFA, C18:3*n*-3 and C20:5*n*-3, at the expense of the MUFA C18:1*n*-9 under FL 5 and 50, compared to CL and FL 500 (Figure 3.27 b). Lastly, *T. chui* showed higher amounts of C16:4*n*-3, C18:3*n*-3 and C18:4*n*-3 and lower C18:1*n*-9 contents upon exposure to FL 5 and FL 50, whereas no effect on C20:5*n*-3 was observed (Figure 3.27c). Similarly, productivities of C20:5*n*-3 increased in FL 5 and FL 50 treated *N. gaditana* and *K. antarctica* cultures by 1.4-1.9 times, while *T. chuii* showed a 1.4 times higher C18:4*n*-3 productivity compared to CL (Supplemental Information).

Apart from effects caused by flashing light, significant correlations between fatty acids and biomass concentration were observed. For example, biomass concentration correlated positively with TFAs, SFA and MUFA in *N. gaditana* (r= 0.8 to 0.9, p< 0.05) and negatively in *T. chui* (r= -0.8 to -0.9, p< 0.01). Conversely, PUFA contents correlated negatively with biomass concentration in all microalgae (r= -0.5 to -0.8). In *N. gaditana*, the major PUFA C20:5*n*-3 decreased with increasing biomass concentration (r= -0.9, p< 0.01), a stronger effect (F= 48.9) compared to the flashing light treatment effects (F= 5.7, p< 0.01) discussed above (Figure 3.27a, Supplemental Information). Considering *K. antarctica*, the major PUFA C18:3*n*-3 and C20:5*n*-3 tended to decrease with increasing biomass concentration (r= -0.8 to -0.6, p<0.5), an effect that was not as strong (F=0.6 to 8.9) as that of the flashing light treatments (Figure 3.27b, F=9.2 to 21.5). In *T. chui*, a correlation between biomass concentration and C18:3*n*-3 (r= 0.7, p< 0.01) and C18:4*n*-3 (r= -0.9, p< 0.01) levels was stronger (F=26-78) as compared to flashing light treatments (Figure 3.27c, F= 9). Notably, strong effects of the prevailing growth stage on major fatty acids have previously been reported for these genera (Fernández-Reiriz et al., 1989; Hodgson et al., 1991; Suzuki et al., 2019) and where indeed important to consider statistically when evaluating effects of flashing light treatments.

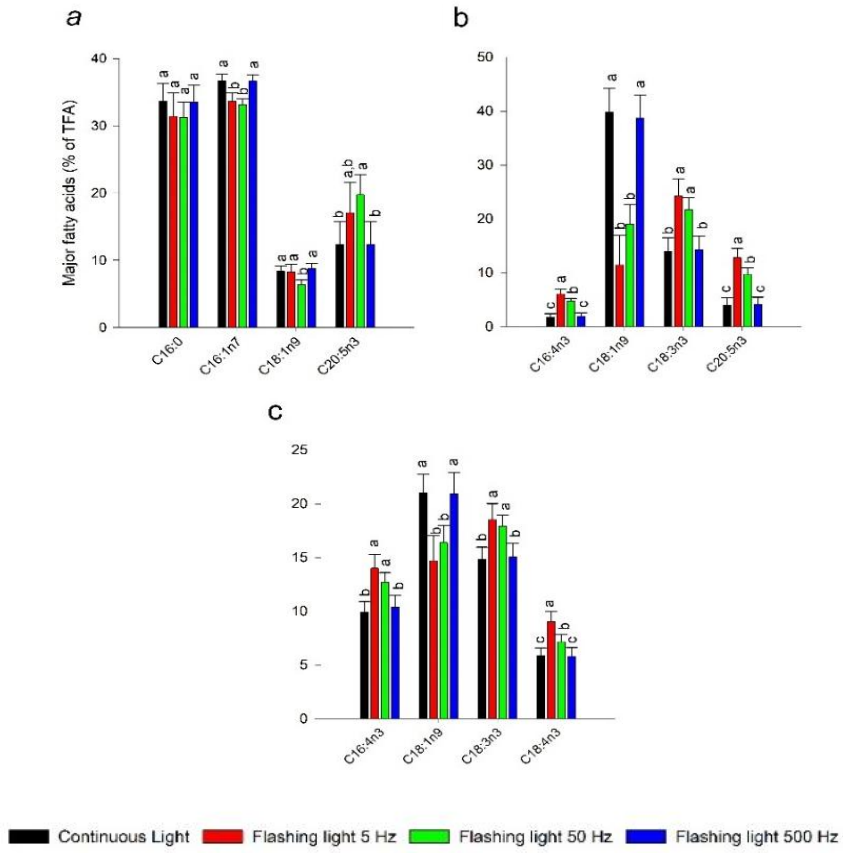

Figure 3.28. Major fatty acids of *Nannochloropsis gaditana* (a), *Koliella antarctica* (b) and *Tetraselmis chui* (c) exposed to flashing light and continuous light. Data given are adjusted means ±95% confidence interval obtained from Tukey´s post hoc test (ANCOVA) for one- and two stage cultivation (*n*= 3). Treatments that do not share the same letter are significantly different to each other. A detailed fatty acid profile is available in the Supplemental Information.

The fact the fatty acid profiles are usually more affected by the biomass concentration than the flashing light treatment in *N. gaditana* and *T. chui* (Supplemental Information) may be linked to a higher biomass productivity and faster transition from one growth stage to another (e.g., lag, exponential and stationary phases), as compared to the slower growing *K. antarctica* (Figure 3.25). Similar species-specific fatty acid shifts under flashing light have been reported previously. For example, *Chlamydomonas reinhardtii* was not affected by flashing light (f= 0.05-5 Hz, DC= 0.5) (Kim et al., 2014), while *Isochrysis galbana* accumulated more phospholipids and docosahexaenoic acid (DHA) when exposed to blue flashing LEDs; e.g., f= 10 KHz, DC= 0.5 (Yoshioka et al., 2012).

Our results indicate that the prevailing growth stage had the strongest effect on the fatty acid profiles of a given microalga (Supplemental Information). Unlike previous suggestions that low frequency flashing light might induce a response similar to that obtained in cells under high light (Schulze et al., 2017b), high PUFA contents usually arise from exposure to low light (Schüler et al., 2017). On the contrary, high light has been related to a decrease in PUFA content (He et al., 2015). These results confirm what found in previous experiments with *N. gaditana* in the "quasi isoactinic" reactor.

Pigments

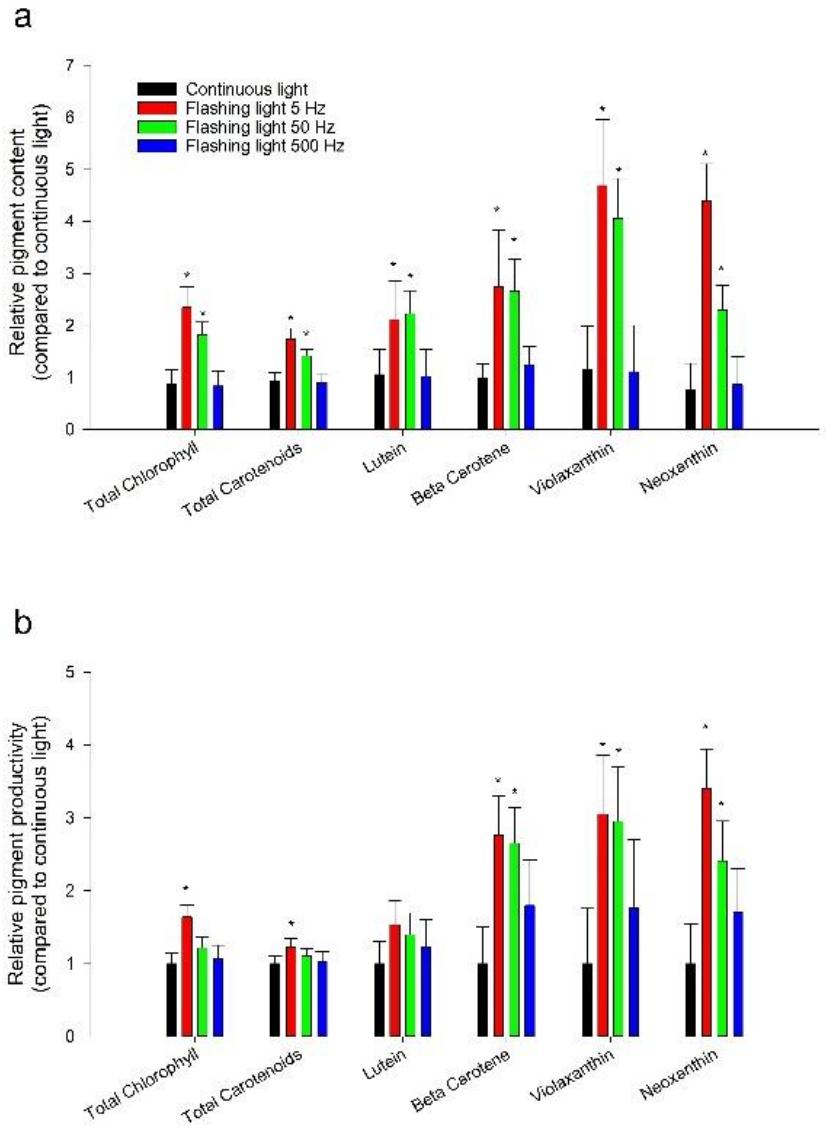

Figure 3.29. Normalised pigment contents (a) and productivities (b) for *Nannochloropsis gaditana*, *Koliella antarctica* and *Tetraselmis chui* exposed to flashing light (f= 5, 50, 500 Hz ; DC= 0.05). Data for each microalgal species were normalised to results obtained under continuous light (= 1) and are given as adjusted mean ±95% confidence interval obtained from Tukey´s tests. Asterisks indicate significant differences compared to continuous light. Neoxanthin was only detected in *T. chui* and *K. antarctica*. Original pigment data are available in the supplementary material (Supplemental Information).

The contents of most pigments were significantly higher in all microalgae exposed to FL 5 and FL 50 as compared to those under CL and FL 500 ($p < 0.05$; Figure 3.29a).

The carotenoids *β*-carotene, violaxanthin, and neoxanthin (in *T. chui* and *K. antarctica*) were on average 3-4 times higher in all microalgae as compared to cultures under CL. Total chlorophyll and total carotenoids as well as lutein increased moderately by 1.7-2.3 times in FL 5 compared to CL treatments (Figure 3.29a). Interestingly, the productivity of the accessory light harvesting pigments neoxanthin and violaxanthin and the photoprotective pigments *β*-carotene and lutein (Mulders et al., 2014) were on average two to three times higher in all microalgae under low frequency flashing light (FL 5 and FL 50) compared to cultures under CL or FL 500 (Figure 3.29b). However, productivities of total carotenoids, chlorophyll and lutein were only slightly enhanced (1.1-1.6 times higher) under FL 5 and FL 50 compared to cells exposed to CL.

Intracellular contents of total chlorophyll and carotenoids ranked among all strains from 1.8-13.8 mg g DW^{-1} and 0.7 to 7.4 mg g DW^{-1}, respectively. The major carotenoid was violaxanthin (0.24-2.07 mg g DW^{-1}) in *N. gaditana*, whereas lutein (0.27-2.05 mg g DW^{-1}) was predominant in *K. antarctica*. *T. chui* contained mostly lutein (0.29-2.2 mg g DW^{-1}) and *β*-carotene (0.40-1.25 mg g DW^{-1}, Supplemental Information). These findings are similar to previous reports for the same algae (Ahmed et al., 2014; Fogliano et al., 2010; Simionato et al., 2013b). Under FL 5, *N. gaditana* was most productive in terms of chlorophyll, total carotenoids and violaxanthin (2.97, 1.34 and 0.45 mg L^{-1} d^{-1}, respectively), whereas *T. chui* was efficient in producing chlorophyll, neoxanthin, lutein and *β*-carotene (2.97, 0.04, 0.47 and 0.35 mg L^{-1} d^{-1}, respectively; Supplemental Information). Conversely, *K. antarctica* was unable to reach any of these productivities.

In accordance with our results, low frequency FL has previously been reported to induce pigments and improve their production (Katsuda et al., 2006). In particular, low frequency FL (e.g., f<30 Hz) often increased pigment production, e.g. in *Chlamydomonas reinhardtii* (f=0.00138-1 Hz, DC=0.5) (Takache et al., 2015) and in *Haematococcus pluvialis (*f=3.49 Hz, DC=0.47; f=0.001–200 Hz, DC=0.17-0.67) (Katsuda et al., 2008; Kim et al., 2006).

The violaxanthin-antheraxanthin-zeaxanthin (VAZ) cycle is an important regulator for the adaptation to different light intensities. Shifts towards the biosynthesis of zeaxanthin occur in plants and algae under high-light stress to avoid photodamage of the photosynthetic apparatus (Jahns et al., 2009). Conversely, violaxanthin accumulates under low-light stress and allows efficient light harvesting (Jahns et al., 2009). Therefore, the presently found increase of violaxanthin levels with decreasing flashing light frequencies may indicate an adaption of cells to low light conditions. In addition, microalgae adapted to low-light also increase their number of thylakoids to harvest light more efficiently (Berner et al., 1989). This requires more PUFA

containing membranes and light harvesting complexes (LHC), which in turn requires more proteins, used by Chlorophytes such as *Koliella* and *Tetraselmis* and Eustigmatophytes (i.e., *Nannochloropsis*) to bind pigments (Basso et al., 2014; Jahns et al., 2009; Sukenik et al., 1992; Thornber, 1986). Therefore, the concomitant increase of proteins (Figure 3.26), PUFA (Figure 3.27, Figure 3.28) and pigments (Figure 3.29) could be attributed to an increase in photosynthetic units in cells treated with low-frequency flashing light which indicates an acclimation of cells to low-light conditions (He et al., 2015; Schüler et al., 2017). Indeed, a low-light adaption was suggested earlier for microalgae exposed to low-frequency FL (Grobbelaar et al., 1996; Yarnold et al., 2016) and was anticipated by previous experiments with *N. gaditana* in the "quasi isoactinic" reactor. However, low frequency flashing light also induced higher levels of β-carotene and lutein, pigments that are usually connected to photoprotection (Mulders et al., 2014) and high-light stress. In the next paragraph further studies will be exposed in order to better understand possible high-light responses of microalgal cells exposed to low frequency FL. Such studies will address metabolic pathways using transcriptomic approaches.

Furthermore, biomass concentration correlated negatively with all the pigments (r= -0.4 to -0.9, p< 0.01-0.7; significance strain-dependent; Supplemental Information). Generally, cells in aging cultures are subject to nutrient depletion or light limitation, leading to downregulation of their photosynthetic activity and decrease in photosynthetic pigments, e.g., chlorophyll, violaxanthin (Oukarroum, 2016). Our statistical analysis revealed that flashing light seemed to counteract this effect significantly because higher pigment contents were found under low frequency FL even after considering the co-variate *biomass concentration*. Therefore, we conclude that the long flash duration (e.g., 1-10 ms) and high instantaneous light intensity (I_l= 6000 μmol s^{-1} m^{-2}) of FL 5 and FL 50 treatments may still stimulate protein, PUFA or pigment biosynthesis even at advanced growth stages where otherwise proteins and pigments decrease or the fatty acids become saturated.

3.6. The transcriptomic of flashing light: the expression levels of selected genes

3.6.1. Materials and Methods

3.6.1.1. Strain and culture conditions

For this experiment *Nannochloropsis gaditana* (CCAP 849/5 Scottish Association for Marine Science, Oban, Scotland), Eustigmatophyceae, was employed. Cultures were maintained in liquid cultures inside Erlenmeyer flasks with F-medium (Guillard, 1975). As growth medium, seawater from the North Atlantic shoreline of Bodø (Norway, 35 ppt) was enriched with a modified F-medium consisting of 5.3 mM $NaNO_3$, 0.22 mM $NaH_2PO_4H_2O$, 35 µM $FeCl_3$ $6H_2O$, 35 µM Na_2EDTA $2H_2O$, 0.12 µM $CuSO_4$ $5H_2O$, 0.078 µM Na_2MoO_4 $2H_2O$, 0.23 µM $ZnSO_4$ $7H_2O$, 0.126 µM $CoCl_2$ $6H_2O$ and 2.73 µM $MnCl_2$ $4H_2O$.

The growth conditions were the same as those in the experiment described in Paragraph 3.5. Tissue culture flasks (Falcon Scientific, Seaton Delaval, UK) with a total volume of 250 mL and 30 mL (light paths: 3.7 and 2.0 cm, respectively) were filled with 200- and 25-mL cultures for one-stage or two-stage cultivation systems, respectively. The cultures were mixed by aeration with humidified and 0.2 µm-filtered air enriched with CO_2 at a flow rate of 160 mL min^{-1}. All algae were cultured during the one-stage batch cultivation for 13 days (n = 3). The two-stage cultivation consisted of a first stage (six days at I_a= 300 µmol s^{-1} m^{-2} under continuous light) and a second stage (five days under the FL treatments). Optical density at 540 nm (OD_{540}) was measured daily (n = 4) for each algal culture using a 96-well plates (Tecan Sunrise A-5082, Männedorf, Switzerland).

3.6.1.2. Flashing light set up

The lighting conditions adopted in this experiment are the same as in experiment of Paragraph 3.5.
The same array of 36 warm-white LEDs (2700 K, 13 W, MHDGWT-0000-000N0HK427G-SB01, emission spectrum provided in Figure 3.24) was employed. The applied flashing light conditions were: continuous light and flashing light with a duty cycle of 0.05 with the frequencies of 5, 50 and 500 Hz. The time-averaged light intensity was I_a= 300 µmol s^{-1} m^{-2} in all conditions, which corresponded to an instantaneous flash intensity of I_l= 6000 µmol s^{-1} m^{-2}.

3.6.1.3. RNA extraction

Total cell RNA from cultivations of *N. gaditana* at a concentration of $1x10^6$ cells/mL was extracted using the E.Z.N.A® total DNA/RNA isolation kit (Omega Bio-tek, Inc., USA). Samples of *N. gaditana* at different conditions of flashing lights were centrifuged at 2000xg, 4 °C for 5 min, the supernatant was discarded and the pellet was stored at -80 °C for at least 24 hours. After this time, 700 uL of lysis buffer provided by the E.Z.N.A® total DNA/RNA isolation kit was added to the sample, and then the cells were disrupted using a bead mill (Bertin technologies, Precellys Evolution, France) using a mixture of 0.1 mm glass beads and 1.4 mm ceramic beads. Samples were centrifuged at 10000xg, 4 °C for 10 min. The supernatant was used for RNA isolation following the manufacturer's protocol.

3.6.1.4. cDNA synthesis

Reverse transcription reactions were performed using the SuperScript™ IV VILO™ Master Mix with ezDNase enzyme (ThermoFisher Scientific) following the manufacturer's protocol. Briefly, a total amount of 1.4 μg of RNA from *N. gaditana* was treated with the ezDNase enzyme (SuperScript™ IV VILO™ Master Mix with ezDNase enzyme, ThermoFisher Scientific) to remove any contaminating DNA. The synthesized cDNA, diluted 1:10 with deionized water (Invitrogen™ Nuclease-Free Water, Fisher scientific, USA), was then used as a template in quantitative PCR reactions.

3.6.1.5. Quantitative (q) PCR reactions

Primers were designed using the PearlPrimer (Marshall, 2004). Sequence data corresponding to the specific targets were retrieved from the database (http://www.nannochloropsis.org/). Primers were designed flanking the intron exon junction to make it specific to the transcripts and avoid binding to the genomic DNA. The qPCR reactions were performed by mixing 5μL of FastStart Universal SYBR Green Master mix (Rox) (Roche Molecular Systems, Inc., USA) with 1 μL of the primer mix (comprising of forward and the reverse primers) at a concentration of 300 nM and 4 μL of the cDNA. The conditions of the thermal cycling were: 95 °C for 600 s of preincubation, followed by 40 cycles of denaturation at 95 °C for 10 s, annealing/extension at 60 °C for 30 s. A melt curve analysis for each sample was performed to check the specificity of the primers. The target gene data was normalized using the normalization factor calculated based on the expression of the 2 most stable reference genes. All the calculations were performed using genorm (Vandesompele et al., 2002). The list of primers and the accession numbers are listed in Supplemental Information.

3.6.1.6. Statistical analysis

Saphiro-Wilk test was used to validate the normal distribution of the data, and Brown-Forsythe test was applied to confirm the homogeneity of the variance amongst treatments. One-way analysis of variance (ANOVA) and *post-hoc* Tukey's multiple comparison test was applied to each set of experiments in order to determine statistical differences among treatments. *P* values smaller than 0.05 were considered statistically significant.

3.6.1.7. Photosynthetic analysis

The photosynthetic performance of cultures was measured by chlorophyll *a* fluorescence using a pulse-amplitude modulated (PAM) fluorometer (Diving-PAM, Walz GmbH, Effeltrich, Germany). For the measurements, algal samples from the cultures were adjusted to 1.0 g DW L^{-1} using seawater (35 ppt) and 1.2 mL was transferred into a 3 mL glass cuvette (1.0 cm light path, VWR, Oslo, Norway) and mixed by a magnet stir. After 1 h under dark, minimum (F_0) and maximum fluorescence (F_m) yields were measured and maximum PSII-quantum yields (F_v/F_m) were calculated (Schreiber et al., 2012):

$$\frac{F_v}{F_m} = \frac{(F_m - F_0)}{F_m} \qquad \text{3-X}$$

Subsequently, a saturation pulse was applied (>9,000 µmol $s^{-1}m^{-2}$, 0.6 s) and effective PSII-quantum yields were measured from minimum (F) and maximum fluorescence (F_m') yields of the algal samples exposed to a series of incrementally increasing actinic light intensities (41-1452 µmol $s^{-1}m^{-2}$). The test light intensities were provided every 10 s Finally, the effective PSII quantum yields were calculated:

$$\frac{Fv'}{Fm'} = \frac{(Fm' - F)}{Fm'} \qquad \text{3-XI}$$

Relative photosynthetic electron transport rates (ETRs) were calculated by multiplying the effective PSII-quantum yields with the incident actinic light intensities. These data sets plotted against the incident actinic light intensities were fitted to the model of Jassby and Platt (1976) using *R* version 2.15 (R Core Team) to estimate the maximum ETRs (ETRmax), the light saturation points of photosynthesis (E_k), and the initial slopes of the ETR vs irradiances curves (α_{ETR}).

3.6.2. Results and discussion

3.6.2.1. Microalgae growth curves

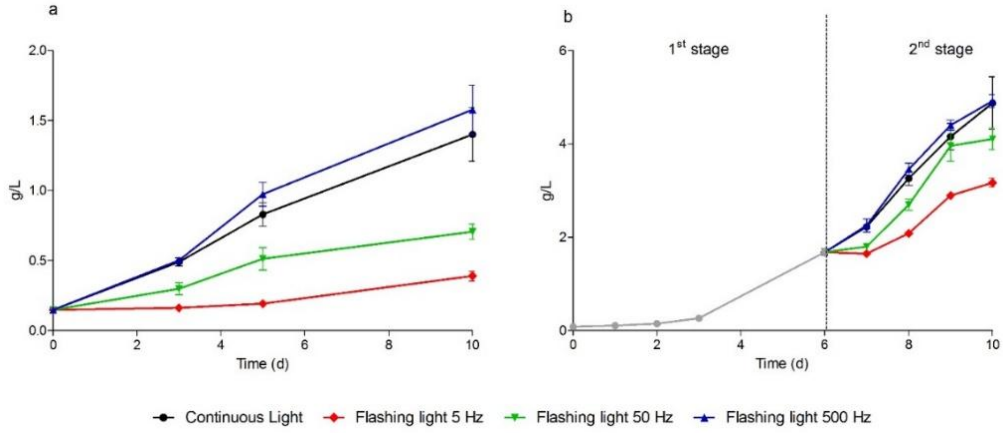

Figure 3.30: Growth curves of miroalgae grown in a one- (a) and two- (b) stage batch culture under different flashing light conditions. *Nannochloropsis gaditana* was cultured under continuous light or flashing light with a duty cycle of 0.05 and frequencies of 5, 50, 500 Hz at an average light intensity of I_a= 300 µmol s^{-1} m^{-2}. Data points with error bars at each day are shown as mean ±SD (n=3).

Figure 3.30 shows the growth curves of *Nannochloropsis gaditana* grown in three flashing light (FL) conditions and a continuous light (CL) control. The adopted flashing light varied in frequency (FL 5, 50 and 500 Hz), while the duty cycle (DC) was kept constant (0.05) and the average light intensity amongst all the light conditions was the same. The algae were grown with two cultivation systems: the first one, in Figure 3.30a, was conducted in one step by lighting the cultures with flashing lights from the start of the cultivation. The second one, in Figure 3.30b, was conducted in two steps: in the first one, the cultivation was illuminated with continuous light. Then, it was split up in four cultures and each of them was illuminated with the same lighting conditions as the one-step cultivations. In both cases, cells showed a higher growth performance in CL and FL 500 Hz compared to FL 50 Hz. FL 5 Hz showed the worst growth performance. In fact, the concentrations reached in CL wew 1.40±0.33 and 4.87±0.97 g/L in one- and two-step cultivation approaches respectively and in the FL 500 Hz is 1.57±0.30 and 4.92±0.25 g/L. In the FL 5 Hz the reached concentrations were instead 0.39±0.06 and 3.17±0.16 g/L, while in FL 50 Hz 0.71±0.09 and 4.11±40 g/L, in one- and two-step cultivation approaches respectively.

These results confirm those of previous experiments (Paragraph 3.5) in which the same cultivation approach was adopted.

3.6.3. Photosynthetic efficiency analysis

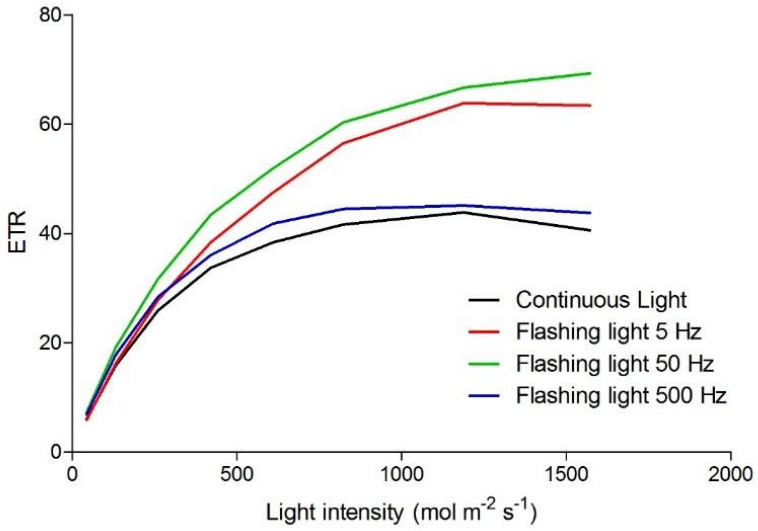

Figure 3.31: Photosynthesis-irradiance (P-I) curves of *Nannochloropsis gaditana* grown under three flashing light (FL) conditions (FL 5, 50, 500 Hz) and a continuous light (CL) control.

Figure 3.31 shows the photosynthesis-irradiance (P-I) curves of *N. gaditana* grown under three flashing light conditions (FL 5, 50 and 500 Hz) and a continuous light control. This analysis is based on the fluorescence of chlorophyll a under different light intensity that can be related to the Electron Transfer Rate (ETR), a measurement of the photosynthetic efficiency of the cell (M. Gilbert et al., 2000). The data set of measurements obtained through the PAM fluorometer was employed in the model of Jassby and Platt (Jassby and Platt, 1976) to get the parameters indicated in Table 3.3.

Table 3.3: Parameters obtained from the modelling of the photosynthesis-irradiance (P-I) curves. Parameters that do not share the same letter in a particular lighting condition are significantly different from each other.

	α	Fv'/Fm'	Etr_{max}	E_k
CL	0.158 a	0.353 b	51.563 b	433.658 a
FL 5 Hz	0.143 a	0.358 b	60.950 ab	477.586 a
FL 50 Hz	0.171 a	0.415 a	72.093 a	459.726 a
FL 500 Hz	0.177 a	0.386 ab	53.850 b	400.771 a
Pr > F	0.000	0.000	0.000	0.001
Significant	Yes	Yes	Yes	Yes

The parameter α is the initial slope of the P-I curve and a measurement of the maximum quantum yield of the PSII (Matthias Gilbert et al., 2000), while Etr_{max} represents the maximum photosynthetic capacity of the cells in that condition (Matthias Gilbert et al., 2000). Fv'/Fm' indicates the effective quantum yield of PSII (Serôdio et al., 2007) and E_k the light-saturation parameter of the P-I curve (Serôdio et al., 2007).

The P-I curves of Figure 3.31 show that cells grown in FL 5 and 50 Hz have a higher photosynthetic efficiency compared to the other two analyzed conditions. By looking, at the α parameter in

Table 3.3, no statistical differences are appreciated. This may indicate that the maximum quantum yield of the PSII is the same amongst all the conditions. The situation of the Fv'/Fm' is slightly different. It indicates, in fact, a significantly higher effective quantum yield of PSII in FL 50 Hz in comparison with the other conditions. These results are interesting as they indicate that the effective quantum yield is higher in FL 50 Hz, although the maximum quantum yield of the PSII is the same. Also the ETR_{max} values indicate that the maximum photosynthetic capacity is higher in FL 50 and 5 Hz compared to other conditions. Oppositely, the E_k values indicate that there is no difference in light saturation amongst the various lighting conditions.

These results may seem in contradiction with the growth curves, in which a lower growth performance is observed for low-frequency FL conditions (Figure 3.30). However, the energy obtained thanks to photosynthesis does not necessarily flow into the Calvin cycle, therefore not necessarily brings to the formation of carbon-related material (James, 1934). Probably, the excess of energy is partially dissipated and partially employed for the production of biocompounds.

3.6.4. Transcriptomic analysis

In order to have a picture about the transcriptional regulation of *N. gaditana* exposed to different flashing light conditions, analysis of mRNA expression have been performed. RNA of the cell was retro-transcribed and the obtained C-DNA was amplified in a quantitative way with selected primers. These allowed to amplify a list of key genes chosen for being essential in pathways of interest.
Results of these analysis are reported below.

Reference genes

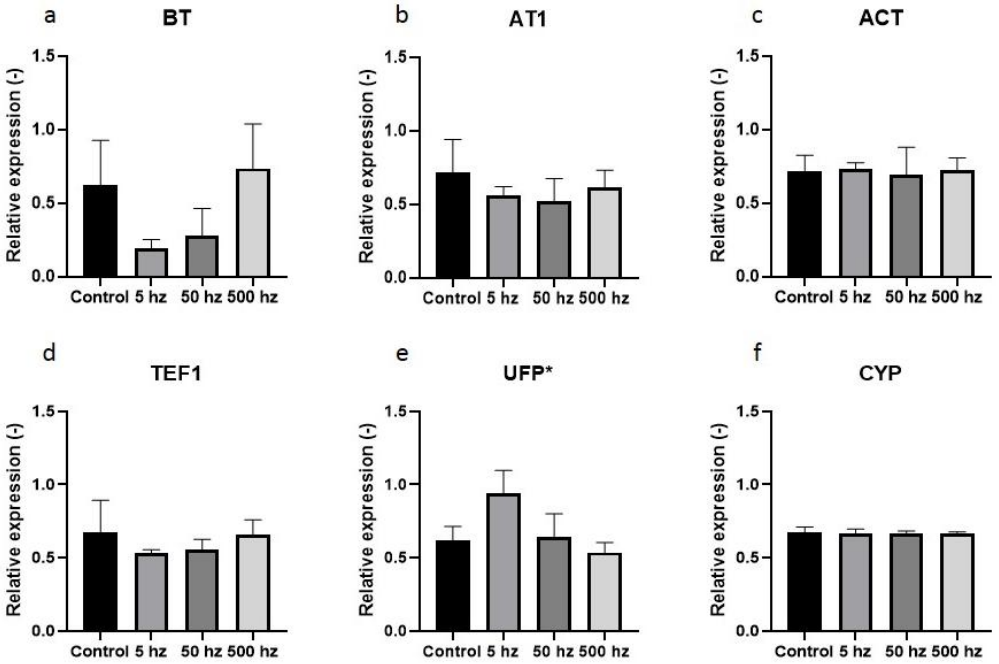

Figure 3.32: Relative expression of selected reference genes in *N. gaditana* exposed to three flashing light conditions and a control. The results are expressed as means (n=3) and error

The relative levels of expression of selected reference genes is reported in Figure 3.32 a-f. Figure 3.32 a shows the expression of *bt* (beta tubulin). Despite statistical analysis does not indicate a statistically significant difference, the expression trend is clear: in FL 5 and 50 the expression is downregulated compared to the control, while it is the same as CL in FL 500. No statistical differences but a similar trend is observed in the *at1* gene and in the *tef1* gene (Figure 3.32b, c, e). Gene *at1* codes for a DNA-binding protein that has the role of a transcriptional factor and, in rice, affects the expression of genes involved in the differentiation of the cells (Meijer et al., 1996). The gene

tef1 codes for an enhancer of transcription (Regad et al., 1995) and in *Arabidopsis thaliana* it may have its key role in the cell cycle, by controlling the expression of genes encoding components of the translational apparatus or involved in regulating the redox state of the cell. The opposite level of expression with a statistical difference is observed in the gene *ufp*, the ubiquitin, (Figure 3.32e) whose functions have been reviewed (Varshavsky, 2017). The overexpression of this gene in the FL 5 Hz suggests a high turnover of proteins in this lighting condition. The other two analysed genes, *act* and *cyp* have a constant level of expression amongst the flashing conditions (Figure 3.32 c, f). They code for the actin and cyclophilin proteins and are used as reference genes in quantitative real time PCR (Niu et al., 2014). In conclusion, although the analysis gave noteworthy indications regarding the expression of some genes, not all the selected genes can be used as reference, because the expression levels vary amongst the analysed conditions.

Genes related to photosynthesis and photoprotection

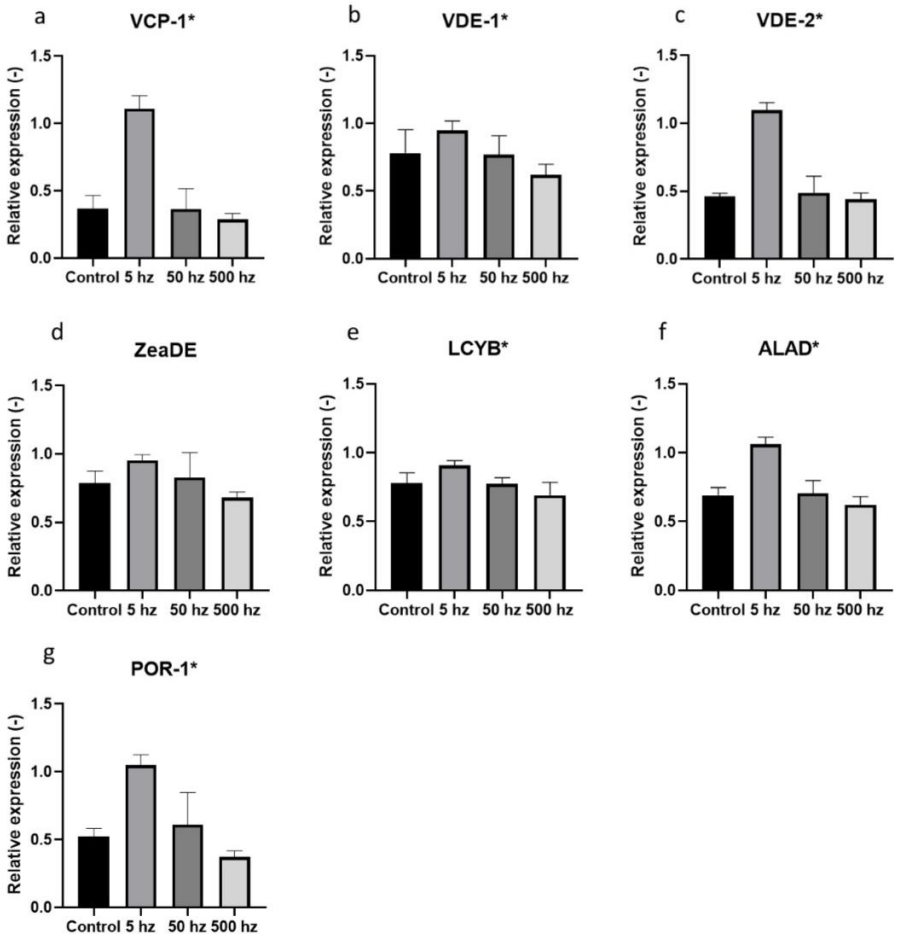

Figure 3.33: Relative expression of selected genes related to photosynthesis and photoprotection in *N. gaditana* exposed to three flashing light conditions and a control. The results are expressed as means (n=3) and error bars report standard deviation. Asterisk indicates a statistical difference between the expression levels.

The levels of expression of relevant genes related to photoprotection and production of carotenoids and photosynthesis were analysed and results are reported in Figure 3.33. All the analysed genes excluding *zeaDE* had statistical differences in the expression levels. The gene *vcp* codes for the violaxanthin–chlorophyll a binding protein, in Figure 3.33a, that is the major light harvesting complex (LHC) of *N. gaditana*. It binds chlorophyll *a* and the carotenoids violaxanthin and vaucheriaxanthin and is involved in triplet–triplet energy transfer (TTET), occurring between chlorophyll and carotenoid molecules to dissipate energy in light stress conditions (Carbonera et al., 2014; Keşan et al., 2016; Litvín et al., 2016). This gene is overexpressed in the FL 5Hz condition, indicating a strong light stress that may be

caused by the high light energy (I_l=6000 μmol m^{-2} s^{-1}) for the light flash period (t_l) of 10 ms, against the 1 and 0.1 ms of the FL 50 and 500 Hz light conditions. Because *vcp* has a fundamental role in photoprotection (Carbonera et al., 2014), these results are related with the previous experimental ones, in Paragraph 3.5 in which symptoms of both high- and low-light adaption were found in algae grown under low-frequencies flashing lights (5 and 50 Hz). In Figure 3.33b, c and d expression of *vde* and *zeaDE* genes expressing violaxanthin de-epoxidase and zeaxanthin epoxidase are reported. These enzymes are involved in another photoprotection mechanism, the xanthophyll cycle, protecting the cells from the oxidative stress that occur under high-light stress (Latowski et al., 2011). All of them are more expressed in FL 5 Hz compared to all the other conditions while *vde-2* and *zeaDE* are overexpressed also in FL 50 while the level of expression in the control and in FL 500 is the same. These results match again the ones found in the previous experiments of Paragraph 3.5 as FL 5 and 50 show symptoms of high-light adaption.

The expression of the gene *lcyB*, coding for the enzyme lycopene β cyclase, is reported in Figure 3.33e. The gene codes for a key enzyme in the biosynthetic pathway of isoprenoids that in particular catalyses the formation of the bi-cyclic β-carotene from the linear, symmetrical lycopene (Cunningham and Gantt, 1998; Paniaqua-Michel et al., 2012). This gene is slightly overexpressed in FL 5 and 50, matching the results of previous experiments in which a higher level of carotenoids on DW was found under low-frequency flashing light conditions (Paragraphs 3.4 and 3.5). However, the marked difference in composition of carotenoids in the low-frequency flashing light conditions previously found may be explained with the differential regulation of other levels in the biosynthetic pathway of isoprenoids. The accumulation of carotenoids can not be directly linked to a low- or a high-light adaption because some carotenoids have been related to a protective function against the oxidation caused by the high-light (Varela et al., 2015) while some others are linked to low-light adaption (Schüler et al., 2017). The accumulation of both groups of carotenoids has been observed in other experiments (Paragraph 3.5) and this validates the hypothesis that algae grown under low-frequency flashing light show both a low- and a high-light adaption.

The expression of genes *alaD* and *por-1* is shown in Figure 3.33f and g. They code for the ALA dehydratase and for the protochlorophyllide oxidoreductase, respectively involved in the tetrapyrrole and in the chlorophyll synthesis (Tanaka and Tanaka, 2007). Both the genes are overexpressed in the FL 5, matching the results of previous experiments (Paragraphs 3.4 and 3.5) in which an accumulation of chlorophyll was observed in low-frequency flashing light conditions.

The expression of genes related to photosynthesis and photoprotection of algae grown under several flashing light conditions shows a double low-and-high light adaption, confirming the results previously observed concerning the accumulation of biocomponents in the biomass.

Furthermore, the overexpression of these genes related to photoprotection, production of carotenoids and production of chlorophyll in low-frequency flashing light answers to the question about the destination of the excess energy provided by the increased photosynthetic efficiency discussed in Paragraph 3.6.3.1.

Lipid synthesis (FA synthetase components)

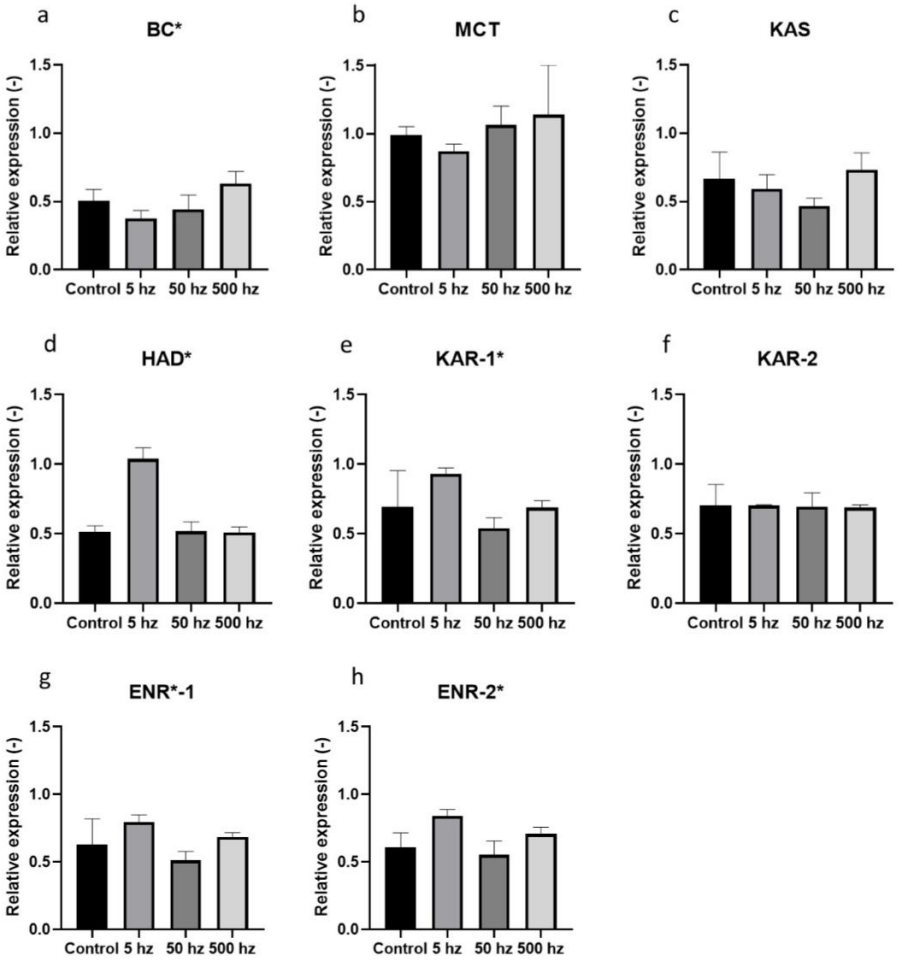

Figure 3.34: Relative expression of selected genes related to de novo lipids biosynthesis in *N. gaditana* exposed to three flashing light conditions and a control. The results are expressed as means (n=3) and error bars report standard deviation. Asterisk indicates a statistical difference between the expression levels.

The levels of expression of relevant genes involved in de novo fatty acid biosynthesis were analysed and results are reported in Figure 3.34. The differences in the expression levels are significant for all the analysed genes excluding *mct*, *kas* and *kar-2*. The gene *bc*, in Figure 3.34 a, codes for the biotin carboxylase, an enzyme that is part of the heteromeric form of the *ACCase* (acetyl-CoA carboxylase), located in the chloroplast of *Nannochloropsis* and responsible for the first step of the de novo synthesis of fatty acids. In fact, it carboxylates acetyl-CoA to produce malonyl-CoA (Li-Beisson et al., 2019; Mühlroth et al., 2013). The gene *mct*, in Figure 3.34b, codes for the malonyl-CoA ACP malonyltransferase that converts malonyl-CoA to malonyl-acyl carrier protein (ACP) (Li-Beisson et al., 2019). These genes are slightly less expressed in FL 5 condition, coherently with the previous results in which lipid content was lower in this condition. The other analysed genes, shown in Figure 3.34c-h, code for enzymes that constitute the Fatty Acid Synthase (FAS) complex. They are the 3-ketoacyl-ACP synthase (*kas*), the hydroxyacyl-ACP dehydrase (*had*), the ketoacyl-ACP reductase (*kar*) and the enoyl-ACP reductase (*enr*) (Li-Beisson et al., 2013). The complex ligates Malonyl-ACP to an acetyl-CoA molecule to form a 3-ketoacyl-ACP by ketoacyl-ACP synthase, while releasing a molecule of CO_2. The 4-carbon 3-ketoacyl-ACP is subsequently reduced (by ke- toacyl-ACP reductase, *kar*), dehydrated (by hydoxyacyl-ACP dehy- drase, *had*), reduced again (by enoyl-ACP reductase, *enr*) until finally a 6-carbon-ACP is formed. FL 5 condition shows an overexpression of all of these genes excluding *kas* and *kar-2*. This result appears to be in contrast with the scarcity of lipids found in the biomass grown in this lighting condition, but it is possible to hypothesize that the control of the expression may intervene at other levels of regulation.

Lipid synthesis (FA trafficking and desaturation)

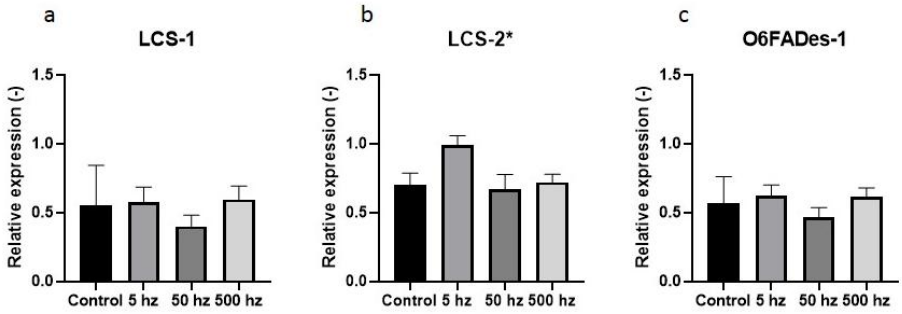

Figure 3.35 Relative expression of selected genes related to fatty acid trafficking and desaturation in *N. gaditana* exposed to three flashing light conditions and a control. The results are expressed as means (n=3) and error bars report standard deviation. Asterisk indicates a statistical difference between the expression levels.

The levels of expression of genes involved in fatty acid trafficking and desaturation were analysed and results are reported in Figure 3.35. Only the expression of *lcs-2* shows statistical differences. In Figure 3.35 a and b the levels of expression of the genes *lcs* (long-chain acyl-coenzyme A synthetase) are shown. The genes of the *lcs* family have been demonstrated to be involved in lipid movement between the endoplasmic reticulum and the plastid in *Arabidopsis* (Jessen et al., 2015); in fact, they activate non-esterified FAs to their CoA esters following their release from a membrane lipid or TAG. Gene *lcs-1* shows no statistical differences in the expression levels, while *lcs-2* is upregulated in FL 5. Although they were identified in algae, the putative orthologues of this family and their functions in FA export have not been yet examined (Li-Beisson et al., 2019), so it is complex to find and explanation for the different levels of expression between *lcs-1* and *2*. The overexpression of *lcs-2* anyway suggests that there is some trafficking of old fatty acids in the low-frequency flashing light conditions, but the response is not clear. In Figure 3.35 c the expression of the gene *o6faDes-1* is shown. It codes for a Δ6 desaturase responsible of making a double bond in both the ALA (α-linoleic acid) and the LA (Linoleic acid) (Khozin-Goldberg et al., 2002; Ma et al., 2011; Wiktorowska-Owczarek et al., 2015) and being therefore a bottle-neck for the creations of all the PUFAs. The differences in expression levels of this gene in the three flashing light conditions are not large enough to explain the accumulation of PUFAs previously observed in FL 5 and 50 Hz, therefore there might be another levels of regulation, for example an overexpression of another desaturase downstream in the biosynthetic chain.

Glycerolipids synthesis

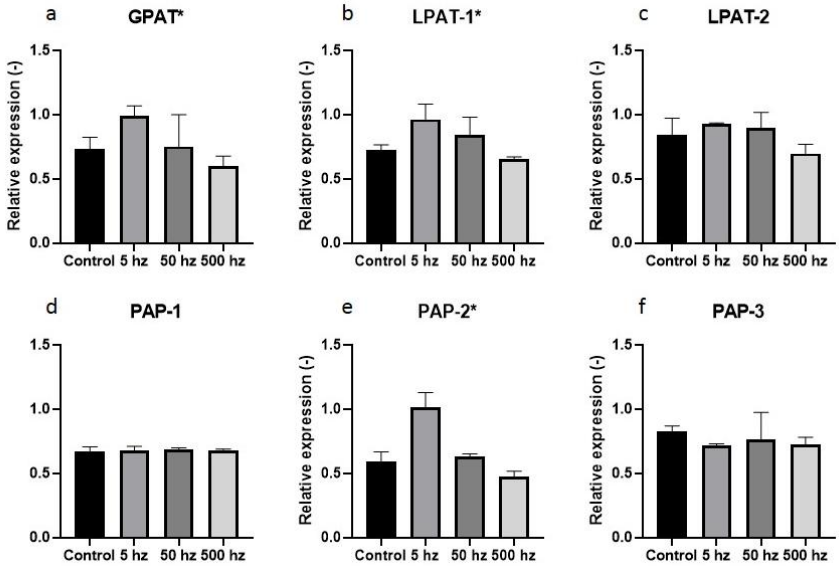

Figure 3.36: Relative expression of selected genes involved in the Kennedy pathway in *N. gaditana* exposed to three flashing light conditions and a control. The results are expressed as means (n=3) and error bars report standard deviation. Asterisk indicates a statistical difference between the expression levels.

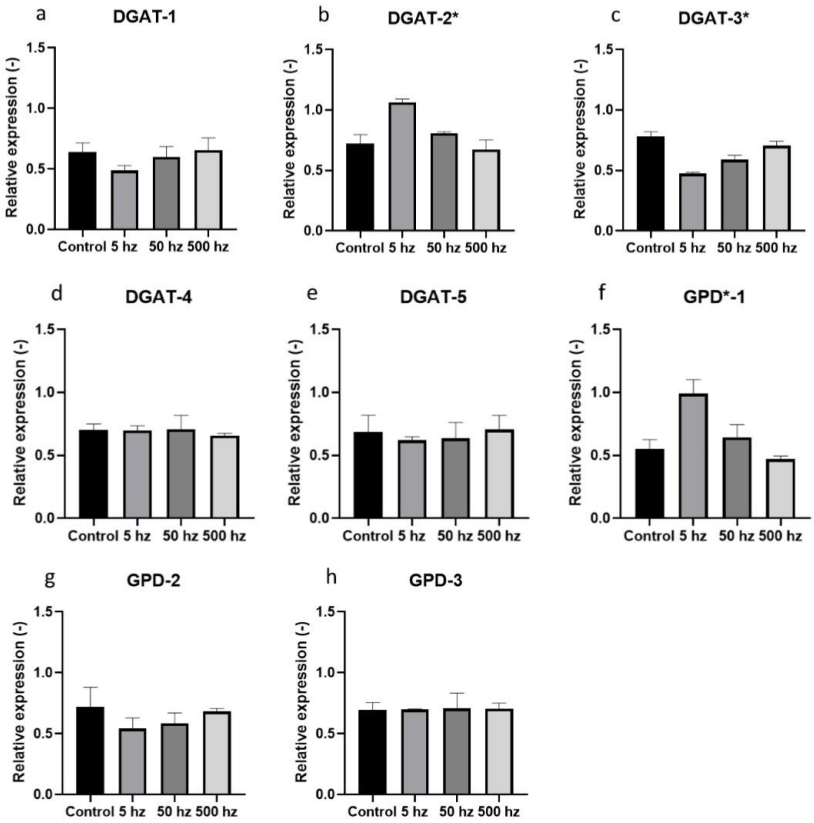

Figure 3.37: Relative expression of selected genes involved in the Kennedy pathway and of glycerol 3 phosphate dehydrogenase (GPD) in *N. gaditana* exposed to three flashing light conditions and a control. The results are expressed as means (n=3) and error bars report standard deviation. Asterisk indicates a statistical difference between the expression levels.

Glycerolipids are synthetized through an ensemble of reactions known as Kennedy pathway. The expression levels of the enzymes of this pathway and the ones of the *gpd* (glycerol 3 phosphate dehydrogenase) are reported in Figure 3.36 and Figure 3.37. The action of the GPD enzyme catalyses the creation of the glycerol backbone for triacylglycerol (TAG) assembly (Li-Beisson et al., 2019). By looking at the results of Figure 3.37 f, g and h, a statistical difference in the expression levels is observed only in *gpd*-1, which is more expressed in FL 5 and 50. This result seems to be in contrast with the decreased level of lipids found in the same conditions of previous experiments (Paragraph 3.5). The isoforms *gpd*-2 and *gpd*-3, that have constant expression levels, have been demonstrated, in *Chlamydomonas reinardtii*, to be inducted in conditions of salt or nutrient stress (Goodenough et al., 2014). The cells of this experiment grew in nutrient abundance and this may be the reason why they are equally expressed.

The Kennedy pathway involves *gpat* (acylCoA:glycerol-3-phosphate acyltransferase), *lpat* (acyl-CoA:lysophosphatidic acyltransferase), *dgat* (diacylglycerol acyltransferase) and *pap* (phosphatidic acid phosphatase). The pathway starts with the acylation of Glycerol 3 phosphate (G3P) by the enzyme GPAT. Then, there is another acyl-CoA dependent acylation catalysed by LPAT that forms the phosphatidic acid (PA). PAP catalyses the release of phosphate to produce diacylglycerol (DAG). The final step is the acylation of DAG to produce TAG, driven by DGAT (Cagliari et al., 2011). GPAT, in Figure 3.36a, shows a statistical difference of expression in the FL 5 and 50 Hz, and this is again in contrast with the lower lipid content found in these conditions of previous experiments (Paragraph 3.5).

In Figure 3.36b and c the expression levels of *lpat 1* and *2* are shown. The only one to show a significant difference is *lpat 1*, in which the expression is augmented in the FL 5 and 50 Hz; this may be correlated with the fact that amongst the several isoforms of LPAT in *Nannochloropsis* only a few were demonstrated to change their level of expression in nitrogen deprivation (Li et al., 2014).

In Figure 3.36d, e and f the expression levels of *pap* genes are shown. The only one that has a statistical difference, and that shows a higher level of expression in FL 5 and 50, is *pap 2*. This genes, in *C. reinhardtii*, has been found to be the only isoform to be complete and was demonstrated to have a correlation with lipid accumulation (Deng et al., 2013). In Figure 3.37 a-e the expression levels of *dgat* are shown. The only two genes to have a statistical difference are *dgat 2* and *3*, while the others show a constant expression amongst the light conditions. In plants, DGAT 1 is the major enzyme for seed oil accumulation, while DGAT2 has a relevant role in the accumulation of unusual fatty acid. The function of the other isoforms is not clear (Cagliari et al., 2011). The expression levels of *dgat 2* is opposite compared to *dgat3*, being overexpressed in FL 5 Hz. This pattern may give some insights on the accumulation of specific fatty acids, such as some PUFAs.

Summarizing, the expression levels of the genes related to the synthesis of TAG are tendentially overexpressed under low-frequency flashing light conditions compared to high-frequency and continuous light. This could mean that there are more TAGs in cells grown under these conditions, even though experimental results of previous works (Paragraph 3.5) showed a decrease of lipids compared to the other two conditions. Anyway, in that experiment only the amounts of total lipids was analysed, but not amount of TAGs. This may bring to the conclusion that, although a decrease of total lipids, under low-frequency flashing light there may be an accumulation of TAGs.

Starch synthesis

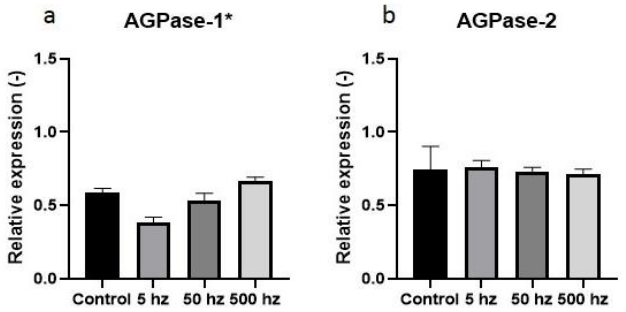

Figure 3.38: Relative expression of selected genes involved in the starch synthesis in *N. gaditana* exposed to three flashing light conditions and a control. The results are expressed as means (n=3) and error bars report standard deviation. Asterisk indicates a statistical difference between the expression levels.

The expression levels of genes *AGPase 1* and *2*, coding for the ADP-glucose pyrophosphorylase are shown in Figure 3.38a and b. This gene is essential for the synthesis of starch and catalyses the reaction of glucose-1-phosphate with ATP to form ADP-glucose and pyrophosphate (Ho et al., 2014). The isoform 1 of the gene is less expressed in FL 5 and 50 Hz, while the isoform 2 has not difference in expression levels. In previous experiments the carbohydrates levels was found to not vary in *N. gaditana*, but it varied both in *Koliella antarctica* and in *Tetraselmis chui*. The expression levels of *AGPase-1* could be correlated with these findings.

Nitrate transport and assimilation

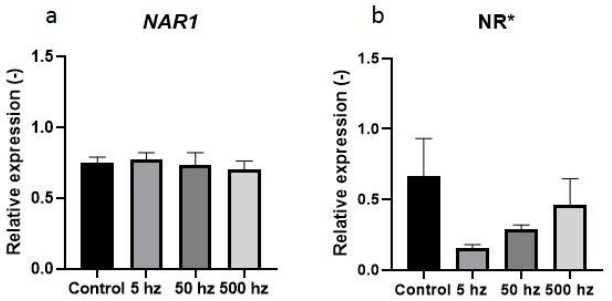

Figure 3.39: Relative expression of selected genes involved in nitrate transport and assimilation in *N. gaditana* exposed to three flashing light conditions and a control. The results are expressed as means (n=3) and error bars report standard deviation. Asterisk indicates a statistical difference between the expression levels.

In Figure 3.39 the relative expression of two genes related to the transport and metabolism of nitrogen are reported. In Figure 3.39a, the levels of expression of the gene *nar1* are shown and they are found to be stable across all the light conditions. The gene *nar1* codes for the Nitrate Assimilation-Related component 1 and has the role of nitrite transporter (Sanz-Luque et al., 2015). The constant expression level suggests that there are no differences among the different lighting conditions in recruiting nitrites. In Figure 3.39 b the expression levels of *nr* (nitrate reductase) is reported and has statistical differences. It is responsible for the first step of nitrogen transport, reducing nitrate to nitrite (Kilian et al., 2011), allowing for the growth with nitrate as a substrate nutrient. It is markedly less expressed in FL 5 and 50 Hz compared to continuous light control. This result does not match with the specie-specific accumulation of proteins in low-frequency flashing light conditions observed in previous experiments (Paragraph 3.5). Anyway, nitrate reductase is a very regulated protein at several levels, for example the post-translational one (Sanz-Luque et al., 2015). This may mean that, although the transcriptional level is down-regulated, there are some other mechanisms that allow the over production of proteins. Another hypothesis is that, because of low division rate of the cells grown in low-frequency flashing light conditions, proteins are produced in excess even if NR is under-expressed.

3.7. Conclusions

In the first part of this work, the effect of flashing light on the growth and biochemical composition of *N. gaditana* grown in two versions of F-medium, one limited in nitrate and phosphate content and one rich in them, was assessed. *N. gaditana* had a worse growth performance under the flashing light conditions than under the continuous light control in both the basic and the enriched version of the medium. The biomass was also analysed to assess its biochemical content that revealed an increase and a decrease of lipid content on DW in the biomass grown under flashing light conditions, as compared to continuous light, in the basic medium and in the enriched medium respectively. The fatty acid content was also analyzed and results showed a decrease and an increase of PUFAs content under the flashing light conditions of 25 and 250 Hz respectively, both with the basic medium and the enriched medium. Furthermore, the chlorophyll content decreased and increased when going to flashing light conditions in the basic and in the enriched medium while, oppositely, the carotenoids content increased and decreased in the same way. All the mentioned variations indicate a combined effect of the frequency of flashing and of the concentration of nutrients when they are limiting. In this case, the flashing light effect increases the effect of the nutrients starvation. When the cells were cultured in nutrient abundance, flashing light had the prevailing effect, showing a low-light acclimation response.

Then, we analysed the effect of flashing light on several species and with higher light intensities. These effects were most discriminative at low frequencies (5 and 50 Hz, DC=0.05), whereas cultures exposed to 500 Hz showed similar growth and biomass composition compared to cells cultured under continuous light. The effects on growth was strain- and culture- concentration depended. Low-frequency flashing light conditions (f= 5 and 50 Hz) induced intracellular biocomponents that typically accumulate under low-light conditions, including proteins, PUFA, chlorophyll, lutein and β-carotene. Strikingly, the productivity of these components was highly improved (up to four times) when using a two-stage cultivation system. Our statistical analysis revealed that most biomolecules were more affected by biomass concentration in the medium, as an indicator for the prevailing culture growth stage, than by the flashing light treatment applied.

Then, we analysed the photosynthetic efficiency and transcriptomic of key genes of *Nannochloropsis gaditana* grown under three flashing light conditions (FL 5, 50 and 500 Hz) and a CL control. The microalgae growth curves confirmed results of previous experiments in which the same conditions of growth were assessed. The growth performance was higher in the CL and FL 500 Hz conditions, while it was markedly decreased in FL 5 and 50 Hz. Photosynthetic analysis revealed that low-frequency flashing light conditions had a higher effective quantum yield and

maximum photosynthetic capacity than both continuous light and high frequency flashing. Transcriptomic analysis revealed that genes related to de novo lipid production (*bc*, *mct* and part of ones constituting the FAS complex) are under-expressed in the low-frequency flashing light conditions. On the contrary, genes related to photoprotection (*vcp*, *vde*, *zeaDE*) and genes related to the production of carotenoids and chlorophyll (*lcyB*, *alaD*, *por-1*) are over expressed in low-frequency flashing light conditions, coherently with the results of previous work in which concentrations of carotenoids and chlorophyll were found to be higher in these than in other light conditions. This may explain how the excess energy produced thanks to a higher photosynthetic efficiency, is used. Also the genes related to the glycerolipids production were analysed and results revealed that they are overexpressed in FL 5 and 50 Hz. This may indicate that in these conditions there is an accumulation of these class of lipids, but they were not analysed in other experiments. Genes related to starch production and nitrate reductase, an enzyme related to the nitrate capture, were under-expressed in FL 5 and 50 Hz.

This work shows that by combining nutrient starvation and flashing light one can address the production of one or another high-value compound, and this knowledge may be applied to industrial productions. Furthermore, microalgal cultivation at high latitudes can benefit from employing artificially emitted low frequency flashing light (e.g., f≤ 50 Hz) to produce high-value microalgal biomass rich in high value metabolites, including PUFA or pigments.

In conclusion, the ensemble of results of this work completes the picture about the response of microalgae to flashing light condition of different frequencies. Probably, at low frequencies microalgae produce more photochemical energy. The photochemical energy produced in these conditions, however, is not employed to produce biomass. It is partly dispersed as heat and partly employed for the production of high-value compounds such as chlorophyll and carotenoids. These findings make the use of flashing light in industry appealing as a strategy to optimize the production of the compounds of interest, by tailoring the frequency of flashing light on the desired compounds.

Section 4: Indigenous microalgal species as a mean for exploiting nutrients in wastewaters

Part of the content of this section was published or submitted for publication as:

- S. Lima, V. Villanova, M. Richiusa, F. Grisafi, F. Scargiali, A. Brucato, Pollutants Removal from Municipal Sewage by Means of Microalgae, in: Chem. Eng. Trans., 2019. doi:10.3303/CET1974208.
- S. Lima, V. Villanova, A. Brucato, F. Grisafi, F. Scargiali. Microalgae as an effective tool for nutrient removal in municipal wastewater. Submitted for publication to *Algal Research*.

4.1. Definition of wastewater

The exponential human population growth together with the industrial development over the past few cwìenturies negatively affected the environment due to a waste disposal increase. Pollution is a phenomenon created by menkind, occurring when there is an increase in artificial or synthetic substance concentrations in the environment. Wastewaters are the consequence of the wastes from industrial, domestic and agricultural activities. Their remediation has become one of the top global priorities.

Several definitions were created for the word "wastewater", but in general one defines them as waters with a negatively altered quality because of anthropogenic activity (WWAP, 2017).

When untreated wastewaters accumulate, the organic matter decomposition leads to annoying conditions including the malodorous gases production. Sewage contains pathogenic microorganisms and nutrients that can stimulate undesirable aquatic plants growth, beyond potentially toxic compounds. For these reasons, wastewater treatment before dispersal into the environment is necessary to protect public health and environment.

The aim of the wastewater treatment is to decrease the pollutants in a way that allow the reintegration of treated water into the environment. In fact, sewages and wastewaters are critical components of water cycle and need to be handled with care to avoid serious consequences for the environment.

4.2. Traditional plant for wastewaters treatment

Wastewater treatment is an important step of industrial production that allows pollutants and toxic agents removal and treated water reuse. The process is summarised in some reviews (*e.g.* Samer, 2015). The traditional process for sewage treatment typically consists of three treatments preceded by a mechanical separation of all materials that could damage the plant during the subsequent phases (Figure 4.1). The primary treatment is done in the first plant section and consists of sedimentation, coagulation and flotation units. It involves the removal of suspended solids and part of the organic matter from sewage water. In the secondary treatment, the biodegradable organic matters and

nutrients removal is obtained via aerobic biological depuration and chemical precipitation. Finally, in the tertiary treatment, the remaining solid matters removal is obtained by a combination of filtration, absorption, denitrification and dephosphatation steps. Sterilization is normally part of these treatments (Metcalf and Eddy, 2003). In order to monitor the sewage depuration process, several chemical analysis are performed, *e.g.* measurement of Biochemical Oxygen Demand (BOD) and Chemical Oxygen Demand (COD) (Pearson et al., 1987). These are organic matter indirect indicators and representative parameters to assess wastewater quality.

The secondary treatment is usually performed by microorganism consortia, employed in the organic matter biological removal. Microorganisms found in the plant are usually heterotrophic bacteria that, in the presence of oxygen, are able to employ the carbon sources in the sewage for their growth and energy. Because of their role in the organic matter biological degradation, in this step an aeration system should be employed to allow the heterotrophic bacteria growth.

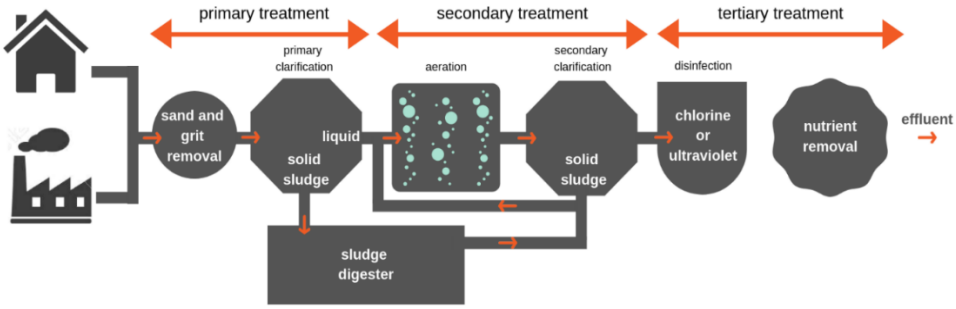

Figure 4.1: Schematic process flow diagram of a typical wastewater treatment plant. The process starts with a mechanical debris separation and continues with primary, secondary and tertiary treatments.

4.3. Biology of the removal of nutrients and symbiosis with heterotrophic bacteria

Microalgae are phototrophic organisms able to convert light energy and inorganic compounds into oxygen and organic compounds. As a matter of fact, it has been shown that the use of microalgae in wastewater treatment secondary steps has several advantages: *i)* the removal of organic pollutants such as ammonia NH_4^+, nitrates NO_3 and phosphates PO_4 (Chamberlin et al., 2018; Lau et al., 1996) deriving from nitrogen compounds and, in some cases, also the removal of inorganic pollutants such as heavy metals (Delrue et al., 2016); *ii)* oxygen production that can be used by the heterotrophic bacteria to degrade compounds present in the matrix (Han et al., 2016).

Moreover, microalgae produce compounds that are useful for the bacterial community growth. These are low molecular weight molecules such as extracellular substances composed by proteins, lipids and nucleic acids, mannitol and arabinose as excretion products, glycolate as photosynthetic by-products under hyperoxic and alkaline conditions, and acetate, propionate, lactate and ethanol as fermentation products (Subashchandrabose et al., 2011). At the same time, heterotrophic bacteria produce compounds, such as vitamins, useful to microalgae, as they are not able to produce them (Han et al., 2016). This symbiotic process is summarized in Figure 4.2, and represents an example of biological application that can be employed during the secondary treatment. Microalgae use CO_2 provided by bacterial metabolism to sustain the photosynthetic reactions, while bacteria use the oxygen keeping its level low and creating a better environment for microalgal growth. The self-oxygenation realized by a consortium of algae and bacteria is also an eco-friendly approach that allows to avoid oxygen supply high costs of the secondary treatment aeration process (Sforza et al., 2018b).

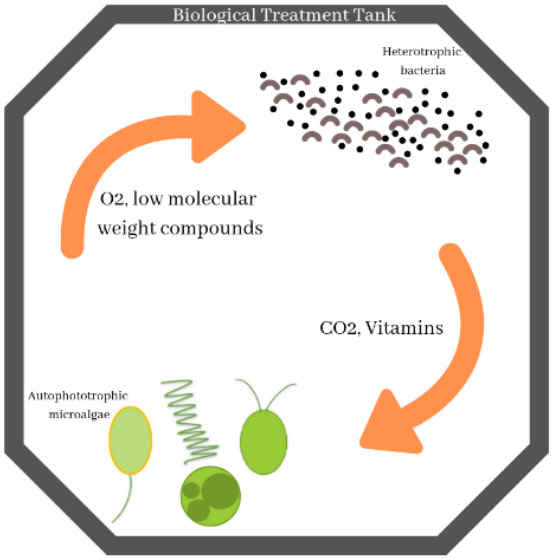

Figure 4.2: Self-oxygenation process aimied at replacing the aeration tank. Microalgae produce O_2 and compounds useful for bacterial metabolism, while bacteria produce vitamins and CO_2 that sustain the microalgal photosynthesis.

Another advantage of microalgae use in wastewater secondary treatment is the production of high-value molecules from microalgal biomass.

4.4. The importance of using indigenous species in commerial applications

In Section 2 microalgae genetic manipulation is discussed as a strategy to make microalgal industry more profitable and thus expanding it in the future. These concepts are undoubtedly innovative and represent a hopeful perspective for the future, but in practice genetic manipulation of microalgae has several downsides, as shown in Section 2. An alternative is the so called "phycoprospecting" (Wilkie et al., 2011), that consists in employing natural engineered microalgae. This, in other words, means exploiting indigenous microalgae for applications in the regional applications. This regionally located-based algal agriculture may bring several benefits, as indigenous microalgae are already adapted to the biotic and abiotic stresses of their environment. This may bring to economic advantages if considering the time and efforts needed for acclimating a strain to a new culture condition. Furthermore, in an outdoor algal facility, contamination risks are very high, therefore local microalgae employment may overcome this obstacle. In an industrial perspective, there is also the possibility of choosing to not employ uni-algal cultures but instead symbiotic cultures, in which there is the coexistence of more microalgal strains and bacteria. This leads to advantages discussed in the next paragraphs. For boosting microalgal industry, one needs to adopt the existing technology to the biology, exploiting the diversity of "Nature's culture collection" (Wilkie et al., 2011) and choosing the most useful microalgae for given purposes. In fact, microalgae selected by nature have hundreds of years of adaption to the environmental conditions, so there they are more resistant than other species. The idea of selecting microalgae from an environment and employ them in it is not new. There are in fact several studies that deepen this concept (Camarena-Bernard and Rout, 2018; Komolafe et al., 2014; Pereira et al., 2015).

Microalgae have furthermore the ability to remediate anthropogenic waters, with several advantages such as saving on fertilisers and the non-utilisation of arable lands. Microalgal bioremediation is part of a circular economy approach, described in Figure 4.3. Phycoprospecting helps in selecting microalgae suitable for regionally-located industrial applications. Microalgae may well grow thanks to sunlight, CO_2 from industrial wastes and nutrients from local sources. The obtained microalgal biomass may then be employed for deriving high-value molecules to be exploited by the society. The residuals are employed for anaerobic digestion to obtain energetic resources and the wastes can be reused for microalgal growth. This circle put together the possibility to expand the microalgal industry and the ideas of green economy and sustainability that nowadays have a significant role in the society.

In order to make this applications feasible, assessments about the selected algae production rate, their biochemical proprieties and the removal effectiveness are needed. Several authors, therefore, performed researches about indigenous microalgae to evaluate

their potential in industrial applications (Camarena-Bernard and Rout, 2018; Jebali et al., 2019; Komolafe et al., 2014; Rao and Vidyapeeth, 2013).
The following research joins the cited ones for the indigenous algae selection and their evaluation for bioremediation applications.

In conclusion, the optimization of wastewater bioremediation by employing microalgae lays the foundations for a future, sustainable, microalgal industry.

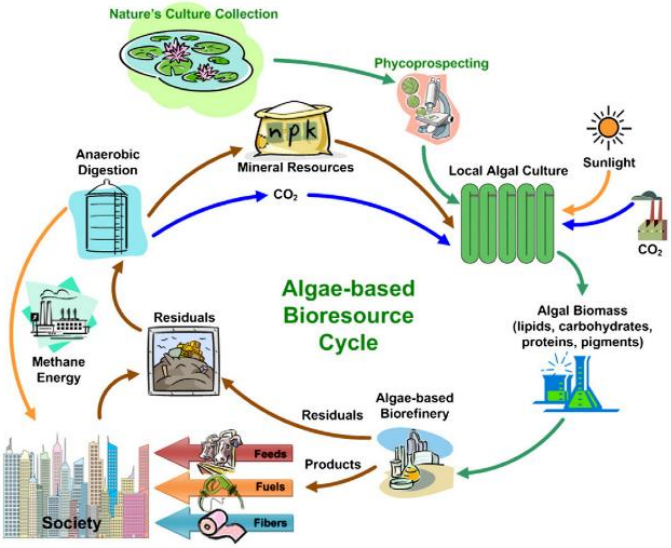

Figure 4.3: Circular economy approach in which phycoprospecting is employed for regionally-located industrial applications of microalgae growing thanks to the wastes of industrial processes. (Wilkie et al., 2011)

4.5. Aim of this section

In this section, four different strains are compared, two of them coming from collections and the other two isolated from Sicilian coastlines. These strains were employed for the first time in wastewater bioremediation of sewage from a municipal plant. In particular, their ability to remove the nutrients from a primary treated sewage was tested. BOD, COD, nitrogen and phosphorous removal were determined in order to evaluate microalgae effectiveness for wastewater treatment. In addition, microalgal biomass composition was also characterised, in order to assess the presence of high value molecules and their industrial production potential.

4.6. Materials and Methods

4.6.1. Isolation of microalgae from marine samples

Figure 4.4: Location of sampling of the microalgal isolates employed in this work. A) Pozzillo beach, in which *Chlorella sp.* (pozzillo) was isolated. B) Vergine maria beach, in which a consortium of *Chlorella sp.* and *Dunaliella sp*. (vergine maria) was isolated. The locations were chosen because of green blooms presence in the water.

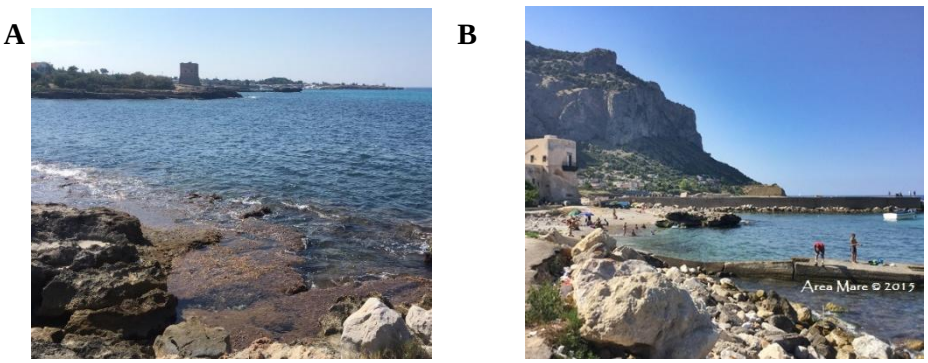

Figure 4.5: Pictures of the location in which algal samples were harvested. A) Pozzillo beach, a location close to the Palermo airport. B) Vergine maria beach, in the periphery of the city.

For this work, some locations in the Sicilian coastline were selected because of the green blooms presence and samples were harvested. The locations chosen were Pozzillo beach (GPS coordinates 38.18372; 13.144250) and Vergine Maria beach (GPS coordinates 38.167149; 13.368573), shown in Figure 4.4 and Figure 4.5.

The isolation of microalgal species was performed by combining filtration method with various pore-size sieves (from 5 to 200 μm) and serial dilutions in microplates. The

employed medium for serial dilutions was F-medium (Guillard, 1975). After obtaining a single strain in each well, the cultures were transferred in solid medium (F- supplemented with agar 1.5%). Monoalgal isolates were then characterized by a microscopic morphological analysis followed by molecular analysis of the rDNA 18S in order to determine the species of the isolated microalgae. Molecular characterization was performed by Colony PCR using Q5 ® high-fidelity DNA Polymerase (NEB), the forward primer A (5′-ACC CTG GTT GAT CCT GCC AG-3’) and primerSSU-inR1 (5′-CAC CAG ACT TGC CCT CCA-3’) and the following program: 95°C (5 min), 32 cycles of 95°C (30 s), 55°C (30 s) and 68°C (60 s) and a final 7 min extension step of 68°C.

4.6.2. Microalgal growth

Four different strains were employed in this work in order to compare their performance in sewage treatment. The first two strains were microalga *N. gaditana* (CCAP 849/5) coming from Scottish Association for Marine Science, and *Chlorella sorokiniana* (CCAP 211/11k) coming from algal collection of Università di Napoli Federico II. The other two algae used in this work were harvested across sicilian coasts, isolated and identified with rDNA 18S sequencing. *Chlorella sp.* (*Pozzillo*) was harvested from Pozzillo beach while the consortium made by *Chlorella sp*. and *Dunaliella sp*. (*Vergine Maria*) was harvested from Vergine Maria beach (see details in previous paragraphs). All the strains were kept in liquid medium. A modified version of F-2 medium (Guillard, 1975) supplemented with 4 times the original nitrate and phosphate concentration was used for *N. gaditana*, *Chlorella sp.* (*Pozzillo*) and the consortium of *Chlorella sp. and Dunaliella sp.* (*Vergine Maria*), while a commercial medium, the Cell-Hi JW (Varicon Aqua Solutions Ltd, UK) was used for culturing the freshwater microalga *Chlorella sorokiniana*. A pre-culture of the microalgae was set up by inoculating 10 ml of sample from a culture flask in 100 ml of fresh medium. When the cells were in late lag phase (around 10 days of cultivation), they were used to inoculate the cultivation flask containing medium or sewage. The algae were cultivated for 15 days. The microalgal suspension concentration was checked by counting the cells using a Burker Chamber and applying the suitable dilution factor in order to have from 100 to 200 cells in a square. Measurements were done in triplicate ($n=3$) and the average value was retained and shown together with the standard deviation (sd).

4.6.3. Set up of the experiment

Microalgae were first cultured in their growth medium. After that, the cells were inoculated in a mixed medium made of the original growth medium with an added quantity of 50% of the original sewage in order to acclimate them (data not shown). A sample from this cultivation was then inoculated into the sewage. We made two

cultivations: the first one had a volume of 400 ml (first cultivation) and the second one of 1 L (second cultivation). The process is shown in Figure 4.6.

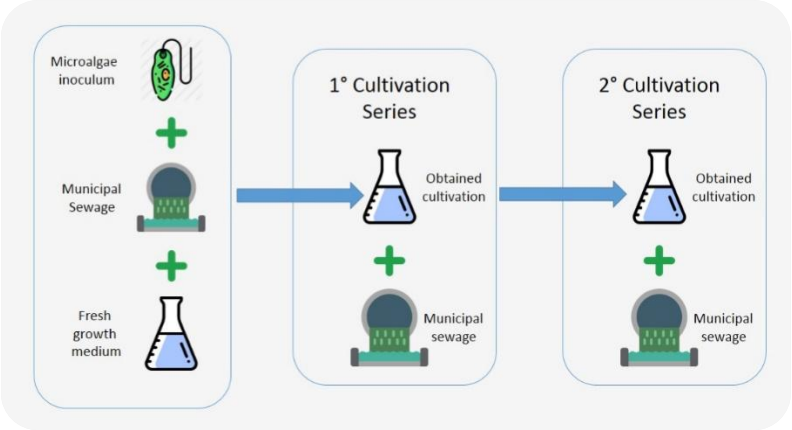

Figure 4.6: Method employed in this experiment. Microalgae were inoculated in the original culture medium mixed with sewage in order to acclimate them to the new growing condition. Then, a sample of this cultivation was inoculated in the sewage with a volume of 400 mL (first cultivation) and subsequently a sample from this last cultivation was employed to inoculate the sewage with a volume of 1 L (second cultivation).

4.6.4. Sample preparation

At the end of the cultivation in the sewage the cell suspension was microfiltered, the biomass was frozen in liquid nitrogen and freeze-dried for 48 h in a bench lyophilizator (FreeZone 2.5L, LABCONCO, US). The biomass was then stored at r.t. for further analysis. The filtered sewage was stored instead at -20°C for further analysis.

4.6.5. Sewage analysis

A pre-treated sewage coming from the municipal treatment plant AMAP Acqua dei Corsari, located in Via Messina Marine, 592, 90121 Palermo PA, was used. This batch was analyzed for COD, BOD, total phosphorous (TP) and total nitrogen (TN) and then stored at -20°C until it was employed for the inoculum. After the microalgal growth the sewage was microfiltered (0.45 μm) and the same analyses were repeated A batch of the sewage was treated in the same way (frozen and microfiltered) and used as reference control. The COD analysis was done following the APAT/CNR Method, IRSA Manuals 117/2014 – Method 513; BOD5 followed OXITOP method, compliant to UNI EN ISO 1899-1:2001; TN was analyzed according to disintegration ISO 11905-1; ISO 7890-1:1986 while TP EPA method 365.2.

4.6.6. Extraction and analysis of Fatty Acids

Extraction and analysis of Fatty Acids was performed according to method described in Paragraph 3.4.1.6.

4.6.7. FTIR analysis

FTIR analysis were performed according to method described in Paragraph 3.4.1.5.

4.6.8. Statistical data analysis

Data from three different experiments were tested for statistical significance of the variations in different strains and treatment. Statistical analysis were performed according to method described in Paragraph 3.4.1.8.

4.7. Results and discussion

4.7.1. Microalgal growth curves

Four microalgae strains were cultured in their growth medium and in urban wastewaters during two cultivation series, differing in the employed cultivation volume: the first cultivation series had a volume of 400 mL and the second one of 1 L. Cells coming from the first series were used for inoculating the second series. Both environmental strains, *Chlorella sp*. (*Pozzillo*) and *Chlorella sp./Dunaliella sp*. (*Vergine Maria*), reached higher cell density than the culture collection strains *N. gaditana* and *C. sorokiniana* in all the tested conditions (Figure 4 A-D). Interestingly, both the *Chlorella* isolates reached higher cells concentrations than other algae belonging to the same genus reported in literature (Ansari et al., 2017; Lau et al., 1996). Almost all the employed species reached higher concentrations in the growth medium (red line) than in the sewage (green and blue lines). However, the consortium of *Chlorella sp./Dunaliella sp*. (*Vergine Maria*) reached comparable cell densities in both control and first cultivation series (Figure 4 D). This strain, hence, showed the best growth performance on sewage in first cultivation series in comparison with the other strains tested.

N. gaditana (Figure 4.7A) during the first cultivation days showed a faster growth in first series with respect to the growth medium but it reached lower final cell density. *C. sorokiniana* (Figure 4.7B) showed the same trend, even if less emphasized. Similar considerations can be done with the isolate *Chlorella sp. (Pozzillo)* (Figure 4.7C), in which there is a marked increase of the first cultivation series growth compared to the second one. The second cultivation series had a worse growth performance in all the tested strains. The anticipated growth observed in the first cultivation series may be due to a best adaptation to the nutrient composition of the sewage compared to the growth medium, in which the growth was delayed.

A different situation is shown in Figure 4.7D where the consortium of *Dunaliella sp./Chlorella sp*. showed a better grown performance in the first cultivation series than in the growth medium. The reason for this may rely on the consortium ability of adaptation and of nutrients removal from wastewaters, as reported for the species *S. obliquus*, *C. vulgaris* and *C. sorokiniana* (Hu et al., 2019), the species *Chlorella protothecoides* and *Brevundimonas diminuta* (Sforza et al., 2018a) and for a mixed-microalgal consortium grown in four different anaerobic digestion effluents (Yu et al., 2019).

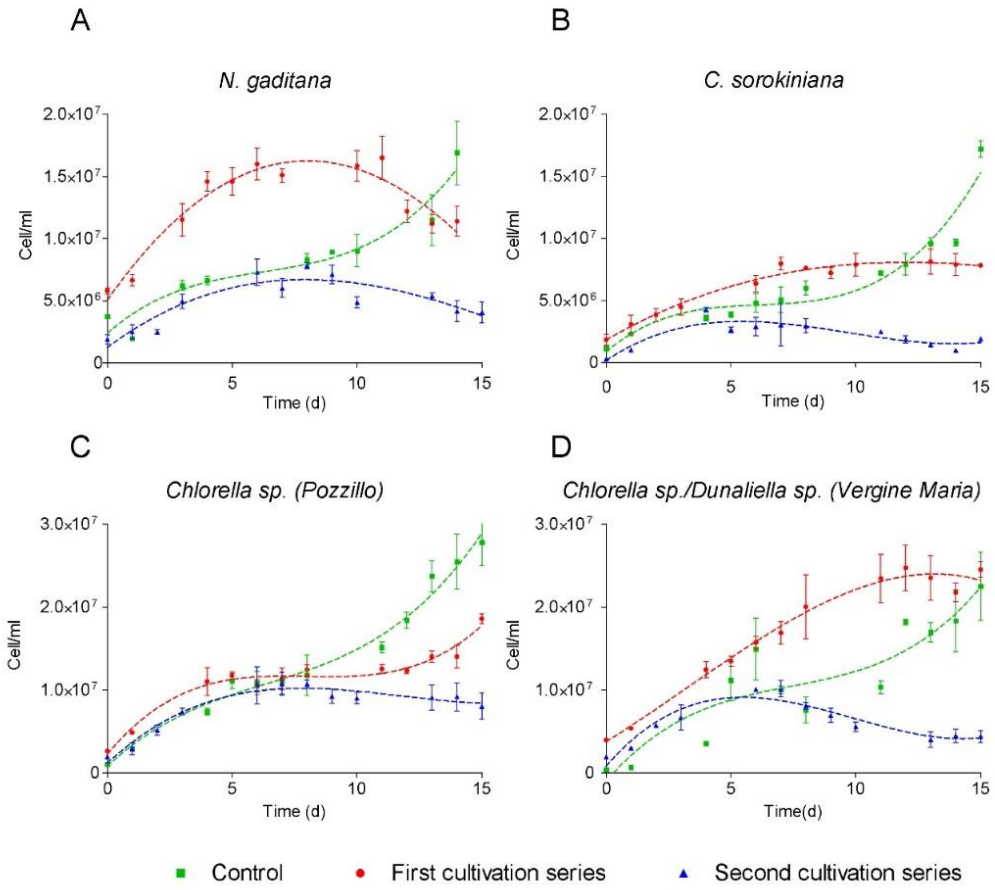

Figure 4.7: Growth curves of four microalgal strains grown in: growth medium (green), first cultivation series (red) and second cultivation series (blue). A) *N. gaditana*; B) *C. sorokiniana*; C) *Chlorella sp*. (Pozzillo); D) *Dunaliella sp./Chlorella sp*. (Vergine Maria). Measurements were done in triplicate (n=3), obtained average and standard deviation values were shown in the graphs.

Although some authors (Hu et al., 2019; Lau et al., 1996) reported that the wastewater treatment optimization goes through the acclimation, the results of the present work show that all the employed microalgae had a poorer growth performance in the second cultivation series compared to the first one, even if cells were expected to be more acclimated. The reason may rely on macronutrient deficiency in the second cultivation series. Probably, they were instead still present in the first cultivation series because in this case the inoculum was obtained from the growth medium, very rich in nitrates and phosphates. As reported also by others (Ahmet Karagunduz et al., 2017; Procházková et al., 2014) and supported by sewage chemical analysis (see next paragraphs), the limiting nutrient may be phosphorous, that is a well-known essential nutrient for plant and microalgae and is often responsible for growth limitation, as reported by Cho and coworkers (Cho et al., 2016) in a wastewater remediation application and reviewed by Singh et al. (Singh et al., 2018).

The usage of microalgae in remediation applications has been widely investigated in literature and several exhaustive reviews may be found about the topic (Abinandan et al., 2018; Delrue et al., 2016; Molazadeh et al., 2019). There are, instead, only a few examples of environmental microalgae isolates employed for this application. In particular, *Scenedesmus sp*. and *Chlorella sp*. isolated from Kallar Kahar Lake, Pakistan, were grown in wastewaters with good results (Ansari et al., 2017). In some cases, microalgae were isolated directly from wastewaters in order to increase their potential in removing nutrients (Doria et al., 2012; Tapia et al., 2019). An interesting feature of the present work is that this is the first time that isolates from Sicily are employed in industrial applications, although there are a few other examples of isolation of microalgae and macroalgae from Sicily (Messina et al., 2019; Pierucci et al., 2017).

It is worth noting also that the environmental isolated microalgae, *Chlorella sp*. (*Pozzillo*) and *Chlorella sp./Dunaliella sp*. (*Vergine Maria*), grown in sewage reached highest cell concentrations than algae from collections and showed a best growth performance. This is in accordance with the sampling locations, selected for their high pollution level. The strains acclimation to their natural habitat has, though, a role in its abilities also after the isolation process, as observed by other authors in different conditions (Tapia et al., 2019; Yun et al., 2014).

4.7.2. Analysis of the biomass

FTIR spectroscopy has been broadly employed to investigate the effect of wastewater properties on the accumulation and changes of biochemical components in microalgal cells (Ansari et al., 2019; Murdock and Wetzel, 2009; Supeng et al., 2012). After the growth, biomass was freeze-dried and analyzed in order to determine its biochemical characteristics. FTIR spectroscopy was used to determine the presence of vibrationally active functional groups (including O–H, N–H, C=O, C–H, CH2, C–O–C) and results are

summarized in the graphs of Figure 4.8A-D. All the original spectra are reported in Supplemental Information (Figure A1 - A4). The peak areas related to the relevant macromolecules, are reported in Figure 4.8 and in Table B of Supplemental Information as ratios between different areas. The decrease of Lipid/Amide I ratio (L/A ratio) can be due to the decrease of the lipid content or to the increase of amide (proteins). By using three ratios, Lipid/Amide I (L/A), Amide I/Carbohydrates (A/C) and Lipid/Carbohydrates (L/C), it is possible to determine the approximate biomass composition evolution amongst the three analyzed conditions.

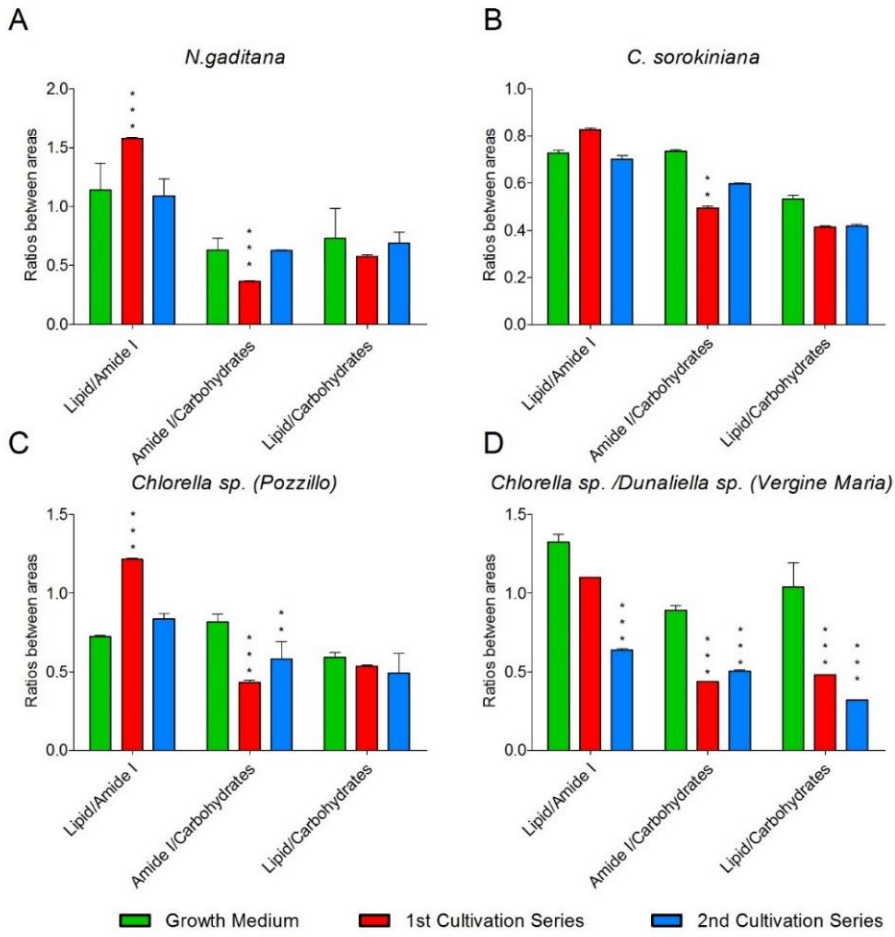

Figure 4.8: FTIR analysis on the microalgal biomass. Here the ratios between areas under peaks related to macromolecules are reported. Following the tendency of different ratio the total composition of the biomass can be estimated. Values are reported as means (n=2) and error bars report the standard deviations. Asterisks indicate if the treatment is statistically different to the control growth medium. Two asterisks indicates a P value <0.01 and three asterisks <0.001.

By looking at the results of this work, under a statistical point of view L/A ratio is affected in the same way by the *treatment* ($F=41.82$, $p<0.01$) and by the *strain* ($F=44.35$, $p<0.01$). On the other hand A/C ratio is significantly affected by the *treatment* ($F=100.7$, $p<0.01$) and poorly by the *strain* ($F= 3.292$, $p<0.1$). Similarly, L/C ratio is affected more by the *treatment* ($F=32.58$, $p<0.01$) and less by the *strain* ($F=16.95$, $p<0.1$).

In the case of *N. gaditana* the L/A ratio increased from the growth medium to the first cultivation and is constant in the second cultivation. As shown in Figure 4.8A, the A/C ratio decreased from the growth medium control to first cultivation series and was the same in the control and in the second cultivation, while the L/C ratio is almost stable in all the cultivations. It may be that both lipid and carbohydrate contents increased from the control to first cultivation series, but carbohydrate level increased more than the lipid one, as shown from the L/C ratio reduction.

The first and second cultivation series of *C. sorokiniana*, in Figure 4.8B, showed similar results as *N. gaditana;* indeed, both lipid and carbohydrate content increased in the first cultivation series, and carbohydrates were more abundant than lipids. Biomass ratios of *C. sorokiniana* in the second cultivation series are similar to the *N. gaditana*'s one with a decrease in lipid content.

For what concerns *Chlorella sp.* (*Pozzillo*), in Figure 4.8C, in the first cultivation series both lipid and carbohydrate content increased compared to the control, but, because the (L/C) ratio remained stable, their content equally increased. In the second cultivation series ratios were stable, not showing big differences in the biochemical composition compared to the control.

Finally, a slightly different situation is displayed by the consortium of *Dunaliella sp.* and *Chlorella sp.* (*Vergine Maria*), in Figure 4.8D. In fact, in this sample the lipid content did not increase from the growth medium control to first and second cultivation series as shown in L/A ratio. The only increasing compounds are the carbohydrates, as shown in the decrease of L/C and A/C ratios in the first and second cultivation series.

Table 4.1: Summary of the effects on microalgal biomass grown in sewage. The composition varies depending on treatment and strain. ↑symbol means that the biomolecules increased compared to the growth medium control, ↓ indicates a decrease, ↔ that the composition has not changed and ↑↑ a marked increase. 1st C= First cultivation, 2nd C= second cultivation.

	N. gaditana		*C. sorokiniana*		*Chlorella sp. (Pozzillo)*		*Dunaliella sp./Chlorella sp. (Vergine Maria)*	
	1st C	2nd C	1st C	2nd C	1st C	2nd C	1st C	2nd C
Lipids	↑	↓	↑	↓	↑	↔	↔	↔
Proteins	↔	↔	↔	↔	↔	↔	↔	↔
Carbohydrates	↑↑	↔	↑↑	↔	↑	↔	↑	↑

Table 4.1 shows a summary of all the changes occurred in the biomass of microalgae cultured in sewage. In general, sewage treatment lead to an increase in both carbohydrates and lipids in microalgal biomass. This may be connected to the nitrogen deficiency at the end of the cultivation, that is a well-known parameter that enhances lipid levels into the biomass, as reported by Liang et al. (Liang et al., 2019) and Metsoviti and collaborators (Metsoviti et al., 2019). Results show that the differential increase of carbohydrates or lipids depends on the species and on the employed volume of the sewage (first or second cultivation). The increase in lipid quantity in algae cultured in wastewaters compared to growth medium control is supported by literature and reported in several cases, *e.g.* in *Nannochloropsis oceanica* grown in industrial wastewaters (Mitra et al., 2016), in *Chlorella minutissima* cultivated in a mix of kitchen waste, poultry litter waste and 5% flue gas (De Bhowmick et al., 2019), in *Chlorella sp*. grown in simulated wastewater (Gao et al., 2019) and in *Dunaliella tertiolecta* cultured in saline sewage (Wu et al., 2017). The observed increase in carbohydrate levels was also previously observed in *Nannochloropsis oculata* and *Tetraselmis suecica* growing in municipal wastewaters (Reyimu and Özçimen, 2017), and in *Desmodesmus spp*. and *Scenedesmus obliquus* cultured in a mixture of raw wastewater with different leachate ratios (Hernández-García et al., 2019).

4.7.3. Characterization of lipid content

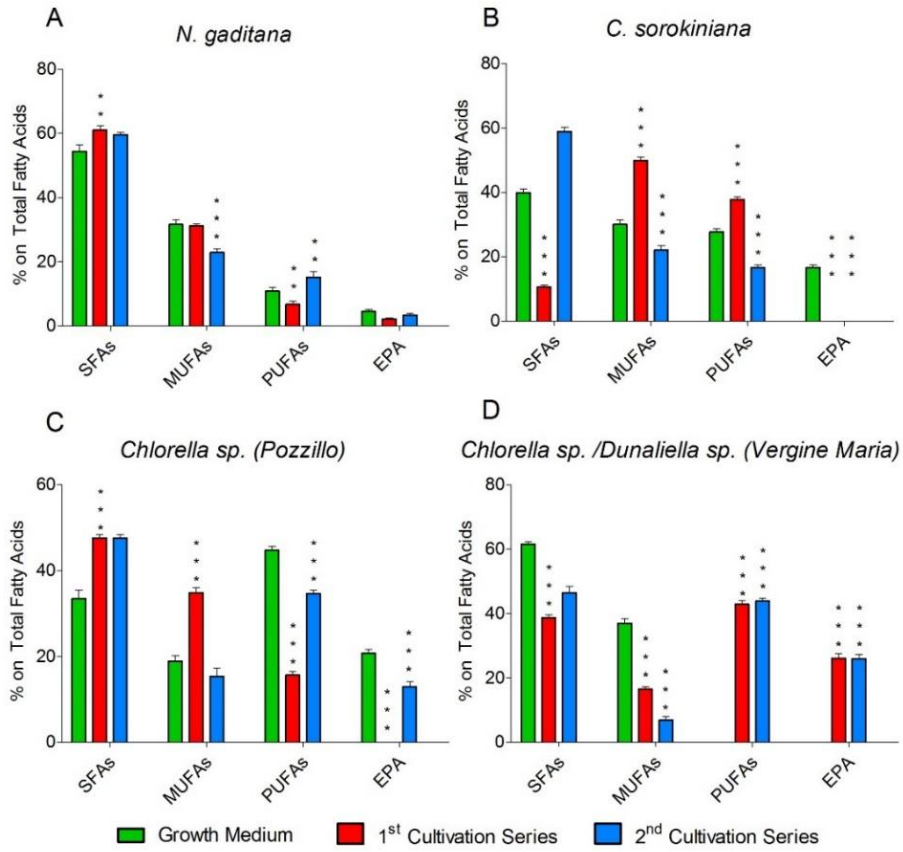

Figure 4.9: Composition in percentage of fatty acid on total fatty acids of microalgal biomass grown in urban wastewaters: A) *N. gaditana*, B) *C. sorokiniana*, C) *Chlorella sp.* (Pozzillo), D) *Chlorella sp./Dunaliella sp*. (Vergine Maria). Fatty acids are shown as saturated fatty acids (SFAs), mono-unsaturated fatty acids (MUFAs), polyunsaturated fatty acids (PUFAs). Eicosapentaenoic acid (EPA) is shown individually because of its economic relevance. Values are reported as means (n=2) and error bars report the standard deviations. Asterisks indicate if the treatment is statistically different to the control growth medium. Two asterisks indicates a P value <0.01 and three asterisks < 0.001.

Biomass samples were analyzed by Gas Chromatography (GC) in order to determine the composition of total fatty acids.

Under a statistical point of view, saturated fatty acids (SFAs) were affected both by the *treatment* ($F=222.7$, $p<0.001$) and by the *strains* ($F=306.9$, $p<0.001$). Mono-unsaturated fatty acids (MUFAs) were affected more by the *treatment* ($F=362.6$, $p<0.001$) than by the *strain* ($F=138.6$, $p<0.001$). By contrast, poly-unsaturated fatty acids (PUFAs) were affected more by the *strain* ($F=494.1$, $p<0.001$) than by the *treatment* ($F=92.08$, $p<0.001$).

As shown in Figure 4.9, the change in fatty acid composition is specie-specific. *N. gaditana*, in Figure 4.9A, did not show a marked shift in composition: there is a slight decrease in SFAs and an increase in PUFAs in the first and second cultivation series compared to the control, while rather small effects were observed on eicosapentaenoic acid (EPA) content. On the other hand, the major effect in *C. sorokiniana* in first cultivation series is a decrease of SFAs and a simultaneous increase of MUFAs and of PUFAs, as shown in Figure 4.9B. By contrast, in second cultivation series the same strain showed an increase in SFAs and a decrease in MUFAs and PUFAs. Furthermore, EPA could not be detected in the two sewage cultivations. *Chlorella sp. (Pozzillo)* in Figure 4.9C showed an increase in SFAs in both first and second cultivation series, while an increase in MUFAs was observed in the first cultivation series and one in PUFAs in the second one. EPA could not be detected in the second cultivation series. The consortium of *Chlorella sp./Dunaliella sp. (Vergine Maria*) showed instead a decrease in MUFAs and an increase in PUFAs both in first and second cultivation series (Figure 4.9D). EPA levels increased in both the cultivation series compared to the control, where it was not detected.

Different factors, such as nutritional condition, physicochemical condition as well as growth phase can act on fatty acid composition (Kim and Hur, 2013; Mata et al., 2010). This was observed also in wastewaters field by Mitra et al. (Mitra et al., 2016), that reported how the fatty acid profile varies in different wastewaters. Other environmental factors such as salinity could modify the fatty acid profile (Wu et al., 2017). The change in fatty acid composition is, therefore, not always easily interpreted. However, this research showed similar results to other works in the same field. For example, *Nannochloropsis oceanica* grown in municipal sewage showed a decrease in SFAs and MUFAs together with an increase in PUFAs on dry weight (Mitra et al., 2016), in a similar way as the algae from the same genus analyzed in the present work. Furthermore, De Bhowmick and coworkers (De Bhowmick et al., 2019), reported a decrease in SFAs together with an increase in PUFAs in *Chlorella minutissima* grown in a mix of kitchen waste, poultry litter waste and 5% flue gas, compared to the growth medium, in a similar way than in *C. sorokiniana* and *Chlorella sp./Dunaliella sp. (Vergine Maria)* in the present work. Regarding EPAs content, even though *Chlorella* genus is not known as a producer of EPA, in many cases good concentrations of this fatty acid were found in this genus: Rismani and Shariati showed that *C. vulgaris* reached 10% EPA under salt stress conditions (Rismani and Shariati, 2017) and Vazhappilly and Chen (Vazhappilly and Chen, 1998), observed *C. minutissima* reaching 37% EPA of total fatty acids. Some authors found that both PUFAs and EPA contents decreased under nutritional (in particular nitrogen) limitation (Hernández-García et al., 2019; Hu et al., 2019) and this may explain the change in fatty acid composition observed with *C. sorokiniana*. A similar observation about PUFAs content was made also by Breuer et al. (Breuer et al., 2012),

studying triacylglycerol (TAG) accumulation under nitrogen-deficient cultivation conditions. Another interesting aspect consists in differences in fatty acid composition observed between the first and the second cultivation series in *C. sorokiniana* and *Chlorella sp. (Pozzillo)*. This is not the first time that in two consequent cultivations a shift in fatty acid composition is observed: a similar situation is depicted also by Daneshvar and collaborators (Daneshvar et al., 2019). In conclusion, the reported results confirm that the fatty acid profile depends both on the analyzed microalgae and on the employed matrix for its cultivation (growth medium, first or second sewage cultivation series).

4.8. Sewage chemical analysis

The sewage treated with microalgae was filtered and analyzed for the determination of Chemical oxygen demand (COD), Biological oxygen demand (BOD), Total Nitrogen (TN) and Total Phosphorous (TP). Results are compared with the control sewage, subjected to the same analytical procedures than the treated samples. Thus, it was frozen and microfiltered to determine whether the process affected the results.

Statistically, the BOD level in the treated sewage is more affected by the *treatment* ($F=37.03$, $p<0.001$) than by the *strain* ($F=14.07$, $p<0.001$). In the same way, the COD level is affected mainly by the *treatment* ($F=550.4$, $p<0.001$) than by the *strain* ($F=41.82$, $p<0.001$). Again, nitrate and phosphate levels are mostly affected by the *treatment* ($F=268.6$, $p<0.001$; $F=152.6$, $p<0.001$) than by the *strain* ($F=5.465$, $p=0.0133$; $F=4.144$, $p<0.1$).

Results obtained in the present work are summarized in Figure 4.10 and Figure 4.11 and in Table A2 of supplementary informations. BOD levels (Figure 4.10A) were stable in all samples except *Chlorella sp. (Pozzillo)* second cultivation series and *C. sorokiniana* second cultivation series, where it reached zero. This may suggest that microalgae were not capable to employ the organic carbon sources present in the sewage. This is of easy understanding if considering that cells were cultured without dark periods, so the carbon metabolism was probably not employed during the growth.

On the other hand, COD levels increased in all the samples (Figure 4.10B). Notably, COD level was higher in the first cultivation series than in the second for all analyzed microalgae, and this correlates with the higher cell concentrations obtained in the first cultivation series compared to the second one. By contrast, several other authors found an opposite trend in the COD values that was decreased by microalgae treatment. For example, *Chlorella vulgaris* decreased COD values of several wastewater kinds (Zhu et al., 2019); in another case, a consortium of *Chlorella prototheicodes* and *Brevundimonas diminuta* decreased COD values of wastewaters in a continuous system (Sforza et al., 2018a); furthermore, COD values were found to decrease in a chemically characterized municipal wastewater by a battery of marine species (Harbi et al., 2017).

Results of the present work showing increased COD values may be due to a microalgal release of chemicals not oxidizable with the BOD test, while are degradable with the COD one. It is probable that these compounds are made of cellulose and hemicellulose, the main carbohydrates of microalgae together with starch (John et al., 2011). Microalgae are, in fact, protected by a lipid-rich plasma membrane and a rigid cell-wall with a complex composition, rich in different carbohydrates (Arnold et al., 2015). Cellulose was detected in *Nannochloropsis* genus (Maffei et al., 2018), in *Chlorella sorokiniana* (Zuorro et al., 2018) and in *Chlorella vulgaris* (Gerken et al., 2013) amongst others. COD analysis can detect the polysaccharide content of a matrix, including cellulose levels, as reported by (Paul et al., 2014). Notably, in the past BOD levels were found to be counterfeit when monitoring of wastes with a high ligno-cellulosic content (Heukelekian and Rand, 1955). In fact, in the usual time of the analysis (5 days), only the more degradable carbohydrates are oxidized, while longer periods would be needed by cellulose or hemicellulose (Raabe, 1968).

Another possible explanation for the COD level increase in treated wastewaters was suggested by Wang et al. (Wang et al., 2010) in a research with *Chlorella sp*. According to the authors, when organic substrates are not available microalgae grow in phototrophy, using CO_2 as carbon source. In these conditions they excrete small molecular organic substances such as glycolic acid as a by-product of photosynthetic carbon reduction cycle, which can explain the COD increase in effluent after algal cultivation.
For what concerns TN and TP analysis, shown in Figure 4.11, their trend is similar in all the analyzed microalgae and consists in their decrease in a progressive way between first and second cultivation series. Results appear coherent with literature data. For example, Chamberlin and coworkers (Chamberlin et al., 2018) showed a decrease of both nitrogen and phosphorous values in wastewaters after the cultivation of *C. vulgaris*. The same strain was found to decrease nitrogen and phosphorous levels also by other authors, that showed the differences between the acclimated strain and the not acclimated one (Lau et al., 1996). Also in the present results there is an example of acclimation, as the reduction of both nitrogen and phosphorous is enhanced in the second cultivation series.

Results show that microalgae appear to excrete biological substances in the matrix that increases the amount of material to be chemically oxidized. Results obtained on TN and TP showed a positive response. They both decreased in all the samples. The second cultivation series was generally more effective in decreasing nutrients, a feature that may be explained with microalgae acclimation.

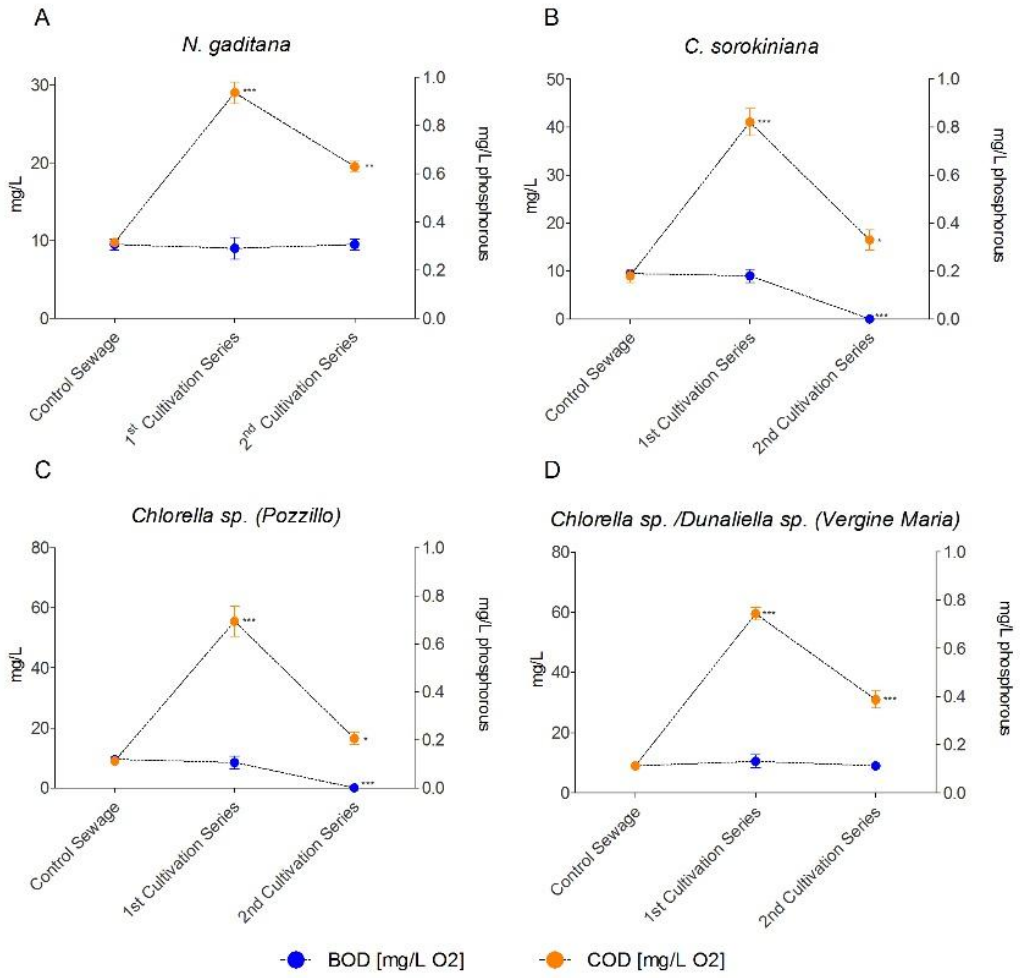

Figure 4.10: Chemical analysis for sewage characterization before and after microalgal treatment: Biological Oxygen Demand (BOD) and Chemical Oxygen Demand (COD) are reported for the untreated sewage (control), first Cultivation Series and second Cultivation Series. Values are reported as means (n=2) and error bars report the standard deviations. Asterisks indicate if the treatment is statistically different from the control sewage. One asterisk indicates a P value <0.1, two asterisks <0.01 and three asterisks < 0.001

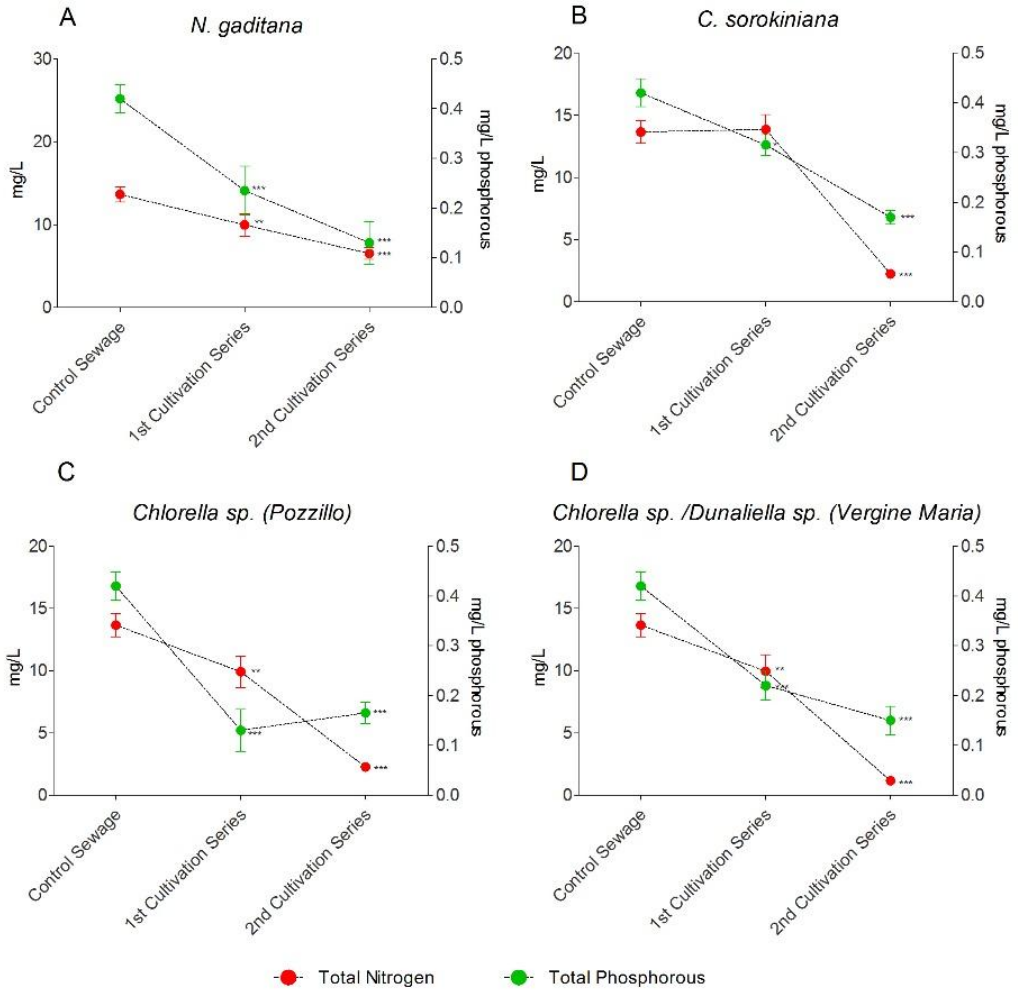

Figure 4.11: Chemical analysis for sewage characterization before and after microalgal treatment: Total nitrogen (TN) and total phosphorous (TP) are reported for the untreated sewage (control), first cultivation series and second cultivation series. Values are reported as means (n=2) and error bars report the standard deviations. Asterisks indicate if the treatment is statistically different from the control sewage. One asterisk indicates a P value <0.1, two asterisks <0.01 and three asterisks < 0.001.

4.9. Conclusions

In this work four different microalgal strains were tested for their ability in bioremediating pretreated municipal wastewaters. Biomass was characterized in order to investigate the effect of wastewaters on the microalgae biochemical composition. Biomass composition was found to be modified by the treatments. In particular, an increase in lipid and carbohydrate fractions was observed in almost all tested strains. A species-specific shift in fatty acid composition was also observed. Chemical analysis were performed to detect the effectiveness of algae in remediating wastewaters. COD value was found to increase in all the samples, probably because of the excretion of some organic compounds by algae themselves, while the BOD value was stable or reduced. On the other side, nitrogen and phosphorous levels decreased. In particular, *Chlorella* strains, especially the one denominated "*Pozzillo*" and the one in consortium with *Dunaliella (Vergine Maria),* were the most effective in bioremediation. This can be related to the location from which the strain was isolated, that was for *Chlorella (Pozzillo)* a polluted area near the airport and for *Chlorella sp./Dunaliella (Vergine Maria)* a polluted area in the outskirts of Palermo. In conclusion, these strains may therefore be good candidates for an industrial bioremediation process and would allow also the accumulation of high-value compounds (*e.g.* PUFAs). To guarantee the decrease of COD and BOD value, the treatment with microalgae could be coupled with another one with heterotrophic bacteria and yeast that would be able to decrease the organic compounds into the matrix. Alternatively, another hypothesis could be that of exploiting the heterotrophic metabolism of microalgae, e.g. by exploiting the dark periods, to pursue the same result.

4.10. Applications in industry: perspectives and limitations

Microalgal wastewaters remediation has an enormous potential as an alternative to traditional treatment because of its many advantages. Amongst them, there is the atmospheric CO2 decrease, the generation of a valuable biomass that could be employed in energetic field, the savings on the substances that support microalgal growth, the possibility to create a circular economy process and others. On the other side, however, there still are challenges to face. Firstly, the process needs to be established on a large scale, which requires technical adjustment on the operation process control. Furthermore, in order to screen a larger number of algae for their remediation capacity, development of high-throughput screening methods is necessary. Another issue regards the contamination control and the consortium protection, especially for plants working outdoors (Delrue et al., 2016). Strategy to enforce the stability on the consortium when growing on different wastewaters are also required, together with the possibility to select and employ different consortia when working with several kinds of wastewaters. Amongst them, in fact, it is more complicated to remediate industrial wastes because of the possible presence of contaminants and heavy metals more concentrated than nutrients

(Molazadeh et al., 2019). Selection and employment of strains resistant to these conditions is therefore needed. Lastly, the possibility to employ CO2 from industrial wastes in order to decrease its emissions leads to other problems, connected to its storage.

Despite several issues that still need to be solved, microalgae usage in wastewater bioremediation remains one of the most promising applications for the future development of microalgal industry.

Section 5: Experiments with an outdoor pilot plant

A few experiments were performed with an existing external pilot plant facility. It is worth mentioning that, due to a still enfuring financial block of the available funds, the plant xould not be modified and revamped as needed. The few experiments performed were therefore only aimed at starting to accumulate experience with an outdoor pilot scale facility. Thanks to novel funds, plant modifications are now planned and future work will hopefully benefit from the previous experiences summarised in this section.

5.1. The photobioreactors world

5.1.1. Advantages of using a photobioreactor compared to open ponds

Microalgae have been cultivated since a long time; some studies testify their consumption as a food up to 2000 years ago (Sathasivam et al., 2019). Traditionally, microalgae are cultured in natural open system, for example in lakes or natural ponds (Ciferri, 1983). They can also be cultivated in artificial open system. Open systems are normally outdoor and rely on natural illumination for sustaining microalgae growth. They are intensively employed because of the low installation and maintenance costs but their utilisation has several drawbacks. Firstly, open cultivation systems are subject to contamination and pollution risks. Contamination is often caused by predator species like rotifers and may cause large production losses. Furthermore, the possibility of contamination by other species of algae affects the final product quality, up to making it unsuitable for market such the pharmaceutical or the nutraceutical ones. Open system do not allow for a thermal control and suffer from evaporative losses. They are subject to environmental conditions, meaning that parameters such as temperature, nutrient concentration and illumination can vary. The consequence of these characteristics is that they cannot be employed for cultivating fragile strains that have difficulties in competing with other strains and need constant cultivation conditions for their growth. Only a relatively small number of algal species can be grown in an open system (Acién Fernández et al., 2013) and usually the extremophiles are a good choice because of the difficulties for other species to growth in their ideal cultivation conditions. In addition, the two major issues for the algae cultivation in any system are the light energy distribution and the mixing for mass transfer enhancing. Open ponds require large areas for exploiting light energy, since they can utilise only the surface layer for the distribution of light (Ugwu et al., 2008). CO_2Mass transfer is also a problem because open ponds are subject to loss by its diffusion to the atmosphere (Pulz, 2001). When the

microalgal market expanded to cosmetics, pharmaceutics and nutraceutics, closed photobioreactors (PBRs) started to be employed. Beside the high costs of installation and maintenance, in PBRs there are several advantages such as an easier control of biological parameters, no CO_2 losses, reduced contamination risks, reproducible cultivation conditions, smaller occupied area (Pulz, 2001). Notably, there are several kinds of PBRs and their efficiency depends on the chosen parameters for their set-up.

5.1.2. Comparison between flat panels and tubular photobioreactors

Amongst the various kinds of closed photobioreactors, the ones most employed are the "flat panels" and the "tubular" ones. Flat plate reactors are made of two overlapped slabs of plastic or glass that create a thin compartment in which algae are cultured in suspension. The thickness between the two slabs determines the light path of the algal cultivation. Usually, this needs to be below 0.07 m to guarantee an optimal light absorption by the culture (Acién Fernández et al., 2013). The optimal light path is a compromise between the growth inhibition in deep layers due to poor illumination and the photoinibition effect in superficial layers. This optimum is species-specific (Xu et al., 2009). Furthermore, as observed in Paragraph 3.3.1, biomass concentration and light penetration are in contrast because of the self-shading effect. Flat plate reactors have a large illuminated surface/volume ratio and this usually leads to very high photosynthetic efficiencies (Nwoba et al., 2019). The oxygen build up is usually low and biomass can be mixed by insufflating air mixed to CO_2 (Acién Fernández et al., 2013; Ugwu et al., 2008). They can be scaled-up by adding different modules and also the orientation can be easily manipulated according to the seasonal needs; in fact, there are several examples of vertical arrangements of flat plate photobioreactors (Rodolfi et al., 2009; Sierra et al., 2008).

Power consumption is mainly due to aeration (Acién Fernández et al., 2013) and depends on the aeration rate or superficial gas velocity in the aerated section, U_G, the density of the liquid, ρ_L, and the gravitational acceleration, g, according to the following equation:

$$\boldsymbol{P = \rho_L U_G g} \qquad \text{5-I}$$

Power input is supplied by aeration at rates between 0.2 and 0.01 v/v/min, equivalent to 10–50 W m^{-3}. This power supply by aeration allows to achieve volumetric mass transfer coefficients of about 0.007 s^{-1}, sufficient to avoid

dissolved oxygen accumulation over saturation with air. This explains the low power supply required by the flat panel photobioreactor and the relatively high mass transfer capacity.

Anyway, the high exposition can easily lead to problems of light inhibition and for the same reason temperature control is a problem; fouling can also be a relevant problem, especially if light path is very short and therefore cleaning the reactor is troublesome.

On the other hand, tubular photobioreactors are the most suitable for the industrial cultivation of microalgae. Tubes are made of glass or plastic and are transparent. The exposed area is also in this case large but illuminated area/volume ratio is lower when compared to flat plate reactors. This has the advantage of lowering photoinibition but at the same time the need arises for mixing the volume in order to avoid cells from sedimenting in the shaded part of the tube. In order to perform the scale-up of this kind of reactor one has to increase tube diameter or tube length. When a tubular PBR is scaled-up by increasing its diameter, the illuminated surface/volume ratio decreases, leading to problems of increased self-shading (Xu et al., 2009). When the tube length is increased, instead problems of O_2 accumulation may occur, generating toxic conditions for the algae. The maximum length L of a tube is given by:

$$\boldsymbol{L = \frac{U_L([O_2]_{out} - [O_2]_{in})}{R_{o_2}}} \qquad \text{5-II}$$

where U_L is the superficial liquid velocity and $[O_2]_{out}$, is the maximum acceptable value that does not inhibit photosynthesis. R_{O2} is the volumetric rate of oxygen generation by photosynthesis in the tube (Molina et al., 2001). Furthermore, by increasing the PBR length, the residence time is increased and this may cause photoinibition problems. In any case, this system cannot be scaled-up indefinitely, and at some point also in this case scale-up by module replication becomes necessary. Furthermore, temperature control also in this case is a problem to solve. Tubular PBRs need a pump to circulate the culture, and it can be an airlift or a centrifugal pump. In any case, it needs high power consumption to work, and this is one of the main drawbacks of this system. To calculate this energy, the Bernoulli equation can be applied. Pressure drop is calculated as the sum of distributed (F_d) and concentrated (F_c) pressure drops (5-III). Distributed pressure drops can be calculated with equation 5-IV, in which *f* is the Fanning friction factor, while concentrated pressure drops are calculated with equation 5-

V, in which C_o, the orifice coefficient, is a factor related to the geometry of the element causing the pressure drop. The friction factor of equation 5-V for Reynolds > 4000 may be calculated with equation 5-VI, known as Churchill's equation.

$$\sum F = F_d + F_c \qquad \text{5-III}$$

$$F_d = 4\, f\, \frac{L}{D}\, \rho\, \frac{v^2}{2} \qquad \text{5-IV}$$

$$F_c = C_o\, \frac{\rho v^2}{2} \qquad \text{5-V}$$

$$\frac{1}{\sqrt{f}} = -4\, log\left[0.27\frac{\varepsilon}{D} + \left(\frac{7}{Re}\right)^{0.9}\right] \qquad \text{5-VI}$$

Furthermore, power consumption ranges from about 100 W m^{-3}, for the airlift-driven configuration, to roughly 500 W m^{-3} for the pump- driven fence configuration (Acién Fernández et al., 2013).

A last point to take into consideration is the spatial dilution of light accomplished by curved surfaces during the cultivation of microalgae. According to Tredici (Tredici and Zittelli, 1998) one of the biggest problems of algae cultivation is the light saturation effect, or light inhibition, which reduces the photosynthetic efficiency of the culture and, hence, its productivity. The proposed solution to this phenomenon is the dilution of light, which can be temporal or spatial. Temporal dilution of light has been discussed in Section 3, dealing with the flashing effect obtained through the tailoring of LED illumination to microalgal cultures. Spatial dilution of light can be achieved through the employment of curved surface for the design of photobioreactors and can lead to significantly higher light conversion efficiency and, consequently, to higher productivity. The higher the light intensity, the higher the beneficial effect of spatial light dilution will be. This theory was confirmed in experiments in which a coiled tubular reactor, a near-horizontal straight tubular reactor and a near-horizontal flat panel were compared. The photosynthetic efficiency achieved in the tubular systems was significantly higher allegedly because their curved surface ''diluted'' the impinging solar radiation and thus reduced the light saturation effect (Tredici and Zittelli, 1998). This explanation may be questionable as new evidences suggested a more uniform light distribution of light in tubular photobioreactors for certain biomass concentrations when compared to flat surface PBRs (Marotta et al.,

2017). In any case, independently of the explanation of the observed effect, fact is that tubular PBRs have been experimentally shown to sport a higher efficiency of light utilisation and therefore they may be regarded as a good option as solar light collectors.

5.1.3. Employment of airlift photobioreactors

Part of this paragraph is adapted from (Molina et al., 2001).
Airlift systems have been widely studied by several authors with special regard to bubble dynamic, overall gas holdup and interfacial area (Fernandes et al., 2014; Molina et al., 1999; Ojha, 2016; Rengel et al., 2012). The system can be employed as a vertical column airlift reactor (Ojha and Al-Dahhan, 2018; Sadeghizadeh et al., 2017) or as a pump for a solar collector, normally made of horizontal tubes (Acién Fernández et al., 2001; Molina et al., 2001). The airlift is made of a riser, full of culture broth and air bubbles, a degasser that allows the gas phase to be separated from the liquid, and a downcomer, mainly filled with the liquid phase. The density difference between riser and downcomer sections generates a pressure difference at the base of the system that allows circulation in the tubes. One of the main advantages of the airlift systems is that circulation is guaranteed without any moving parts. This generates a robust culture that resists to contaminations. Additionally, airlift works as a gas-liquid contactor that efficiently removes oxygen produced by photosynthesis. Furthermore, microalgae in outdoor photobioreactors seem to undergo light-dark cycles that might improve the productivity. This topic has been studied by several authors (Merchuk et al., 2000; Wu and Merchuk, 2004) and it was proposed that a regular dark-light cycle could improve biomass productivity (Degen et al., 2001). This is the case of airlift photobioreactors, which presents a regular mixing which guarantees an alternation of light and dark when each cell moves from the dark riser/downcomer to the enlighted section. This is opposed to random mixing found in bubble columns (Fernandes et al., 2014). It is worth noting, however, that the quoted dark-light cycles are way too long to give rise to the flashing effect described in Section 3. To maximise the circulation in the plant, a complete separation of liquid from gas at the head zone of the airlift has to be achieved. This is obtained when the distance between the entrance and the exit of the degasser (L_D) is large enough to allow for the smallest bubbles to rise out from the fluid before entering into the downcomer. All the fluid that is in the riser enters into the degasser, so we have:

$$U_L A_r = U_{LD} A_{LD} \quad \text{5-VII}$$

where U_{LD} is the mean superficial liquid velocity in the degasser, A_r is the section of the riser and A_{LD} the vertical mean liquid occupied section in the downcomer. The section A_r is equal to $h_D * d_t$, equal to the mean height of the fluid in the degasser and the distance between the parallel degasser walls. To allow for the disengagement of the air bubble is necessary that:

$$\frac{L_D}{U_{LD}} \geq \frac{h_D}{U_b} \quad \text{5-VIII}$$

where U_b is bubble rise velocity (Chisti and Moo-Young, 1993). Substitution of 5 VII in 5 VIII gives the following equation:

$$L_D = \frac{U_L A_r}{d_t U_b} = \frac{\pi d_t}{4} \frac{U_L}{U_b} \quad \text{5-IX}$$

In the airlift system the flow velocity depends on the configuration on the system and on the difference in gas hold up in the riser and in the downcomer. According to Chisti, (Chisti, 1989) the relationship may be expressed as:

$$U_L = \sqrt{\frac{2g(\varepsilon_r - \varepsilon_d) h_r}{\frac{K_T}{(1-\varepsilon_r)^2} + K_B \left(\frac{A_r}{A_d}\right)^2 \frac{1}{(1-\varepsilon_d)^2}}} \quad \text{5-X}$$

where K_T and K_B are respectively the frictional loss coefficient for the top and the bottom connecting sections of the airlift, h_r is the height of the riser zone, A_d is the cross-sectional areas of the downcomer, ε_r is the gas holdup in the riser, and ε_d is the holdup in the downcomer. The frictional loss coefficient K_B can be approximated as:

$$K_B = 0.3164 \left(\frac{\rho U_L d_t}{\mu_L}\right)^{-0.25} \frac{L_{eq}}{d_t} \quad \text{5-XI}$$

where L_{eq} is the equivalent length of the loop considering concentrated pressure drops as an increase of length and d_t is the tube diameter. For external, well designed airlifts, no bubbles recirculate in the downcomer, so ε_d is equal to zero and by substituting equation 5-XI in equation 5-XII one obtains:

$$U_L = \left(\frac{g \varepsilon_r h d_t^{1.25}}{0.3164 \left(\frac{\mu_L}{\rho}\right)^{0.25} L_{eq}}\right)^{4/7} \quad \text{5-XII}$$

The gas holdup ε_r in the riser is calculated through the Zuber and Findlay (Zuber and Findlay, 1965) equation:

$$\varepsilon_r = \frac{\beta}{\lambda + \frac{U_b}{U_G + U_L}} \qquad \text{5-XIII}$$

where U_G and U_L are the superficial velocities of the gas and liquid in the riser zone, β is the ratio of the superficial gas velocity to the total superficial velocity, λ is a characteristic parameter. By solving equation 5-XIII for U_G, one obtains:

$$U_g = \frac{\varepsilon\lambda U_L + \varepsilon U_b}{1 - \varepsilon\lambda} \qquad \text{5-XIV}$$

The following equation links density in the riser (ρ_r) and density of the gas (ρ_G) and of the liquid to the hold up:

$$\varepsilon = \frac{\rho_L - \rho_r}{\rho_L - \rho_G} \qquad \text{5-XV}$$

In order to estimate the capability of oxygen removal in the airlift column, the following equation by Chisti (Chisti, 1989) can be used:

$$\frac{k_L}{d_B} = \frac{k_L a_L (1 - \varepsilon_r)}{6\varepsilon_r} \qquad \text{5-XVI}$$

where $k_L a_L$ is the volumetric mass transfer coefficient, ε_r is gas holdup, d_B is mean bubble diameter and k_L is mass transfer coefficient.

5.2. Case study at Palermo University: Outdoor airlift pilot plant

5.2.1. Aim of the project

In order to develop microalgal industry and make the whole supply chain economically sustainable, a cut of costs in industrial cultivation is needed. Therefore, it is necessary to develop efficient photobioreactors that allow the right photosynthetic efficiency and productivity to be obtained while keeping costs low enough. Furthermore, in an industrial perspective harvesting and downstream processing of microalgae add further significant costs. In this way, a relatively high production costs in incurred, possibly making microalgae not competitive with other sources of bioactive compounds.

Sicily, in the heart of Mediterranean Sea, is a favourable location for outdoor cultivation of microalgae because of the ideal climate with high solar irradiations during the whole year. These conditions suggest a good potential of economic development of microalgal market in Sicily.

This part of my project aims to fill the technological gap of Sicily through optimization of an already existing pilot plant at Palermo University with the final goal of cultivating local microalgae in it. My aim is that of providing the needed know-how for the Sicilian microalgal industry expansion.

The outdoor pilot plant treated in this section is supplied with an airlift system. In this research several configurations for the solar collector were tested. In the original plant project the, it was supplied with soft Low Density Polyethylene film tubes, chosen for their affordability and simplicity to replace. Because of the very low hydrostatic pressure resistance of these tubes, another kind of tubes made of soft Polyvinyl chloride (PVC) were employed in order to perform some hydraulic tests. These tubes, anyway, were not resistant to sunlight and weather conditions, so it was necessary to replace them from time to time.

In order to fulfil the initial project purpose and employ film tubes, a modification on the set up of the airlift was necessary, consisting on the placement of a new degasser section at a lower height. This resulted in a lower hydrostatic pressure on the entire system at the cost of a smaller circulating flow-rate. In this way polyolefin tubing could be employed and it was possible to start the system with the inoculum of microalgae of the species *Chlorella sorokiniana*.

In the attempt to optimize the solar collector, other two configurations were chosen: a flat alveolar plate PBR, employed for hydraulic tests, and a rigid tubular PBRs made in polymethyl methacrylate (PMMA) that will be provided by a German company, *Algoliner*.

5.2.2. Description of the plant

The PBR pilot system was built inside Palermo University campus (Italy), as shown in Figure 5.1, in May 2016. This location is ideal for microalgae growth, as it s located in the south of the Mediterranean area, the climate is warm, and on average there are no temperature values below 15 °C throughout the year (Thangavel and Sridevi, 2015).

(a) (b)

Figure 5.1: (a) Location of the PBR pilot plant within Palermo University Campus; (b) Satellite image of the pilot plant location.

5.2.2.1. Original Pilot Plant Design

The photobioreactor located at Palermo University has two main sections:

- *Solar collector*: made of horizontal transparent pipes exposed to sunlight (outdoor system). The pipe construction material should be low-cost, characterized by high solar radiation transparency and sufficient UV resistance and, depending on their thickness and rigidity, may be either laid down on the ground (simply flattened and covered by a low-cost plastic protection cloth), or suspended on suitable pipe-racks (Marotta et al., 2017);
- *External loop Air-Lift section:* the main components are the riser, the downcomer and the degasser. In the riser section, the medium coming from the photobioreactor ascends together with air supplemented with a

CO_2 gas stream injected through a suitable sparger. The separation between gas and liquid phase takes place in the degasser section. The gas-freed liquid phase descends *via* the downcomer and feeds the photobioreactor tubes.

In the riser bottom a gas sparger, fed by a compressor air-line, is inserted for culture broth movimentation, CO_2 input and O_2 removal. Then, the gas separated in the degasser section (top airlift) is released to environment or connected to the vacuum pump for vacuum operation of the section. Figure 5.2 and Figure 5.3 show in particular, CAD designs of the two sections.

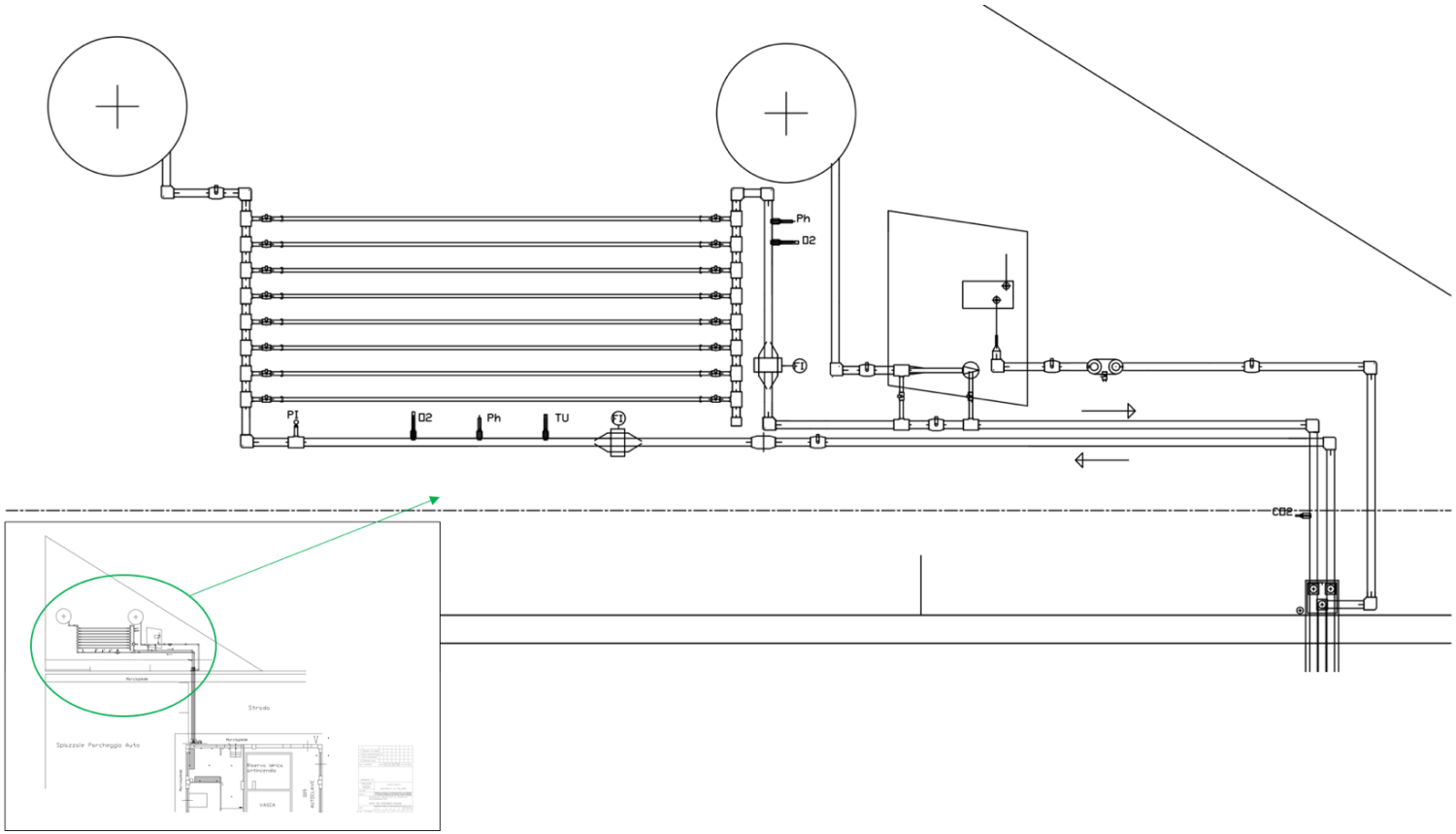

Figure 5.2: PBR pilot plant CAD design: Original solar collector section configuration.

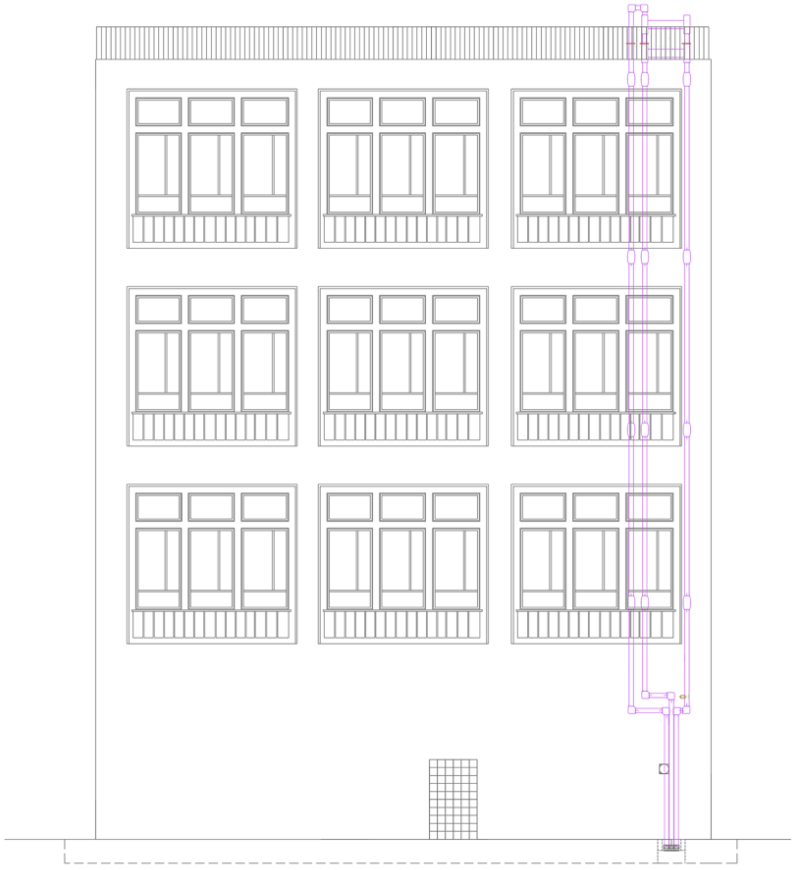

Figure 5.3: PBR pilot plant CAD design: airlift section.

5.2.2.2. Experimental site and apparatus

The 20 meters high airlift unit was built by the photobiorector and was supported by the walls of a university campus building as shown in Figure 5.4a. It is connected to the photobioreaction section by means of a trail carved along the street road, as shown in Figure 5.4b. All main pipelines are in polyethylene (PE). Table 5.1 shows the main pilot plant sizes.

.

(a) (b)

Figure 5.4: (a) Evacuated-head airlift installed on the side of Building 6, in front of the pilot area; (b) Trail carved along the street road to connect the evacuated-head airlift to the photobioreaction section.

(b)

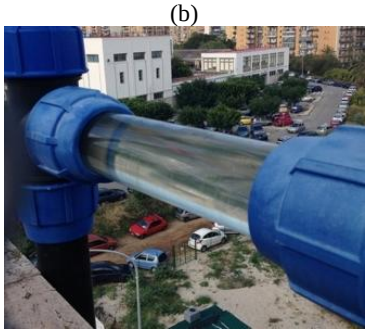

(a) (c)

Figure 5.5: (a) Dual transparent degasser (b) full of air in the highest section and (c) of aqueous solution in the lower section.

Regarding the airlift unit, it is worth noting that the degasser section consists of two horizontal parallel pipes, one above the other, of the same diameter as the riser and downcomers, simply connected to these by standard T junctions. The degasser is shown in Figure 5.5. Notably this design was found to effectively sort out two different problems observed when using a single connection: (i) the strong liquid circulation rate dependence on the liquid height in the degasser and (ii) significant bubble entrainment in the downcomer section, due to the relatively high velocities in the partially filled single degaser system. After the modification realised to decrease the hydrostatic pressure at the base of the system, the degasser height decreased from 18 m to 5.5 m. Considering 1.5 m of depth of the trail carved along the street road, the hydrostatic pressures dropped from 1.7 to 0.4 Bar.

Figure 5.6: Modified degasser, at 5.7 m from the ground.

Figure 5.6 shows the new degasser that is constituted only by a single tube, creating some problems on the hydraulic profile that will be shown in next paragraphs.

Table 5.1: Characteristics and size of the PBR pilot plant.

Section	ID [m]	Length [m]	Volume [L]
Riser	0.08	18	~ 90
Downcomer	0.08	18	~ 90
PBR line connection	0.08	17	~ 84
Degaser	0.10	0.80	~ 6
PBR	0.06	81	~ 230
Total Volume [L]			~ 500

5.2.2.3. Solar collector

According to the original project, the first version of the solar collector was made of thin tubes made in low density polyethylene (LDPE). The photobioreactor section consisted of eight horizontal 10 m tubes connected in parallel as shown in Figure 5.7. It is worth noting that in this PBR Unit, VICTAULIC® grooved piping, fittings and couplings were chosen, supplied by the Sicilian company *Plastica Alfa*, for easy replacement and modification of the entire section. In order to enable or disable individual parallel photobioreactors, manual polypropylene (PP) ball valves were inserted in the inlet and outlet manifolds. In the solar collector second version only one tube was installed with a total length of about 20 m. Several tubes were connected together through flanged connections and a U curve was realised thanks to two orange PVC L curves glued together.

Two pipe typologies were employed in the photobioreactor unit. The first ones were transparent with thin LDPE film pipes 60 mm in internal diameter, able to capture light radiation for microalgae growth. The second ones, in mixed polyolefin, had a thickness of 0.6 mm and a diameter of 60 mm. The two tube typologies are shown in Figure 5.8.

The first tube typology, when employed with the 5.7 m airlift, underwent to a dilation of their diameter to 70-75 mm, causing consequent problems on the system hydrodynamics. Furthermore, these tubes never resisted for more than 48 h while the system was operating, as they exploded under the plant hydrostatic pressure, as shown in Figure 5.9.

The second tube typology, when employed with the 5.7 m airlift, underwent as well to a dilation of the diameter to 73-78 mm. Also in this case it was necessary to increase the liquid volume inside the PBR, but in this case they resisted for more than one month of usage.

(a)

(b)

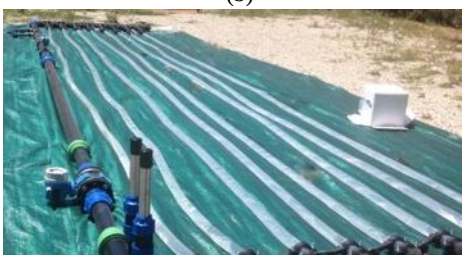

(c)

Figure 5.7: First version of the photobioreactor unit with LDPE film tubes according to the original project.

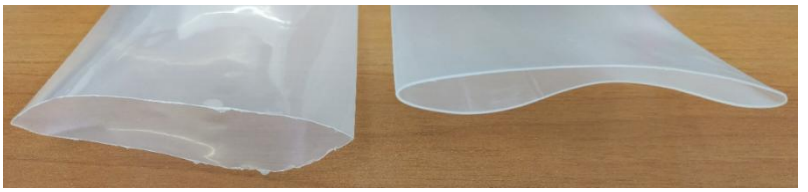

Figure 5.8: On the left the LDPE tube firstly employed is shown, while the mixed polyolefin tube successively employed is on the right

Figure 5.9: LDPE tubes firstly employed in the solar collector of the plant. They exploded under the airlift hydrostatic pressure.

5.2.2.4. Instrumentation

The plant is supplied with two pumps, a centrifugal one (Calpeda NM40/16B/B) and a vacuum one (Edwards ES65), shown in Figure 5.10. The first one can be employed for supplying fresh water or inocula to the plant, while the second one can be used to perform the gas stripping from the degasser.

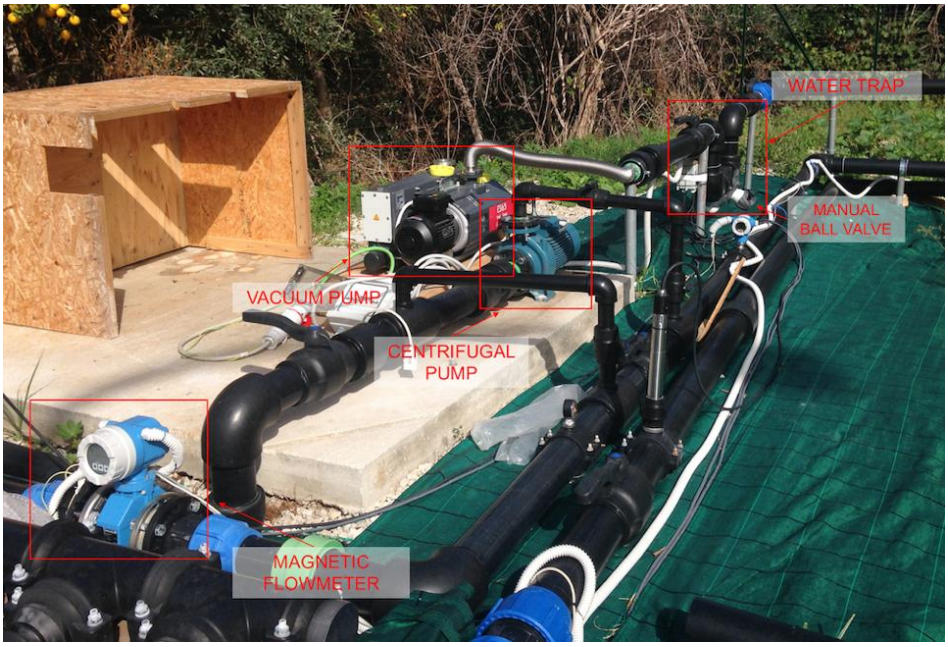

Figure 5.10: Detail of the circulation/input system in which a centrifugal pump and a vacuum pump are shown.

The measuring instrumentation comprises pH/temperature sensors/transmitters (WTW Sensolyt 700 IQ), oxygen sensors/transmitters (WTW FDO 700 IQ), turbidity sensor/transmitter (WTW Visoturb 700 IQ), and digital pressure sensor (EH Cerabar S PMC 71) for both inlet/outlet PBR Unit section. An additional digital pressure sensor is installed at the airlift top, and a CO_2 sensor/transmitter (Mettler Toledo ISM INPRO 5000i), is installed near PBR inlet section. The inlet/outlet flow rate of the liquid is measured by magnetic flowmeters (EH Promag 10L). The measuring instrumentation is handled by the laboratory through the three data loggers shown in Figure 5.11. The first one is a terminal/controller (MIQ/TC 220 XT, WTW) supplied with two modules (MIQ/PS and MIQ/C6) responsible for sending and receiving the signal from and to the transducers through two additional modules located in the plant area (MIQ/JB). The sensors powered (12 V) by this controller are the pH probes, the O_2 probes and the turbidity sensor. These sensors send back to the data logger the recorded data minute by minute and they are saved in an internal memory. The second

controller (Memograph M, Endress Hauser) powers the plant pressure transducers, two in the plant area and one at the airlift top. They send back the signal to the data logger, together with the flowmeters, which are at the contrary powered by an electrical panel present in the plant. This electrical panel powers also the two system pumps and a monophasic plug. All the electrical connections in the plant are depicted in Figure 5.12, while the electrical panel, recently built, is shown in Figure 5.13. The back side of the Endress/Hauser data logger is shown in Figure 5.14. It contains several channels; each of them is connected to a different probe transducer. The employed channel list with the correspondent transducer is shown in Table 5 2.

Figure 5.11: Pilot plant data loggers inside the laboratory

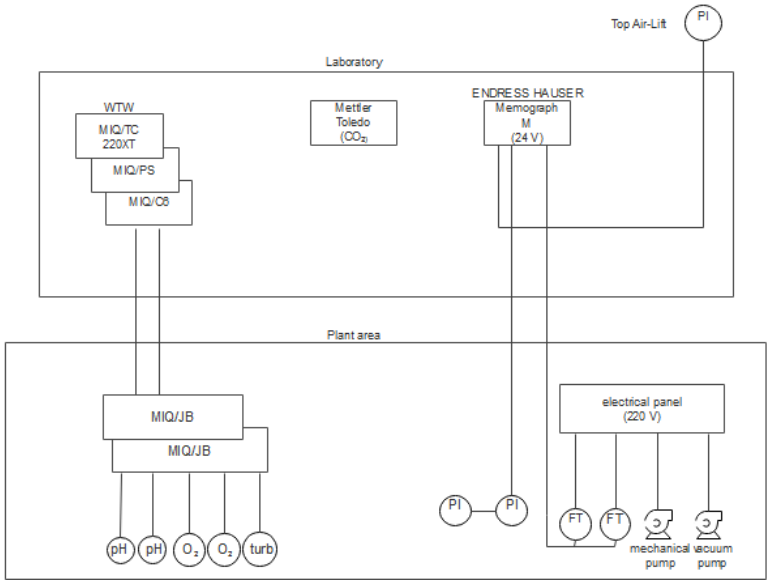

Figure 5.12: Scheme of the electrical connections between transducers (in the plant) and the controllers (in the laboratory)

Figure 5.13: Electrical panel in the plant area. It is possible to see a master switch, the switch for the monophase plug, the two switches for the pumps and a general switch followed by single ones for the flowmeters.

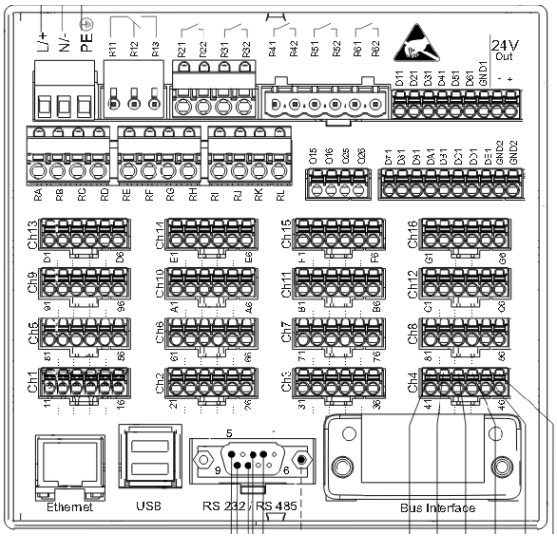

Figure 5.14: Back side of Memograph M data logger. Each channel is connected to a different probe transducer.

Table 5.2: List of probe transducer connected to the Memograph M and of the connected channels.

Trasducer	Channel	Cable colour
Pressure sensor-P1 (in)	CH 1	+orange -white/orange
Pressure sensor-P2 (out)	CH 8	+blue -white/blue
Pressure sensor-P3 (Top Air-Lift)	CH 5	+brown -white/brown
Flowmeter-Flow 1 (in)	CH 4	+green -white/green
Flowmeter-Flow 2 (out)	CH 6	+brown -white/brown

5.2.3. Results and Discussion

5.2.3.1. Performance test on circulation flow rate

Performance tests on circulation liquid flow (Ql) and circulation liquid velocity (v) in relation to gas flow in the airlift (Qg) were conducted with a single soft PVC tube of 20 m. Results are shown in Figure 5.15 and Figure 5.16. The tests were carried out with the entire airlift length, 17 m, and with the modified degasser, 5.7 m.

Considering that with the degasser modification the hydraulic head provided by the airlift decreased, the results returned a poorer circulation performance (Figure 5.15) and smaller liquid velocities for the same gas flow rate fed into the system (Figure 5.16).

Microalgae culture in outdoor photobioreactor needs a good circulation rate in order to prevent sedimentation and fouling in the tubes. The needed velocities vary according to the species but the range is between 0.17 and 0.8 m/s (Molina et al., 2001). Figure 5.16 shows how the circulation rates in 5.7 m airlift are barely acceptable with air flows higher than 3.5 L/min. The 17 m airlift performance is markedly higher, as with 1 L/min of gas flow the circulation flow reaches 0.2 L/s.

The unavailability of a pipe resistant to the hydrostatic pressure caused by the 17 m airlift together with the low circulation rates caused by the employment of the 5.7 m airlift motivated the decision to avoid the employment of the collector located in the photobioreactor section that would have caused a further circulation rate decrease. For this reason, a single polyolefin tube with one curve was employed.

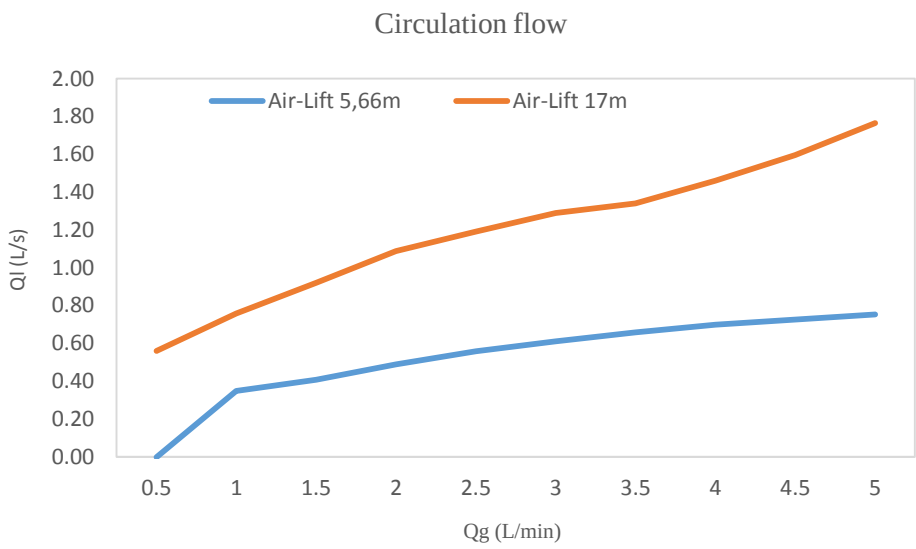

Figure 5.15: Liquid flow (Ql) performance related to gas flow (Qg).

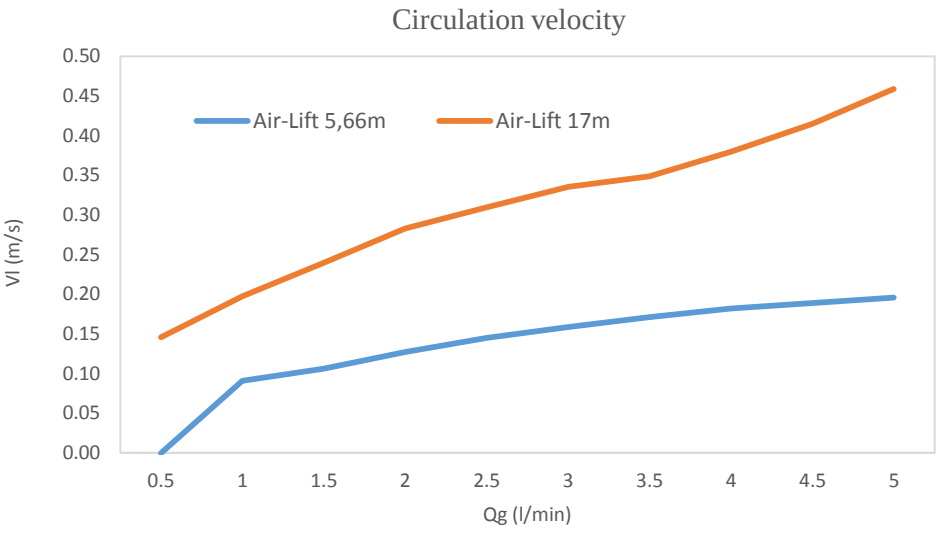

Figure 5.16: Liquid velocity (v) performance related to gas flow (Qg).

5.2.3.2. Microalgal growth in the photobioreactor and monitoring by transducers from the plant

Microalgae *Chlorella sorokiniana* was inoculated into the outdoor pilot plant and the growth was monitored. The inoculum was realised with 40 L of microalgal suspension previously grown in the laboratory, and the growth medium was made by adding 1.25 Kg of commercial fertilizer (Spray feed 20.20.20, Pavoni) to 460 L of water coming from the water pipe line. The total cultivation volume was 500 L. The inoculum was introduced into the plant from a tank placed in the plant area by employing the centrifugal pump. Microalgae growth curve in the outdoor pilot plant was monitored by manually taking a sample every day and measuring its absorbance at 500 nm for 25 days (from 15th June 2017 to 10th July 2018). The growth curve is depicted in Figure 5.17. The algal growth was monitored also by employing the turbidity probe located in the plant. Its signal is provided in Figure 5.22, which shows the signal provided by the turbidity probe in the plant. In the same figure, also the oxygen level is detected.

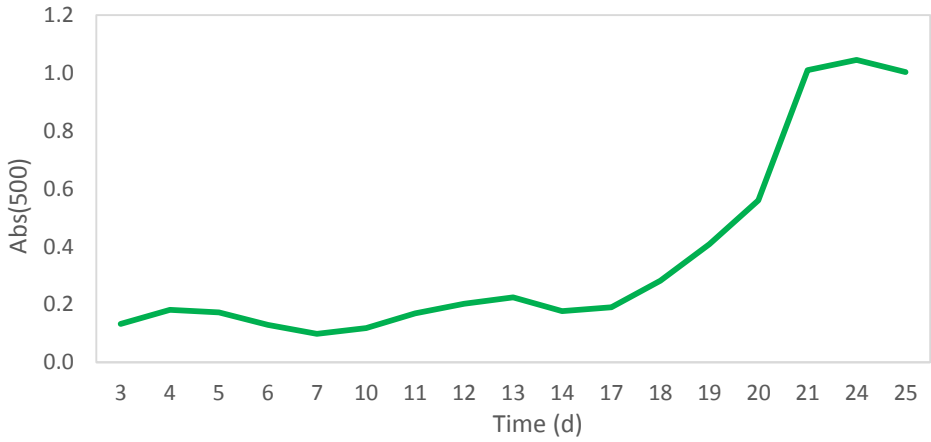

Figure 5.17: Growth curve of microalgae *Chlorella sorokiniana* growing into the pilot plant.

By looking at Figure 5.17 and Figure 5.22 it is possible to observe that until day 14 the growth was still in latency phase, while the exponential phase started from day 15. This is probably due by the usual acclimation phase due to a new environment but also to the temperatures that were really high, especially between the 15th and 17th of June (1st-3rd days) and the 27th and 28th of June (11th-12th days). The species inoculated in the plant has an ideal temperature of growth around 30°C (Lizzul et al., 2018), while the temperatures in the plant reached over 47°C, as shown in Figure 5.23, in which temperature and pH data recorded by probes in the plant are shown.

In order to decrease the temperature, a heat reflecting isolation material (Actis, Leroy Melin) was placed on the black tube top constituting the portion of the plant that connects the airlift to the photobioreactor. Irradiation and internal and external temperature data of two days, with and without insulator, are reported in Figure 5.18, Figure 5.19 and Figure 5.20. These data are adapted from the ones of Figure 5.24 and recorded by the probes present in the plant. One observes how the maximum decrease of temperature was of 2.5°C in the warmest hours of the day; this decrease is clearly insufficient to guarantee an optimal microalgal growth.

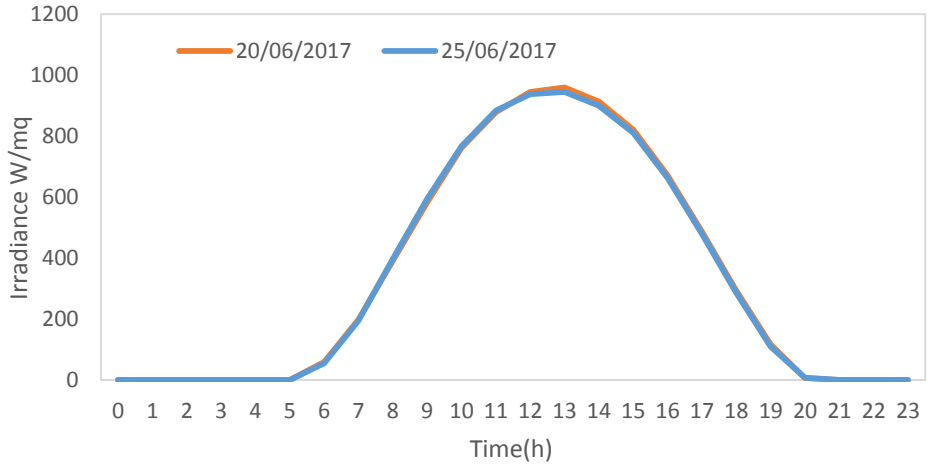

Figure 5.18: Average irradiance during two days of cultivation.

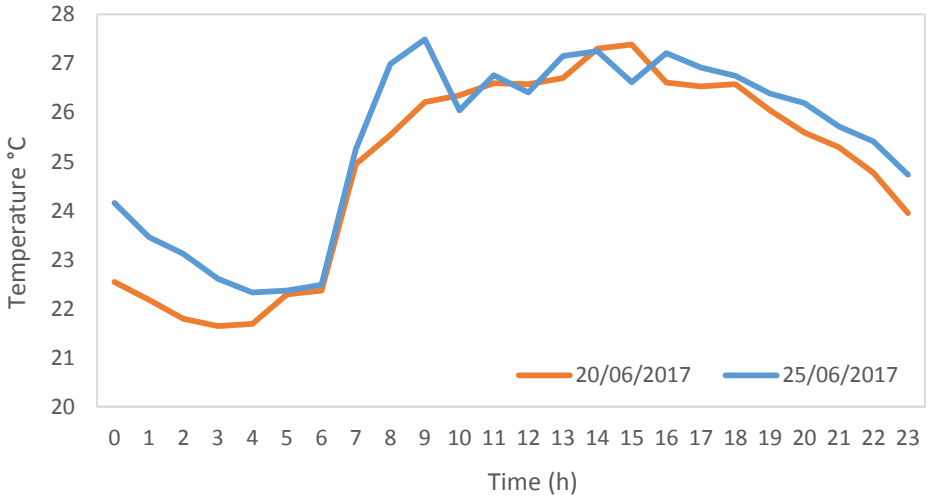

Figure 5.19: External temperatures during two days of cultivation.

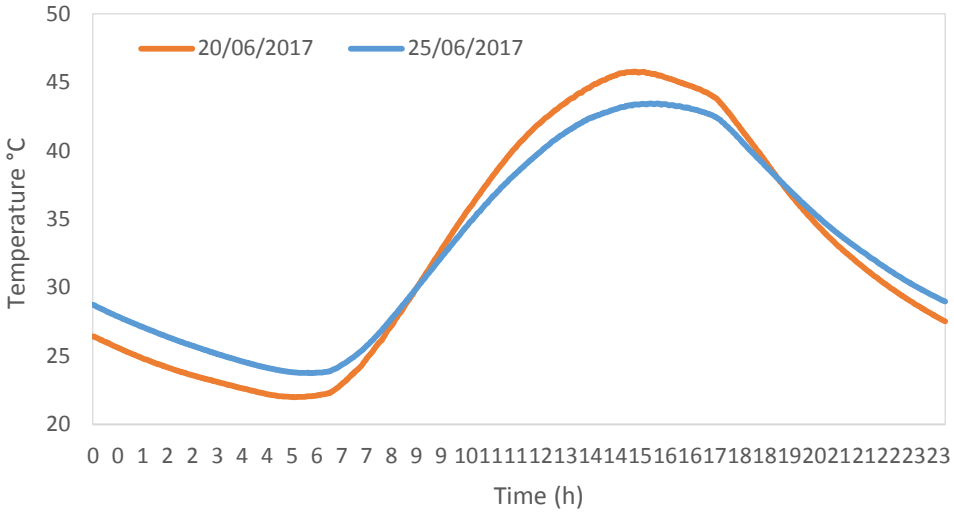

Figure 5.20: Internal temperature during two day of cultivation.

From 10th day of cultivation, CO_2 was manually inserted from the air sparger in order to regulate the culture pH, which naturally tends to reach basic values, and as carbon source. CO_2 was injected with a pressure of 2.5 bar and with a flow of 17 L/m for 4 minutes. In this way, at every injection 68 L of CO_2 were inserted into the system. The pH monitoring by the probes in the plant is observed in Figure 5.23.

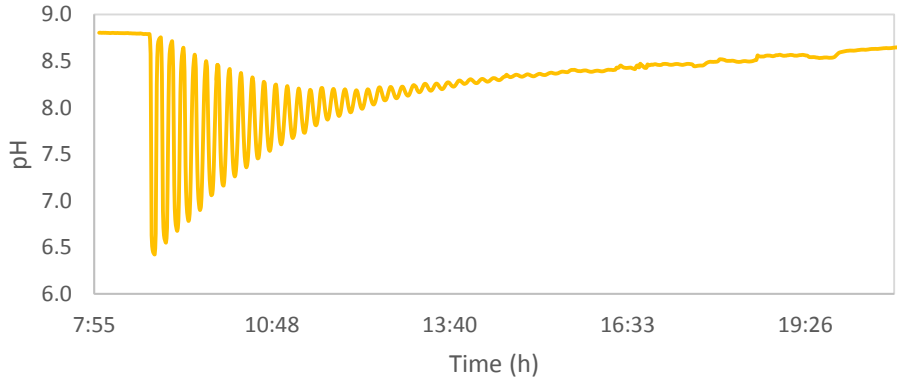

Figure 5.21: Variation of pH caused by the CO_2 injection.

By monitoring the system in the hours after the CO_2 injection one observes how the signal oscillates for about 8 hours before obscillations are damped out. This means that the mixing time in the plant is quite slow, as it could have been expected, due to the tubular nature of the reactor. Clearly from the data in Figure 5.21, showing the pH evolution after the CO_2 injection, a plug flow with axial dispersion appears to be

a suitable model for the system, which is however made of sections (PBR, riser, downcamer) with different axial dispersion features. The parameter that can be easily expected from those data is circulation time that can be used to match that expected from flow rate and from measured values.

By observing the data shown from Figure 5.22 to Figure 5.24 one observes that temperature, and thus also the irradiation, are the main factors affecting microalgae life cycle. All the biological data, in fact, followed the circadian rhythm of the photobioreactor internal temperature, made even more evident by Sicilian summer temperatures that caused temperature obscillations between night and day larger than 25 °C (Figure 5.23). The pH value is as well proportional to temperatures (Figure 5.23). In the figure, the points in which CO_2 was added manually are highlighted by relevant drops in the pH curve. In Figure 5.22, the oxygen concentration trend is regular in the first part of the curve and follows that of temperature as the oxygen solubility in water varies with it. In this first part, thus, the microalgae were not enough to affect the oxygen concentration in water. When microalgae started to growth exponentially, on the other hand, oxygen concentration started to develop in an irregular way, until the day concentration doubles thatof the night. This is probably due to the presence of algae that produced and consumed oxygen during the day and during the night respectively. This effect is also enhanced by the different oxygen solubility at different temperatures.

Flow and pressure trends inside the plant are reported in Figure 5.24. Both the parameters are dependent on temperature as fluids densities varywith it. This means that during the night the liquid flow and the pressure decreased. This effect is enhanced by the single-tube degasser that offer a reduced section for the liquid flow in that point. The consequence is that the volume decrease of the night causes a small variation sufficient to decrease the liquid level in the degasser and in this way prevent the circulation into the downcomer to occur. Clearly also water evaporation and relevant discontinuous addition played a role in the flow rate dynamics observed.

In all cases, the aforementioned figures show that modelling an outdoor PBR as a steady state device is very far from reality. They also give an idea of the many parameters that need to be taken into account when setting up a realistic phenomenological dynamic model of outdoor PBRs.

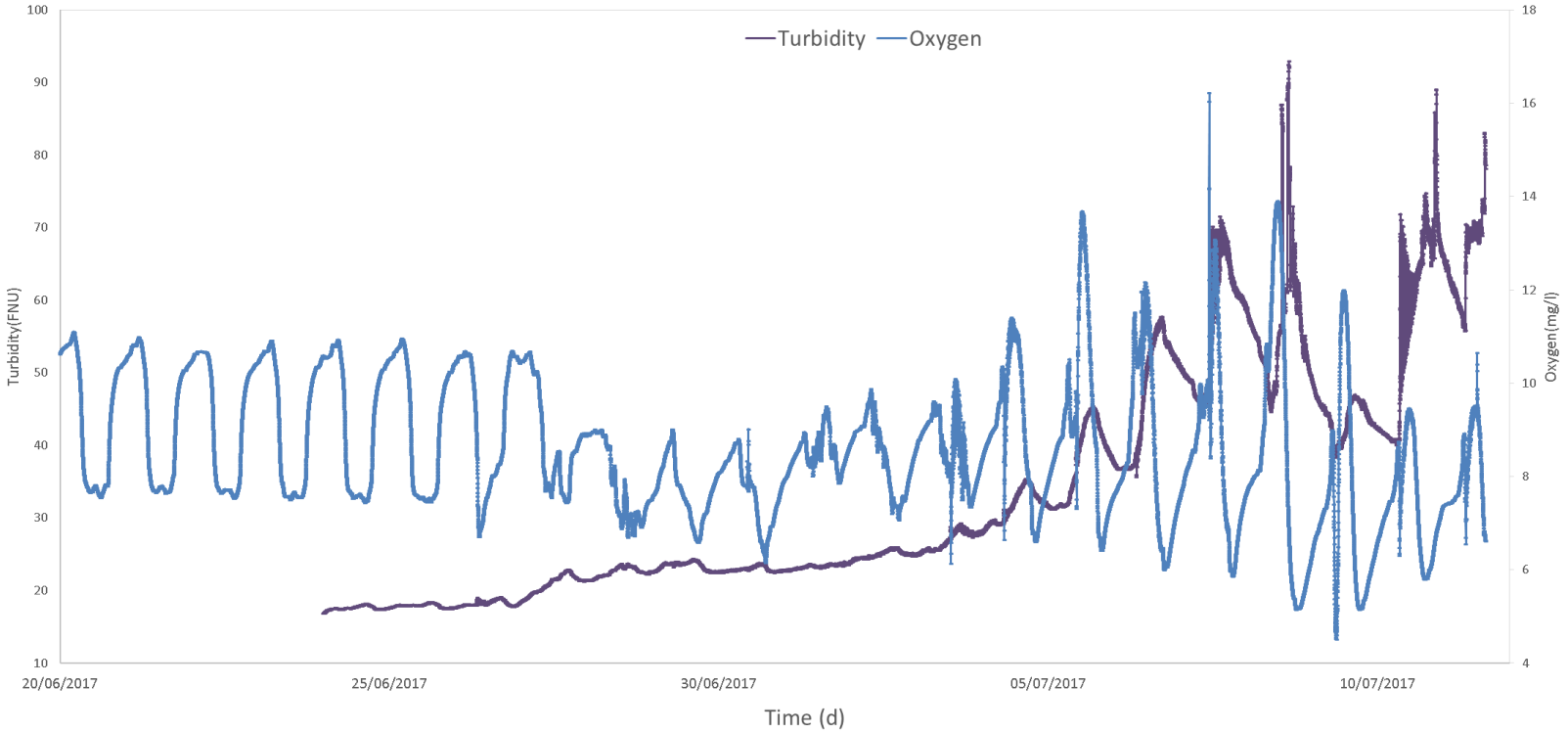

Figure 5.22: Turbidity and Oxygen concentration

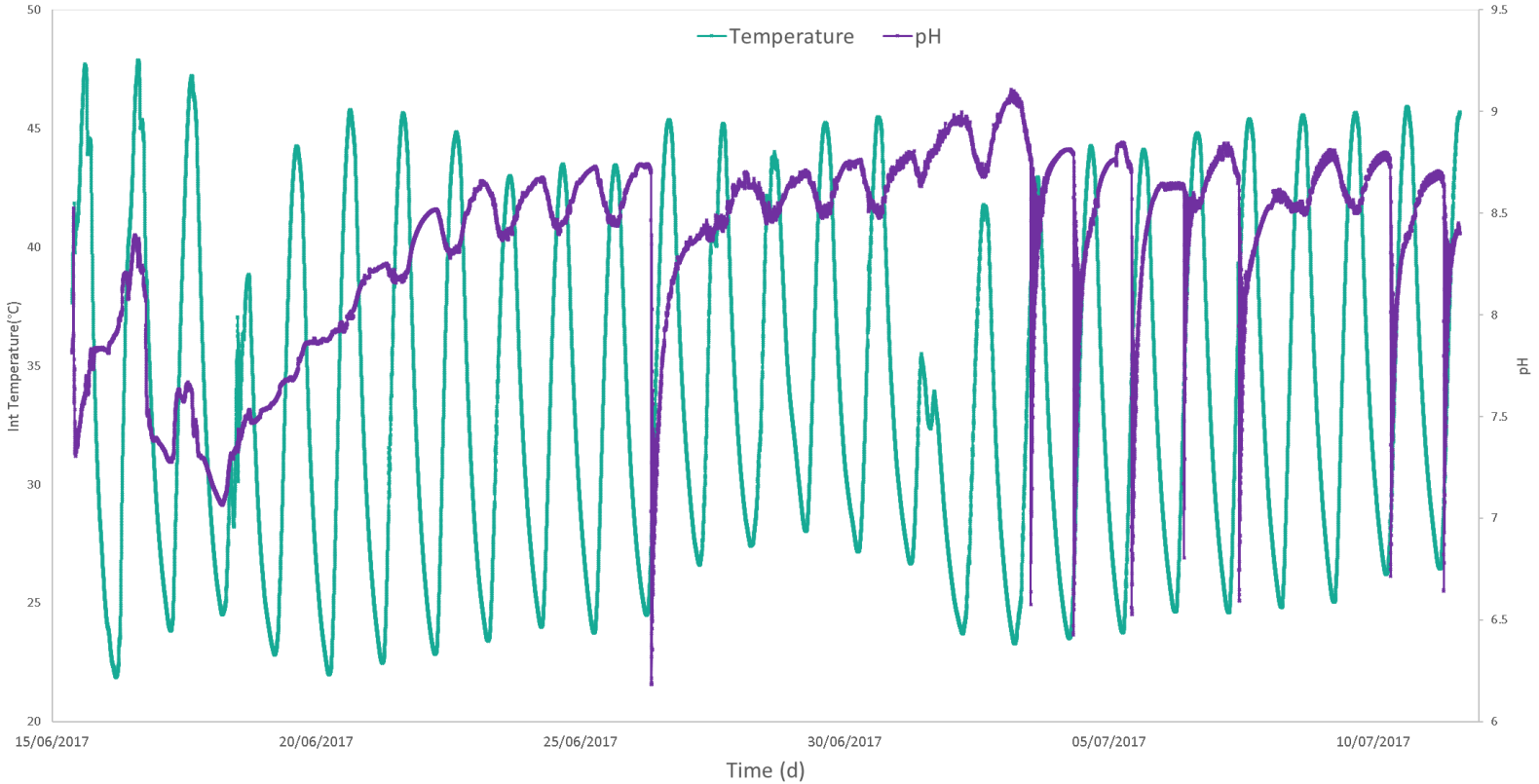

Figure 5.23: pH and temperature inside the plant.

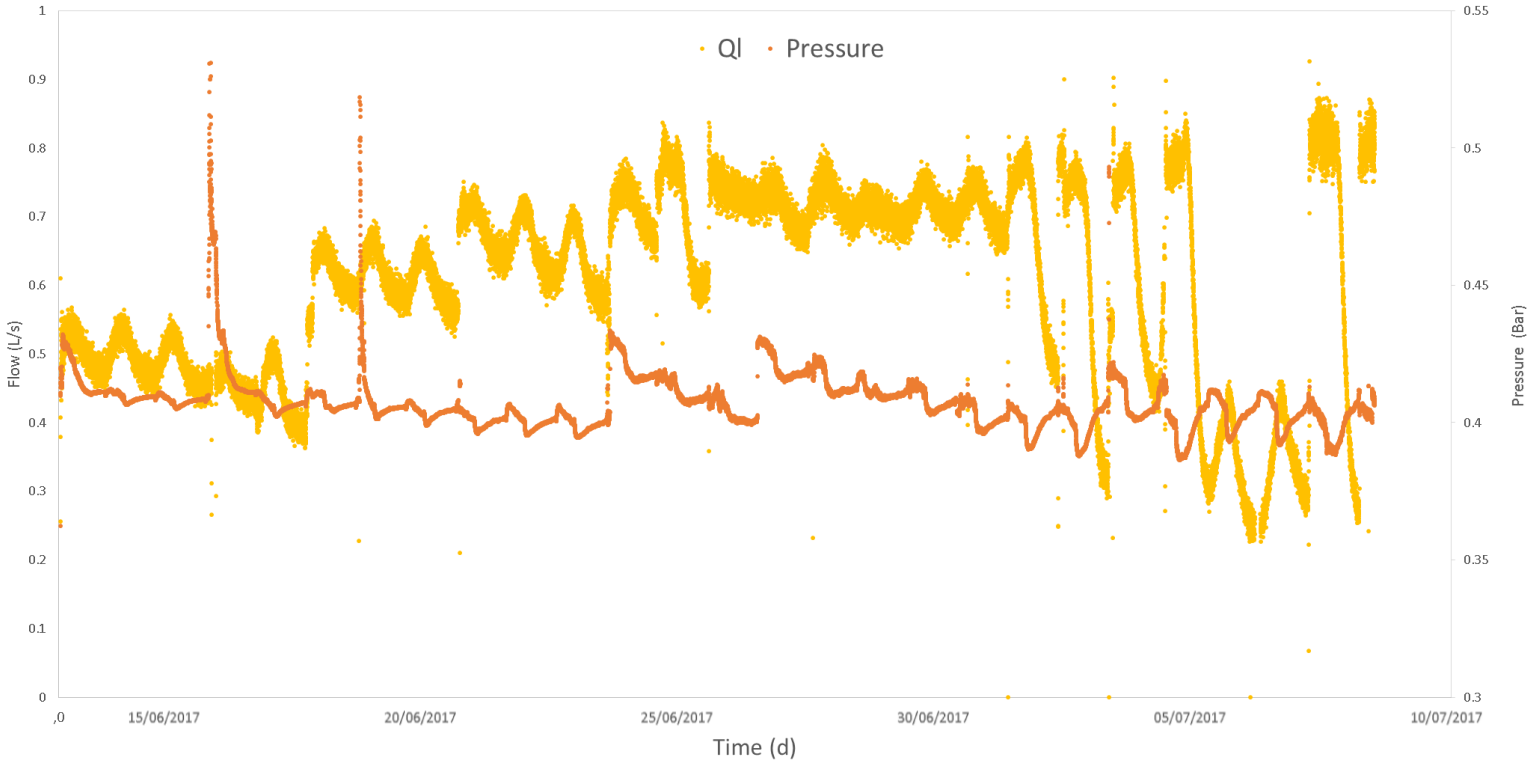

Figure 5.24: Liquid flow and pressure in the plant.

5.3. Plant optimization

5.3.1. Flat alveolar plate

In order to improve the surface-to-volume ratio, an attempt to set-up a flat-plate photobioreactor was made. The flat-plate is an alveolar plate made of transparent MakrolonR polycarbonate (PC), produced by *Covestro* and supplied by *Tecnoriv*. This material has a transparency of 77% to the visible fraction of solar radiation, it is able to resist to a wide temperature range (up to + 120°C), and it is provided with a UV-radiation resistant external layer with a guaranteed lifetime of 20 years. The alveolar PBR geometry is characterized by a length of 6 m and a total width of 1.20 m in which there is a single layer of 40 channels with 29.1 x 13.5 mm rectangular section. It has been connected to the plant and employed as solar collector. The flat alveolar plate is observed in Figure 5.25.

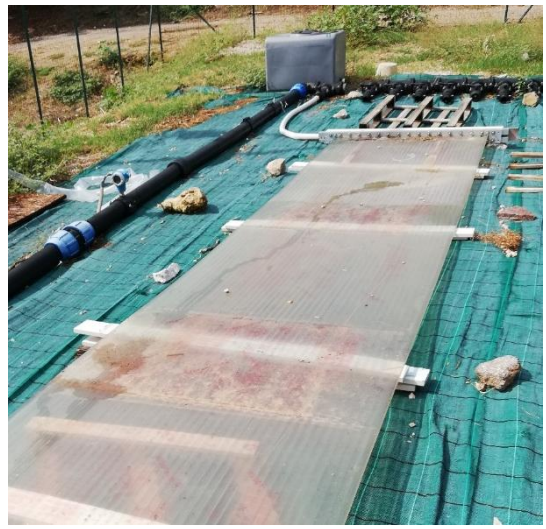

Figure 5.25: Flat plate alveolar photobioreactor employed as solar collector.

5.3.1.1. Test with flat-plate photoreactor

The flat plate alveolar photobioreactor was employed to perform hydrodynamics tests on the entire system. Data about pressure and flow trends were recorded during the tests and results are shown in Figure 5.26 and Figure 5.27. The records started during water filling of the plant. The red arrow indicates the moment in which the centrifugal pump was started to perform circulation inside the reactor. As it is evident from the graph of Figure 5.27, the pressure, after increasing during the filling of the system,

dropped after the pump was turned on. Also the liquid flow, in Figure 5.27, reached 0.4 L/s after about 20 minutes from the activation of the pump, while it started to decrease after less than one hour from start.

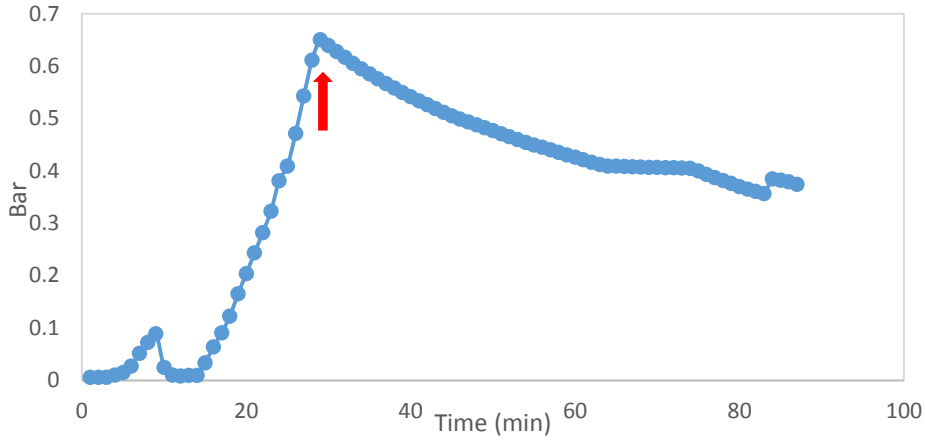

Figure 5.26: Pressure monitoring in the flat plate photobioreactor during the filling of the plant and the actuation of the pump.

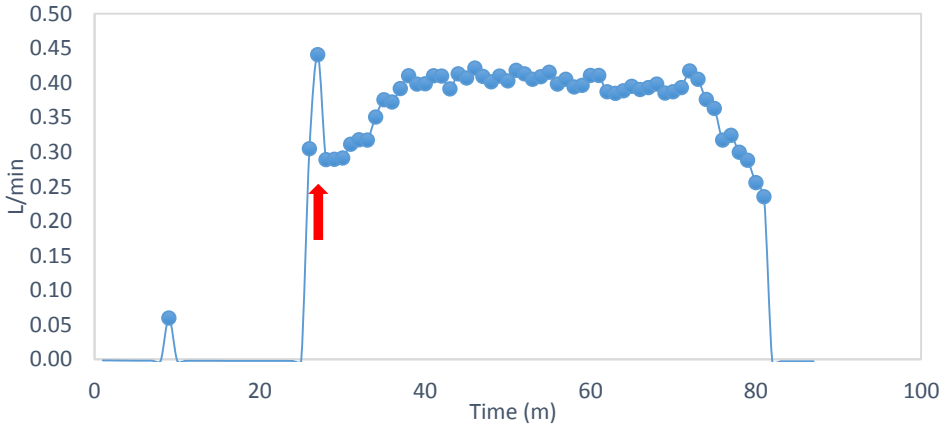

Figure 5.27: Liquid flow monitoring in the photobioreactor.

5.3.2. Rigid PMMA tubes

The new tubular solar PBR designed in cooperation with *Algoliner* is shown in Figure 5.28 and involves in the reuse of the collector employed in the original version of the photobioreactor. This collector will be modified and valves will be introduced amongst its outputs. The distance amongst them will increase from the present 26 cm to 61 cm, allowing to fit a photobioreactor module of 5 pipes in series, each 9.61 m long. The pipes will have an inner diameter of 51 mm. The total volume of the solar

collector will be 724 L for a total illuminated surface of 18.56 m^2. The introduction of valves amongst the outputs in the collector will allow to employ the system in series or in parallel and the valves before and after each module will allow to exclude it in case of need. The employed outputs will be 7 instead of 8 in order to allocate the new collector, 5 m long, in the available space of the experimental area. The pipes will be tilled by 1° in order to help the air removal. The system has been designed to stand a pressure of about 2.5 bar. The tubes are supported by an aluminium profile, shown in Figure 5.29. Since all elements are screwed together, they can be easily assembled and modified later if necessary. All the flanges are foreseen to be screwed together. Therefore the system can be opened for cleaning and/or repairing. In case one element is defect, it can be easily replaced. The profiles are every 2 meters stabilized to the side.

This configuration is the one that allows the greatest possible flexibility and will enable configuring the system with the modules in parallel or in series, allowing for experimental optimization of the configuration.

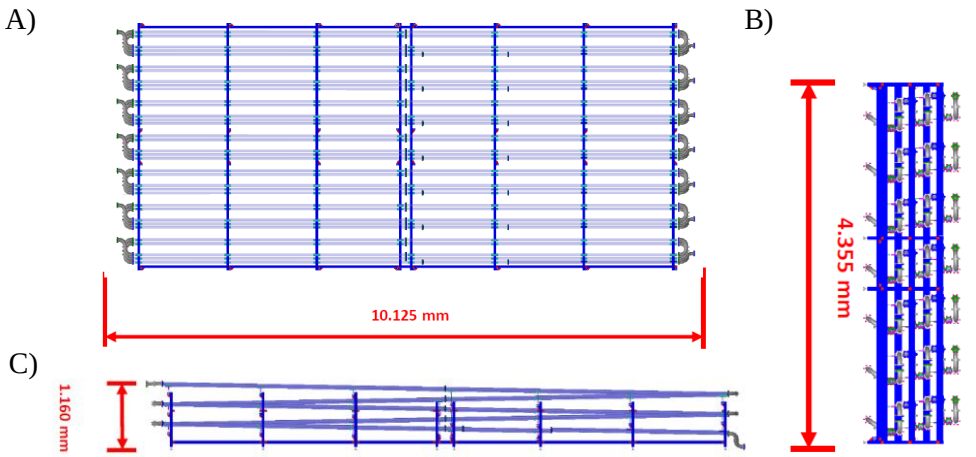

Figure 5.28: A) Sketch of the new project of solar collector designed by the company *Algoliner* as solar collector for the outdoor pilot plant of Palermo University. B) Side view. C) lateral view.

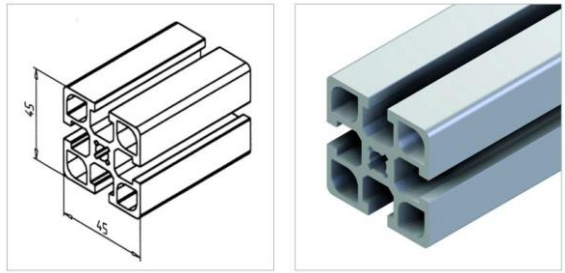

Figure 5.29: Detail of the aluminium profile employed for the supporting of PMMA tubes.

5.3.3. Prediction of the hydrodynamic performance in three alternative photobioreactor set-ups

In order to estimate the airlift performance in relation to several solar collector hydraulic configurations, some equations shown in the first part of this chapter were applied. Equations 5 IV to 5 VII were employed to calculate pressure drops to overcome in the solar collector to guarantee the fluid circulation. Considering that $\Delta P = gh(\rho r - \rho L)$, the gas hold up ε was calculated with equation 5 XV. Then, equation 5 XIV was employed to calculate U_G. The factors λ and U_b were taken from literature (Molina et al., 2001), and UL was used as variable. The input gas flow (Qg) was plotted against liquid flow (Ql) and circulation rate in the tubes (v). Results are reported from **Errore. L'origine riferimento non è stata trovata.** to Figure 5.32.

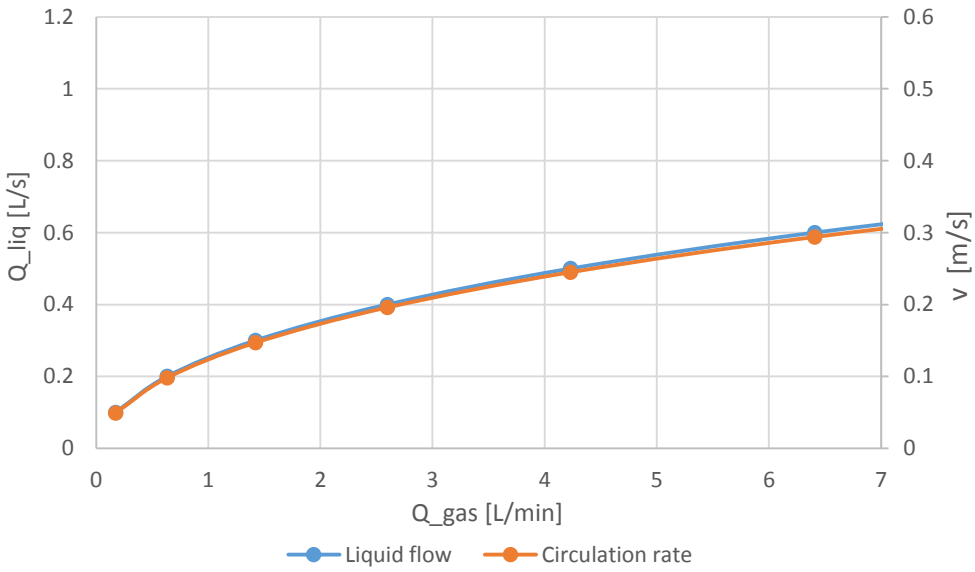

Figure 5.30: Previewed liquid circulation performance in the airlift system with the projected PMMA tubes of 356 m length as solar collector.

The previewed circulation flow in the first project by *Algoliner*, in Figure 5.30, consisting in a single tube 356 m long, with a gas input of 5 L/min consists in a liquid flow of about 0.5 L/s, with a circulation rate of about 0.25 m/s. Although the objective is closer, it is still not there.

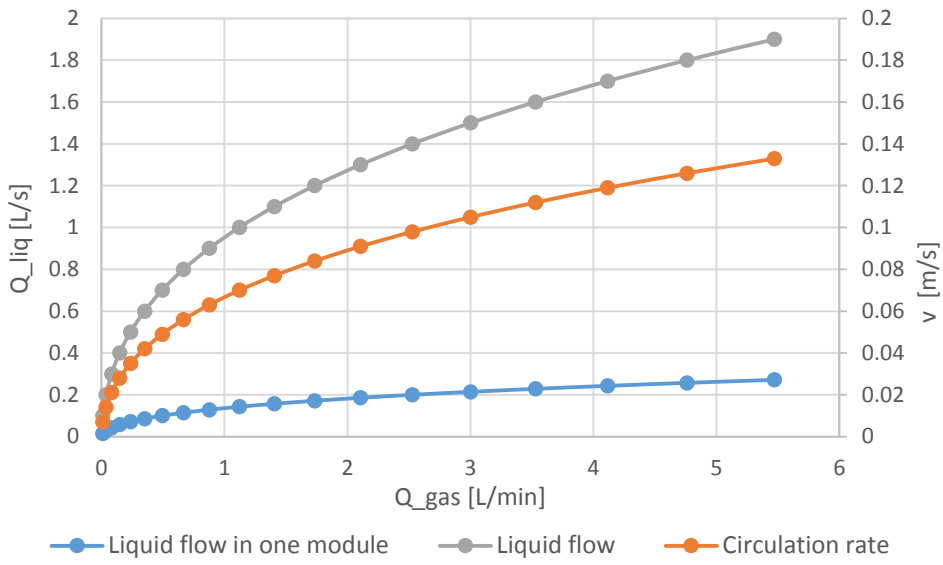

Figure 5.31: Previewed liquid circulation performance in the airlift system with the projected PMMA tubes divided in 7 parallel modules, each one made of 5 tubes.

In Figure 5.31 one observes the prediction with the solar collector arranged in 7 parallel modules, each one made of 5 tubes. In this case, the circulation flow performance would increase. In fact, with 2 L/m of input gas flow, the overall liquid flow is about 1.25 L/s, while the liquid flow in one module is about 0.19 L/s. Anyway, the circulation rate is still far away from the goal of 0.5 m/s, as in one module it reaches about 0.1 m/s.

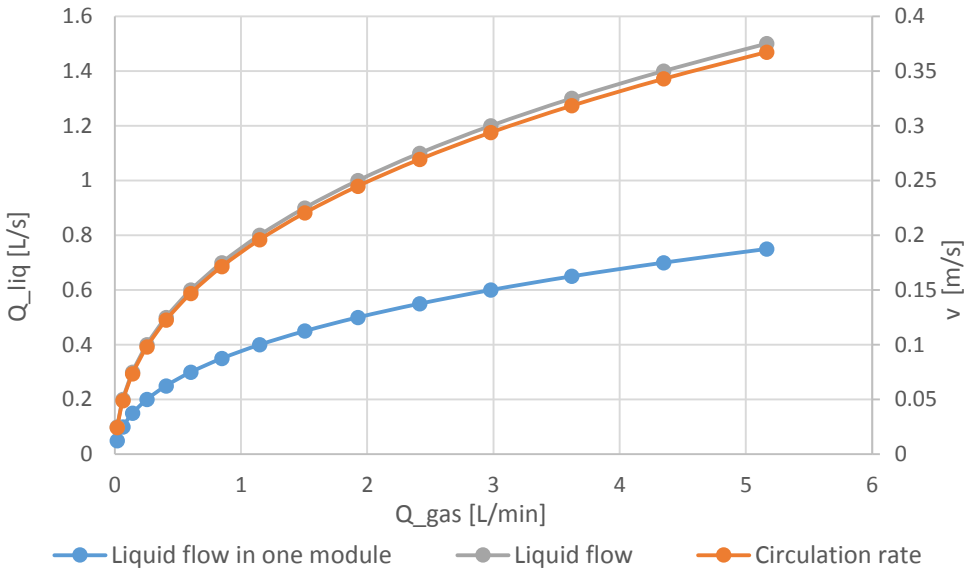

Figure 5.32: Previewed liquid circulation performance of in the airlift system with the projected PMMA tubes divided in 2 modules, each of one constituted by 5 tubes.

In Figure 5.32 the case in which only two of the seven modules are employed in parallel between them is shown. We observe how the circulation performance is increased as with 2 L/min of gas input flow the circulation flow reaches almost 1.5 L/s, while the circulation rate in the tubes is almost 0.3 m/s.

These data show that amongst the possible solar collectors for the outdoor pilot plant driven by the airlift pump, the best configuration is the last proposed, consisting in a plastic system that allows to employ the rigid PMMA tubes in series or in parallel. Furthermore, it will be possible to exclude modules if desired.

5.4. Conclusions and future perspectives

This part of the work was aimed at the development of an outdoor pilot plant driven by an airlift pump located at Palermo University. The cultivation of the microalgae *Chlorella sorokiniana* in the plant was realised during the Sicilian summer, thus with high temperatures and irradiation. The cultivation was realised by employing a single polyolefin tube and the modified degasser located at 5.6 m. Although it was not possible to operate the system at its circulation performance, microalgae grew and data about turbidity, circulation flow, pH, oxygen concentration and pressure were recorded. All the data were affected by the internal temperature of the system, including the microalgal growth. Thus, introducing a method for controlling the temperature of the system would be useful. In order to test the characteristic of a plate system, also an alveolar flat plate was employed but it did not result in a good working performance. With the aim of operating the system at his best circulation performance, it is necessary to employ the total height of the airlift (17 m). This implies using a solar collector resistant to the hydrostatic pressure of the system, equal to 1.7 bar. For this reason, we decided to adopt a new PMMA tubular system supplied by the company *Algoliner*. According to hydrodynamic calculations, the first proposed system, consisting of a single tube 396 m long, would not lead to an optimal circulation performance. Thus, we designed a new system containing seven modules of five tubes that can be employed either in series or in parallel. This will guarantee the needed flexibility when operating the system. Next steps will be installing the designed system and to perform hydrodynamic tests in order to validate the hydraulic model developed. At that point, we will start the cultivation of a model microalgae into the system in order to estimate productivity data in the Sicilian territory. Finally, the cultivation of indigenous microalgal strains will be performed, in order to explore the potential of Sicily as an ideal region for expanding the microalgal industrial market.

Final remarks

Final remarks

This thesis work focuses on several industrial applications of microalgae and deals with different microalgal species and with different techniques, all directed towards the exploitation of the photosynthetic machinery as a mean to reach industrial goals through microalgal cultivation. This conclusion presents a summary of the main scientific findings and of the work that still needs to be done in order to exploit the scientific output of this research.

The first part of this work was focused on molecular biology techniques on the model microalgae *Chlamydomonas reinhardtii*. It was demonstrated that the human glycoprotein Intrinsic Factor can be expressed in *Chlamydomonas reinhardtii* by the nuclear genome. The addition of an *ARS2* signal peptide leads to efficient secretion towards the medium. Furthermore, the secreted IF protein directly binds B_{12}. This study was a first proof-of-concept utilizing a human B_{12} binding protein as a tool for enriching B_{12} in microalgae and can contribute to the future development of microalgal market of functional foods.

Considering the limitations associated with the clear gap between the results obtained in proof-of-concept studies and the transition to an industrial scale of genetic manipulation techniques, in this thesis some alternatives were also explored.

Among them, the first one to be addressed was the tailoring of light in short packages, referred to as flashing light. In this part of the research, a "quasi isoactinic" reactor was firstly set up in order to homogeneously distribute light inside it. This reactor was employed for the cultivation of the microalgae *Nannochloropsis gaditana* under several regimes of flashing light and with a growth medium both supplemented with nutrients or not. A combined effect of the flashing frequency and of the nutrient concentration was observed when nutrients are limiting. In this case, the flashing light increases nutrient starvation effects leading to accumulation of lipids. When the cells were cultivated in richness of nutrients, flashing light led instead to low-light acclimation responses such as PUFAs and pigments accumulation. In a second moment, the effect of flashing light on several species (*Nannochloropsis gaditana, Koliella antarctica and Tetraselmis chuii*) and under higher light intensities was investigated. The results confirmed that these effects were stronger at relatively low frequencies. Also in this case, low-frequency flashing light conditions induced intracellular biocomponents that typically accumulate under low-light conditions, including protein, PUFA, chlorophyll, lutein and β-carotene. To further deepen the scenario about the effects of flashing light on microalgae, the photosynthetic efficiency and transcriptomic of key genes of *Nannochloropsis gaditana,* grown under flashing light conditions, were analyzed. The results were coherent with composition data and prooved that the photosynthetic machinery is enhanced by low-

frequency flashing light. This photochemical energy, however, is dispersed as heat or employed for the production of high-value biocompounds. The combination of these results makes the usage of flashing light in industry as a promising strategy to optimize the production of the compounds of interest. Considering furthermore that flashing light was found to be a good strategy for inducing high-value compounds, a future application may be that of cultivating microalgae that naturally produce high amounts of carotenoids, such as *Dunaliella salina* or *Haematococcus pluvialis*, under pulsed light.

The second analyzed alternative to the genetic manipulation was the selection of microalgae from the environment and their cultivation in wastewaters, according to a process called *phycoprospecting*. Some microalgal strains were isolated from the Sicilian coastline and two of them, *Chlorella (Pozzillo)* and *Chlorella sp./Dunaliella (Vergine Maria)*, were employed for the bioremediation of urban wastewaters. They were compared with two collection strains, *Nannochloropsis gaditana* CCAP 849/5 and *Chlorella sorokiniana* CCAP 211/11k. The results of biochemical and chemical analysis on treated sewages indicated that the environmental strains may be good candidates for an industrial bioremediation process, in particular a tertiary one. They would also allow the accumulation of high-value compounds (*e.g.* PUFAs).

As last topic of this work, the problems of industrial cultivation of microalgae inside photobioreactors started to be addressed. In particular, we tried to revamp an already existing outdoor airlift pilot plant located at Palermo University. The microalgae *Chlorella sorokiniana* CCAP 211/11k was cultivated inside the photobioreactor and we observed how all the parameters related to the hydraulic performance and to the microalgal growth are related to the temperature of the system. We also designed a new solar collector made of rigid PMMA tubes that is expected to result in a more resistant photobioreactor system to be coupled with the airlift reactor. About this part of the thesis, significant work still remains to be carried out. Once the tubes will be installed, the system will be employed to assess the productivities of Sicilian migroalgae grown under their natural environmental conditions.

Supplemental Information

Supplemental informations

Section 2

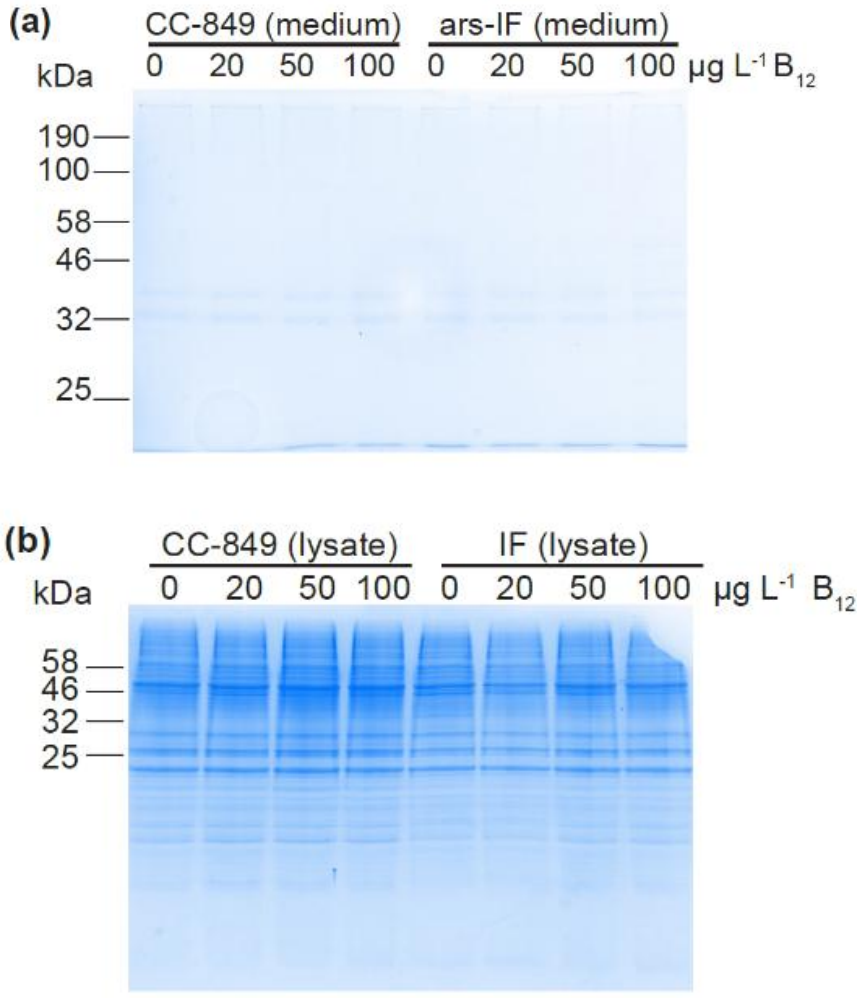

Figure A1: Coomassie-stained polyacrylamide gels of samples shown in figure 3. (a) medium harvested from CC-849 and ars-IF cultures grown to late log phase containing 0, 20, 50 and 100 µg L–1 Vitamin B12. 20 µL of culture supernatant loaded per lane. (b) Cellular lysates from CC-849 and IF cultures grown to late log phase with 0, 20, 50 and 100 µg L–1 Vitamin B12 supplemented. Equal amounts of cellular lysate standardized by OD_{750} loaded.

Picture of the Vitamin B12 assay plates with different fractions from ion exchange chromatography.

Ars-IF, medium (20 µg L–1 Vitamin B12 supplemented) on the first row
CC-849, medium (20 µg L–1 Vitamin B12 supplemented) on the second row

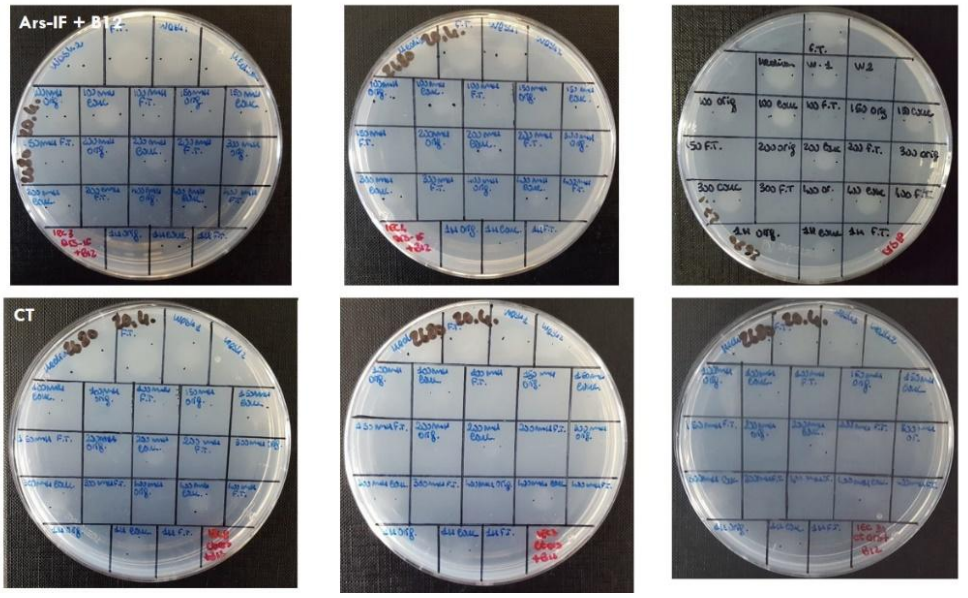

Ars-IF, medium (no Vitamin B12 supplemented) on the first row
CC-849, medium (no Vitamin B12 supplemented) on the second row

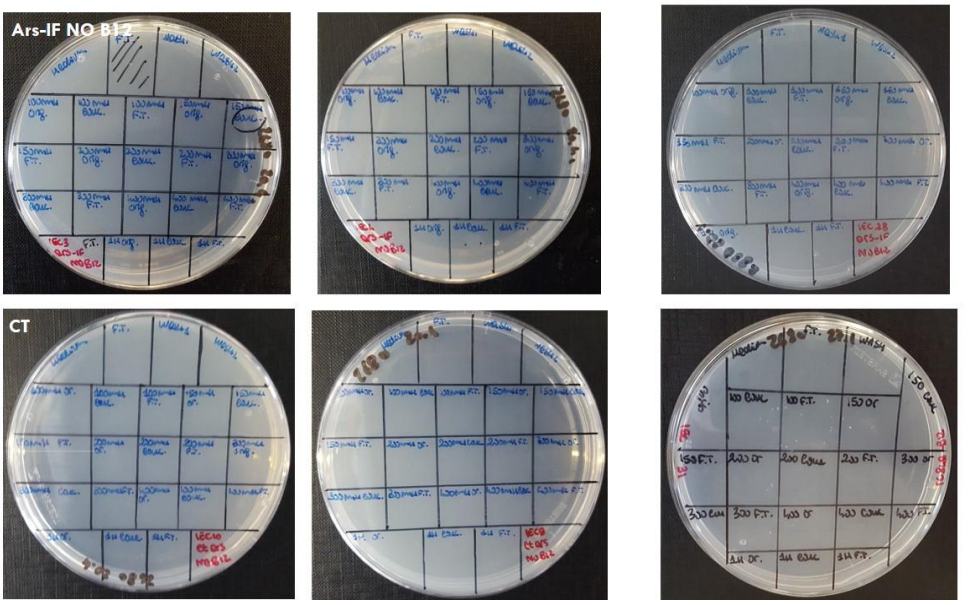

IF, lysate (20 µg L–1 Vitamin B12 supplemented)
CC-849, lysate (20 µg L–1 Vitamin B12 supplemented)

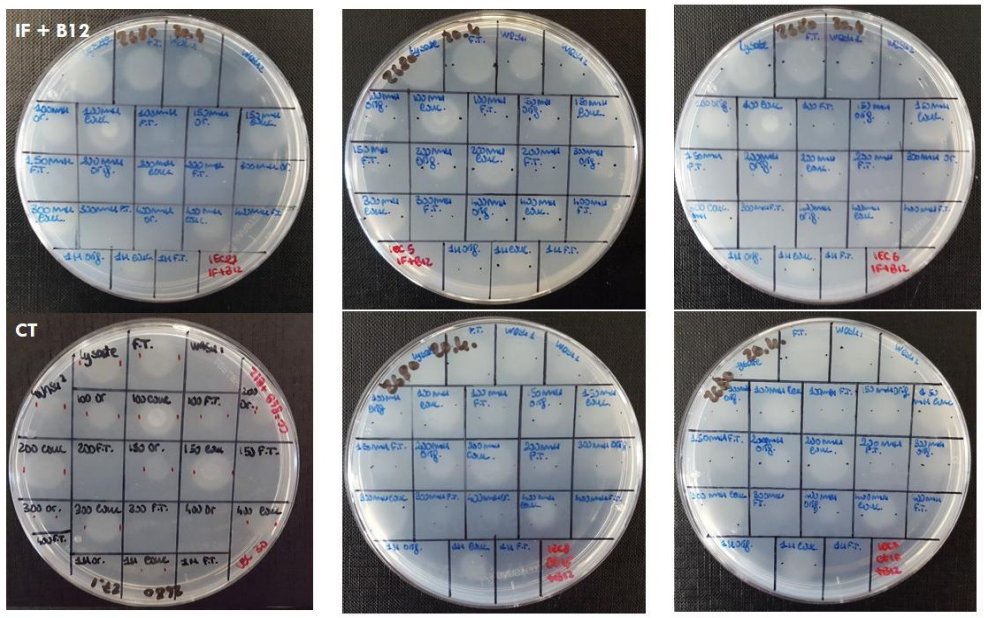

IF, lysate (no Vitamin B12 supplemented)
CC-849, lysate (no Vitamin B12 supplemented)

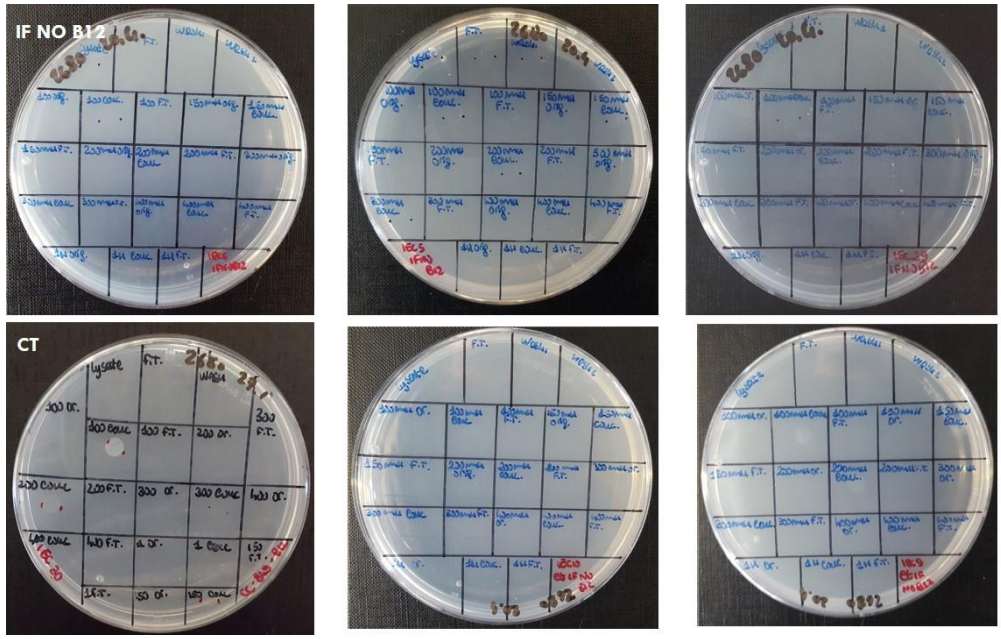

Vitamin B12 assay plaque diameters measured in different fractions from ion exchange chromatography and calculated Vitamin B12 content of samples (nM).

ars-IF. medium (20 µg L–1 Vitamin B12 supplemented)

	plaque diameter (cm)			Vitamin B12 (mg/L)		
Fraction	replicate 1	replicate 2	replicate 3	replicate 1	replicate 2	replicate 3
Medium	0.95	1.25	1.25	2.97	13.30	13.30
Flow Through	1.00	1.15	1.20	3.93	8.43	10.64
Wash 1	0.80	0.95	0.90	1.16	2.97	2.21
Wash 2	0.50	0.50	0.00	0.09	0.09	0.00
100 mM	0.60	0.60	0.60	0.24	0.24	0.24
150 mM	0.50	0.60	0.55	0.09	0.24	0.15
200 mM	0.00	0.00	0.00	0.00	0.00	0.00
300 mM	0.00	0.00	0.00	0.00	0.00	0.00
400 mM	0.50	0.00	0.00	0.09	0.00	0.00
1 M	0.00	0.00	0.00	0.00	0.00	0.00

ars-IF, medium (no Vitamin B12 supplemented)

	plaque diameter (cm)			Vitamin B12 (mg/L)		
Fraction	replicate 1	replicate 2	replicate 3	replicate 1	replicate 2	replicate 3
Medium	0	0	0	0	0	0
Flow Through	0	0	0	0	0	0
Wash 1	0	0	0	0	0	0
Wash 2	0	0	0	0	0	0
100 mM	0	0	0	0	0	0
150 mM	0	0	0	0	0	0
200 mM	0	0	0	0	0	0
300 mM	0	0	0	0	0	0
400 mM	0	0	0	0	0	0
1 M	0	0	0	0	0	0

CC-849. medium (20 µg L–1 Vitamin B12 supplemented)

	plaque diameter (cm)			Vitamin B12 (mg/L)		
Fraction	replicate 1	replicate 2	replicate 3	replicate 1	replicate 2	replicate 3
Medium	0.95	1.20	1.20	2.97	10.64	10.64
Flow Through	1.00	1.20	1.10	3.93	10.64	6.61
Wash 1	0.60	0.80	0.85	0.24	1.16	1.62
Wash 2	0.00	0.00	0.00	0.00	0.00	0.00
100 mM	0.00	0.00	0.00	0.00	0.00	0.00
150 mM	0.00	0.00	0.00	0.00	0.00	0.00
200 mM	0.00	0.00	0.00	0.00	0.00	0.00
300 mM	0.00	0.00	0.00	0.00	0.00	0.00
400 mM	0.00	0.00	0.00	0.00	0.00	0.00
1 M	0.00	0.00	0.00	0.00	0.00	0.00

CC-849, medium (no Vitamin B12 supplemented)

	plaque diameter (cm)			Vitamin B12 (mg/L)		
Fraction	replicate 1	replicate 2	replicate 3	replicate 1	replicate 2	replicate 3
Medium	0	0	0	0	0	0
Flow Through	0	0	0	0	0	0
Wash 1	0	0	0	0	0	0
Wash 2	0	0	0	0	0	0
100 mM	0	0	0	0	0	0
150 mM	0	0	0	0	0	0
200 mM	0	0	0	0	0	0
300 mM	0	0	0	0	0	0
400 mM	0	0	0	0	0	0
1 M	0	0	0	0	0	0

IF. lysate (20 μg L–1 Vitamin B12 supplemented)

	plaque diameter (cm)			Vitamin B12 (mg/L)		
Fraction	replicate 1	replicate 2	replicate 3	replicate 1	replicate 2	replicate 3
Lysate	1.40	1.35	1.30	24.69	20.24	16.47
F.T.	1.00	1.20	1.15	3.93	10.64	8.43
Wash 1	0.85	1.00	1.00	1.62	3.93	3.93
Wash 2	0.65	0.70	0.75	0.37	0.56	0.82
100 mM	0.85	0.90	0.90	1.62	2.21	2.21
150 mM	0.95	0.95	0.70	2.97	2.97	0.56
200 mM	0.85	0.95	0.80	1.62	2.97	1.16
300 mM	0.70	0.90	0.75	0.56	2.21	0.82
400 mM	0.65	0.85	0.00	0.37	1.62	0.00
1 M	0.00	0.65	0.00	0.00	0.37	0.00

IF. lysate (no Vitamin B12 supplemented)

	plaque diameter (cm)			Vitamin B12 (mg/L)		
Fraction	replicate 1	replicate 2	replicate 3	replicate 1	replicate 2	replicate 3
Lysate	1.15	1.20	1.20	8.43	10.64	10.64
F.T.	1.15	1.20	1.20	8.43	10.64	10.64
Wash 1	0.80	1.00	0.95	1.16	3.93	2.97
Wash 2	0.00	0.80	0.80	0.00	1.16	1.16
100 mM	1.00	0.70	0.90	3.93	0.56	2.21
150 mM	0.80	0.80	0.90	1.16	1.16	2.21
200 mM	0.70	0.85	0.95	0.56	1.62	2.97
300 mM	0.65	0.85	0.75	0.37	1.62	0.82
400 mM	0.00	0.70	0.60	0.00	0.56	0.24
1 M	0.00	0.00	0.00	0.00	0.00	0.00

CC-849. lysate (20 µg L–1 Vitamin B12 supplemented)

	plaque diameter (cm)			Vitamin B12 (mg/L)		
Fraction	replicate 1	replicate 2	replicate 3	replicate 1	replicate 2	replicate 3
lysate	1.15	1.20	1.20	8.43	10.64	10.64
F.T.	1.15	1.20	1.20	8.43	10.64	10.64
Washing 1	0.80	1.00	0.95	1.16	3.93	2.97
Washing 2	0.00	0.80	0.80	0.00	1.16	1.16
100 mM	1.00	0.70	0.90	3.93	0.56	2.21
150 mM	0.80	0.80	0.90	1.16	1.16	2.21
200 mM	0.70	0.85	0.95	0.56	1.62	2.97
300 mM	0.65	0.85	0.75	0.37	1.62	0.82
400 mM	0.00	0.70	0.60	0.00	0.56	0.24
1 M	0.00	0.00	0.00	0.00	0.00	0.00

CC-849, lysate (no Vitamin B12 supplemented)

	plaque diameter (cm)			Vitamin B12 (mg/L)		
Fraction	replicate 1	replicate 2	replicate 3	replicate 1	replicate 2	replicate 3
Medium	0	0	0	0	0	0
F.T.	0	0	0	0	0	0
Wash 1	0	0	0	0	0	0
Wash 2	0	0	0	0	0	0
100 mM	0	0	0	0	0	0
150 mM	0	0	0	0	0	0
200 mM	0	0	0	0	0	0
300 mM	0	0	0	0	0	0
400 mM	0	0	0	0	0	0
1 M	0	0	0	0	0	0

Section 3

Part 1

Paragraph 3.4.

Cell concentration of *Nannochloropsis gaditana* grown in basic medium.

Time (d)	CL [1]	CL [2]	CL [3]	FL 25Hz [1]	FL 25Hz [2]	FL 25Hz [3]	FL 250Hz [1]	FL 250Hz [2]	FL 250Hz [3]	FL 2500 Hz [1]	FL 2500 Hz [2]	FL 2500 Hz [3]
0	8.48E+05	7.67E+05	7.78E+05	1.11E+06	1.14E+06	1.53E+06	1.23E+06	1.34E+06	1.26E+06	1.12E+06	1.20E+06	1.17E+06
1	4.64E+05	9.73E+05	1.01E+06	4.93E+06	5.71E+06	5.37E+06				1.50E+06	1.50E+06	1.65E+06
2	1.44E+06	1.45E+06	8.23E+05				4.15E+06	3.20E+06	3.65E+06	4.40E+06	3.95E+06	4.80E+06
3	6.25E+06	4.44E+06	3.23E+06				5.50E+06	5.30E+06	4.50E+06	1.04E+07	9.00E+06	1.10E+07
4	7.57E+06	6.86E+06	5.00E+06	7.89E+06	4.94E+06	1.04E+07	1.19E+07	1.32E+07	1.22E+07	1.79E+07	2.00E+07	1.93E+07
5				1.14E+07	1.44E+07	1.56E+07	3.30E+07	3.00E+07	2.95E+07	2.76E+07	2.52E+07	2.52E+07
6				1.56E+07	1.68E+07	1.74E+07	2.94E+07	3.48E+07	3.90E+07	3.70E+07	4.40E+07	3.40E+07
7	6.76E+07	2.77E+07	4.00E+07	3.66E+07	3.66E+07	3.00E+07				4.20E+07	3.50E+07	4.05E+07
8	5.07E+07	7.12E+07	6.93E+07	4.20E+07	5.11E+07	3.29E+07				3.18E+07	3.60E+07	4.62E+07
9	7.27E+07	8.25E+07	8.43E+07	6.75E+07	5.49E+07	4.14E+07	6.57E+07	7.47E+07	5.85E+07	4.06E+07	3.22E+07	4.48E+07
10	6.75E+07	7.62E+07	8.52E+07	4.70E+07	4.00E+07	4.40E+07	5.58E+07	4.95E+07	5.85E+07	4.14E+07	3.78E+07	3.66E+07
11	6.14E+07	8.93E+07	6.22E+07	6.20E+07	4.70E+07	3.80E+07	5.68E+07	5.20E+07	5.68E+07			
12	6.14E+07	8.93E+07	6.22E+07	6.00E+07	6.10E+07	5.30E+07	5.76E+07	5.60E+07	4.80E+07			
13	6.14E+07	8.93E+07	6.22E+07	4.60E+07	5.30E+07	4.20E+07	4.48E+07	5.04E+07	5.04E+07	4.20E+07	3.50E+07	4.05E+07

Cell concentration of *Nannochloropsis gaditana* grown in enriched medium.

Time (d)	CL [1]	CL [2]	CL [3]	FL 25Hz [1]	FL 25Hz [2]	FL 25Hz [3]	FL 250Hz [1]	FL 250Hz [2]	FL 250Hz [3]	FL 2500 Hz [1]	FL 2500 Hz [2]	FL 2500 Hz [3]
0	3.27E+06	4.08E+06	3.54E+06	3.90E+06	4.60E+06	4.15E+06	2.75E+06	3.00E+06	3.05E+06	9.50E+05	1.09E+06	1.05E+06
1	6.36E+06	5.94E+06	6.12E+06	4.25E+06	4.85E+06	4.90E+06	4.53E+06	5.25E+06	4.86E+06	1.18E+06	1.36E+06	1.28E+06
2	8.30E+06	8.00E+06	8.45E+06	9.60E+06	1.13E+07	9.00E+06	6.72E+06	6.00E+06	7.80E+06	3.60E+06	2.78E+06	3.34E+06
3	9.80E+06	9.40E+06	9.20E+06	2.11E+07	2.61E+07	2.34E+07				1.05E+07	1.08E+07	1.02E+07
4	3.88E+07	3.76E+07	3.80E+07	2.24E+07	2.46E+07	2.74E+07				2.57E+07	2.90E+07	2.78E+07
5	4.80E+07	5.30E+07	5.60E+07				2.20E+07	2.74E+07	2.41E+07	5.31E+07	4.41E+07	4.83E+07
6	8.10E+07	7.30E+07	8.50E+07				4.30E+07	4.12E+07	4.34E+07	4.64E+07	4.52E+07	4.76E+07
7	1.06E+08	9.50E+07	1.42E+08	5.07E+07	5.07E+07	4.77E+07	5.55E+07	5.46E+07	5.25E+07	5.10E+07	5.16E+07	5.04E+07
8	1.64E+08	1.82E+08	1.74E+08	7.80E+07	6.96E+07	6.75E+07	8.04E+07	7.04E+07	7.00E+07	5.85E+07	6.00E+07	5.20E+07
9	1.84E+08	2.18E+08	2.08E+08	7.28E+07	7.88E+07	7.68E+07	9.55E+07	8.65E+07	9.70E+07	5.80E+07	5.70E+07	5.40E+07
10	1.86E+08	2.32E+08	1.96E+08	9.85E+07	1.00E+08	9.85E+07				5.80E+07	5.70E+07	5.40E+07
11	1.86E+08	2.32E+08	1.96E+08	1.20E+08	1.22E+08	1.38E+08				5.80E+07	5.70E+07	5.40E+07
12	1.86E+08	2.32E+08	1.96E+08				9.80E+07	9.45E+07	1.21E+08	5.80E+07	5.70E+07	5.40E+07
13	1.86E+08	2.32E+08	1.96E+08	1.13E+08	9.17E+07	1.11E+08	1.19E+08	1.04E+08	1.12E+08	5.80E+07	5.70E+07	5.40E+07

FTIR analysis. basic medium

	Lipid/amide I			AmideI/carb			Lipid/carb		
CL	1.05	0.86	0.93	0.67	0.67	0.63	0.70	0.58	0.58
FL 25 Hz	1.57	1.48	1.49	0.66	0.64	0.64	1.04	0.94	0.96
FL 250 Hz	1.72	1.83	1.61	0.65	0.66	0.66	1.12	1.20	1.07
FL 2500 Hz	0.92	1.08	1.08	0.69	0.82	0.81	0.63	0.89	0.88

FTIR ratios. enriched medium

	Lipid/amide I			AmideI/carb			Lipid/carb		
CL	0.72	0.75	0.81	1.02	0.91	0.92	0.74	0.68	0.74
FL 25 Hz	0.80	0.80	0.75	1.06	1.23	1.16	0.85	0.99	0.86
FL 250 Hz	1.38	0.81	0.89	0.87	0.99	0.66	0.68	0.81	0.59
FL 2500 Hz	0.75	0.90	0.77	1.07	0.93	0.98	0.80	0.83	0.76

Total lipids. (% on DW)

	CL [1]	CL [2]	CL [3]	FL 25Hz [1]	FL 25Hz [2]	FL 25Hz [3]	FL 250Hz [1]	FL 250Hz [2]	FL 250Hz [3]	FL 2500 Hz [1]	FL 2500 Hz [2]
Basic medium	27.3	19.64	17.6	34.6	33.8	31.6	41.7	47.6	43.1	39.2	38.9
Enriched medium	53.8	60.4	63.8	32	30.5	26.27	25.12	25.96	29.6	44.3	42.1

Chlorophyll a content (µg/g DW)

	CL [1]	CL [2]	CL [3]	FL 25Hz [1]	FL 25Hz [2]	FL 25Hz [3]	FL 250Hz [1]	FL 250Hz [2]	FL 250Hz [3]	FL 2500 Hz [1]	FL 2500 Hz [2]	FL 2500 Hz [3]
Basic medium	4.7	5.1	5.3	4.5	3.8	4.8	2.2	3.9	4.3	2.6	2.6	2.9
Enriched medium	1.3	1.9	1.4	4.3	2.1	3.5	3.5	4.7	4.5	6.2	6.4	5.1

Total carotenoids (µg/g DW)

	CL [1]	CL [2]	CL [3]	FL 25Hz [1]	FL 25Hz [2]	FL 25Hz [3]	FL 250Hz [1]	FL 250Hz [2]	FL 250Hz [3]	FL 2500 Hz [1]	FL 2500 Hz [2]	FL 2500 Hz [3]
Basic medium	0.48	0.57	0.60	0.40	0.32	0.40	0.47	1.12	1.14	2.22	2.38	2.77
Enriched medium	1.51	1.83	2.11	3.66	2.16	2.99	3.05	4.16	3.80	1.07	1.16	1.60

Fatty acid. basic medium (% on TFA)

	SFAs		MUFAs		PUFAs	
CL	55.17	52.16	33.65	32.65	11.18	12.19
FL 25 Hz	57.17	59.17	36.05	34.05	6.78	6.79
FL 250 Hz	56.89	54.88	37.54	37.54	5.57	7.58
FL 2500 Hz	51.16	49.16	39.12	41.11	9.72	9.73

Fatty acid. enriched medium (% on TFA)

	SFAs		MUFAs		PUFAs	
CL	44.88	42.87	36.96	37.96	18.16	19.17
FL 25 Hz	40.86	39.78	35.95	33.74	24.14	26.48
FL 250 Hz	38.45	37.35	37.95	36.45	23.60	26.20
FL 2500 Hz	42.38	40.37	36.46	37.45	21.16	22.21

Original FTIR spectra of *Nannochloropsis gaditana* biomass grown in flashing light conditions in two different media.

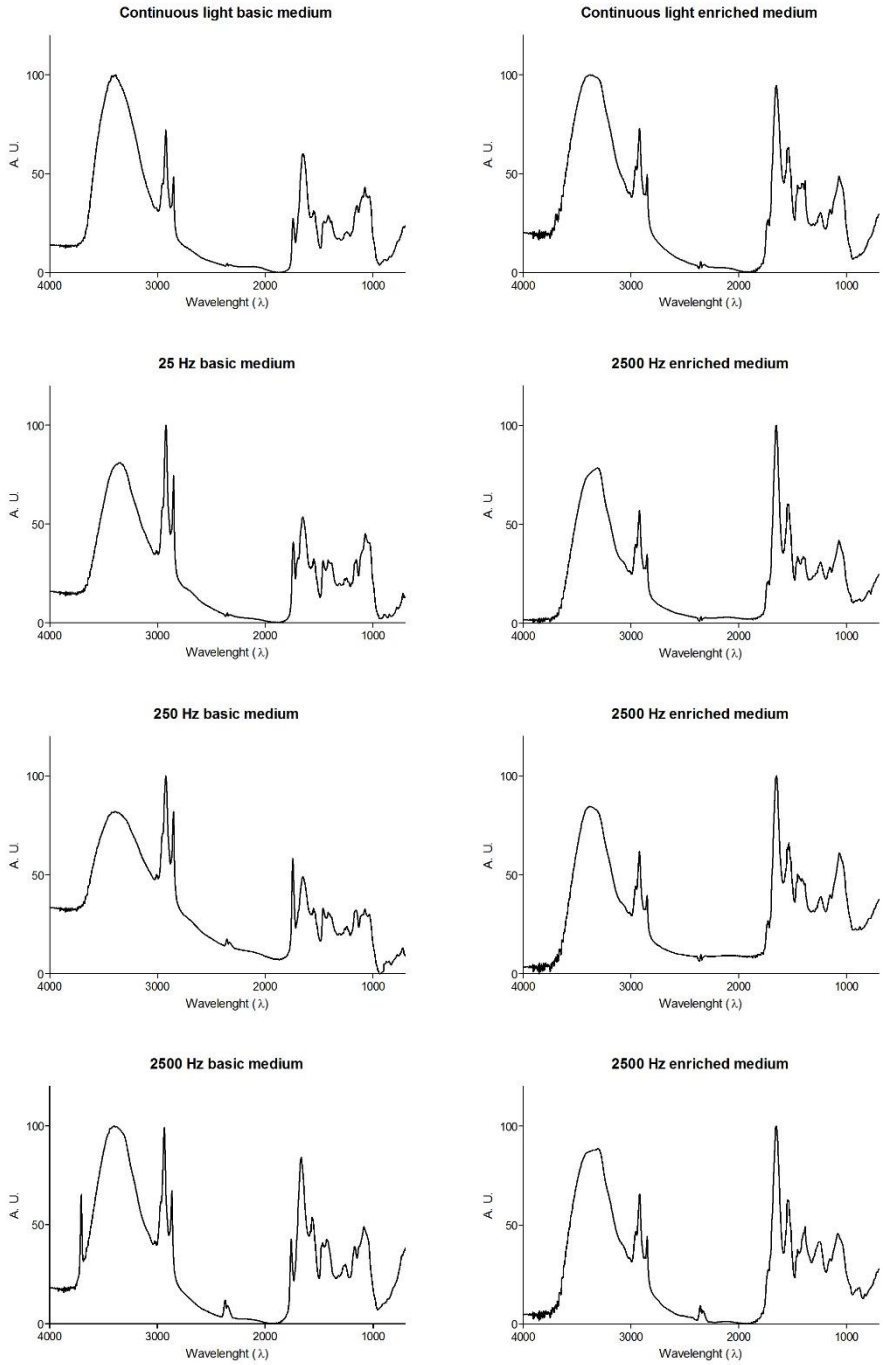

Statistical analysis

Growth factor

Two-way ANOVA

Source of Variation	% of total variation	P value
Interaction	16.02	< 0.0001
Flashing treatment	80.66	< 0.0001
medium	3.32	< 0.0001

Source of Variation	P value summary	Significant?
Interaction	***	Yes
Flashing treatment	***	Yes
medium	***	Yes

Source of Variation	Df	Sum-of-squares	Mean square	F
Interaction	3	0.02783	0.009276	1.782E+15
Flashing treatment	3	0.1402	0.04672	8.977E+15
medium	1	0.005769	0.005769	1.108E+15
Residual	16	0.0000	0.0000	

Number of missing values	0

Bonferroni posttests

CL vs 25 Hz

medium	CL	25 Hz	Difference	95% CI of diff.
Basic medium	0.3060	0.1825	-0.1235	-0.1235 to -0.1235
Enriched medium	0.2367	0.1369	-0.09980	-0.09980 to -0.0998

medium	Difference	t	P value	Summary
Basic medium	-0.1235	66320000	P<0.001	***
Enriched medium	-0.09980	53580000	P<0.001	***

CL vs 250 Hz

medium	CL	250 Hz	Difference	95% CI of diff.
Basic medium	0.3060	0.2638	-0.04223	-0.04223 to -0.04223
Enriched medium	0.2367	0.1713	-0.0654	-0.06540 to -0.0654

medium	Difference	t	P value	Summary
Basic medium	-0.04223	22670000	P<0.001	***
Enriched medium	-0.0654	35110000	P<0.001	***

CL vs 2500 Hz

medium	CL	2500 Hz	Difference	95% CI of diff.
Basic medium	0.3060	0.3256	0.01957	0.01957 to 0.01957
Enriched medium	0.2367	0.4090	0.1723	0.1723 to 0.1723

medium	Difference	t	P value	Summary
Basic medium	0.01957	10510000	P<0.001	***
Enriched medium	0.1723	92500000	P<0.001	***

Lipid/amide I

Two-way ANOVA

Source of Variation	% of total variation	P value
Interaction	20.92	< 0.0001
Treatment	22.06	< 0.0001
medium	54.17	< 0.0001
Source of Variation	P value summary	Significant?
Interaction	***	Yes
Treatment	***	Yes
medium	***	Yes

Source of Variation	Df	Sum-of-squares	Mean square	F
Interaction	3	0.6185	0.2062	39.13
Treatment	3	0.6521	0.2174	41.26
medium	1	1.602	1.602	304.0
Residual	16	0.08431	0.005269	
Number of missing values	0			

Bonferroni posttests

Continuous Light vs 25 Hz				
medium	Continuous Light	25 Hz	Difference	95% CI of diff.
basic medium	0.9470	1.513	0.5656	0.3873 to 0.7439
enriched medium	0.7618	0.7709	0.009091	-0.1692 to 0.1874

medium	Difference	t	P value	Summary
basic medium	0.5656	9.543	P<0.001	***
enriched medium	0.009091	0.1534	P > 0.05	ns

Continuous Light vs 250 Hz				
medium	Continuous Light	250 Hz	Difference	95% CI of diff.
basic medium	0.9470	1.722	0.7752	0.5969 to 0.9535
enriched medium	0.7618	0.8014	0.03958	-0.1387 to 0.2179

medium	Difference	t	P value	Summary
basic medium	0.7752	13.08	P<0.001	***
enriched medium	0.03958	0.6678	P > 0.05	ns

Continuous Light vs 2500 Hz				
medium	Continuous Light	2500 Hz	Difference	95% CI of diff.
basic medium	0.9470	1.028	0.08108	-0.09722 to 0.2594
enriched medium	0.7618	0.8089	0.04710	-0.1312 to 0.2254

medium	Difference	t	P value	Summary
basic medium	0.08108	1.368	P > 0.05	ns
enriched medium	0.04710	0.7947	P > 0.05	ns

Amide/carb

Two-way ANOVA

Source of Variation	% of total variation	P value
Interaction	11.17	0.0162
treatment	14.04	0.0069
medium	61.94	< 0.0001

Source of Variation	P value summary	Significant?
Interaction	*	Yes
treatment	**	Yes
medium	***	Yes

Source of Variation	Df	Sum-of-squares	Mean square	F
Interaction	3	0.07052	0.02351	4.636
treatment	3	0.08867	0.02956	5.829
medium	1	0.3911	0.3911	77.13
Residual	16	0.08113	0.005070	

Number of missing values	0

Bonferroni posttests

Continuous Light vs 25 Hz				
medium	Continuous Light	25 Hz	Difference	95% CI of diff.
basic medium	0.6543	0.6435	-0.01078	-0.1857 to 0.1641
enriched medium	0.9488	1.025	0.07638	-0.09853 to 0.2513

medium	Difference	t	P value	Summary
basic medium	-0.01078	0.1854	P > 0.05	ns
enriched medium	0.07638	1.314	P > 0.05	ns

Continuous Light vs 250 Hz				
medium	Continuous Light	250 Hz	Difference	95% CI of diff.
basic medium	0.6543	0.6692	0.01495	-0.1600 to 0.1899
enriched medium	0.9488	0.9305	-0.01831	-0.1932 to 0.1566

medium	Difference	t	P value	Summary
basic medium	0.01495	0.2571	P > 0.05	ns
enriched medium	-0.01831	0.3149	P > 0.05	ns

Continuous Light vs 2500 Hz				
medium	Continuous Light	2500 Hz	Difference	95% CI of diff.
basic medium	0.6543	0.9068	0.2526	0.07765 to 0.4275
enriched medium	0.9488	0.9905	0.04167	-0.1332 to 0.2166

medium	Difference	t	P value	Summary
basic medium	0.2526	4.344	P<0.01	**
enriched medium	0.04167	0.7166	P > 0.05	ns

Lipid/carb

Two-way ANOVA

Source of Variation	% of total variation	P value
Interaction	36.31	0.0013
treatment	31.55	0.0024
medium	9.52	0.0195

Source of Variation	P value summary	Significant?
Interaction	**	Yes
treatment	**	Yes
medium	*	Yes

Source of Variation	Df	Sum-of-squares	Mean square	F
Interaction	3	0.2259	0.07530	8.561
treatment	3	0.1963	0.06544	7.440
medium	1	0.05922	0.05922	6.733
Residual	16	0.1407	0.008795	

Number of missing values	0

Bonferroni posttests

Continuous Light vs 25 Hz				
medium	Continuous Light	25 Hz	Difference	95% CI of diff.
basic medium	1.131	0.8008	-0.3306	-0.5609 to -0.1002
enriched medium	0.7217	0.9004	0.1787	-0.05162 to 0.4091

medium	Difference	t	P value	Summary
basic medium	-0.3306	4.317	P<0.01	**
enriched medium	0.1787	2.334	P > 0.05	ns

Continuous Light vs 250 Hz				
medium	Continuous Light	250 Hz	Difference	95% CI of diff.
basic medium	1.131	0.6692	-0.4621	-0.6925 to -0.2318
enriched medium	0.7217	0.6907	-0.03096	-0.2613 to 0.1994

medium	Difference	t	P value	Summary
basic medium	-0.4621	6.035	P<0.001	***
enriched medium	-0.03096	0.4043	P > 0.05	ns

Continuous Light vs 2500 Hz				
medium	Continuous Light	2500 Hz	Difference	95% CI of diff.
basic medium	1.131	0.9068	-0.2245	-0.4549 to 0.005850
enriched medium	0.7217	0.7980	0.07629	-0.1541 to 0.3067

medium	Difference	t	P value	Summary
basic medium	-0.2245	2.932	P < 0.05	*
enriched medium	0.07629	0.9963	P > 0.05	ns

Total Lipids

Two-way ANOVA

Source of Variation	% of total variation	P value
Interaction	79.23	< 0.0001
treatment	10.32	0.0010
medium	4.33	0.0036

Source of Variation	P value summary	Significant?
Interaction	***	Yes
treatment	***	Yes
medium	**	Yes

Source of Variation	Df	Sum-of-squares	Mean square	F
Interaction	3	2478	826.1	72.44
treatment	3	322.7	107.6	9.433
medium	1	135.4	135.4	11.87
Residual	15	171.1	11.40	

Number of missing values	1

Bonferroni posttests

Continuous Light vs 25 Hz

medium	Continuous Light	25 Hz	Difference	95% CI of diff.
Row 1	21.51	33.33	11.82	3.448 to 20.19
Row 2	59.33	29.59	-29.74	-38.12 to -21.37

medium	Difference	t	P value	Summary
Row 1	11.82	4.287	P<0.01	**
Row 2	-29.74	10.79	P<0.001	***

Continuous Light vs 250 Hz

medium	Continuous Light	250 Hz	Difference	95% CI of diff.
Row 1	21.51	44.13	22.62	14.25 to 30.99
Row 2	59.33	26.89	-32.44	-40.81 to -24.07

medium	Difference	t	P value	Summary
Row 1	22.62	8.203	P<0.001	***
Row 2	-32.44	11.76	P<0.001	***

Continuous Light vs 2500 Hz

medium	Continuous Light	2500 Hz	Difference	95% CI of diff.
Row 1	21.51	39.05	17.54	8.176 to 26.90
Row 2	59.33	41.80	-17.53	-25.91 to -9.161

medium	Difference	t	P value	Summary
Row 1	17.54	5.688	P<0.001	***
Row 2	-17.53	6.359	P<0.001	***

Chlorophyll a

Two-way ANOVA

Source of Variation	% of total variation	P value
Interaction	77.88	< 0.0001
treatment	6.77	0.1080
medium	0.18	0.6682

Source of Variation	P value summary	Significant?
Interaction	***	Yes
treatment	ns	No
medium	ns	No

Source of Variation	Df	Sum-of-squares	Mean square	F
Interaction	3	35.31	11.77	27.37
treatment	3	3.069	1.023	2.379
medium	1	0.08200	0.08200	0.1907
Residual	16	6.880	0.4300	

Number of missing values	0

Bonferroni posttests

Continuous Light vs 25 Hz				
medium	Continuous Light	25 Hz	Difference	95% CI of diff.
basic medium	5.021	4.336	-0.6849	-2.296 to 0.9258
enriched medium	1.545	3.422	1.878	0.2670 to 3.488

medium	Difference	t	P value	Summary
basic medium	-0.6849	1.279	P > 0.05	ns
enriched medium	1.878	3.507	P<0.01	**

Continuous Light vs 250 Hz				
medium	Continuous Light	250 Hz	Difference	95% CI of diff.
basic medium	5.021	3.498	-1.523	-3.134 to 0.08727
enriched medium	1.545	4.237	2.693	1.082 to 4.304

medium	Difference	t	P value	Summary
basic medium	-1.523	2.845	P < 0.05	*
enriched medium	2.693	5.029	P<0.001	***

Continuous Light vs 2500 Hz				
medium	Continuous Light	2500 Hz	Difference	95% CI of diff.
basic medium	5.021	2.695	-2.326	-3.937 to -0.7152
enriched medium	1.545	5.878	4.333	2.722 to 5.944

medium	Difference	t	P value	Summary
basic medium	-2.326	4.344	P<0.01	**
enriched medium	4.333	8.093	P<0.001	***

Total carotenoids

Two-way ANOVA

Source of Variation	% of total variation	P value
Interaction	46.10	< 0.0001
treatment	11.88	0.0018
medium	34.01	< 0.0001

Source of Variation	P value summary	Significant?
Interaction	***	Yes
treatment	**	Yes
medium	***	Yes

Source of Variation	Df	Sum-of-squares	Mean square	F
Interaction	3	14.84	4.945	30.71
treatment	3	3.824	1.275	7.916
medium	1	10.94	10.94	67.96
Residual	16	2.577	0.1611	

Number of missing values	0

Bonferroni posttests

Continuous Light vs 25 Hz				
medium	Continuous Light	25 Hz	Difference	95% CI of diff.
basic medium	0.5500	0.3726	-0.1774	-1.163 to 0.8084
enriched medium	1.815	2.937	1.122	0.1364 to 2.108

medium	Difference	t	P value	Summary
basic medium	-0.1774	0.5413	P > 0.05	ns
enriched medium	1.122	3.425	P<0.01	**

Continuous Light vs 250 Hz				
medium	Continuous Light	250 Hz	Difference	95% CI of diff.
basic medium	0.5500	0.9115	0.3615	-0.6242 to 1.347
enriched medium	1.815	3.670	1.855	0.8694 to 2.841

medium	Difference	t	P value	Summary
basic medium	0.3615	1.103	P > 0.05	ns
enriched medium	1.855	5.662	P<0.001	***

Continuous Light vs 2500 Hz				
medium	Continuous Light	2500 Hz	Difference	95% CI of diff.
basic medium	0.5500	2.460	1.910	0.9241 to 2.896
enriched medium	1.815	1.275	-0.5397	-1.525 to 0.4460

medium	Difference	t	P value	Summary
basic medium	1.910	5.829	P<0.001	***
enriched medium	-0.5397	1.647	P > 0.05	ns

SFA

Two-way ANOVA

Source of Variation	% of total variation	P value
Interaction	8.69	0.0021
treatment	3.67	0.0257
medium	85.81	< 0.0001

Source of Variation	P value summary	Significant?
Interaction	**	Yes
treatment	*	Yes
medium	***	Yes

Source of Variation	Df	Sum-of-squares	Mean square	F
Interaction	3	74.97	24.99	12.69
treatment	3	31.65	10.55	5.356
medium	1	740.1	740.1	375.7
Residual	8	15.76	1.970	

Number of missing values	0

Bonferroni posttests

Continuous Light vs 25 Hz				
medium	Continuous Light	25 Hz	Difference	95% CI of diff.
basic medium	53.66	58.17	4.507	-0.3758 to 9.390
enriched medium	43.87	40.32	-3.555	-8.437 to 1.328

medium	Difference	t	P value	Summary
basic medium	4.507	3.211	P < 0.05	*
enriched medium	-3.555	2.533	P > 0.05	ns

Continuous Light vs 250 Hz				
medium	Continuous Light	250 Hz	Difference	95% CI of diff.
basic medium	53.66	55.88	2.220	-2.663 to 7.103
enriched medium	43.87	37.90	-5.975	-10.86 to -1.092

medium	Difference	t	P value	Summary
basic medium	2.220	1.582	P > 0.05	ns
enriched medium	-5.975	4.257	P<0.01	**

Continuous Light vs 2500 Hz				
medium	Continuous Light	2500 Hz	Difference	95% CI of diff.
basic medium	53.66	50.16	-3.502	-8.385 to 1.381
enriched medium	43.87	41.37	-2.500	-7.383 to 2.383

medium	Difference	t	P value	Summary
basic medium	-3.502	2.495	P > 0.05	ns
enriched medium	-2.500	1.781	P > 0.05	ns

MUFA

Two-way ANOVA

Source of Variation	% of total variation	P value
Interaction	39.39	0.0073
treatment	48.04	0.0040
medium	0.13	0.7839

Source of Variation	P value summary	Significant?
Interaction	**	Yes
treatment	**	Yes
medium	ns	No

Source of Variation	Df	Sum-of-squares	Mean square	F
Interaction	3	28.62	9.541	8.440
treatment	3	34.90	11.63	10.29
medium	1	0.09097	0.09097	0.08047
Residual	8	9.043	1.130	

Number of missing values	0

Bonferroni posttests

Continuous Light vs 25 Hz				
medium	Continuous Light	25 Hz	Difference	95% CI of diff.
basic medium	33.15	35.05	1.899	-1.800 to 5.598
enriched medium	37.46	34.85	-2.616	-6.315 to 1.083

medium	Difference	t	P value	Summary
basic medium	1.899	1.786	P > 0.05	ns
enriched medium	-2.616	2.461	P > 0.05	ns

Continuous Light vs 250 Hz				
medium	Continuous Light	250 Hz	Difference	95% CI of diff.
basic medium	33.15	37.54	4.391	0.6919 to 8.089
enriched medium	37.46	37.20	-0.2611	-3.960 to 3.438

medium	Difference	t	P value	Summary
basic medium	4.391	4.130	P<0.01	**
enriched medium	-0.2611	0.2456	P > 0.05	ns

Continuous Light vs 2500 Hz				
medium	Continuous Light	2500 Hz	Difference	95% CI of diff.
basic medium	33.15	40.11	6.963	3.264 to 10.66
enriched medium	37.46	36.95	-0.5062	-4.205 to 3.193

medium	Difference	t	P value	Summary
basic medium	6.963	6.549	P<0.001	***
enriched medium	-0.5062	0.4761	P > 0.05	ns

PUFA

Two-way ANOVA

Source of Variation	% of total variation	P value
Interaction	10.50	0.0002
treatment	0.18	0.7359
medium	88.22	< 0.0001

Source of Variation	P value summary	Significant?
Interaction	***	Yes
treatment	ns	No
medium	***	Yes

Source of Variation	Df	Sum-of-squares	Mean square	F
Interaction	3	92.63	30.88	25.44
treatment	3	1.573	0.5242	0.4319
medium	1	778.1	778.1	641.1
Residual	8	9.710	1.214	

Number of missing values	0

Bonferroni posttests

Continuous Light vs 25 Hz				
medium	Continuous Light	25 Hz	Difference	95% CI of diff.
basic medium	11.69	6.784	-4.901	-8.734 to -1.069
enriched medium	18.66	25.31	6.646	2.813 to 10.48

medium	Difference	t	P value	Summary
basic medium	-4.901	4.449	P<0.01	**
enriched medium	6.646	6.032	P<0.001	***

Continuous Light vs 250 Hz				
medium	Continuous Light	250 Hz	Difference	95% CI of diff.
basic medium	11.69	6.575	-5.111	-8.943 to -1.278
enriched medium	18.66	24.90	6.236	2.403 to 10.07

medium	Difference	t	P value	Summary
basic medium	-5.111	4.639	P<0.01	**
enriched medium	6.236	5.660	P<0.001	***

Continuous Light vs 2500 Hz				
medium	Continuous Light	2500 Hz	Difference	95% CI of diff.
basic medium	11.69	9.725	-1.961	-5.793 to 1.872
enriched medium	18.66	21.69	3.021	-0.8112 to 6.854

medium	Difference	t	P value	Summary
basic medium	-1.961	1.780	P > 0.05	ns
enriched medium	3.021	2.743	P > 0.05	ns

Part 2

Paragraph 3.5.

Growth data for one- and two stage cultivation

N. gaditana: one stage cultvation (gDW L-1)

Time (d)	CL [1]	CL [2]	CL [3]	FL 5Hz [1]	FL 5Hz [2]	FL 5Hz [3]	FL 50Hz [1]	FL 50Hz [2]	FL 50Hz [3]	FL 500Hz [1]	FL 500Hz [2]	FL 500Hz [3]
0	0.16	0.15	0.14	0.09	0.09	0.09	0.09	0.09	0.10	0.15	0.15	0.15
1	0.23	0.20	0.21	0.09	0.09	0.09	0.10	0.10	0.11	0.21	0.21	0.22
2	0.41	0.36	0.37	0.09	0.09	0.10	0.12	0.12	0.12	0.39	0.40	0.41
3	0.49	0.64	0.61	0.11	0.10	0.09	0.14	0.15	0.15	0.69	0.67	0.67
4	0.91	1.12	1.07	0.11	0.11	0.10	0.17	0.17	0.18	1.08	1.18	1.18
5	1.81	2.07	2.00	0.13	0.12	0.13	0.22	0.24	0.25	1.76	1.97	1.94
6	2.52	2.44	2.56	0.14	0.13	0.13	0.30	0.32	0.34	1.90	2.48	2.50
7	2.83	2.96	3.04	0.14	0.14	0.14	0.38	0.42	0.42	2.60	2.85	3.00
8	2.96	2.91	3.06	0.14	0.14	0.15	0.46	0.51	0.49	2.32	2.67	3.03
9	3.38	3.30	3.47	0.14	0.14	0.12	0.58	0.61	0.56	2.79	3.13	3.96
10	3.55	3.51	3.48	0.17	0.16	0.16	0.72	0.80	0.75	2.84	3.08	3.58
11	3.62	3.89	3.77	0.18	0.16	0.17	0.92	1.01	0.92	3.16	3.29	3.91
12	4.20	3.97	3.86	0.19	0.17	0.18	1.34	1.52	1.35	3.19	3.42	3.95
13	4.41	4.10	3.97	0.19	0.17	0.18	1.56	1.89	1.71	3.40	3.66	4.35
	Biomass productivity* (g L-1 d-1)											
	0.63	0.74	0.68	0.42	0.43	0.45	0.58	0.61	0.61	0.65	0.69	0.62

K. antarctica: one stage cultvation (gDW L-1)

Time (d)	CL [1]	CL [2]	CL [3]	FL 5Hz [1]	FL 5Hz [2]	FL 5Hz [3]	FL 50Hz [1]	FL 50Hz [2]	FL 50Hz [3]	FL 500Hz [1]	FL 500Hz [2]	FL 500Hz [3]
0	0.15	0.15	0.15	0.15	0.15	0.15	0.15	0.15	0.15	0.15	0.15	0.15
1	0.14	0.13	0.14	0.13	0.13	0.12	0.13	0.13	0.13	0.14	0.14	0.14
2	0.17	0.15	0.14	0.13	0.13	0.12	0.12	0.13	0.13	0.15	0.14	0.15
3	0.17	0.16	0.16	0.13	0.13	0.13	0.13	0.14	0.13	0.17	0.15	0.16
4	0.19	0.17	0.18	0.12	0.13	0.13	0.13	0.14	0.14	0.17	0.17	0.17
5	0.23	0.21	0.22	0.13	0.13	0.13	0.14	0.15	0.15	0.22	0.19	0.21
6	0.29	0.27	0.28	0.13	0.12	0.12	0.15	0.16	0.16	0.28	0.23	0.27
7	0.40	0.35	0.41	0.14	0.13	0.13	0.18	0.19	0.19	0.35	0.28	0.36
8	0.49	0.44	0.55	0.14	0.13	0.13	0.19	0.20	0.21	0.43	0.37	0.45
9	0.56	0.61	0.77	0.14	0.14	0.14	0.24	0.24	0.26	0.59	0.42	0.59
10	0.75	0.89	1.12	0.15	0.15	0.15	0.30	0.30	0.31	0.81	0.68	0.87
11	1.12	1.12	1.28	0.14	0.16	0.16	0.34	0.35	0.36	1.08	0.90	1.18
12	1.33	1.40	1.45	0.15	0.17	0.17	0.39	0.44	0.42	1.32	1.15	1.40
13	1.80	1.75	1.93	0.18	0.18	0.18	0.53	0.64	0.56	1.73	1.56	1.85
	Biomass productivity* (g L-1 d-1)											
	0.10	0.11	0.14	0.02	0.04	0.07	0.03	0.04	0.03	0.11	0.09	0.12

T. chui: one stage cultvation (gDW L-1)

Time (d)	CL [1]	CL [2]	CL [3]	FL 5Hz [1]	FL 5Hz [2]	FL 5Hz [3]	FL 50Hz [1]	FL 50Hz [2]	FL 50Hz [3]	FL 500Hz [1]	FL 500Hz [2]	FL 500Hz [3]
0	0.32	0.32	0.32	0.32	0.32	0.32	0.32	0.32	0.32	0.32	0.32	0.32
1	0.27	0.30	0.30	0.27	0.26	0.25	0.27	0.27	0.27	0.28	0.28	0.30
2	0.33	0.38	0.37	0.28	0.27	0.26	0.28	0.30	0.28	0.34	0.36	0.34
3	0.40	0.43	0.48	0.26	0.26	0.26	0.31	0.33	0.32	0.40	0.44	0.42
4	0.70	0.78	0.80	0.25	0.26	0.25	0.35	0.38	0.35	0.59	0.67	0.66
5	0.94	0.88	0.99	0.25	0.26	0.27	0.43	0.48	0.47	0.76	0.79	0.84
6	1.57	1.54	1.64	0.27	0.26	0.25	0.52	0.57	0.53	1.22	1.27	1.23
7	1.73	1.63	2.12	0.25	0.25	0.25	0.81	0.86	0.85	1.95	2.10	1.91
8	2.18	1.83	2.40	0.28	0.27	0.26	0.97	1.17	1.18	1.92	2.18	1.92
9	2.67	2.81	3.27	0.27	0.27	0.27	1.31	1.44	1.71	2.80	2.96	2.58
10	2.73	2.97	3.24	0.33	0.28	0.27	1.53	1.72	2.04	2.52	2.53	2.23
11	3.41	3.48	3.73	0.32	0.29	0.27	2.11	2.38	2.52	2.80	3.05	2.82
12	3.33	3.60	4.13	0.30	0.27	0.26	2.19	2.13	2.87	3.37	3.50	3.49
13	3.71	3.64	4.04	0.31	0.31	0.27	2.41	2.63	3.10	3.75	3.63	3.44
	Biomass productivity* (g L-1 d-1)											
	0.25	0.23	0.28	0.00	0.00	0.00	0.16	0.17	0.22	0.26	0.26	0.22

N. gaditana: two stage cultvation (gDW L-1)

Time (d)	CL [1]	CL [2]	CL [3]	FL 5Hz [1]	FL 5Hz [2]	FL 5Hz [3]	FL 50Hz [1]	FL 50Hz [2]	FL 50Hz [3]	FL 500Hz [1]	FL 500Hz [2]	FL 500Hz [3]
0	0.38	0.39	0.39	0.38	0.39	0.39	0.38	0.39	0.39	0.38	0.39	0.39
1	0.51	0.50	0.54	0.51	0.50	0.54	0.51	0.50	0.54	0.51	0.50	0.54
2	0.62	0.62	0.63	0.62	0.62	0.63	0.62	0.62	0.63	0.62	0.62	0.63
3	0.67	0.65	0.68	0.67	0.65	0.68	0.67	0.65	0.68	0.67	0.65	0.68
4	0.76	0.77	0.78	0.76	0.77	0.78	0.76	0.77	0.78	0.76	0.77	0.78
5	1.22	1.22	1.22	1.22	1.22	1.22	1.22	1.22	1.22	1.22	1.22	1.22
6	1.72	1.72	1.72	1.72	1.72	1.72	1.72	1.72	1.72	1.72	1.72	1.72
7	3.21	3.12	2.88	2.36	2.37	2.45	2.74	2.66	2.78	3.14	2.55	2.86
8	3.83	3.72	3.65	2.64	2.69	2.71	3.16	3.20	3.22	3.56	3.15	3.27
9	4.66	4.45	4.85	3.17	3.27	3.16	4.10	4.29	4.11	4.67	4.31	4.15
10	6.05	5.68	6.20	3.42	3.51	3.41	5.03	5.16	5.30	5.62	5.63	5.36
	Biomass productivity* (g L-1 d-1)											
	0.36	0.36	0.36	0.01	0.01	0.01	0.08	0.09	0.08	0.28	0.33	0.38

K. antarctica: two stage cultvation (gDW L-1)

Time (d)	CL [1]	CL [2]	CL [3]	FL 5Hz [1]	FL 5Hz [2]	FL 5Hz [3]	FL 50Hz [1]	FL 50Hz [2]	FL 50Hz [3]	FL 500Hz [1]	FL 500Hz [2]	FL 500Hz [3]
0	0.25	0.25	0.25	0.25	0.25	0.25	0.25	0.25	0.25	0.25	0.25	0.25
1	0.35	0.34	0.35	0.35	0.34	0.35	0.35	0.34	0.35	0.35	0.34	0.35
2	0.43	0.42	0.42	0.43	0.42	0.42	0.43	0.42	0.42	0.43	0.42	0.42
3	0.57	0.58	0.59	0.57	0.58	0.59	0.57	0.58	0.59	0.57	0.58	0.59
4	0.99	1.05	1.03	0.99	1.05	1.03	0.99	1.05	1.03	0.99	1.05	1.03
5	1.22	1.29	1.33	1.22	1.29	1.33	1.22	1.29	1.33	1.22	1.29	1.33
6	2.01	1.96	1.98	2.01	1.96	1.98	2.01	1.96	1.98	2.01	1.96	1.98
7	2.40	2.47	2.59	1.89	1.92	1.96	2.03	1.95	1.98	2.63	2.18	2.23
8	3.41	3.34	3.67	2.15	2.21	2.17	2.50	2.45	2.32	3.78	2.98	3.31
9	4.26	4.28	4.60	2.45	2.60	2.57	3.15	2.98	2.98	4.67	3.63	4.13
10	5.23	4.88	5.06	2.96	3.10	2.82	3.74	3.40	3.57	5.66	4.79	4.45
	Biomass productivity* (g L-1 d-1)											
	0.69	0.68	0.75	0.33	0.35	0.35	0.43	0.38	0.41	0.66	0.56	0.51

T. chui: two stage cultvation (gDW L-1)

Time (d)	CL [1]	CL [2]	CL [3]	FL 5Hz [1]	FL 5Hz [2]	FL 5Hz [3]	FL 50Hz [1]	FL 50Hz [2]	FL 50Hz [3]	FL 500Hz [1]	FL 500Hz [2]	FL 500Hz [3]
0	0.60	0.61	0.61	0.60	0.61	0.61	0.60	0.61	0.61	0.60	0.61	0.61
1	0.98	0.94	0.98	0.98	0.94	0.98	0.98	0.94	0.98	0.98	0.94	0.98
2	1.20	1.05	1.24	1.20	1.05	1.24	1.20	1.05	1.24	1.20	1.05	1.24
3	1.26	1.23	1.27	1.26	1.23	1.27	1.26	1.23	1.27	1.26	1.23	1.27
4	1.57	1.44	1.50	1.57	1.44	1.50	1.57	1.44	1.50	1.57	1.44	1.50
5	1.40	1.29	1.36	1.40	1.29	1.36	1.40	1.29	1.36	1.40	1.29	1.36
6	2.21	2.26	2.31	2.21	2.26	2.31	2.21	2.26	2.31	2.21	2.26	2.31
7	2.35	2.27	2.08	1.95	1.84	2.06	2.15	2.03	2.23	2.57	2.78	2.38
8	2.59	2.98	2.92	2.39	2.33	2.34	2.24	2.90	3.09	3.10	2.91	2.88
9	3.35	3.09	3.70	3.00	2.93	3.12	3.80	3.56	4.00	3.78	4.33	3.75
10	3.56	4.52	4.54	3.43	3.45	3.21	4.19	4.29	4.65	5.26	5.71	5.04
	Biomass productivity* (g L-1 d-1)											
	0.44	0.48	0.54	0.39	0.40	0.39	0.55	0.50	0.55	0.60	0.71	0.60

Biochemical composition for one- and two stage cultivation

Biochemical composition of *N. gaditana* during one stage cultivation.

			mg gDW-1				ug gDW-1			% of DW			mg gDW-1	% of DW		
Treatment	DW	log10(DW)	Chl a	Chl b	Total Chl	Total Carot	Neoxanthin	Violaxanthin	Lutein	Beta carotene	Protein	Carbohydrate	Lipids	TFA	N	C	H
5 Hz	0.19	-0.73	7.83	n.d.	7.83	4.64	n.d.	n.d.	n.d.	n.d.	49.21	14.00	23.15	137.49	n.d.	n.d.	n.d.
5 Hz	0.17	-0.78	13.76	n.d.	13.76	7.04	n.d.	n.d.	n.d.	n.d.	46.01	13.58	25.39	158.36	n.d.	n.d.	n.d.
5 Hz	0.18	-0.75	8.81	n.d.	8.81	4.68	n.d.	n.d.	n.d.	n.d.	39.67	12.76	24.21	132.13	n.d.	n.d.	n.d.
50 Hz	1.56	0.19	8.16	n.d.	8.16	2.81	n.d.	2071.16	808.16	622.32	22.66	12.31	33.35	184.00	2.84	27.79	3.70
50 Hz	1.89	0.28	5.52	n.d.	5.52	2.17	n.d.	1241.76	472.47	390.10	19.51	6.24	31.29	224.48	5.88	54.68	8.32
50 Hz	1.71	0.23	10.92	n.d.	10.92	3.91	n.d.	1490.17	580.48	545.40	21.85	12.06	32.10	162.38	6.72	54.58	8.31
500 Hz	3.40	0.53	1.98	n.d.	1.98	1.34	n.d.	266.76	89.69	24.56	13.01	7.84	39.51	339.28	2.72	58.12	8.96
500 Hz	3.66	0.56	1.93	n.d.	1.93	1.22	n.d.	376.81	116.09	37.39	13.60	11.23	37.02	267.67	2.85	61.73	9.46
500 Hz	4.35	0.64	2.24	n.d.	2.24	1.44	n.d.	243.44	91.15	31.84	12.90	9.78	38.25	276.58	2.70	62.13	9.63
CL	4.41	0.64	2.55	n.d.	2.55	1.73	n.d.	295.21	117.11	32.30	12.39	8.42	39.17	261.48	2.59	62.03	9.45
CL	4.10	0.61	2.83	n.d.	2.83	1.85	n.d.	273.23	91.20	22.16	11.91	9.85	39.05	290.93	2.49	61.18	9.35
CL	3.97	0.60	2.35	n.d.	2.35	1.59	n.d.	370.35	149.14	26.22	12.82	7.52	43.22	305.67	2.68	61.27	9.41

Fatty acid composition of *N. gaditana* during one stage cultivation.

% of TFA														
Treatment	C14:0	C16:0	C16:1n7	C16:2n3	C16:3n3	C16:4n3	C18:0	C18:1n9	C18:2n6	18:3n-6	C18:3n3	C18:4n3	C20:1n9	C20:5n3
5 Hz	4.46	9.04	24.56	1.69	0.42	0.64	1.71	6.09	1.98	1.28	0.97	1.04	3.01	41.09
5 Hz	4.28	9.65	23.04	1.77	0.43	0.66	3.94	5.74	1.85	1.21	n.d.	0.99	2.99	41.51
5 Hz	4.40	11.46	23.46	1.67	0.40	0.62	4.59	5.72	1.89	1.18	n.d.	0.96	2.80	38.83
50 Hz	3.83	21.25	29.22	0.35	0.32	0.37	2.12	5.04	2.06	1.20	0.94	n.d.	n.d.	31.34
50 Hz	2.84	30.29	31.84	0.19	0.17	0.19	1.38	4.09	1.66	0.95	0.47	n.d.	0.44	24.50
50 Hz	3.46	24.27	29.47	0.32	0.37	0.30	1.58	4.86	2.07	1.32	0.84	n.d.	n.d.	29.43
500 Hz	1.51	37.37	37.94	0.13	0.24	0.00	2.13	9.98	1.62	0.82	0.35	n.d.	0.36	6.72
500 Hz	1.39	39.57	38.84	0.07	0.20	0.06	1.59	9.36	1.52	0.72	0.18	n.d.	0.19	5.84
500 Hz	1.56	40.10	37.35	0.12	0.25	0.11	1.44	9.53	1.49	0.78	n.d.	n.d.	0.32	6.26
CL	1.55	39.64	39.06	0.08	0.20	0.07	1.39	8.78	1.46	0.71	n.d.	n.d.	0.19	6.25
CL	1.52	40.14	38.05	0.09	0.22	0.09	1.34	9.07	1.45	0.74	n.d.	n.d.	0.25	6.47
CL	1.52	39.64	38.45	0.09	0.22	0.08	1.35	8.89	1.49	0.71	n.d.	n.d.	0.24	6.77

Biochemical composition of *K. antarctica* during one stage cultivation.

			mg gDW-1				ug gDW-1				% of DW			mg gDW-1	% of DW		
Treatment	DW	log10(DW)	Chl a	Chl b	Total Chl	Total Carot	Neoxanthin	Violaxanthin	Lutein	Beta carotene	Protein	Carbohydrate	Lipids	TFA	N	C	H
CL	4.41	0.64	2.55	n.d.	2.55	1.73	n.d.	295.21	117.11	32.30	12.39	8.42	39.17	261.48	2.59	62.03	9.45
CL	4.10	0.61	2.83	n.d.	2.83	1.85	n.d.	273.23	91.20	22.16	11.91	9.85	39.05	290.93	2.49	61.18	9.35
CL	3.97	0.60	2.35	n.d.	2.35	1.59	n.d.	370.35	149.14	26.22	12.82	7.52	43.22	305.67	2.68	61.27	9.41
5 Hz	0.14	-0.85	2.33	0.63	2.97	1.61	33.69	208.04	1481.20	497.21	25.01	4.60	23.91	124.07	5.23	26.82	4.83
5 Hz	0.14	-0.85	3.10	0.86	3.96	1.77	47.03	176.03	1715.51	494.85	37.12	13.12	13.44	101.48	n.d.	n.d.	n.d.
5 Hz	0.14	-0.86	3.92	1.16	5.09	2.33	60.37	206.35	2050.96	532.74	36.86	10.06	14.56	94.76	7.71	39.48	6.71
50 Hz	0.50	-0.30	4.28	1.16	5.44	2.71	25.48	168.94	1582.29	303.92	42.85	14.60	16.03	106.04	8.97	45.70	6.89
50 Hz	0.62	-0.21	5.10	1.59	6.69	2.67	15.09	136.40	1675.01	379.75	46.92	19.52	16.54	87.80	9.28	47.64	7.70
50 Hz	0.53	-0.28	4.39	1.28	5.68	2.68	18.84	160.74	1307.09	268.76	42.73	12.98	14.23	99.47	8.94	46.73	7.67
500 Hz	1.74	0.24	3.85	1.23	5.08	2.25	10.23	39.25	889.17	128.40	21.27	23.17	13.21	91.16	4.45	52.08	7.91
500 Hz	1.56	0.19	2.67	1.01	3.69	2.35	8.51	23.83	880.49	159.80	22.99	36.93	13.19	91.04	4.81	51.73	7.89
500 Hz	1.87	0.27	2.25	0.71	2.96	1.44	8.42	31.43	679.50	99.45	21.26	33.48	12.23	84.42	4.45	53.77	8.03

Fatty acid composition of *K. antarctica* during one stage cultivation.

% of TFA														
Treatment	C14:0	C16:0	C16:1n7	C16:2n3	C16:3n3	C16:4n3	C18:0	C18:1n9	C18:2n6	18:3n-6	C18:3n3	C18:4n3	C20:1n9	C20:5n3
CL	1.55	39.64	39.06	0.08	0.20	0.07	1.39	8.78	1.46	0.71	n.d.	n.d.	0.19	6.25
CL	1.52	40.14	38.05	0.09	0.22	0.09	1.34	9.07	1.45	0.74	n.d.	n.d.	0.25	6.47
CL	1.52	39.64	38.45	0.09	0.22	0.08	1.35	8.89	1.49	0.71	n.d.	n.d.	0.24	6.77
5 Hz	2.56	7.97	2.67	1.60	7.69	4.38	1.40	12.44	4.13	2.12	28.66	4.55	6.54	11.06
5 Hz	1.76	10.29	2.17	1.31	8.35	5.46	0.86	9.30	3.10	1.25	33.90	4.61	3.69	12.59
5 Hz	1.78	10.20	2.22	1.45	9.05	4.87	1.08	9.86	3.43	1.31	33.71	4.25	3.89	11.44
50 Hz	2.06	11.36	2.36	2.01	7.21	5.74	1.55	10.77	5.29	1.84	28.42	5.00	1.72	12.83
50 Hz	1.82	11.41	2.26	2.43	8.50	5.35	1.29	10.85	6.19	1.76	30.11	4.36	1.54	10.46
50 Hz	2.05	11.80	2.47	2.22	7.67	5.20	1.69	11.16	5.71	1.86	28.16	4.68	1.69	11.79
500 Hz	0.80	8.45	1.65	2.67	3.83	2.40	0.89	38.80	12.34	4.31	12.21	2.15	3.33	4.65
500 Hz	0.93	9.02	1.35	2.33	4.39	2.85	0.94	34.73	12.04	4.27	14.93	2.54	3.05	4.96
500 Hz	0.75	8.66	1.51	2.48	4.14	2.00	0.96	40.72	12.14	3.89	12.44	1.90	2.99	3.96

Biochemical composition of *T. chui* during one stage cultivation.

			mg gDW-1				ug gDW-1			% of DW				mg gDW-1	% of DW		
Treatment	DW	log10(DW)	Chl a	Chl b	Total Chl	Total Carot	Neoxanthin	Violaxanthin	Lutein	Beta carotene	Protein	Carbohydrate	Lipids	TFA	N	C	H
5 Hz	0.31	-0.51	1.85	1.28	3.13	1.13	n.d.	n.d.	2223.83	764.23	26.79	19.90	11.98	143.40	5.85	34.62	6.30
5 Hz	0.31	-0.51	1.85	1.34	3.19	1.05	n.d.	n.d.	1587.92	594.86	29.87	18.24	15.67	117.46	6.13	35.80	6.17
5 Hz	0.27	-0.57	1.17	0.89	2.05	0.75	n.d.	n.d.	1905.88	679.55	25.96	20.35	14.77	125.95	6.14	32.23	5.88
50 Hz	2.41	0.38	5.37	3.77	9.14	2.55	103.56	90.68	1292.30	972.30	11.82	29.83	13.99	92.45	2.47	44.32	7.16
50 Hz	2.63	0.42	4.44	2.67	7.10	2.51	117.69	149.42	1338.19	1060.54	13.78	24.11	17.18	89.36	2.88	44.02	7.16
50 Hz	3.10	0.49	4.00	2.83	6.83	2.08	54.12	32.64	798.36	680.64	9.50	32.95	14.29	82.01	1.99	61.87	10.16
500 Hz	3.75	0.57	2.70	1.66	4.36	1.82	47.94	30.22	596.65	785.97	6.43	26.29	12.81	77.49	1.35	29.20	4.86
500 Hz	3.63	0.56	2.55	1.40	3.95	1.80	50.98	31.83	517.03	674.47	6.76	29.11	13.50	76.24	1.41	43.37	7.18
500 Hz	3.44	0.54	2.90	1.71	4.61	1.98	34.12	29.22	437.41	588.53	8.32	15.02	11.83	79.60	1.74	43.20	7.10
CL	3.71	0.57	2.89	1.98	4.86	1.84	71.35	48.86	685.91	846.95	7.91	29.41	11.25	82.95	1.66	42.59	7.24
CL	3.64	0.56	2.92	1.76	4.69	1.94	56.10	34.73	672.63	868.52	7.88	40.11	12.76	89.54	1.65	43.41	7.04
CL	4.04	0.61	2.76	1.60	4.35	1.88	45.38	16.12	602.75	819.20	7.69	30.77	13.50	92.56	1.61	43.85	7.17

Fatty acid composition of *T. chui* during one stage cultivation.

% of TFA														
Treatment	C14:0	C16:0	C16:1n7	C16:2n3	C16:3n3	C16:4n3	C18:0	C18:1n9	C18:2n6	18:3n-6	C18:3n3	C18:4n3	C20:1n9	C20:5n3
5 Hz	1.73	14.21	1.94	0.52	1.17	12.90	1.28	14.43	2.12	n.d.	13.08	16.18	9.11	11.33
5 Hz	2.11	12.75	2.20	0.65	1.33	12.22	1.65	15.27	2.61	n.d.	13.10	15.56	9.97	10.58
5 Hz	2.86	12.23	3.03	0.00	1.32	9.46	1.94	19.87	3.08	n.d.	10.81	13.08	12.90	9.41
50 Hz	0.97	14.75	2.02	0.56	2.46	13.36	0.56	16.25	7.87	1.11	18.88	6.49	2.83	10.44
50 Hz	1.04	14.24	1.48	0.43	2.49	14.31	0.50	13.76	7.18	1.10	20.11	7.21	2.64	12.23
50 Hz	0.99	15.13	2.74	0.65	2.38	12.26	0.44	19.02	7.52	1.01	17.97	5.67	3.08	9.78
500 Hz	1.26	15.92	3.81	0.97	2.57	10.29	0.94	22.86	8.35	n.d.	15.53	4.10	3.50	9.89
500 Hz	1.41	15.66	3.93	0.97	2.47	9.94	1.03	23.18	8.59	n.d.	15.00	4.04	3.72	10.06
500 Hz	1.34	15.51	3.92	0.93	2.68	10.20	1.01	22.75	8.94	n.d.	15.03	3.87	3.76	10.07
CL	1.64	14.62	3.00	0.80	2.45	10.61	1.33	20.03	7.92	1.80	16.13	4.82	3.62	11.23
CL	1.29	15.45	3.81	0.98	2.51	9.92	1.11	22.30	8.59	1.53	15.01	3.91	3.71	9.88
CL	1.53	15.26	4.10	1.11	2.41	9.43	1.23	23.11	8.26	1.67	14.76	4.27	3.80	9.07

Biochemical composition of *N. gaditana* during two stage cultivation.

			mg gDW-1				ug gDW-1			% of DW				mg gDW-1	% of DW		
Treatment	DW	log10(DW)	Chl a	Chl b	Total Chl	Total Carot	Neoxanthin	Violaxanthin	Lutein	Beta carotene	Protein	Carbohydrate	Lipids	TFA	N	C	H
5 Hz	3.42	0.53	7.67	0.00	7.67	3.48	n.d.	1353.54	64.88	279.86	20.07	11.94	29.00	228.75	4.20	54.05	8.34
5 Hz	3.51	0.55	9.10	0.00	9.10	3.97	n.d.	1188.57	61.20	219.80	21.26	10.02	29.09	219.00	4.45	54.63	8.41
5 Hz	3.41	0.53	9.05	0.00	9.05	4.20	n.d.	1362.65	67.56	249.45	22.43	7.42	33.62	218.21	4.69	54.75	8.39
50 Hz	5.03	0.70	4.83	0.00	4.83	2.44	n.d.	561.81	39.36	126.72	15.43	7.17	36.83	304.22	3.23	58.20	8.95
50 Hz	5.16	0.71	4.98	0.00	4.98	2.39	n.d.	577.16	42.45	115.27	15.40	6.43	34.94	344.80	3.22	58.69	9.04
50 Hz	5.30	0.72	3.36	0.00	3.36	1.90	n.d.	498.13	40.87	117.39	15.44	8.44	33.98	292.97	3.23	58.93	9.15
500 Hz	5.62	0.75	2.90	0.00	2.90	1.82	n.d.	256.35	38.62	52.83	12.62	9.46	34.11	260.14	2.64	60.93	9.33
500 Hz	5.63	0.75	3.06	0.00	3.06	1.82	n.d.	390.55	35.50	70.77	14.58	12.04	32.62	248.77	3.05	60.38	9.27
500 Hz	5.36	0.73	4.03	0.00	4.03	2.23	n.d.	431.76	32.60	64.04	13.39	9.68	34.33	261.77	2.80	60.77	9.38
CL	5.68	0.75	3.56	0.00	3.56	2.04	n.d.	573.06	53.76	26.94	12.76	7.97	37.39	258.84	2.67	62.08	9.45
CL	6.20	0.79	2.66	0.00	2.66	1.75	n.d.	501.52	41.83	33.95	12.03	8.26	35.86	258.12	2.52	60.92	9.35
CL	6.05	0.78	3.52	0.00	3.52	2.18	n.d.	519.26	41.34	55.97	12.26	12.26	40.06	315.78	2.56	61.17	9.41

Fatty acid composition of *N. gaditana* during two stage cultivation.

% of TFA														
Treatment	C14:0	C16:0	C16:1n7	C16:2n3	C16:3n3	C16:4n3	C18:0	C18:1n9	C18:2n6	18:3n-6	C18:3n3	C18:4n3	C20:1n9	C20:5n3
5 Hz	2.54	31.10	34.67	0.25	0.00	0.25	1.52	8.31	2.00	0.96	n.d.	n.d.	0.68	16.33
5 Hz	2.43	31.35	34.65	0.21	0.00	0.21	1.35	8.38	1.93	0.86	n.d.	n.d.	0.57	16.86
5 Hz	2.41	31.37	33.98	0.22	0.41	0.21	1.83	8.37	1.91	0.87	n.d.	n.d.	0.56	16.64
50 Hz	1.77	38.97	36.79	0.12	0.25	0.11	1.59	8.12	1.47	0.57	n.d.	n.d.	0.31	9.23
50 Hz	1.80	39.15	36.80	0.14	0.00	0.13	1.40	8.37	1.49	0.62	n.d.	n.d.	0.37	8.92
50 Hz	1.76	38.46	37.01	0.12	0.25	0.12	1.32	8.18	1.50	0.61	n.d.	n.d.	0.32	9.65
500 Hz	1.49	38.61	38.85	0.19	0.22	0.09	1.41	8.73	1.36	0.68	n.d.	n.d.	0.25	7.55
500 Hz	1.42	37.09	38.87	0.11	0.25	0.10	1.75	8.95	1.60	0.84	n.d.	n.d.	0.29	8.01
500 Hz	1.53	36.20	39.76	0.11	0.25	0.11	1.55	9.23	1.47	0.86	n.d.	n.d.	0.30	7.97
CL	1.43	38.44	39.50	0.09	0.22	0.08	1.70	8.97	1.41	0.78	n.d.	n.d.	0.23	6.62
CL	1.56	37.61	40.01	0.09	0.24	0.08	1.55	9.30	1.38	0.78	n.d.	n.d.	0.23	6.61
CL	1.59	38.58	38.66	0.10	0.23	0.09	1.52	8.68	1.33	0.70	n.d.	n.d.	0.25	7.19

Biochemical composition of *K. anctartica* during two stage cultivation.

			mg gDW-1				ug gDW-1				% of DW			mg gDW-1	% of DW		
Treatment	DW	log10 (DW)	Chl a	Chl b	Total Chl	Total Carot	Neoxanthin	Violaxanthin	Lutein	Beta carotene	Protein	Carbohydrate	Lipids	TFA	N	C	H
5 Hz	2.96	0.47	2.67	0.97	3.65	1.63	33.69	155.30	697.09	233.01	29.95	34.07	10.50	73.97	6.27	45.32	6.83
5 Hz	3.10	0.49	2.59	0.92	3.51	1.59	47.03	138.13	621.27	197.52	26.60	17.94	16.57	128.46	5.56	40.28	5.78
5 Hz	2.82	0.45	4.08	1.38	5.46	2.36	60.37	120.97	545.46	162.03	20.55	27.66	21.19	107.19	4.30	33.38	4.47
50 Hz	3.74	0.57	1.81	0.62	2.43	1.28	25.48	124.85	883.33	233.48	25.47	30.34	17.86	131.45	5.33	50.64	7.77
50 Hz	3.40	0.53	2.30	0.90	3.20	1.82	15.09	126.04	693.42	204.02	24.69	31.65	16.35	120.31	5.16	44.83	6.71
50 Hz	3.57	0.55	2.72	1.07	3.79	1.95	18.84	130.83	869.33	272.39	20.23	40.71	15.15	111.51	4.23	41.08	5.98
500 Hz	5.66	0.75	1.29	0.55	1.83	1.04	10.23	16.78	453.58	94.51	17.75	29.36	14.96	110.07	3.71	54.21	8.36
500 Hz	4.79	0.68	1.70	0.56	2.26	1.08	8.51	21.88	533.25	105.09	19.09	37.75	15.61	114.89	3.99	47.09	7.18
500 Hz	4.45	0.65	1.57	0.62	2.18	1.04	8.42	26.98	612.92	115.66	16.37	36.03	16.70	122.91	3.42	45.04	6.65
CL	5.23	0.72	1.52	0.52	2.04	1.06	9.53	8.52	273.01	41.04	7.96	29.08	13.30	97.88	1.67	27.01	3.24
CL	4.88	0.69	1.47	0.43	1.91	1.07	7.22	17.65	491.83	35.76	12.83	41.18	15.06	110.83	2.68	35.98	5.39
CL	5.06	0.70	1.49	0.49	1.97	1.10	7.16	18.80	477.78	46.32	16.66	37.69	12.32	90.67	3.49	50.25	7.54

Fatty acid composition of *K. anctartica* during two stage cultivation.

% of TFA														
Treatment	C14:0	C16:0	C16:1n7	C16:2n3	C16:3n3	C16:4n3	C18:0	C18:1n9	C18:2n6	18:3n-6	C18:3n3	C18:4n3	C20:1n9	C20:5n3
5 Hz	1.37	10.94	1.53	1.97	2.49	5.94	0.55	12.10	10.85	3.34	22.98	3.15	7.00	12.86
5 Hz	1.18	10.82	1.33	1.80	2.43	6.44	0.48	10.76	10.74	3.39	24.42	3.24	6.65	13.45
5 Hz	1.83	9.28	1.76	2.00	2.35	5.71	0.87	12.37	10.40	3.58	22.46	3.46	7.97	12.39
50 Hz	1.31	10.53	1.84	2.67	2.59	3.29	1.03	30.34	12.66	3.81	14.23	2.34	3.75	7.39
50 Hz	1.50	11.34	1.66	2.52	2.76	4.07	1.08	23.68	12.69	4.10	17.23	2.87	3.42	8.43
50 Hz	1.62	10.71	1.90	2.68	2.78	3.80	1.19	26.65	12.61	4.13	15.92	2.82	3.80	6.73
500 Hz	0.77	9.52	1.75	2.28	2.93	1.75	0.91	43.49	12.01	4.08	9.97	1.39	3.99	3.59
500 Hz	0.93	10.62	1.61	2.31	3.04	2.49	0.88	35.96	12.37	4.70	12.63	2.00	3.99	4.61
500 Hz	0.87	9.75	1.69	2.38	3.02	2.04	0.93	39.42	12.17	4.52	11.32	1.67	4.05	4.43
CL	0.90	9.65	1.74	2.22	2.83	1.90	1.05	41.18	11.99	4.37	10.51	1.63	4.16	4.11
CL	0.81	9.66	1.71	2.27	2.91	1.88	0.91	41.76	12.13	4.35	10.37	1.54	4.12	3.89
CL	0.77	9.50	1.74	2.21	2.83	1.79	0.93	42.93	12.05	4.22	10.16	1.43	4.11	3.71

Biochemical composition of *T. chui* during two stage cultivation.

			mg gDW-1				ug gDW-1				% of DW			mg gDW-1	% of DW		
Treatment	DW	log10 (DW)	Chl a	Chl b	Total Chl	Total Carot	Neoxanthin	Violaxanthin	Lutein	Beta carotene	Protein	Carbohydrate	Lipids	TFA	N	C	H
5 Hz	3.43	0.54	4.65	3.04	7.69	2.28	147.86	170.05	1594.90	1245.99	17.86	24.34	11.47	90.18	3.74	41.80	6.36
5 Hz	3.45	0.54	4.30	2.87	7.16	2.12	118.87	145.93	1281.71	945.50	18.04	20.93	11.06	93.40	3.77	41.74	6.35
5 Hz	3.21	0.51	7.13	4.70	11.83	3.42	83.83	146.23	1267.00	948.27	18.26	17.37	11.30	88.94	3.82	41.98	6.42
50 Hz	4.19	0.62	3.26	1.91	5.17	1.87	80.85	79.57	918.46	771.24	15.78	22.43	9.27	74.91	3.30	42.06	6.49
50 Hz	4.29	0.63	3.30	2.04	5.34	1.98	78.68	121.66	847.06	736.33	12.88	25.47	8.66	65.09	2.69	42.01	6.54
50 Hz	4.65	0.67	3.11	2.01	5.12	1.89	53.07	65.92	642.25	520.52	12.06	21.04	8.24	69.74	2.52	41.00	6.43
500 Hz	5.71	0.76	2.55	1.56	4.10	1.66	58.75	76.96	547.31	662.24	10.32	33.35	14.52	68.32	2.16	42.67	6.66
500 Hz	5.04	0.70	2.44	1.41	3.85	1.48	60.16	81.49	576.41	683.50	10.53	29.82	13.83	74.33	2.20	42.78	6.73
CL	3.59	0.55	3.27	1.84	5.11	1.96	50.73	81.19	583.89	731.23	10.38	28.03	8.10	76.04	2.17	41.86	6.51
CL	4.52	0.65	2.56	1.50	4.06	1.65	27.73	42.01	363.77	444.36	9.43	34.86	9.60	73.66	1.97	42.98	6.71
CL	4.54	0.66	1.90	1.11	3.01	1.29	16.64	22.24	293.57	403.70	8.97	45.37	7.74	73.07	1.88	42.55	6.79
5 Hz	3.43	0.54	4.65	3.04	7.69	2.28	147.86	170.05	1594.90	1245.99	17.86	24.34	11.47	90.18	3.74	41.80	6.36

Fatty acid composition of *T. chui* during two stage cultivation.

% of TFA														
Treatment	C14:0	C16:0	C16:1n7	C16:2n3	C16:3n3	C16:4n3	C18:0	C18:1n9	C18:2n6	18:3n-6	C18:3n3	C18:4n3	C20:1n9	C20:5n3
5 Hz	1.74	14.01	1.99	0.64	1.78	13.95	1.28	13.57	6.28	n.d.	19.22	9.32	3.37	12.85
5 Hz	1.80	13.55	2.01	0.63	1.74	15.38	1.21	13.33	5.94	n.d.	19.21	9.04	3.50	12.66
5 Hz	1.68	14.10	1.96	0.63	1.86	13.84	1.15	13.56	7.03	n.d.	19.54	8.62	3.38	12.64
50 Hz	0.92	15.10	1.83	0.49	2.03	13.35	0.39	14.97	7.02	1.06	19.52	6.50	3.04	12.72
50 Hz	1.81	14.89	2.41	0.78	2.11	12.43	1.25	16.65	7.40	n.d.	17.09	6.90	3.77	12.52
50 Hz	1.69	15.03	2.48	0.87	2.30	11.79	1.16	17.11	7.72	1.80	17.63	5.88	3.56	10.97
500 Hz	0.87	15.98	2.40	0.60	2.45	12.04	0.47	17.97	7.63	1.04	17.91	4.79	3.04	11.77
500 Hz	1.13	15.08	2.57	0.72	2.41	11.60	0.63	18.16	7.64	1.27	17.57	4.92	3.22	11.50
CL	1.78	14.89	2.74	0.92	2.39	11.22	1.23	18.70	7.50	n.d.	17.11	5.51	3.72	12.29
CL	1.83	15.14	3.04	0.96	2.51	10.53	1.36	20.13	8.14	n.d.	16.31	5.04	3.87	11.13
CL	1.78	15.22	3.37	0.98	2.58	10.22	1.34	21.08	8.23	n.d.	16.02	4.80	3.91	10.48
5 Hz	1.74	14.01	1.99	0.64	1.78	13.95	1.28	13.57	6.28	n.d.	19.22	9.32	3.37	12.85

Biocomponent productivity in *N. gaditana* during two-stage cultivation

Treatment	Tot. Chl	Tot. Caro t	Neo xant hin	Viol axan thin	Lute in	Beta caro tene	Prot ein	Carb ohy drat e	Lipi ds	TFA	C14: 0	C16: 0	C16: 1n7	C16: 2n3	C16: 3n3	C16: 4n3	C18: 0	C18: 1n9	C18: 2n6	18:3 n-6	C18: 3n3	C18: 4n3	C20: 1n9	C20: 5n3
5 Hz	2.63	1.19		0.46	0.02	0.10	68.73	40.87	99.31	78.34	0.87	10.65	11.87	0.08		0.08	0.52	2.85	0.69	0.33			0.23	5.59
5 Hz	3.19	1.39		0.42	0.02	0.08	74.65	35.19	102.13	76.88	0.85	11.00	12.16	0.07		0.08	0.47	2.94	0.68	0.30			0.20	5.92
5 Hz	3.09	1.43		0.46	0.02	0.09	76.54	25.32	114.70	74.46	0.82	10.70	11.59	0.07	0.14	0.07	0.62	2.86	0.65	0.30			0.19	5.68
50 Hz	2.43	1.23		0.28	0.02	0.06	77.61	36.08	185.24	153.03	0.89	19.60	18.50	0.06	0.12	0.06	0.80	4.08	0.74	0.29			0.15	4.64
50 Hz	2.57	1.23		0.30	0.02	0.06	79.37	33.14	180.11	177.76	0.93	20.18	18.97	0.07		0.07	0.72	4.32	0.77	0.32			0.19	4.60
50 Hz	1.78	1.01		0.26	0.02	0.06	81.85	44.76	180.16	155.35	0.93	20.39	19.62	0.06	0.13	0.06	0.70	4.34	0.80	0.32			0.17	5.12
500 Hz	1.63	1.02		0.14	0.02	0.03	70.84	53.13	191.57	146.08	0.83	21.68	21.82	0.11	0.13	0.05	0.79	4.90	0.76	0.38			0.14	4.24
500 Hz	1.73	1.03		0.22	0.02	0.04	82.16	67.83	183.81	140.16	0.80	20.90	21.90	0.06	0.14	0.06	0.99	5.04	0.90	0.47			0.17	4.51
500 Hz	2.16	1.20		0.23	0.02	0.03	71.80	51.90	184.07	140.36	0.82	19.41	21.32	0.06	0.13	0.06	0.83	4.95	0.79	0.46			0.16	4.27
CL	2.02	1.16		0.33	0.03	0.02	72.52	45.28	212.40	147.05	0.81	21.84	22.44	0.05	0.12	0.05	0.97	5.09	0.80	0.44			0.13	3.76
CL	1.65	1.09		0.31	0.03	0.02	74.62	51.27	222.45	160.14	0.97	23.34	24.82	0.05	0.15	0.05	0.96	5.77	0.86	0.48			0.14	4.10
CL	2.13	1.32		0.31	0.03	0.03	74.13	74.14	242.24	190.97	0.96	23.33	23.38	0.06	0.14	0.05	0.92	5.25	0.80	0.42			0.15	4.35

Biocomponent productivity in *K. antarctica* during two-stage cultivation

Treatment	Tot. Chl	Tot. Carot	Neoxanthin	Violaxanthin	Lutein	Beta carotene	Protein	Carbohydrate	Lipids	TFA	C14:0	C16:0	C16:1n7	C16:2n3	C16:3n3	C16:4n3	C18:0	C18:1n9	C18:2n6	18:3n-6	C18:3n3	C18:4n3	C20:1n9	C20:5n3
5 Hz	1.08	0.48	0.01	0.05	0.21	0.07	88.67	100.88	31.10	21.90	0.41	3.24	0.45	0.58	0.74	1.76	0.16	3.58	3.21	0.99	6.80	0.93	2.07	3.81
5 Hz	1.09	0.49	0.01	0.04	0.19	0.06	82.53	55.64	51.40	39.86	0.37	3.36	0.41	0.56	0.75	2.00	0.15	3.34	3.33	1.05	7.58	1.00	2.06	4.17
5 Hz	1.54	0.66	0.02	0.03	0.15	0.05	57.88	77.92	59.68	30.19	0.51	2.61	0.50	0.56	0.66	1.61	0.24	3.48	2.93	1.01	6.33	0.97	2.24	3.49
50 Hz	0.91	0.48	0.01	0.05	0.33	0.09	95.25	113.47	66.81	49.17	0.49	3.94	0.69	1.00	0.97	1.23	0.39	11.35	4.73	1.42	5.32	0.87	1.40	2.76
50 Hz	1.09	0.62	0.01	0.04	0.24	0.07	84.04	107.74	55.65	40.96	0.51	3.86	0.57	0.86	0.94	1.39	0.37	8.06	4.32	1.39	5.86	0.98	1.16	2.87
500 Hz	1.35	0.70	0.01	0.05	0.31	0.10	72.28	145.48	54.14	39.85	0.58	3.83	0.68	0.96	0.99	1.36	0.42	9.52	4.50	1.48	5.69	1.01	1.36	2.41
500 Hz	1.04	0.59	0.01	0.01	0.26	0.05	100.55	166.30	84.70	62.34	0.43	5.39	0.99	1.29	1.66	0.99	0.52	24.63	6.80	2.31	5.65	0.78	2.26	2.03
500 Hz	1.08	0.52	0.00	0.01	0.26	0.05	91.50	180.89	74.81	55.06	0.45	5.09	0.77	1.11	1.46	1.19	0.42	17.23	5.93	2.25	6.05	0.96	1.91	2.21
Hz	0.97	0.46	0.00	0.01	0.27	0.05	72.81	160.31	74.31	54.69	0.39	4.34	0.75	1.06	1.34	0.91	0.41	17.54	5.42	2.01	5.04	0.74	1.80	1.97
CL	1.06	0.56	0.00	0.00	0.14	0.02	41.63	152.08	69.54	51.18	0.47	5.05	0.91	1.16	1.48	0.99	0.55	21.53	6.27	2.28	5.50	0.85	2.17	2.15
CL	0.93	0.52	0.00	0.01	0.24	0.02	62.61	201.03	73.51	54.10	0.40	4.72	0.84	1.11	1.42	0.92	0.44	20.39	5.92	2.12	5.06	0.75	2.01	1.90
CL	1.00	0.55	0.00	0.01	0.24	0.02	84.26	190.63	62.31	45.85	0.39	4.80	0.88	1.12	1.43	0.90	0.47	21.71	6.10	2.14	5.14	0.72	2.08	1.88

Biocomponent productivity in *T. chui* during two-stage cultivation

Treatment	Tot. Chl	Tot. Carot	Neoxanthin	Violaxanthin	Lutein	Beta carotene	Protein	Carbohydrate	Lipids	TFA	C14:0	C16:0	C16:1n7	C16:2n3	C16:3n3	C16:4n3	C18:0	C18:1n9	C18:2n6	18:3 n-6	C18:3n3	C18:4n3	C20:1n9	C20:5n3
5 Hz	2.64	0.78	0.05	0.06	0.55	0.43	61.27	83.50	39.35	30.94	0.60	4.81	0.68	0.22	0.61	4.79	0.44	4.66	2.15		6.59	3.20	1.16	4.41
5 Hz	2.47	0.73	0.04	0.05	0.44	0.33	62.27	72.27	38.18	32.25	0.62	4.68	0.69	0.22	0.60	5.31	0.42	4.60	2.05		6.63	3.12	1.21	4.37
5 Hz 50	3.80	1.10	0.03	0.05	0.41	0.30	58.59	55.73	36.26	28.54	0.54	4.52	0.63	0.20	0.60	4.44	0.37	4.35	2.26		6.27	2.77	1.08	4.06
Hz 50	2.16	0.78	0.03	0.03	0.38	0.32	66.06	93.90	38.80	31.36	0.39	6.32	0.76	0.21	0.85	5.59	0.16	6.27	2.94	0.44	8.17	2.72	1.27	5.33
Hz 50	2.29	0.85	0.03	0.05	0.36	0.32	55.29	109.35	37.19	27.94	0.78	6.39	1.03	0.33	0.91	5.34	0.54	7.15	3.17		7.34	2.96	1.62	5.37
Hz 500	2.38	0.88	0.02	0.03	0.30	0.24	56.13	97.89	38.36	32.45	0.79	7.00	1.15	0.40	1.07	5.48	0.54	7.96	3.59	0.84	8.20	2.73	1.66	5.11
Hz 500	2.34	0.95	0.03	0.04	0.31	0.38	58.95	190.48	82.93	39.02	0.50	9.12	1.37	0.34	1.40	6.87	0.27	10.26	4.36	0.59	10.23	2.73	1.74	6.72
Hz	1.94	0.75	0.03	0.04	0.29	0.34	53.09	150.38	69.74	37.48	0.57	7.60	1.30	0.37	1.22	5.85	0.32	9.16	3.85	0.64	8.86	2.48	1.62	5.80
CL	1.83	0.70	0.02	0.03	0.21	0.26	37.23	100.59	29.06	27.29	0.64	5.34	0.98	0.33	0.86	4.03	0.44	6.71	2.69		6.14	1.98	1.33	4.41
CL	1.83	0.74	0.01	0.02	0.16	0.20	42.60	157.41	43.36	33.26	0.83	6.84	1.37	0.43	1.13	4.75	0.62	9.09	3.67		7.36	2.28	1.75	5.02
CL	1.37	0.59	0.01	0.01	0.13	0.18	40.71	206.02	35.12	33.18	0.81	6.91	1.53	0.44	1.17	4.64	0.61	9.57	3.74		7.27	2.18	1.78	4.76

Normalised biocomponent productivity in *N. gaditana* during two-stage cultivation

Treatment	Tot. Chl	Tot. Caro t	Neo xanthin	Viol axanthin	Lute in	Beta caro tene	Prot ein	Carb ohy drat e	Lipi ds	TFA	C14: 0	C16: 0	C16: 1n7	C16: 2n3	C16: 3n3	C16: 4n3	C18: 0	C18: 1n9	C18: 2n6	18:3 n-6	C18: 3n3	C18: 4n3	C20: 1n9	C20: 5n3
5 Hz	1.36	1.00		1.46	0.82	4.09	0.93	0.72	0.44	0.47	0.95	0.47	0.50	1.54		1.70	0.55	0.53	0.84	0.73			1.65	1.37
5 Hz	1.65	1.17		1.32	0.79	3.30	1.01	0.62	0.45	0.46	0.93	0.48	0.52	1.37		1.52	0.50	0.55	0.83	0.68			1.42	1.45
5 Hz 50	1.60	1.21		1.47	0.85	3.64	1.04	0.45	0.51	0.45	0.90	0.47	0.49	1.34	1.02	1.48	0.66	0.53	0.80	0.66			1.37	1.40
Hz 50	1.26	1.03		0.89	0.73	2.72	1.05	0.63	0.82	0.92	0.97	0.86	0.79	1.07	0.91	1.14	0.84	0.76	0.90	0.64			1.10	1.14
Hz 50	1.33	1.04		0.94	0.81	2.54	1.08	0.58	0.80	1.07	1.01	0.88	0.81	1.30		1.36	0.76	0.80	0.94	0.72			1.34	1.13
Hz 500	0.92	0.85		0.83	0.80	2.66	1.11	0.79	0.80	0.94	1.02	0.89	0.83	1.17	0.96	1.24	0.74	0.81	0.97	0.72			1.19	1.26
Hz 500	0.84	0.86		0.45	0.80	1.27	0.96	0.93	0.85	0.88	0.91	0.95	0.93	1.96	0.92	1.02	0.83	0.91	0.93	0.85			0.98	1.04
Hz 500	0.89	0.86		0.69	0.74	1.70	1.11	1.19	0.81	0.84	0.88	0.92	0.93	1.16	1.03	1.18	1.04	0.94	1.10	1.05			1.18	1.11
Hz	1.12	1.01		0.73	0.64	1.47	0.97	0.91	0.82	0.85	0.89	0.85	0.91	1.10	0.97	1.14	0.87	0.92	0.96	1.03			1.15	1.05
CL	1.05	0.97		1.03	1.12	0.65	0.98	0.80	0.94	0.89	0.89	0.96	0.95	0.92	0.89	0.91	1.02	0.95	0.98	0.99			0.91	0.92
CL	0.85	0.91		0.98	0.96	0.90	1.01	0.90	0.99	0.96	1.06	1.02	1.05	0.99	1.08	1.02	1.01	1.07	1.04	1.07			1.01	1.01
CL	1.10	1.11		0.99	0.92	1.45	1.01	1.30	1.07	1.15	1.05	1.02	0.99	1.09	1.03	1.07	0.97	0.98	0.98	0.94			1.07	1.07

Normalised biocomponent productivity in *K. antarctica* during two-stage cultivation

Treatment	Tot. Chl	Tot. Carot	Neoxanthin	Violaxanthin	Lutein	Betacarotene	Protein	Carbohydrate	Lipids	TFA	C14:0	C16:0	C16:1n7	C16:2n3	C16:3n3	C16:4n3	C18:0	C18:1n9	C18:2n6	18:3n-6	C18:3n3	C18:4n3	C20:1n9	C20:5n3
5 Hz	1.08	0.89	2.47	6.11	0.99	3.32	1.41	0.56	0.45	0.43	0.97	0.67	0.52	0.52	0.51	1.87	0.33	0.17	0.53	0.45	1.30	1.20	0.99	1.93
5 Hz	1.09	0.90	3.61	5.69	0.93	2.95	1.31	0.31	0.75	0.79	0.87	0.69	0.47	0.49	0.52	2.13	0.30	0.16	0.55	0.48	1.45	1.29	0.99	2.11
5 Hz	1.54	1.22	4.21	4.53	0.74	2.20	0.92	0.43	0.87	0.60	1.23	0.54	0.57	0.50	0.46	1.72	0.50	0.16	0.48	0.46	1.21	1.26	1.08	1.77
50 Hz	0.91	0.88	2.36	6.21	1.59	4.20	1.52	0.63	0.98	0.98	1.17	0.81	0.79	0.88	0.67	1.31	0.80	0.54	0.78	0.65	1.02	1.13	0.67	1.40
50 Hz	1.09	1.14	1.27	5.70	1.13	3.34	1.34	0.59	0.81	0.81	1.22	0.80	0.65	0.76	0.65	1.48	0.76	0.38	0.71	0.64	1.12	1.26	0.56	1.45
50 Hz	1.36	1.28	1.67	6.21	1.49	4.68	1.15	0.80	0.79	0.79	1.38	0.79	0.78	0.85	0.69	1.45	0.87	0.45	0.74	0.68	1.09	1.30	0.65	1.22
500 Hz	1.04	1.09	1.43	1.26	1.23	2.58	1.60	0.92	1.24	1.24	1.04	1.11	1.13	1.15	1.15	1.06	1.06	1.16	1.12	1.06	1.08	1.01	1.08	1.03
500 Hz	1.08	0.95	1.01	1.39	1.23	2.42	1.46	1.00	1.09	1.09	1.07	1.05	0.88	0.98	1.01	1.27	0.87	0.81	0.97	1.03	1.16	1.23	0.91	1.12
500 Hz	0.97	0.85	0.93	1.60	1.31	2.48	1.16	0.88	1.09	1.09	0.93	0.89	0.86	0.94	0.93	0.97	0.85	0.83	0.89	0.92	0.96	0.96	0.86	1.00
CL	1.07	1.02	1.23	0.59	0.69	1.03	0.66	0.84	1.02	1.02	1.13	1.04	1.04	1.03	1.02	1.06	1.13	1.02	1.03	1.05	1.05	1.10	1.04	1.09
CL	0.93	0.96	0.87	1.14	1.15	0.84	1.00	1.11	1.07	1.07	0.94	0.97	0.95	0.98	0.98	0.98	0.91	0.96	0.97	0.97	0.97	0.97	0.96	0.96
CL	1.00	1.02	0.90	1.26	1.16	1.13	1.34	1.05	0.91	0.91	0.93	0.99	1.00	0.99	0.99	0.96	0.96	1.02	1.00	0.98	0.98	0.93	1.00	0.95

Normalised biocomponent productivity in *T. chuii* during two-stage cultivation

Treatment	Tot. Chl	Tot. Carot	Neoxanthin	Violaxanthin	Lutein	Betacarotene	Protein	Carbohydrate	Lipids	TFA	C14:0	C16:0	C16:1n7	C16:2n3	C16:3n3	C16:4n3	C18:0	C18:1n9	C18:2n6	18:3n-6	C18:3n3	C18:4n3	C20:1n9	C20:5n3
5 Hz	1.57	1.15	3.98	3.01	3.24	1.98	1.52	0.54	1.10	0.99	0.79	0.76	0.53	0.55	0.58	1.07	0.79	0.55	0.64		0.95	1.49	0.71	0.93
5 Hz	1.47	1.08	3.22	2.60	2.62	1.52	1.55	0.47	1.06	1.03	0.82	0.73	0.54	0.54	0.57	1.19	0.76	0.54	0.61		0.96	1.46	0.75	0.92
5 Hz	2.26	1.62	2.11	2.42	2.41	1.41	1.46	0.36	1.01	0.91	0.71	0.71	0.49	0.50	0.57	0.99	0.66	0.51	0.67		0.91	1.29	0.67	0.86
50 Hz	1.29	1.15	2.65	1.72	2.27	1.50	1.64	0.61	1.08	1.00	0.51	0.99	0.59	0.51	0.81	1.25	0.30	0.74	0.87		1.18	1.27	0.79	1.13
50 Hz	1.37	1.26	2.65	2.69	2.15	1.47	1.38	0.71	1.04	0.89	1.02	1.00	0.80	0.83	0.86	1.19	0.97	0.85	0.94		1.06	1.38	1.00	1.14
50 Hz	1.42	1.30	1.94	1.58	1.77	1.12	1.40	0.63	1.07	1.04	1.04	1.10	0.89	1.00	1.02	1.23	0.98	0.94	1.07		1.18	1.28	1.02	1.08
500 Hz	1.40	1.39	2.63	2.27	1.85	1.76	1.47	1.23	2.31	1.25	0.66	1.43	1.06	0.85	1.33	1.54	0.48	1.21	1.29		1.48	1.28	1.07	1.42
500 Hz	1.15	1.10	2.38	2.12	1.72	1.60	1.32	0.97	1.95	1.20	0.75	1.19	1.00	0.91	1.16	1.31	0.57	1.08	1.14		1.28	1.16	1.00	1.23
CL	1.09	1.04	1.43	1.50	1.24	1.22	0.93	0.65	0.81	0.87	0.84	0.84	0.76	0.82	0.81	0.90	0.79	0.79	0.80		0.89	0.92	0.82	0.93
CL	1.09	1.10	0.98	0.98	0.97	0.93	1.06	1.02	1.21	1.06	1.09	1.07	1.06	1.08	1.08	1.06	1.11	1.07	1.09		1.06	1.06	1.08	1.06
CL	0.81	0.87	0.59	0.52	0.79	0.85	1.01	1.33	0.98	1.06	1.07	1.09	1.18	1.10	1.11	1.04	1.10	1.13	1.11		1.05	1.02	1.10	1.01

Statistical analysis

Overall ANCOVA on contents in all strains cultivated in a one- and two stage approach

		Proteins	Carbohydrates	Lipids
Model	R^2	0.836	0.689	0.831
	F	45.846	19.957	44.226
	p	< 0.0001	< 0.0001	< 0.0001
log10(DW)	F	55.772	1.385	2.805
	p	< 0.0001	0.244	0.099
Pearson´s	r	-0.804	0.230	0.192
Strain	F	16.710	56.339	141.615
	p	< 0.0001	< 0.0001	< 0.0001
Cultivation	F	5.299	0.215	2.055
	p	0.025	0.644	0.157
Treatment	F	5.711	2.317	1.691
	p	0.002	0.084	0.178

ANCOVA on contents in *Nannochlorpsis gaditana* cultivated in a one- and two stage approach

		Proteins	Carbohydrates	Lipids
Model	R^2	0.977433	0.465122	0.877916
	F	155.9262	3.130503	25.88789
	p	< 0.0001	0.033118	< 0.0001
log10(DW)	F	175.6744	5.288627	21.4839
	p	< 0.0001	0.033648	0.000206
Pearson´s r		-0.962	-0.610	0.775
Cultivation	F	11.0697	0.490567	9.347528
	p	0.00375	0.492629	0.006782
Treatment	F	1.907757	0.961045	3.702407
	p	0.164529	0.432474	0.03098

ANCOVA on contents in *Koliella antarctica* cultivated in a one- and two stage approach

		Proteins	Carbohydrates	Lipids
Model	R^2	0.800	0.740	0.322
	F	14.372	10.250	1.708
	p	< 0.0001	< 0.0001	0.184
log10(DW)	F	0.882	6.092	1.381
	p	0.360	0.024	0.255
Pearson´s	r	-0.693	0.820	-0.214
Cultivation	F	0.884	0.281	1.977
	p	0.360	0.603	0.177
Treatment	F	9.054	0.441	0.367
	p	0.001	0.727	0.778

ANCOVA on contents in *Tetraselmis chui* cultivated in a one- and two stage approach

		Proteins	Carbohydrates	Lipids
Model	R^2	0.969	0.542	0.571
	F	105.233	4.031	4.522
	p	< 0.0001	0.014	0.008
log10(DW)	F	84.636	0.023	0.108
	p	< 0.0001	0.882	0.747
Pearson´s	r	-0.848	0.442	-0.382
Cultivation	F	26.165	0.071	9.844
	p	< 0.0001	0.793	0.006
Treatment	F	13.341	4.048	1.874
	p	0.000	0.024	0.172

Overall ANCOVA on normalised productivities in all strains cultivated in the two-stage approach

		Proteins	Carbohydrates	Lipids
Model	R^2	0.549	0.709	0.638
	F	7.056	14.163	10.207
	p	0.000	< 0.0001	< 0.0001
Strain	F	10.002	0.432	17.056
	p	0.000	0.653	< 0.0001
Treatment	F	5.293	23.297	6.517
	p	0.005	< 0.0001	0.002

Overall ANCOVA on FA contents in all strains cultivated in a one- and two stage approach

		TFAs	SFA	MUFA	PUFA
Model	R^2	0.792	0.800	0.821	0.753
	F	34.240	35.951	41.170	27.385
	p	< 0.0001	< 0.0001	< 0.0001	< 0.0001
log10(DW)	F	2.739	4.432	3.915	7.609
	p	0.103	0.039	0.052	0.008
Pearson´s	r	0.250	0.323	0.342	-0.700
Strain	F	106.569	104.687	117.157	10.316
	p	< 0.0001	< 0.0001	< 0.0001	0.000
Cultivation	F	0.391	0.594	0.133	0.060
	p	0.534	0.444	0.716	0.808
Treatment	F	1.564	1.351	3.583	12.905
	p	0.207	0.266	0.019	< 0.0001

ANCOVA on FA contents in *Nannochloropsis gaditana* cultivated in a one- and two stage approach

		TFA	SFA	MUFA	PUFA
Model	R^2	0.671	0.765	0.753	0.895
	F	7.348	11.697	10.951	30.596
	p	0.001	< 0.0001	< 0.0001	< 0.0001
log10(DW)	F	5.705	9.391	6.792	14.481
	p	0.028	0.007	0.018	0.001
Pearson´s	r	0.799	0.849	0.831	-0.831
Cultivation	F	0.020	0.098	0.026	0.160
	p	0.889	0.758	0.873	0.694
Treatment	F	0.321	0.553	1.239	11.027
	p	0.810	0.653	0.325	0.000

ANCOVA on FA contents in *Koliella antarctica* cultivated in a one- and two stage approach

		TFA	SFA	MUFA	PUFA
Model	R^2	0.447	0.755	0.847	0.783
	F	2.905	11.109	19.870	12.986
	p	0.043	< 0.0001	< 0.0001	< 0.0001
log10(DW)	F	2.933	7.303	1.833	1.914
	p	0.104	0.015	0.192	0.183
Pearson´s	r	0.129	-0.098	0.726	-0.533
Cultivation	F	7.349	13.789	11.656	1.238
	p	0.014	0.002	0.003	0.280
Treatment	F	1.060	8.243	11.924	5.107
	p	0.391	0.001	0.000	0.010

ANCOVA on FA contents in *Tetraselmis chuii* cultivated in a one- and two stage approach

		TFA	SFA	MUFA	PUFA
Model	R^2	0.921	0.908	0.882	0.807
	F	39.832	33.513	25.410	14.233
	p	< 0.0001	< 0.0001	< 0.0001	< 0.0001
log10(DW)	F	18.563	18.329	29.346	1.043
	p	0.000	0.001	< 0.0001	0.322
Pearson´s	r	-0.921	-0.901	-0.831	-0.778
Cultivation	F	7.885	5.850	3.610	2.571
	p	0.012	0.027	0.075	0.127
Treatment	F	4.828	5.401	5.918	5.720
	p	0.013	0.009	0.006	0.007

Overall ANCOVA on normalised productivities of FA in all strains cultivated in the two-stage approach.

		TFA	SFA	MUFA	PUFA
Model	R^2	0.688	0.705	0.763	0.476
	F	12.796	13.843	18.655	5.270
	p	< 0.0001	< 0.0001	< 0.0001	0.001
Strain	F	16.465	16.718	6.687	12.197
	p	< 0.0001	< 0.0001	0.004	0.000
Treatment	F	10.910	12.276	27.250	0.774
	p	< 0.0001	< 0.0001	< 0.0001	0.518

ANCOVA on specific FA in *Nannochloropsis gaditana* cultivated in a one- and two stage approach

		C16:0	C16:1n7	C18:1n9	C20:5n3
	R^2	0.946	0.973	0.808	0.937
Model	F	62.524	128.319	15.163	53.334
	p	< 0.0001	< 0.0001	< 0.0001	< 0.0001
log10(DW)	F	74.216	94.643	9.406	48.889
	p	< 0.0001	< 0.0001	0.007	< 0.0001
Pearson´s	r	0.956	0.949	0.693	-0.931
Cultivation	F	2.538	0.466	0.143	0.167
	p	0.129	0.504	0.709	0.688
Treatment	F	0.991	14.903	10.221	5.708
	p	0.419	< 0.0001	0.000	0.006

ANCOVA on specific FA in *Koliella antarctica* cultivated in a one- and two stage approach

		C16:0	C16:3n3	C16:4n3	C16:1n7	C18:2n6	C18:3n3	C20:5n3
	R^2	0.641	0.940	0.886	0.926	0.925	0.928	0.907
Model	F	6.439	56.564	27.848	45.078	44.261	46.500	35.119
	p	0.001	< 0.0001	< 0.0001	< 0.0001	< 0.0001	< 0.0001	< 0.0001
log10(DW)	F	0.307	60.319	4.326	0.023	52.747	8.867	0.594
	p	0.586	< 0.0001	0.052	0.880	< 0.0001	0.008	0.451
Pearson´s	r	-0.024	-0.940	-0.519	0.665	0.924	-0.841	-0.589
Cultivation	F	1.791	1.868	6.278	1.642	9.173	0.022	2.215
	p	0.197	0.189	0.022	0.216	0.007	0.885	0.154
Treatment	F	7.362	5.196	23.030	23.333	0.442	9.183	21.512
	p	0.002	0.009	< 0.0001	< 0.0001	0.726	0.001	< 0.0001

ANCOVA on specific FA in *Tetraselmis chui* cultivated in a one- and two stage approach

		C16:0	C16:4	C18:1n9	C18:2n6	C18:3n3	C18:4n3	C20:5n3
Model	R^2	0.816	0.717	0.774	0.950	0.807	0.965	0.627
	F	15.038	8.621	11.641	64.420	14.217	93.043	5.716
	p	< 0.0001	0.000	< 0.0001	< 0.0001	< 0.0001	< 0.0001	0.003
log10(DW)	F	4.348	5.210	0.152	81.397	26.085	77.687	0.924
	p	0.052	0.036	0.702	< 0.0001	< 0.0001	< 0.0001	0.350
Pearson´s r	0.757	-0.008	0.232	0.912	0.656	-0.894	0.234	
Cultivation	F	0.194	0.083	3.860	13.385	0.021	10.461	7.631
	p	0.665	0.777	0.066	0.002	0.888	0.005	0.013
Treatment	F	4.691	11.197	10.149	0.837	9.245	9.604	1.837
	p	0.015	0.000	0.000	0.165	0.001	0.001	0.179

Overall ANCOVA on carotenoids content in a one- and two stage approach

		Total Chlorophyll mg/g	Total carotenoids mg/gDW	Neoxanthin [ug/g DW]	Violaxanthin [ug/g DW]	Lutein [ug/g DW]	Beta carotene [ug/g DW]
Model	R^2	0.585	0.483	0.580	0.644	0.866	0.887
	F	10.682	7.083	10.459	13.678	48.798	59.147
	p	< 0.0001	< 0.0001	< 0.0001	< 0.0001	< 0.0001	< 0.0001
log10(DW)	F	0.634	0.012	1.452	0.127	25.382	1.619
	p	0.429	0.914	0.234	0.723	< 0.0001	0.209
Pearson´s	r	-0.165	-0.191	-0.063	-0.005	-0.744	-0.127
Strain	F	5.999	4.779	8.408	35.490	53.773	165.378
	p	0.004	0.012	0.001	< 0.0001	< 0.0001	< 0.0001
Cultivation	F	3.857	1.370	6.905	0.159	0.644	4.154
	p	0.055	0.247	0.011	0.692	0.426	0.047
Treatment	F	12.647	7.501	10.738	4.064	5.178	9.314
	p	< 0.0001	0.000	< 0.0001	0.011	0.003	< 0.0001

Overall ANOVA on carotenoid productivities in all strains cultivated in a two stage approach.

		Total Chlorophyll mg/g	Total carotenoids mg/gDW	Neoxanthin [ug/g DW]	Violaxanthin [ug/g DW]	Lutein [ug/g DW]	Beta carotene [ug/g DW]
	R^2	0.807	0.857	0.668	0.902	0.820	0.929
Model	F	21.701	31.282	10.479	47.788	23.657	67.955
	p	< 0.0001	< 0.0001	< 0.0001	< 0.0001	< 0.0001	< 0.0001
Strain	F	35.740	74.998	14.269	110.771	54.491	159.479
	p	< 0.0001	< 0.0001	< 0.0001	< 0.0001	< 0.0001	< 0.0001
Treatment	F	11.831	2.226	7.756	6.482	2.716	7.431
	p	< 0.0001	0.109	0.001	0.002	0.065	0.001

ANCOVA on carotenoids in *Nannochloropsis gaditana* cultivated in a one- and two stage approach

		Total Chlorophyll mg/g	total carotenoids mg/gDW	Violaxanthin [ug/g DW]	Lutein [ug/g DW]	Beta carotene [ug/g DW]
	R^2	0.879	0.852	0.949	0.949	0.955
Model	F	21.883	17.269	56.314	56.215	64.312
	p	< 0.0001	< 0.0001	< 0.0001	< 0.0001	< 0.0001
log10(DW)	F	20.378	9.318	93.030	96.203	102.038
	p	0.000	0.008	0.000	< 0.0001	< 0.0001
Pearson´s r		-0.638	-0.436	-0.786	-0.895	-0.872
Cultivation	F	10.684	7.750	37.443	13.245	31.672
	p	0.005	0.014	< 0.0001	0.002	< 0.0001
Treatment	F	2.015	4.818	3.646	14.662	3.162
	p	0.155	0.015	0.037	< 0.0001	0.056

ANCOVA on carotenoids in *Koliella antarctica* cultivated in a one- and two stage approach

		Total Chlorophyll mg/g	total carotenoids mg/gDW	Neoxanthin [ug/g DW]	Violaxanthin [ug/g DW]	Lutein [ug/g DW]	Beta carotene [ug/g DW]
	R^2	0.667	0.699	0.461	0.981	0.909	0.939
Model	F	6.022	6.954	2.565	152.646	29.948	46.578
	p	0.003	0.002	0.072	< 0.0001	< 0.0001	< 0.0001
log10(DW)	F	4.246	3.697	0.189	15.769	19.453	26.792
	p	0.057	0.074	0.670	0.001	0.001	0.000
Pearson´s	r	-0.527	-0.530	-0.423	-0.707	-0.922	-0.875
Cultivation	F	12.117	12.432	0.410	1.871	0.195	4.052
	p	0.003	0.003	0.532	0.192	0.665	0.062
Treatment	F	5.076	5.800	1.739	52.293	3.174	3.400
	p	0.013	0.008	0.202	< 0.0001	0.055	0.046

ANCOVA on carotenoids in *Tetraselmis chui* cultivated in a one- and two stage approach

		Total Chlorophyll mg/g	total carotenoids mg/gDW	Neoxanthin [ug/g DW]	Violaxanthin [ug/g DW]	Lutein [ug/g DW]	Beta carotene [ug/g DW]
	R^2	0.813	0.704	0.663	0.750	0.849	0.616
Model	F	11.312	6.190	5.119	7.802	14.636	4.174
	p	0.000	0.004	0.008	0.001	< 0.0001	0.018
log10(DW)	F	5.770	3.542	0.399	2.620	2.277	0.449
	p	0.032	0.082	0.538	0.130	0.155	0.515
Pearson´s	r	-0.692	-0.702	-0.508	-0.314	-0.645	-0.621
Cultivation	F	0.320	0.011	0.023	4.092	0.042	1.122
	p	0.581	0.919	0.883	0.064	0.840	0.309
Treatment	F	3.002	1.518	2.874	2.384	6.565	2.338
	p	0.069	0.257	0.077	0.116	0.006	0.121

Paragraph 3.6. List of primers with the biological functions employed in transcriptomic analysis.

GENE ID	Primer	Biological function	Symbol
Naga_100106g21 F	TGC CTT GTT GTC GTC ATA CTC	Glycerol-3-phosphate acyltransferase (GPAT)	GPAT
Naga_100106g21 R	TTG GGA GTG AGT GAG GAA GAG		
Naga_100005g43 F	TTC GGA TTG CCA GAA GAT GTC	LCYB Lycopene beta cyclase	LCYB
Naga_100005g43 R	ATG GAG TTT GCC TTG ACG AG		
Naga_100007g86 F	AGG TTT GGA GAA CAT ACC CG	1-Acyl-sn-glycerol-3-phosphate acyltransferase (LPAT)	LPAT-2
Naga_100007g86 R	ATT TGA CTG CGT TTG TCA TCT C		
Naga_100010g4 F	CAT CCT CAC GGA ATT CTG ACC	Diacylglycerol acyltransferase	DGAT-5
Naga_100010g4 R	GAG AGG AAA TCG CTG ATG AAG G		
Naga_100010g65 F	GAA ACA GGC CAC AAA CTT ACC	ALAD 5-aminolevulinic acid dehydratase/porphobilinogen synthase	ALAD
Naga_100015g9 R	GCT CCT CCT TAT TCT TTC CCA		
Naga_100016g50 F	CTT GAG CAT GGT GGT GTT TGG	VDE- violaxanthin de-epoxidase chloroplastic	VDE-2
Naga_100016g50 R	GCC ATC GTC ATT GTC ATT GC		
Naga_100020g8 F	CGA ATA AAC AGG CTC TTC ATG G	Glucose-1-phosphate adenylyltransferase	AGPase-2
Naga_100020g8 R	CCA TCA CCA GTT TCT TTC CGT		
Naga_100024g16 F	GGT GCT CTG GCT AGT TTG AC	3-Oxoacyl-[acyl carrier protein] reductase (KAR)	KAR-2
Naga_100024g16 R	GGA TAC TGT TCA ACA CTT GAA CG		
Naga_100037g12 F	AAC TTG CCC AAC ATG GAG TG	3-Oxoacyl-[acyl carrier protein] reductase (KAR)	KAR-1
Naga_100037g12 R	CAT GTC AGC CTT GAT AGC CA		
Naga_100038g41 F	TCC TCG GAA GAT AAG AGT GCT	Phosphatidic acid phosphatase	PAP-3
Naga_100038g41 R	ACA TCT TGA GGC TGT TGG TG		
Naga_100041g46 F	GAC TTG AAG GAG AAC CCG AC	VDE- violaxanthin de-epoxidase chloroplastic	VDE-1
Naga_100041g46 R	CCT TCT CCT CCA TCA TGA TCG		
Naga_100042g20 F	GGC ATA CAA CTA CCT ACA AAC G	Glycerol-3-phosphate dehydrogenase	GPD-3
Naga_100042g20 R	GTA GGC ATG AAG AGA TCC GC		
Naga_100046g34 F	GCC AAG ACA GAG TTC AAG ACG	Malonyl-CoA:ACP transacylase (MCT)	MCT
Naga_100046g34 R	CAG GTC GTT CAT GGT GGT CTC		

Naga_100046g36 F	ATG TTT GTC GGA CCC TTC GG	nitrite transporter NAR1	NAR1
Naga_100046g36 R	CCC GCT ATG ATA TTT CCA ATG GT		
Naga_100055g16 F	CCC GCT ATG ATA TTT CCA ATG GT	Biotin-acetyl-CoA-carboxylase ligase (BC)	BC
Naga_100055g16 R	CGT CCA TTT CGA TCA ATA GGC		
Naga_100061g21 F	CGG TGG TGA AAG AGT GGA GAC	Delta 6 saturase	D6S
Naga_100061g21 R	TGT GTT GAC GCA CCT CAT CC		
Naga_100071g18 F	GAA TCG CAG AAA TGT TCA TGC T	Diacylglycerol acyltransferase	DGAT-4
Naga_100071g18 R	CGT GTG GTT AAA GTG GTA AAT GG		
Naga_100113g7 F	GAC ACT CTG GTC ATG GAG GT	3-Hydroxyacyl-ACP dehydratase (HAD)	HAD
Naga_100113g7 R	AAG TCA TCT CCT TGA TTT CGA CG		
Naga_100158g20 F	CTC CAG TAC ATC TAC CAG AAC AG	Long-chain acyl-CoA synthetase (LCS)	LCS-2
Naga_100158g20 R	GAA AGA GGA CGA GGA TGA AGC		
Naga_100174g4 F	CTT CCC GAT TCC TGA AAT TGG	3-Ketoacyl-CoA-synthase 11 (KAS)	KAS
Naga_100174g4 R	GCA CGA ATT CCT TGA TCT CG		
Naga_100194g2 F	CCT TCA CCT CAG CCT TCC TC	zeaxanthin de-epoxidase Chloroplastic	ZeaDE
Naga_100194g2 R	CTC CCG CAG ACT ACC ATA CTG		
Naga_100217g6 F	CCT TCA TCA TCC ACG CAG TC	Glycerol-3-phosphate dehydrogenase	GPD-2
Naga_100217g6 R	GTC TCC AAG AGG ATG TCC TG		
Naga_100234g7 F	GGT AGA AGG CGT TGA AAT CGT	Phosphatidic acid phosphatase	PAP-2
Naga_100234g7 R	CTT TGC CAT CCC AAT CAT TGC		
Naga_100251g9 F	GGA GTC ACG ACT TCC TTC TG	Phosphatidic acid phosphatase	PAP-1
Naga_100251g9 R	CCT ACT TGT TCC ATC ATC CCT G		
Naga_100258g4 F	GGG ACT TGA AAG GGA TGC AG	POR light-dependent NADPH:protochlorophyllide oxidoreductase	POR-1
Naga_100258g4 R	CAT GTT GCA CAT CTT GCT GTC C		
Naga_100343g3 F	ACT TCC ACT ACG AAT ACA TTC TGG	Diacylglycerol acyltransferase	DGAT-3
Naga_100343g3 R	CTG CTT GGT GAT GGA GAT GG		
Naga_100427g6 R	TCT GAA TAG CCT CCC AGT CC		
Naga_100545g1 F	ATG CTT CCA GAA ATC ACT TCT CC	Long-chain acyl-CoA synthetase (LCS)	LCS-1
Naga_100545g1 R	TGA CCG ATC ACA AAG AGA CAC		
Naga_100649g1 F	CGT CAA TCG TTG CTG AAG GA	Diacylglycerol acyltransferase	DGAT-2

Naga_100649g1 R	ACT TCT GGG TAG GAG TGA GG		
Naga_100682g2 R	GCC TGA AGC AAC ATG AAT TTC G		
Naga_100699g1 F	CCT TTG GCA TTT GGA TGT CG	Nitrate reductase	NR
Naga_100699g1 R	GCT GTT GTT CAT CAT TCC GAG G		
Naga_100904g1 F	GCG TTG TTG TAT CAA TCT GGG	1-Acyl-sn-glycerol-3-phosphate acyltransferase (LPAT)	LPAT-1
Naga_100904g1 R	AAA TCC AAC CGA GCA AGA GG		
Naga_101053g1 F	GGG AAG AAG ACC TTC ATC GAG	Enoyl-[acyl carrier protein] reductase (ENR)	ENR-2
Naga_101053g1 R	CCA CAT ACA TAG TCA CGC CC		
Naga_101227g1 F	GGC GTG CTG GGT ATT TGG AT	VCP- violaxanthin-chlorophyll protein	VCP-1
Naga_101227g1 R	GCT GAA GGA GAC CTG GAG GA		
Naga_101286g2 F	TCT AAT ATC ATC ACA AGC ACC AGC	Glucose-1-phosphate adenylyltransferase	AGPase-1
Naga_101286g2 R	AGG CTT CAC TCA ATT CCA CC		
Naga_101365g1 F	AGG GTG TTA GGA GAC TGA TGG	Glycerol-3-phosphate dehydrogenase	GPD-1
Naga_101365g1 R	ACC TCT TTC CTT GTC CAC TG		
Naga_101525g2 F	GCT GTC CCT TCT GCT TTG TC	Enoyl-[acyl carrier protein] reductase (ENR)	ENR-1
Naga_101525g2 R	CAA GTG TTT GGT GAT GGC CC		
Naga_101968g1 F	CCA TCA TCC AGA GCA CTA TGG	Diacylglycerol acyltransferase	DGAT-1
Naga_101968g1 R	ATC TCG GCA AAC AAA TTC AGC		
Naga_102294g1 F	CTT GCT CCA CAC CTT CTT ACG	1-Acyl-sn-glycerol-3-phosphate acyltransferase (LPAT)	deleted
Naga_102294g1 R	GGA CCA AGG CCA AGA AGG AC		
Naga_102739g1 F	ATC GGC TCC ATG TAT TTG ATC C	Omega 6 fatty acid desaturase	O6FADes-1
Naga_102739g1 R	CCC TTG ATG TAG CTC CAC TC		
rNaga_100257g1 F	GCGTCTTGGGTTAC ACAGAG	glyceraldehyde-3-phosphate dehydrogenase	Gly3PDH
rNaga_100257g1 R	GAGTAGCCCATCTC ATTGTCG		
rNaga_100009g3 F	TCTTCCGCCCAGAT AATTTCG	beta-tubulin	BT
rNaga_100009g3 R	GCCTCTTTCCTGAC TACATCC		
rNaga_100021g70 F	CTTTCAAATTAACT CTCAACCCGC	alpha tubulin 1	AT1
rNaga_100021g70 R	CTCCGATGGTCTTC TCAGAC		

rNaga_102100g1 F	GGACCTGTACTCCA ACATCG	Actin	ACT
rNaga_102100g1 R	CACGACCTTCACCT TCATGG		
rNaga_100019g64 F	CACGATTCAACGA GATCAAGG	translation elongation factor 1-	TEF1
rNaga_100019g64R	CTTGTACCAGGCCA TGTTAGTG		
rNaga_100044g34F	GCAGATCAACGTG AAGACAC	ubiquitin family protein	UFP
rNaga_100044g34R	CCTCCAAAGATGA GACGCTG		
rNaga_100067g11F	TTTAAGGGCTCCAC CTTCCA	cyclophilin	CYP
rNaga_100067g11R	AATTTGTTCCCGTA GATAGACTCG		

Section 4

Figure A1: Original Infra Red spectra of the *N. gaditana* cultured in growth medium and in wastewaters during first cultivation series and second cultivation series

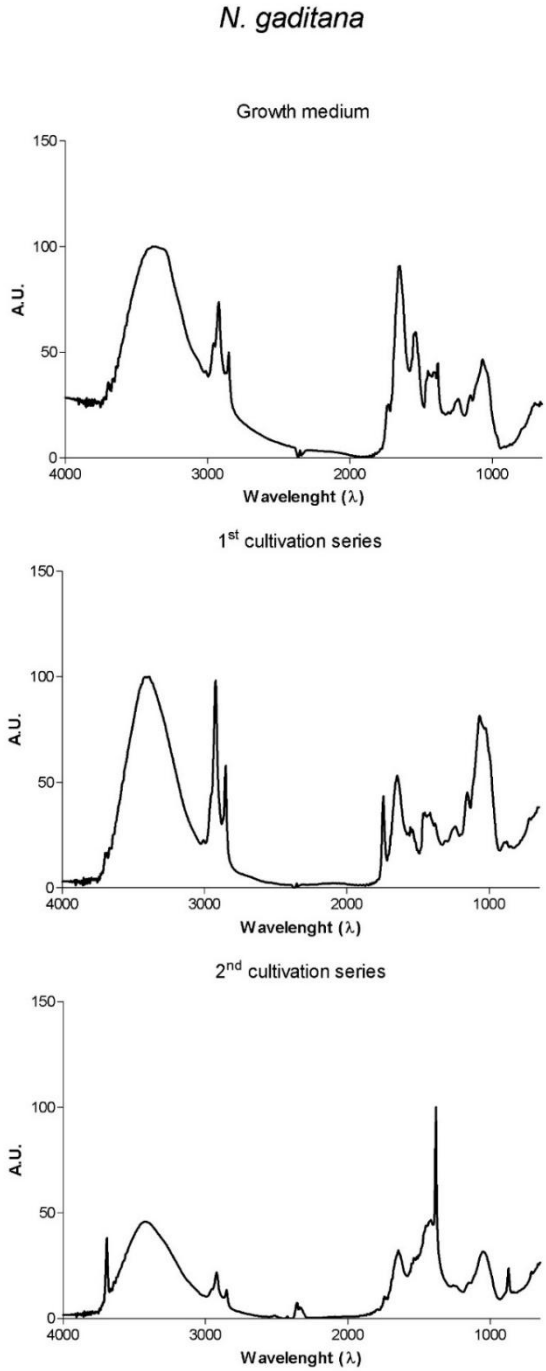

Figure A2: Original Infra Red spectra of the biomass of *C. sorokiniana* cultured in growth medium and in wastewaters during first and second cultivation series.

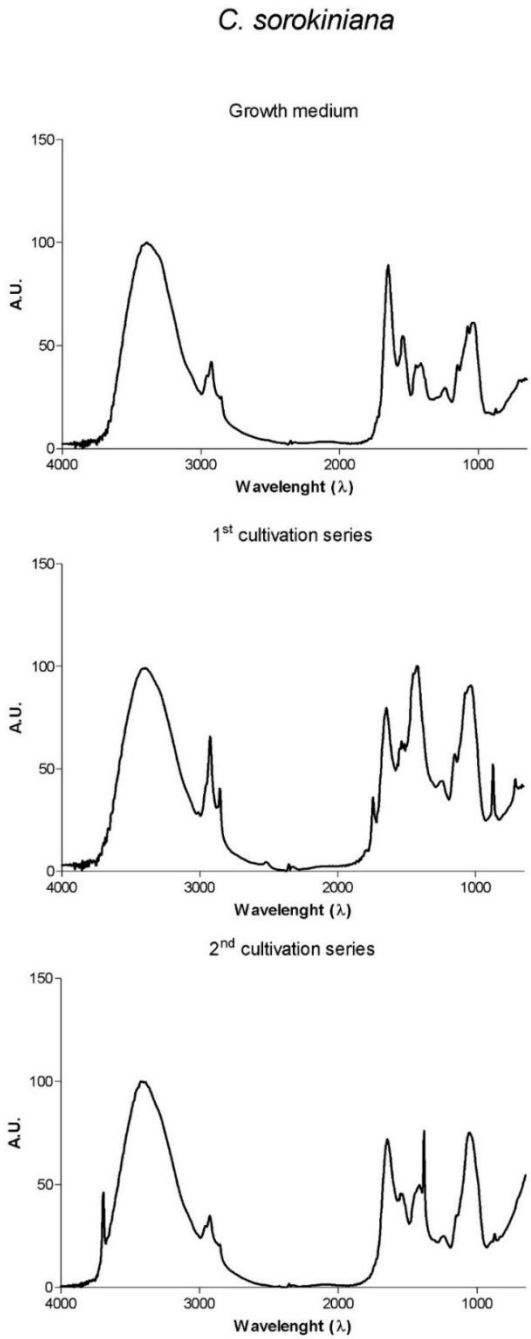

Figure A3: Original Infra Red spectrum of *Chlorella sp. (Pozzillo)* cultured in growth medium and in wastewaters during first and second cultivation series.

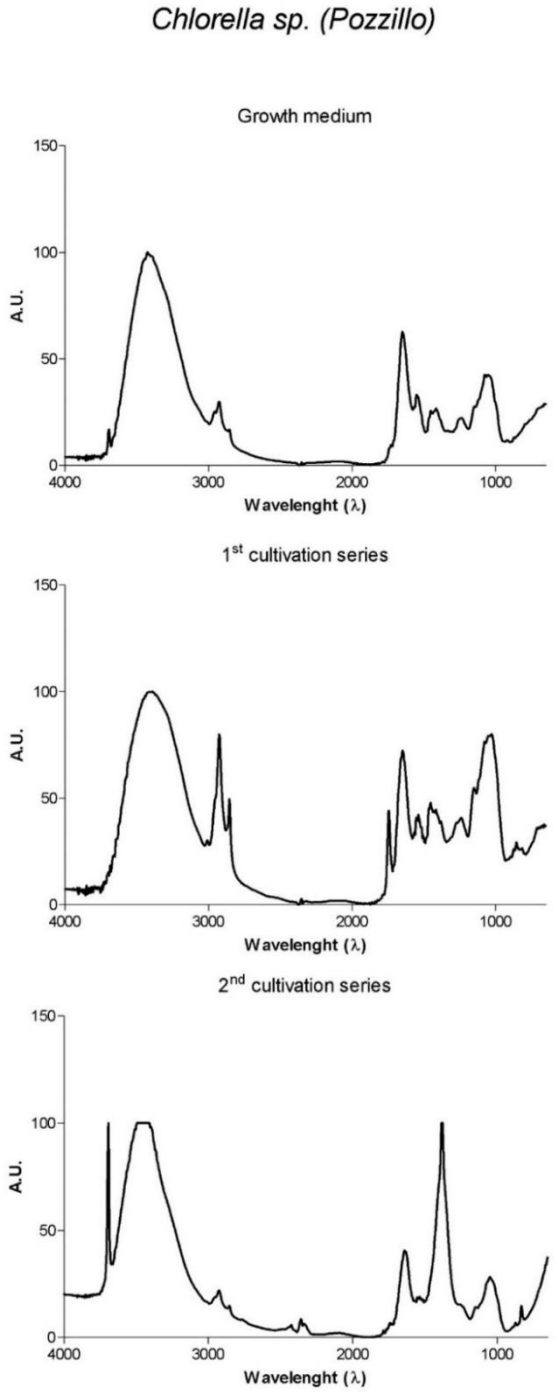

Figure A4: Original Infra Red spectra of *Chlorella sp./Dunaliella sp. (Vergine Maria)* cultured in growth medium and in wastewaters during first and second cultivation series.

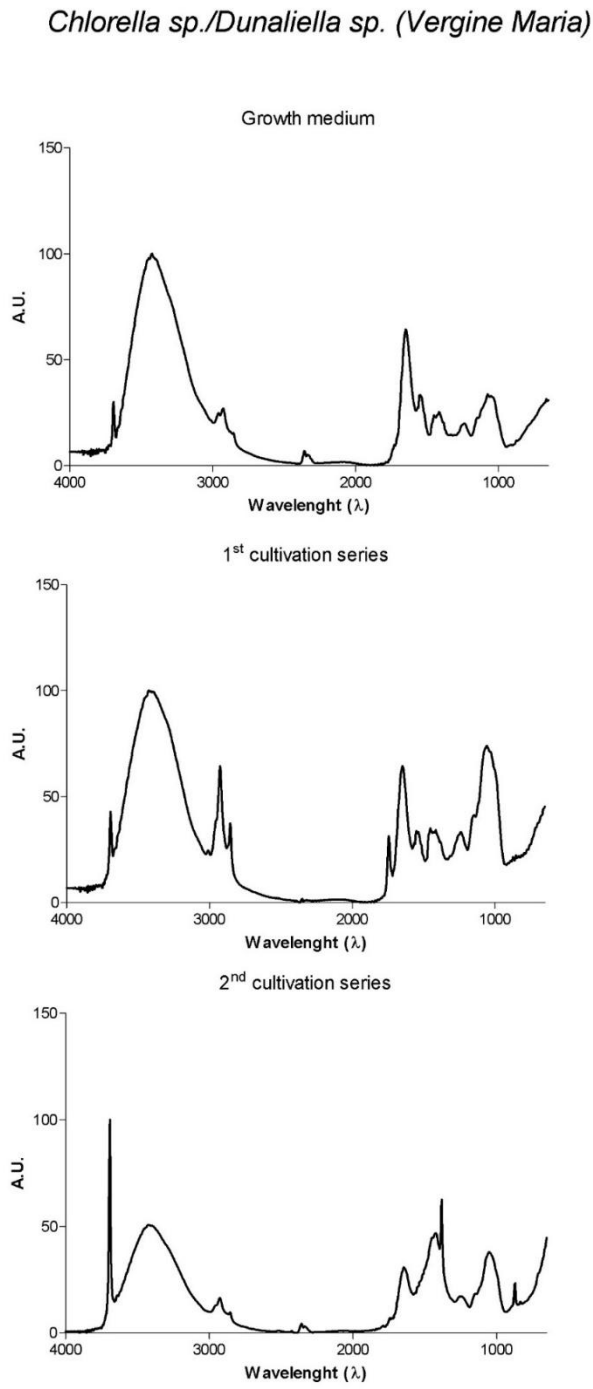

Table A.1: Detail of ratios of the peaks areas connected to biomolecules.

Abbreviations: GM= Growth medium; 1st C= first cultivation; 2nd C= second cultivation; L/A= Lipid/amide I; A/C= Amide I/carbohydrates; L/C= Lipid/carbohydrates.

	N. gaditana			***C. sorokiniana***			***Chlorella sp. (Pozzillo)***			***Consortium Dunaliella sp./Chlorella sp. (Vergine Maria)***		
	GM	1st C	2nd C	GM	1st C	2nd C	GM	1st C	2nd C	GM	1st C	2nd C
L/A	1.30; 0.98	1.57; 1.58	0.99; 1.19	0.74; 0.72	0.83; 0.82	0.69; 0.71	0.73; 0.72	1.22; 0.21	0.86; 0.81	1.36; 1.29	1.10; 1.10	0.63; 0.65
A/C	0.70; 0.56	0.37; 0.36	0.62; 0.63	0.74; 0.73	0.50; 0.49	0.60; 0.59	0.78; 0.85	0.44; 0.42	0.66; 0.50	0.87; 0.91	0.44; 0.44	0.51; 0.49
L/C	0.91; 0.54	0.57; 0.59	0.62; 0.75	0.54; 0.52	0.42; 0.41	0.41; 0.42	0.57; 0.61	0.53; 0.54	0.58; 0.41	1.15; 0.93	0.48 0.48	0.32; 0.32

Table A.2: Summary of microalgal treatment effects on municipal wastewater chemical proprieties. The result is reported as percentage of difference compared to the original sewage. ↔ symbol means that there is no effect compared to the original sample. Abbreviations: CS= Control Sewage, 1st C= first cultivation; 2nd C= second cultivation; TR= Total Removal.

	CS	***N. gaditana***		***C. sorokiniana***		***Chlorella sp. (Pozzillo)***		***Consortium Dunaliella sp./Chlorella sp. (Vergine Maria)***	
		1st C	2nd C	1st C	2nd C	1st C	2nd C	1st C	2nd C
BOD [mg/L O_2]	↔	↔	↔	↔	T R	↔	T R	+20.0%	↔
COD [mg/L O_2]	-9.1%	+154.5 %	+72.7%	+254.5 %	+63.6%	+436.4 %	+254.5 %	+454.5 %	+200.0 %
TN	+30.0 %	-0.9%	-36.4%	+33.6%	-77.3%	-1.8%	-76.4%	-0.9%	-88.2%
TP	+7.3%	-34.1%	-61.0%	-19.5%	-56.1%	-61.0%	-17.1%	-41.5%	-58.5%

List of abbreviations

List of abbreviations

A/C	Amide I/carbohydrates
ACCase	Acetyl-CoA carboxylase
ACP	Acyl carrier protein
ADP	Adenosine diphosphate
ADP	Adenosine diphosphate
ADP Glc	ADP glucose
AGPase	ADP-glucose pyrophosphorylase
ALA	A-linoleic acid
ALAD	ALA dehydratase
ARS	Arsylsulfatase
ATP	Adenosine triphosphate
ATPase	ATP synthase
BC	Biotin carboxylase
BCCP	Biotin carboxyl carrier protein
BE	Branching enzymes
BKT	Beta-carotene ketolase
BOD	Biological oxygen demand
BT	Beta tubulin
C_a	Chlorophyll a
CAGR	Compounded average growth rate
C_b	Chlorophyll b
C_{carot}	Total carotenoids
CEF	Cyclic electron transport
CL	Continuous light
COD	Chemical oxygen demand
DAG	Diacylglycerol
DC	Duty cycle
DGAT	Diacylglycerol acyltransferase
DHA	Docosahexaenoic acid
DHLAT	Dihydrolipoyl acyltransferase
DMAPP	Dimathylallyl pyrophosphate
DW	Dry weight
EET	Eletron energy transfer
E_k	Light saturation points of photosynthesis
ENR	Enoyl-acp reductase
EPA	Eicosapentaenoic acids
ER	Endoplasmic reticulum
ETR	Electron transfer rate
ETRmax	Maximum ETRs
f	Frequency
FAMEs	Fatty acid methyl esters
FAO	Food and Agriculture Organization of the United Nations

FAS	Fatty acid synthase
FDA	Food and drug administration
Fe	Ferrodoxin
FL	Flashing light
FL 250	250 Hz flashing light condition
FL 2500	2500 Hz flashing light condition
FL 50	50 Hz flashing light condition
FL 500	500 Hz flashing light condition
FL 25	25Hz flashing light condition
FL 5	5Hz flashing light condition
FNR	Ferrodoxin nadp+ reductase
FPP	Farnesylpyrophosphate
FTIR	Fourier transform infrared spectroscopy
G3P	Glycerol 3 phosphate
GBSS	Granule bound starch synthase
GC	Gas chromatography
Gcl1P	Glucose 1 phosphate
GGPP	Geranylgeranylpyrophosphate
Gly3PDH	Glycerol 3-phosphate dehydrogenase
glycerate-P	Phosphoglycerate
GM	Genetic modified
GPAT	Acylcoa:glycerol-3-phosphate acyltransferase
GPP	Geranylpyrophosphate
GWD	Glucan, water dikinases
HAD	Hydroxyacyl-acp dehydrase
I_a	Averaged light intensity
IEC	Ion exchange chromatography
IF	Intrinsic factor
I_l	Instantaneous light intensity
IPCC	Intergovernmental panel on climate change
IPP	Isopentenyl pyrophosphate
ISO	Isoamylase
KAR	Ketoacyl-acp reductase
KAS	3-ketoacyl-acp synthase
L/A)	Lipid/amide I
L/C	Lipid/carbohydrates
LA	Linoleic acid
LCS	Long-chain acyl-coenzyme a synthetase
LCYB	Lycopene β cyclase
LCY-b	Lycopene beta-cyclase
LCY-e	Lycopene e-cyclase
LDPE	Low density polyethylene
LED	Light emitting diode
LEF	Linear electron transfer

LHC	Light harvesting complex
LPAT	Acyl-CoA:lysophosphatidic acyltransferase
LPCAT	Lysophosphatidylcholine acyltransferase
LPD	Dihydrolipoamide dehydrogenase
LS	Lipoic acid synthase
LT	Lipoyltransferase
LVRPA	Local volumetric rate of photon absorption
MCT	Malonyl-coa acp malonyltransferase
MEP	2- C -methyl- D -erythritol 4-phosphate
MUFA	Monounsaturated fatty acid
MVA	Mevalonate
NAD	Nicotinamide adenine dinucleotide
NADP	Nicotinamide adenine dinucleotide phosphate
NAR1	Nitrate assimilation-related component 1
NPQ	Non photochemical quenching
NR	Nitrate reductase
O6FADes-1	Δ6 desaturase
PA	Phosphatidic acid
PAM	Pulse-amplitude modulated
PAP	Phosphatidic acid phosphatase
PAR	Photosynthetic active radiation
PBR	Photobioreactor
PC	Plastocyanin
PDCH	Plastidial pyruvate dehydrogenase complex
PDH	Pyruvate dehydrogenase
PDHC	Plastidial pyruvate dehydrogenase complex
PDS	Phytoene desaturase
PE	Polyethylene
PET	Photosynthetic electron transfer
Phe	Pheophytin
Pi	Pyrophosphate
P-I curves	Photosynthesis-irradiance curves
PMMA	Polymethyl methacrylate
POR-1	Protochlorophyllide oxidoreductase
PP	Polypropylene
PQ	Plastoquinone
PSII and PSI	Photosystems ii and i
PTOX	Quinol terminal oxidase
PUFA	Polyunsaturated fatty acid
PVC	Polyvinyl chloride
PWD	Phosphoglucan,water phosphatases
Qg	Gas flow
Ql	Liquid flow
RC	Reaction centre

RGB	Red-green-blue
Ribulose-bis-P	Ribulose bisphosphate
Rubisco	Ribulose bisphosphate carboxylase/oxygenase
SAD	ACP desaturase
SFA	Saturated fatty acid
SSs	Starch synthases
TAG	Triacylglycerol
TAP	Tris acetate phosphate
tc	Flashing cycle
td	Dark periods
TFA	Total fatty acid
tl	Light periods
TN	Total nitrogen
TP	Total phosphorous
Tris	Tris(hydroxymethyl)aminomethane
TTET	Triplet–triplet energy transfer
VCP	Violaxanthin–chlorophyll a binding protein
VDE	Violaxanthin de-epoxidase
WWAP	World water assessment programme
ZDS	Z-carotene desaturase
ZeaDE	Zeaxanthin epoxidase
αETR	Initial slopes of the ETR vs irradiances curves

Notation

Notation

$\frac{dx}{dt}$	Rate of cell concentration change
$\sum \boldsymbol{F}$	Pressure drop
$\frac{\boldsymbol{Fv'}}{\boldsymbol{Fm'}}$	Effective PSII-quantum yield
$[O_2]_{out}$	Maximum acceptable oxygen value
μ	Specific growth rate
μ_{max}	Maximum value of specific growth rate μ
A_d	Cross-sectional areas of the downcomer
A_{LD}	Section of the degasser
a_p	Capture cross section
A_r	Section of the riser
C_o	Orifice coefficient
d_B	Mean bubble diameter
d_t	Tube diameter
ε_d	Gas holdup in the downcomer
ε_r	Gas holdup in the riser
f	Friction factor
F	Minimum fluorescence
F_0	Minimum fluorescence yield
F_c	Concentrated pressure drops
F_d	Distributed pressure drops
F_m	Maximum fluorescence yield
F_m'	Maximum fluorescence
F_v/F_m	Maximum PSII-quantum yield
g	Gravitational acceleration
G_0	Inlet irradiation intensity
h	Plank constant
h_D	Height of the fluid in the degasser
h_r	Height of the riser
K_B	Frictional loss coefficient for the bottom connecting section of the airlift
K_i	Light saturation constant
k_L	Mass transfer coefficient
k_La_L	Volumetric mass transfer coefficient
Ks	Substrate constant
K_T	Frictional loss coefficient for the top connecting section of the airlift
L	Maximum length of a photobioreactor tube
L_D	Distance between the entrance and the exit of the degasser

L_E	Characteristic extension lenght
L_{eq}	Equivalent length of the loop considering concentrated pressure drops as an increase of length
L_r	Reactor thickness
L_t	Distance between the parallel degasser walls
n_p	Number of particles per unit suspension volume
P	Power input
Re	Reynolds number
R_{O2}	Volumetric rate of oxygen generation
r_x	Volumetric rate of biomass production
S	Nutrient concentration
U_b	Bubble rise velocity in the riser
U_G	Aeration rate in the riser
U_L	Mean superficial liquid velocity in the riser
U_{LD}	Mean superficial liquid velocity in the degasser
x_0	Viable cell concentration at time zero
β	Ratio of superficial gas velocity to the total (gas and liquid) superficial velocity
λ	Characteristic parameter in eq. Errore. Nel documento non esiste testo dello stile specificato.-I
ρ_G	Density of the gas
ρ_L	Liquid density
ρ_r	Density in the riser
υ	Photon frequency
A	Illuminated surface area
I	Photon flux density in the photosynthetically available range
V	Culture volume
Y	Photosynthetic yield
x	Viable cell concentration

Bibliography

Bibliography

Abdel-Raouf, N., Al-Homaidan, A.A., Ibraheem, I.B.M., 2012. Microalgae and wastewater treatment. Saudi J. Biol. Sci. 19, 257–275. https://doi.org/10.1016/j.sjbs.2012.04.005

Abdulqader, G., Barsanti, L., Tredici, M.R., 2000. Harvest of Arthrospira platensis from Lake Kossorom (Chad) and its household usage among the Kanembu. J. Appl. Phycol. 12, 493–498.

Abinandan, S., Subashchandrabose, S.R., Venkateswarlu, K., Megharaj, M., 2018. Nutrient removal and biomass production: advances in microalgal biotechnology for wastewater treatment. Crit. Rev. Biotechnol. 38, 1244–1260. https://doi.org/10.1080/07388551.2018.1472066

Abu-Ghosh, S., Fixler, D., Dubinsky, Z., Iluz, D., 2016. Flashing light in microalgae biotechnology. Bioresour. Technol. 203, 357–363. https://doi.org/10.1016/j.biortech.2015.12.057

Abu-Ghosh, S., Fixler, D., Dubinsky, Z., Iluz, D., 2015. Continuous background light significantly increases flashing-light enhancement of photosynthesis and growth of microalgae. Bioresour. Technol. 187, 144–148. https://doi.org/10.1016/j.biortech.2015.03.119

Acién Fernández, F.G., Fernández Sevilla, J.M., Molina Grima, E., 2013. Photobioreactors for the production of microalgae. Rev. Environ. Sci. Bio/Technology 12, 131–151. https://doi.org/10.1007/s11157-012-9307-6

Acién Fernández, F.G., Fernández Sevilla, J.M., Sánchez Pérez, J.A., Molina Grima, E., Chisti, Y., 2001. Airlift-driven external-loop tubular photobioreactors for outdoor production of microalgae: assessment of design and performance. Chem. Eng. Sci. 56, 2721–2732. https://doi.org/10.1016/S0009-2509(00)00521-2

Ahmed, F., Fanning, K., Netzel, M., Turner, W., Li, Y., Schenk, P.M., 2014. Profiling of carotenoids and antioxidant capacity of microalgae from subtropical coastal and brackish waters. Food Chem. 165, 300–306. https://doi.org/10.1016/j.foodchem.2014.05.107

Ahmet Karagunduz, N.O., Bayar, S., Gurol, M.D., Karagunduz, A., 2017. Submerged microfiltration membrane performances of microalgal biomass cultivated in secondary effluent. Desalin. WATER Treat. 66, 42–49. https://doi.org/10.5004/dwt.2017.20326

Allen, J.F., de Paula, W.B.M., Puthiyaveetil, S., Nield, J., 2011. A structural phylogenetic map for chloroplast photosynthesis. Trends Plant Sci. 16, 645–655. https://doi.org/10.1016/j.tplants.2011.10.004

Alonso, D.L., Belarbi, E.-H., Fernández-Sevilla, J.M., Rodríguez-Ruiz, J., Grima, E.M., 2000. Acyl lipid composition variation related to culture age and nitrogen concentration in continuous culture of the microalga Phaeodactylum tricornutum. Phytochemistry 54, 461–471. https://doi.org/10.1016/S0031-9422(00)00084-4

Alpers, D.H., Russell-Jones, G., 2013. Gastric intrinsic factor: The gastric and small intestinal stages of cobalamin absorption. A personal journey. Biochimie 95, 989–994. https://doi.org/10.1016/j.biochi.2012.12.006

Ambati, R.R., Gogisetty, D., Aswathanarayana, R.G., Ravi, S., Bikkina, P.N., Bo, L., Yuepeng, S., 2019. Industrial potential of carotenoid pigments from microalgae: Current trends and future prospects. Crit. Rev. Food Sci. Nutr. 59, 1880–1902. https://doi.org/10.1080/10408398.2018.1432561

Ansari, A.A., Khoja, A.H., Nawar, A., Qayyum, M., Ali, E., 2017. Wastewater treatment by local microalgae strains for CO2 sequestration and biofuel production. Appl. Water Sci. 7, 4151–4158. https://doi.org/10.1007/s13201-017-0574-9

Ansari, F.A., Ravindran, B., Gupta, S.K., Nasr, M., Rawat, I., Bux, F., 2019. Techno-economic estimation of wastewater phycoremediation and environmental benefits using Scenedesmus obliquus microalgae. J. Environ. Manage. 240, 293–302. https://doi.org/10.1016/j.jenvman.2019.03.123

Ariede, M.B., Candido, T.M., Jacome, A.L.M., Velasco, M.V.R., de Carvalho, J.C.M., Baby, A.R., 2017. Cosmetic attributes of algae - A review. Algal Res. 25, 483–487. https://doi.org/10.1016/j.algal.2017.05.019

Arnold, A.A., Genard, B., Zito, F., Tremblay, R., Warschawski, D.E., Marcotte, I., 2015. Identification of lipid and saccharide constituents of whole microalgal cells by 13C solid-state NMR. Biochim. Biophys. Acta - Biomembr. 1848, 369–377. https://doi.org/10.1016/j.bbamem.2014.07.017

Baliga, R., Powers, S.E., 2010. Sustainable Algae Biodiesel Production in Cold Climates. Int. J. Chem. Eng. 2010, 1–13. https://doi.org/10.1155/2010/102179

Banerjee, A., Maiti, S.K., Guria, C., Banerjee, C., 2017. Metabolic pathways for lipid synthesis under nitrogen stress in Chlamydomonas and Nannochloropsis. Biotechnol. Lett. 39, 1–11. https://doi.org/10.1007/s10529-016-2216-y

Barahimipour, R., Neupert, J., Bock, R., 2016. Efficient expression of nuclear transgenes in the green alga Chlamydomonas: synthesis of an HIV antigen and development of a new selectable marker. Plant Mol. Biol. 90, 403–418. https://doi.org/10.1007/s11103-015-0425-8

Basso, S., Simionato, D., Gerotto, C., Segalla, A., Giacometti, G.M., Morosinotto, T., 2014. Characterization of the photosynthetic apparatus of the Eustigmatophycean Nannochloropsis gaditana: Evidence of convergent evolution in the supramolecular organization of photosystem I. Biochim. Biophys. Acta - Bioenerg. 1837, 306–314. https://doi.org/10.1016/j.bbabio.2013.11.019

Becker, E.W., 2007. Micro-algae as a source of protein. Biotechnol. Adv. 25, 207–210. https://doi.org/10.1016/j.biotechadv.2006.11.002

Benemann, J., 2013. Microalgae for Biofuels and Animal Feeds. Energies 6, 5869–5886. https://doi.org/10.3390/en6115869

Berner, T., Dubinsky, Z., Wyman, K., Falkowski, P.G., 1989. Photoadaptation and the "package" effect in Dunaliella tertiolecta (Chlorophyceae). J. Phycol. 25, 70–78. https://doi.org/10.1111/j.0022-3646.1989.00070.x

Bertrand, E.M., Allen, A.E., Dupont, C.L., Norden-Krichmar, T.M., Bai, J., Valas, R.E., Saito, M.A., 2012. Influence of cobalamin scarcity on diatom molecular physiology and

identification of a cobalamin acquisition protein. Proc. Natl. Acad. Sci. U. S. A. 109, E1762-71. https://doi.org/10.1073/pnas.1201731109

Bertucco, A., Sforza, E., Fiorenzato, V., Strumendo, M., 2015. Population balance modeling of a microalgal culture in photobioreactors: Comparison between experiments and simulations. AIChE J. 61, 2702–2710. https://doi.org/10.1002/aic.14893

Bito, T., Bito, M., Asai, Y., Takenaka, S., Yabuta, Y., Tago, K., Ohnishi, M., Mizoguchi, T., Watanabe, F., 2016. Characterization and Quantitation of Vitamin B 12 Compounds in Various Chlorella Supplements. J. Agric. Food Chem. 64, 8516–8524. https://doi.org/10.1021/acs.jafc.6b03550

Blanken, W., Cuaresma, M., Wijffels, R.H., Janssen, M., 2013. Cultivation of microalgae on artificial light comes at a cost. Algal Res. 2, 333–340. https://doi.org/10.1016/j.algal.2013.09.004

Bligh, E.G., Dyer, W.J., 1959. A rapid method of total lipid extraction and purification. Can. J. Biochem. Physiol. 37, 911–917. https://doi.org/10.1139/o59-099

Borowitzka, M.A., 2013. High-value products from microalgae—their development and commercialisation. J. Appl. Phycol. 25, 743–756. https://doi.org/10.1007/s10811-013-9983-9

Bottino, N.., Newman, R.., Cox, E.., Stockton, R., Hoban, M., Zingaro, R.., Irgolic, K.., 1978. The effects of arsenate and arsenite on the growth and morphology of the marine unicellular algae Tetraselmis chui (Chlorophyta) and Hymenomonas carterae (Chrysophyta). J. Exp. Mar. Bio. Ecol. 33, 153–168. https://doi.org/10.1016/0022-0981(78)90005-9

Boynton, J., Gillham, N., Harris, E., Hosler, J., Johnson, A., Jones, A., Randolph-Anderson, B., Robertson, D., Klein, T., Shark, K., Et, A., 1988. Chloroplast transformation in Chlamydomonas with high velocity microprojectiles. Science (80-.). 240, 1534–1538. https://doi.org/10.1126/science.2897716

Brennan, L., Owende, P., 2010. Biofuels from microalgae—A review of technologies for production, processing, and extractions of biofuels and co-products. Renew. Sustain. Energy Rev. 14, 557–577. https://doi.org/10.1016/j.rser.2009.10.009

Breuer, G., Lamers, P.P., Martens, D.E., Draaisma, R.B., Wijffels, R.H., 2012. The impact of nitrogen starvation on the dynamics of triacylglycerol accumulation in nine microalgae strains. Bioresour. Technol. 124, 217–226. https://doi.org/10.1016/j.biortech.2012.08.003

Brower, V., 1998. Nutraceuticals: poised for a healthy slice of the healthcare market? Nat. Biotechnol. 16, 728–731.

Brown, M.R., Dunstan, G.A., Norwood, S.J., Miller, K.A., 1996. Effects of harvest stage and light on the biochemical composition of the diatom Thalassiosira pseudonana. J. Phycol. 32, 64–73. https://doi.org/10.1111/j.0022-3646.1996.00064.x

Brucato, A., Rizzuti, L., 1997. Simplified Modeling of Radiant Fields in Heterogeneous Photoreactors. 1. Case of Zero Reflectance. Ind. Eng. Chem. Res. 36, 4740–4747. https://doi.org/10.1021/ie960259j

Brucato, A., Grisafi, F., Rizzuti, L., Sclafani, A., Vella, G., 2007. Quasi-isoactinic reactor for photocatalytic kinetics studies. Ind. Eng. Chem. Res. 46, 7684–7690. https://doi.org/10.1021/ie0703991

Buléon, A., Colonna, P., Planchot, V., Ball, S., 1998. Starch granules: structure and biosynthesis. Int. J. Biol. Macromol. 23, 85–112. https://doi.org/10.1016/S0141-8130(98)00040-3

Burlew, J.S., 1953. Algal culture, from laboratory to pilot plant.

Busi, M. V., Barchiesi, J., Martín, M., Gomez-Casati, D.F., 2014. Starch metabolism in green algae. Starch - Stärke 66, 28–40. https://doi.org/10.1002/star.201200211

Cagliari, A., Margis, R., Dos Santos Maraschin, F., Turchetto-Zolet, A.C., Loss, G., Margis-Pinheiro, M., 2011. Biosynthesis of Triacylglycerols (TAGs) in plants and algae. Int. J. Plant Biol. 2, 10. https://doi.org/10.4081/pb.2011.e10

Camacho-Rodríguez, J., Cerón-García, M.C., Fernández-Sevilla, J.M., Molina-Grima, E., 2015. The influence of culture conditions on biomass and high value product generation by Nannochloropsis gaditana in aquaculture. Algal Res. 11, 63–73. https://doi.org/10.1016/j.algal.2015.05.017

Camarena-Bernard, C., Rout, N.P., 2018. Native Microalgae from Eutrophic Water: Potential for Wastewater Treatment, Low-Cost Biomass, and Lipid Production. Ind. Biotechnol. 14, 257–264. https://doi.org/10.1089/ind.2018.0009

Caporgno, M.P., Mathys, A., 2018. Trends in Microalgae Incorporation Into Innovative Food Products With Potential Health Benefits. Front. Nutr. 5. https://doi.org/10.3389/fnut.2018.00058

Carbonera, D., Agostini, A., Di Valentin, M., Gerotto, C., Basso, S., Giacometti, G.M., Morosinotto, T., 2014. Photoprotective sites in the violaxanthin–chlorophyll a binding Protein (VCP) from Nannochloropsis gaditana. Biochim. Biophys. Acta - Bioenerg. 1837, 1235–1246. https://doi.org/10.1016/j.bbabio.2014.03.014

Cardenas, D., Fuchs-Tarlovsky, V., 2018. Is multi-level marketing of nutrition supplements a legal and an ethical practice? Clin. Nutr. ESPEN 25, 133–138. https://doi.org/10.1016/j.clnesp.2018.03.118

Cereghino, G.P.L., Cregg, J.M., 1999. Applications of yeast in biotechnology: protein production and genetic analysis. Curr. Opin. Biotechnol. 10, 422–427. https://doi.org/10.1016/S0958-1669(99)00004-X

Cerutti, H., Johnson, A.M., Gillham, N.W., Boynton, J.E., 1997. Epigenetic silencing of a foreign gene in nuclear transformants of Chlamydomonas. Plant Cell 9, 925–945. https://doi.org/10.1105/tpc.9.6.925

Cezare-Gomes, E.A., Mejia-da-Silva, L. del C., Pérez-Mora, L.S., Matsudo, M.C., Ferreira-Camargo, L.S., Singh, A.K., de Carvalho, J.C.M., 2019. Potential of Microalgae Carotenoids for Industrial Application. Appl. Biochem. Biotechnol. 188, 602–634. https://doi.org/10.1007/s12010-018-02945-4

Chamberlin, J., Harrison, K., Zhang, W., 2018. Impact of Nutrient Availability on Tertiary Wastewater Treatment by Chlorella vulgaris. Water Environ. Res. 90, 2008–2016. https://doi.org/10.2175/106143017X15131012188114

Cheng, R., Ma, R., Li, K., Rong, H., Lin, X., Wang, Z., Yang, S., Ma, Y., 2012. Agrobacterium tumefaciens mediated transformation of marine microalgae Schizochytrium. Microbiol. Res. 167, 179–186. https://doi.org/10.1016/j.micres.2011.05.003

Chisti, M.Y., 1989. Airlift bioreactors, London ; New York : Elsevier Applied Science. John Wiley & Sons, Ltd. https://doi.org/10.1002/cjce.5450680228

Cho, D.-H., Ramanan, R., Heo, J., Shin, D.-S., Oh, H.-M., Kim, H.-S., 2016. Influence of limiting factors on biomass and lipid productivities of axenic Chlorella vulgaris in photobioreactor under chemostat cultivation. Bioresour. Technol. 211, 367–373. https://doi.org/10.1016/j.biortech.2016.03.109

Choi, Y.K., Kim, Hyun Joong, Kumaran, R.S., Song, H.J., Song, K.G., Kim, K.J., Lee, S.H., Yang, Y.H., Kim, Hyung Joo, 2017. Enhanced growth and total fatty acid production of microalgae under various lighting conditions induced by flashing light. Eng. Life Sci. 17, 976–980. https://doi.org/10.1002/elsc.201700001

Chu, L., Robinson, D.K., 2001. Industrial choices for protein production by large-scale cell culture. Curr. Opin. Biotechnol. 12, 180–187. https://doi.org/10.1016/S0958-1669(00)00197-X

Ciferri, O., 1983. Spirulina, the Edible Microorganism. Microbiol. Rev. 47, 551–578.

Combe, C., Hartmann, P., Rabouille, S., Talec, A., Bernard, O., Sciandra, A., 2015. Long-term adaptive response to high-frequency light signals in the unicellular photosynthetic eukaryote Dunaliella salina. Biotechnol. Bioeng. 112, 1111–1121. https://doi.org/10.1002/bit.25526

Corteggiani Carpinelli, E., Telatin, A., Vitulo, N., Forcato, C., D'Angelo, M., Schiavon, R., Vezzi, A., Giacometti, G.M., Morosinotto, T., Valle, G., 2014. Chromosome scale genome assembly and transcriptome profiling of Nannochloropsis gaditana in nitrogen depletion. Mol. Plant 7, 323–335. https://doi.org/10.1093/mp/sst120

Couso, I., Vila, M., Vigara, J., Cordero, B.F., Vargas, M.Á., Rodríguez, H., León, R., 2012. Synthesis of carotenoids and regulation of the carotenoid biosynthesis pathway in response to high light stress in the unicellular microalga Chlamydomonas reinhardtii. Eur. J. Phycol. 47, 223–232. https://doi.org/10.1080/09670262.2012.692816

Croce, R., van Amerongen, H., 2013. Light-harvesting in photosystem I. Photosynth. Res. 116, 153–166. https://doi.org/10.1007/s11120-013-9838-x

Croft, M.T., Lawrence, A.D., Raux-Deery, E., Warren, M.J., Smith, A.G., 2005. Algae acquire vitamin B12 through a symbiotic relationship with bacteria. Nature 438, 90–93. https://doi.org/10.1038/nature04056

Cunningham, F.X., Gantt, E., 1998. Genes and enzymes of carotenoid biosynthesis in plants. Annu. Rev. Plant Physiol. Plant Mol. Biol. 49, 557–583. https://doi.org/10.1146/annurev.arplant.49.1.557

Daneshvar, E., Zarrinmehr, M.J., Koutra, E., Kornaros, M., Farhadian, O., Bhatnagar, A., 2019. Sequential cultivation of microalgae in raw and recycled dairy wastewater: Microalgal growth, wastewater treatment and biochemical composition. Bioresour. Technol. 273, 556–564. https://doi.org/10.1016/j.biortech.2018.11.059

De Bhowmick, G., Sarmah, A.K., Sen, R., 2019. Performance evaluation of an outdoor algal biorefinery for sustainable production of biomass, lipid and lutein valorizing flue-gas carbon dioxide and wastewater cocktail. Bioresour. Technol. 283, 198–206. https://doi.org/10.1016/j.biortech.2019.03.075

De Mooij, T., De Vries, G., Latsos, C., Wijffels, R.H., Janssen, M., 2016. Impact of light colour on photobioreactor productivity. Algal Res. 15, 32–42. https://doi.org/10.1016/j.algal.2016.01.015

Dean, A.P., Sigee, D.C., Estrada, B., Pittman, J.K., 2010. Using FTIR spectroscopy for rapid determination of lipid accumulation in response to nitrogen limitation in freshwater microalgae. Bioresour. Technol. 101, 4499–4507. https://doi.org/10.1016/j.biortech.2010.01.065

Debuchy, R., Purton, S., Rochaix, J.D., 1989. The argininosuccinate lyase gene of Chlamydomonas reinhardtii: an important tool for nuclear transformation and for correlating the genetic and molecular maps of the ARG7 locus. EMBO J. 8, 2803–9.

DeCicco, J.M., Liu, D.Y., Heo, J., Krishnan, R., Kurthen, A., Wang, L., 2016. Carbon balance effects of U.S. biofuel production and use. Clim. Change 138, 667–680. https://doi.org/10.1007/s10584-016-1764-4

Degen, J., Uebele, A., Retze, A., Schmid-Staiger, U., Trösch, W., 2001. A novel airlift photobioreactor with baffles for improved light utilization through the flashing light effect. J. Biotechnol. 92, 89–94. https://doi.org/10.1016/S0168-1656(01)00350-9

Del Campo, J.A., Rodriguez, H., Moreno, J., Vargas, M.Á., Rivas, J., Guerrero, M.G., 2004. Accumulation of astaxanthin and lutein in Chlorella zofingiensis (Chlorophyta). Appl. Microbiol. Biotechnol. 64, 848–854. https://doi.org/10.1007/s00253-003-1510-5

Delrue, F., Álvarez-Díaz, P., Fon-Sing, S., Fleury, G., Sassi, J.-F., 2016. The environmental biorefinery: using microalgae to remediate wastewater, a win-win paradigm. Energies 9, 132. https://doi.org/10.3390/en9030132

Deng, X., Cai, J., Fei, X., 2013. Involvement of phosphatidate phosphatase in the biosynthesis of triacylglycerols in Chlamydomonas reinhardtii. J. Zhejiang Univ. Sci. B 14, 1121–1131. https://doi.org/10.1631/jzus.B1300180

Dinesh Kumar, S., Ro, K.-M., Santhanam, P., Dhanalakshmi, B., Latha, S., Kim, M.-K., 2018. Initial population density plays a vital role to enhance biodiesel productivity of Tetraselmis sp. under reciprocal nitrogen concentration. Bioresour. Technol. Reports 3, 15–21. https://doi.org/10.1016/j.biteb.2018.05.008

Doran, P.M., 2013. Homogeneous Reactions, in: Bioprocess Engineering Principles. Elsevier, pp. 599–703. https://doi.org/10.1016/B978-0-12-220851-5.00012-5

Doria, E., Longoni, P., Scibilia, L., Iazzi, N., Cella, R., Nielsen, E., 2012. Isolation and characterization of a Scenedesmus acutus strain to be used for bioremediation of urban wastewater. J. Appl. Phycol. 24, 375–383. https://doi.org/10.1007/s10811-011-9759-z

Drop, B., Webber-Birungi, M., Yadav, S.K.N., Filipowicz-Szymanska, A., Fusetti, F., Boekema, E.J., Croce, R., 2014. Light-harvesting complex II (LHCII) and its supramolecular organization in Chlamydomonas reinhardtii. Biochim. Biophys. Acta - Bioenerg. 1837, 63–72. https://doi.org/10.1016/j.bbabio.2013.07.012

Dubinsky, Z., Falkowski, P.G., Wyman, K., 1986. Light Harvesting and Utilization by Phytoplankton. Plant Cell Physiol. 27, 1335–1349. https://doi.org/10.1093/oxfordjournals.pcp.a077232

Eberhard, S., Finazzi, G., Wollman, F.-A., 2008. The Dynamics of Photosynthesis. Annu. Rev. Genet. 42, 463–515. https://doi.org/10.1146/annurev.genet.42.110807.091452

Economou, C., Wannathong, T., Szaub, J., Purton, S., 2014. A Simple, Low-Cost Method for Chloroplast Transformation of the Green Alga Chlamydomonas reinhardtii. Humana Press, Totowa, NJ, pp. 401–411. https://doi.org/10.1007/978-1-62703-995-6_27

Eichler-Stahlberg, A., Weisheit, W., Ruecker, O., Heitzer, M., 2009. Strategies to facilitate transgene expression in Chlamydomonas reinhardtii. Planta 229, 873–883. https://doi.org/10.1007/s00425-008-0879-x

Espín, J.C., García-Conesa, M.T., Tomás-Barberán, F.A., 2007. Nutraceuticals: Facts and fiction. Phytochemistry 68, 2986–3008. https://doi.org/10.1016/j.phytochem.2007.09.014

FAO, 2017. The future of food and agriculture : trends and challenges.

Fedosov, S.N., Laursen, N.B., Nexo, E., Moestrup, S.K., Petersen, T.E., Jensen, E.O., Berglund, L., 2003. Human intrinsic factor expressed in the plant Arabidopsis thaliana. Eur. J. Biochem. 270, 3362–3367. https://doi.org/10.1046/j.1432-1033.2003.03716.x

Fernandes, B.D., Mota, A., Ferreira, A., Dragone, G., Teixeira, J.A., Vicente, A.A., 2014. Characterization of split cylinder airlift photobioreactors for efficient microalgae cultivation. Chem. Eng. Sci. 117, 445–454. https://doi.org/10.1016/j.ces.2014.06.043

Fernández-Reiriz, M.J., Perez-Camacho, A., Ferreiro, M.J., Blanco, J., Planas, M., Campos, M.J., Labarta, U., 1989. Biomass production and variation in the biochemical profile (total protein, carbohydrates, RNA, lipids and fatty acids) of seven species of marine microalgae. Aquaculture 83, 17–37. https://doi.org/10.1016/0044-8486(89)90057-4

Fogliano, V., Andreoli, C., Martello, A., Caiazzo, M., Lobosco, O., Formisano, F., Carlino, P.A., Meca, G., Graziani, G., Rigano, V.D.M., Vona, V., Carfagna, S., Rigano, C., 2010. Functional ingredients produced by culture of Koliella antarctica. Aquaculture 299, 115–120. https://doi.org/10.1016/j.aquaculture.2009.11.008

Forján, E., Garbayo, I., Casal, C., Vílchez, C., Forján Lozano, E., Garbayo Nores, I., Casal Bejarano, C., Vílchez Lobato, C., Forján, E., Garbayo, I., Casal, C., Vílchez, C., 2007. Enhancement of carotenoid production in Nannochloropsis by phosphate and sulphur limitation. Commun. Curr. Res. Educ. Top. Trends Appl. Microbiol. 1, 356–364.

Fu, W., Nelson, D.R., Mystikou, A., Daakour, S., Salehi-Ashtiani, K., 2019. Advances in microalgal research and engineering development. Curr. Opin. Biotechnol. https://doi.org/10.1016/j.copbio.2019.05.013

Fumio Watanabe, Yoshihisa Nakano, Yoshiyuki Tamura, Hiroyuki Yamanaka, 1991. Vitamin B12 metabolism in a photosynthesizing green alga, Chlamydomonas reinhardtii. Biochim. Biophys. Acta - Gen. Subj. 1075, 36–41. https://doi.org/10.1016/0304-4165(91)90071-N

Gangl, D., Zedler, J.A.Z., Rajakumar, P.D., Martinez, E.M.R., Riseley, A., Włodarczyk, A., Purton, S., Sakuragi, Y., Howe, C.J., Jensen, P.E., Robinson, C., 2015a. Biotechnological exploitation of microalgae. J. Exp. Bot. 66, 6975–6990. https://doi.org/10.1093/jxb/erv426

Gangl, D., Zedler, J.A.Z., Włodarczyk, A., Jensen, P.E., Purton, S., Robinson, C., 2015b. Expression and membrane-targeting of an active plant cytochrome P450 in the chloroplast of the green alga Chlamydomonas reinhardtii. Phytochemistry 110, 22–28. https://doi.org/10.1016/j.phytochem.2014.12.006

Gao, F., Yang, H.-L., Li, C., Peng, Y.-Y., Lu, M.-M., Jin, W.-H., Bao, J.-J., Guo, Y.-M., 2019. Effect of organic carbon to nitrogen ratio in wastewater on growth, nutrient uptake and lipid accumulation of a mixotrophic microalgae Chlorella sp. Bioresour. Technol. 282, 118–124. https://doi.org/10.1016/j.biortech.2019.03.011

Gao, K., 1998. Chinese studies on the edible blue-green alga, Nostoc flagelliforme: A review. J. Appl. Phycol. 10, 37–49. https://doi.org/10.1023/A:1008014424247

Gerken, H.G., Donohoe, B., Knoshaug, E.P., 2013. Enzymatic cell wall degradation of Chlorella vulgaris and other microalgae for biofuels production. Planta 237, 239–253. https://doi.org/10.1007/s00425-012-1765-0

Gifuni, I., Olivieri, G., Pollio, A., Marzocchella, A., 2018. Identification of an industrial microalgal strain for starch production in biorefinery context: The effect of nitrogen and carbon concentration on starch accumulation. N. Biotechnol. 41, 46–54. https://doi.org/10.1016/j.nbt.2017.12.003

Gilbert, M., Domin, A., Becker, A., Wilhelm, C., 2000. Estimation of Primary Productivity by Chlorophyll a in vivo Fluorescence in Freshwater Phytoplankton. Photosynthetica 38, 111–126. https://doi.org/https://doi.org/10.1023/A:1026708327185

Gilbert, Matthias, Wilhelm, C., Richter, M., 2000. Bio-optical modelling of oxygen evolution using in vivo fluorescence: Comparison of measured and calculated photosynthesis/irradiance (P-I) curves in four representative phytoplankton species. J. Plant Physiol. 157, 307–314. https://doi.org/10.1016/S0176-1617(00)80052-8

Gimpel, J.A., Hyun, J.S., Schoepp, N.G., Mayfield, S.P., 2015. Production of recombinant proteins in microalgae at pilot greenhouse scale. Biotechnol. Bioeng. 112, 339–345. https://doi.org/10.1002/bit.25357

Giordano, M., Beardall, J., Raven, J.A., 2005. CO2 Concentrating Mechanisms in Algae: Mechanisms, Environmental Modulation and Evolution. Annu. Rev. Plant Biol. 56, 99–131. https://doi.org/10.1146/annurev.arplant.56.032604.144052

Glemser, M., Heining, M., Schmidt, J., Becker, A., Garbe, D., Buchholz, R., Brück, T., 2016. Application of light-emitting diodes (LEDs) in cultivation of phototrophic microalgae: current

state and perspectives. Appl. Microbiol. Biotechnol. 100, 1077–1088. https://doi.org/10.1007/s00253-015-7144-6

Goiris, K., Muylaert, K., Fraeye, I., Foubert, I., De Brabanter, J., De Cooman, L., 2012. Antioxidant potential of microalgae in relation to their phenolic and carotenoid content. J. Appl. Phycol. 24, 1477–1486. https://doi.org/10.1007/s10811-012-9804-6

Goodenough, U., Blaby, I., Casero, D., Gallaher, S.D., Goodson, C., Johnson, S., Lee, J.H., Merchant, S.S., Pellegrini, M., Roth, R., Rusch, J., Singh, M., Umen, J.G., Weiss, T.L., Wulan, T., 2014. The path to triacylglyceride obesity in the sta6 strain of Chlamydomonas reinhardtii. Eukaryot. Cell 13, 591–613. https://doi.org/10.1128/EC.00013-14

Gordon, M.M., Hu, C., Chokshi, H., Hewitt, J.E., Alpers, D.H., 1991. Glycosylation is not required for ligand or receptor binding by expressed rat intrinsic factor. Am. J. Physiol. Liver Physiol. 260, G736–G742. https://doi.org/10.1152/ajpgi.1991.260.5.G736

Gorman, D.S., Levine, R.P., 1965. Cytochrome f and plastocyanin: their sequence in the photosynthetic electron transport chain of Chlamydomonas reinhardii. Proc. Natl. Acad. Sci. 54, 1665–1669. https://doi.org/10.1073/pnas.54.6.1665

Green, R., Allen, L.H., Bjørke-Monsen, A.-L., Brito, A., Guéant, J.-L., Miller, J.W., Molloy, A.M., Nexo, E., Stabler, S., Toh, B.-H., Ueland, P.M., Yajnik, C., 2017. Vitamin B12 deficiency. Nat. Rev. Dis. Prim. 3, 17040. https://doi.org/10.1038/nrdp.2017.40

Greiner, A., Kelterborn, S., Evers, H., Kreimer, G., Sizova, I., Hegemann, P., 2017. Targeting of Photoreceptor Genes in Chlamydomonas reinhardtii via Zinc-Finger Nucleases and CRISPR/Cas9. Plant Cell 29, 2498–2518. https://doi.org/10.1105/tpc.17.00659

Gris, B., Morosinotto, T., Giacometti, G.M., Bertucco, A., Sforza, E., 2014. Cultivation of Scenedesmus obliquus in Photobioreactors: Effects of Light Intensities and Light–Dark Cycles on Growth, Productivity, and Biochemical Composition. Appl. Biochem. Biotechnol. 172, 2377–2389. https://doi.org/10.1007/s12010-013-0679-z

Grobbelaar, J.U., Nedbal, L., Tichý, V., 1996. Influence of high frequency light/dark fluctuations on photosynthetic characteristics of microalgae photoacclimated to different light intensities and implications for mass algal cultivation. J. Appl. Phycol. 8, 335–343. https://doi.org/10.1007/BF02178576

Guillard, R.R.L., 1975. Culture of Phytoplankton for Feeding Marine Invertebrates, in: Smith, W.L., Chanley, M.H. (Eds.), Culture of Marine Invertebrate Animals. Springer US, Boston, MA, pp. 29–60. https://doi.org/10.1007/978-1-4615-8714-9_3

Han, J., Zhang, L., Wang, S., Yang, G., Zhao, L., Pan, K., 2016. Co-culturing bacteria and microalgae in organic carbon containing medium. J. Biol. Res. 23, 8. https://doi.org/10.1186/s40709-016-0047-6

Harbi, K., Makridis, P., Koukoumis, C., Papadionysiou, M., Vgenis, T., Kornaros, M., Ntaikou, I., Giokas, S., Dailianis, S., 2017. Evaluation of a battery of marine species-based bioassays against raw and treated municipal wastewaters. J. Hazard. Mater. 321, 537–546. https://doi.org/10.1016/j.jhazmat.2016.09.036

Hardy, G., 2000. Nutraceuticals and functional foods: introduction and meaning. Nutrition 16, 688–689. https://doi.org/10.1016/S0899-9007(00)00332-4

Harris, E.H., 2001. Chlamhydomonas as model organism. Annu. Rev. Plant Physiol. Plant Mol. Biol. 52, 363–406. https://doi.org/10.1146/annurev.arplant.52.1.363

He, Q., Yang, H., Wu, L., Hu, C., 2015. Effect of light intensity on physiological changes, carbon allocation and neutral lipid accumulation in oleaginous microalgae. Bioresour. Technol. 191, 219–228. https://doi.org/10.1016/j.biortech.2015.05.021

Helliwell, K.E., Lawrence, A.D., Holzer, A., Kudahl, U.J., Sasso, S., Kräutler, B., Scanlan, D.J., Warren, M.J., Smith, A.G., 2016. Cyanobacteria and Eukaryotic Algae Use Different Chemical Variants of Vitamin B12. Curr. Biol. 26, 999–1008. https://doi.org/10.1016/j.cub.2016.02.041

Helliwell, K.E., Pandhal, J., Cooper, M.B., Longworth, J., Kudahl, U.J., Russo, D.A., Tomsett, E. V., Bunbury, F., Salmon, D.L., Smirnoff, N., Wright, P.C., Smith, A.G., 2018. Quantitative proteomics of a B 12 -dependent alga grown in coculture with bacteria reveals metabolic tradeoffs required for mutualism. New Phytol. 217, 599–612. https://doi.org/10.1111/nph.14832

Helliwell, K.E., Wheeler, G.L., Leptos, K.C., Goldstein, R.E., Smith, A.G., 2011. Insights into the Evolution of Vitamin B12 Auxotrophy from Sequenced Algal Genomes. Mol. Biol. Evol. 28, 2921–2933. https://doi.org/10.1093/molbev/msr124

Hempel, F., Lau, J., Klingl, A., Maier, U.G., 2011. Algae as Protein Factories: Expression of a Human Antibody and the Respective Antigen in the Diatom Phaeodactylum tricornutum. PLoS One 6, e28424. https://doi.org/10.1371/journal.pone.0028424

Hempel, F., Maier, U.G., 2012. An engineered diatom acting like a plasma cell secreting human IgG antibodies with high efficiency. Microb. Cell Fact. 11, 126. https://doi.org/10.1186/1475-2859-11-126

Henriques, M., Silva, A., Rocha, J., 2007. Extraction and quantification of pigments from a marine microalga : a simple and reproducible method. Commun. Curr. Res. Educ. Top. Trends Appl. Microbiol. 586–593.

Henríquez, V., Escobar, C., Galarza, J., Gimpel, J., 2016. Carotenoids in Microalgae, in: Sub-Cellular Biochemistry. Springer New York, pp. 219–237. https://doi.org/10.1007/978-3-319-39126-7_8

Hernández-García, A., Velásquez-Orta, S.B., Novelo, E., Yáñez-Noguez, I., Monje-Ramírez, I., Orta Ledesma, M.T., 2019. Wastewater-leachate treatment by microalgae: Biomass, carbohydrate and lipid production. Ecotoxicol. Environ. Saf. 174, 435–444. https://doi.org/10.1016/j.ecoenv.2019.02.052

Heukelekian, H., Rand, M.C., 1955. Biochemical Oxygen Demand of Pure Organic Compounds: A Report of the Research Committee.

Hill, R., Bendall, F., 1960. Function of the Two Cytochrome Components in Chloroplasts: A Working Hypothesis. Nature 186, 136–137. https://doi.org/10.1038/186136a0

Ho, S.-H., Ye, X., Hasunuma, T., Chang, J.-S., Kondo, A., 2014. Perspectives on engineering strategies for improving biofuel production from microalgae — A critical review. Biotechnol. Adv. 32, 1448–1459. https://doi.org/10.1016/j.biotechadv.2014.09.002

Hodgson, P.A., Henderson, R.J., Sargent, J.R., Leftley, J.W., Hodgson A., P., Henderson James, R., Sargent R., J., Leftley W., J., 1991. Patterns of variation in the lipid class and fatty acid composition of Nannochloropsis oculata (Eustigmatophyceae) during batch culture. J. Appl. Phycol. 3, 169–181.

Hu, Q., Guterman, H., Richmond, A., 1996. A flat inclined modular photobioreactor for outdoor mass cultivation of photoautotrophs. Biotechnol. Bioeng. New York 51, 51–60.

Hu, X., Meneses, Y.E., Stratton, J., Wang, B., 2019. Acclimation of consortium of micro-algae help removal of organic pollutants from meat processing wastewater. J. Clean. Prod. 214, 95–102. https://doi.org/10.1016/j.jclepro.2018.12.255

Hubble, D.S., Harper, D.M., 2001. Impact of light regimen and self-shading by algal cells on primary productivity in the water column of a shallow tropical lake (Lake Naivasha, Kenya). Lakes & Reservoirs: Research and. Management 6, 143–150. https://doi.org/10.1046/j.1440-1770.2001.00133.x

Hulatt, C.J., Wijffels, R.H., Bolla, S., Kiron, V., 2017. Production of Fatty Acids and Protein by Nannochloropsis in Flat-Plate Photobioreactors. PLoS One 12, e0170440. https://doi.org/10.1371/journal.pone.0170440

Ip, P.-F., Chen, F., 2005. Production of astaxanthin by the green microalga Chlorella zofingiensis in the dark. Process Biochem. 40, 733–738. https://doi.org/10.1016/j.procbio.2004.01.039

IPCC, 2019a. IPCC, 2019: Summary for Policymakers. In: IPCC Special Report on the Ocean and Cryosphere in a Changing Climate. https://doi.org/https://www.ipcc.ch/report/srocc/

IPCC, 2019b. IPCC Special Report on Climate Change, Desertification, Land Degradation, Sustainable Land Management, Food Security, and Greenhouse gas fluxes in Terrestrial Ecosystems. Edward Elgar Publishing.

IPCC, 20018: Global Warming of 1.5°C. An IPCC Special Report on the impacts of global warming of 1.5°C above pre-industrial levels and related global greenhouse gas emission pathways, in the context of strengthening the global response to the threat of cli.

Ipek, B., Uner, D., 2012. Artificial Photosynthesis from a Chemical Engineering Perspective, in: Artificial Photosynthesis. InTech. https://doi.org/10.5772/26909

Jahns, P., Latowski, D., Strzalka, K., 2009. Mechanism and regulation of the violaxanthin cycle: The role of antenna proteins and membrane lipids. Biochim. Biophys. Acta - Bioenerg. 1787, 3–14. https://doi.org/10.1016/j.bbabio.2008.09.013

James, W.O., 1934. The dynamics of photosynthesis. New Phytol. 33, 8–40. https://doi.org/10.1111/j.1469-8137.1934.tb06793.x

Jassby, A.D., Platt, T., 1976. Mathematical formulation of the relationship between photosynthesis and light for phytoplankton. Limnol. Oceanogr. 21, 540–547. https://doi.org/10.4319/lo.1976.21.4.0540

Jebali, A., Acién, F.G., Jiménez-Ruiz, N., Gómez, C., Fernández-Sevilla, J.M., Mhiri, N., Karray, F., Sayadi, S., Molina-Grima, E., 2019. Evaluation of native microalgae from Tunisia using the pulse-amplitude-modulation measurement of chlorophyll fluorescence and a

performance study in semi-continuous mode for biofuel production. Biotechnol. Biofuels 12, 119. https://doi.org/10.1186/s13068-019-1461-4

Jessen, D., Roth, C., Wiermer, M., Fulda, M., 2015. Two Activities of Long-Chain Acyl-Coenzyme A Synthetase Are Involved in Lipid Trafficking between the Endoplasmic Reticulum and the Plastid in Arabidopsis. Plant Physiol. 167, 351–366. https://doi.org/10.1104/pp.114.250365

Jiang, W., Brueggeman, A.J., Horken, K.M., Plucinak, T.M., Weeks, D.P., 2014. Successful Transient Expression of Cas9 and Single Guide RNA Genes in Chlamydomonas reinhardtii. Eukaryot. Cell 13, 1465–1469. https://doi.org/10.1128/EC.00213-14

Jin, E., Juergen, P.W., Kum, L.H., Min, H.S., Man, C., 2003. Xanthophylls in Microalgae: From Biosynthesis to Biotechnological Mass Production and Application 13, 165–174.

Jinkerson, R.E., Jonikas, M.C., 2015. Molecular techniques to interrogate and edit the Chlamydomonas nuclear genome. Plant J. 82, 393–412. https://doi.org/10.1111/tpj.12801

Jishi, T., Matsuda, R., Fujiwara, K., 2015. A kinetic model for estimating net photosynthetic rates of cos lettuce leaves under pulsed light. Photosynth. Res. 124, 107–116. https://doi.org/10.1007/s11120-015-0107-z

John, R.P., Anisha, G.S., Nampoothiri, K.M., Pandey, A., 2011. Micro and macroalgal biomass: A renewable source for bioethanol. Bioresour. Technol. 102, 186–193. https://doi.org/10.1016/j.biortech.2010.06.139

Johnston, M.L., Luethy, M.H., Miernyk, J.A., Randall, D.D., 1997. Cloning and molecular analyses of the Arabidopsis thaliana plastid pyruvate dehydrogenase subunits. Biochim. Biophys. Acta 1321, 200–6. https://doi.org/10.1016/s0005-2728(97)00059-5

Jyonouchi, H., Sun, S., Tomita, Y., Gross, M.D., 1995. Astaxanthin, a Carotenoid without Vitamin A Activity, Augments Antibody Responses in Cultures Including T-helper Cell Clones and Suboptimal Doses of Antigen. J. Nutr. 125, 2483–2492. https://doi.org/10.1093/jn/125.10.2483

Jyonouchi, H., Zhang, L., Tomita, Y., 1993. Studies of immunomodulating actions of carotenoids. II. astaxanthin enhances in vitro antibody production to T-dependent antigens without facilitating polyclonal B-cell activation. Nutr. Cancer 19, 269–280. https://doi.org/10.1080/01635589309514258

Kang, N.K., Choi, G.-G., Kim, E.K., Shin, S.-E., Jeon, S., Park, M.S., Jeong, K.J., Jeong, B., Chang, Y.K., Yang, J.-W., Lee, B., 2015. Heterologous overexpression of sfCherry fluorescent protein in Nannochloropsis salina. Biotechnol. Reports 8, 10–15. https://doi.org/10.1016/j.btre.2015.08.004

Katsuda, T., Shimahara, K., Shiraishi, H., Yamagami, K., Ranjbar, R., Katoh, S., 2006. Effect of flashing light from blue light emitting diodes on cell growth and astaxanthin production of Haematococcus pluvialis. J. Biosci. Bioeng. 102, 442–446. https://doi.org/10.1263/jbb.102.442

Katsuda, T., Shiraishi, H., Ishizu, N., Ranjbar, R., Katoh, S., 2008. Effect of light intensity and frequency of flashing light from blue light emitting diodes on astaxanthin production by

Haematococcus pluvialis. J. Biosci. Bioeng. 105, 216–220. https://doi.org/10.1263/jbb.105.216

Kazamia, E., Czesnick, H., Nguyen, T.T. Van, Croft, M.T., Sherwood, E., Sasso, S., Hodson, S.J., Warren, M.J., Smith, A.G., 2012. Mutualistic interactions between vitamin B12-dependent algae and heterotrophic bacteria exhibit regulation. Environ. Microbiol. 14, 1466–1476. https://doi.org/10.1111/j.1462-2920.2012.02733.x

Kazamia, E., Riseley, A.S., Howe, C.J., Smith, A.G., 2014. An Engineered Community Approach for Industrial Cultivation of Microalgae. Ind. Biotechnol. 10, 184–190. https://doi.org/10.1089/ind.2013.0041

Keşan, G., Litvín, R., Bína, D., Durchan, M., Šlouf, V., Polívka, T., 2016. Efficient light-harvesting using non-carbonyl carotenoids: Energy transfer dynamics in the VCP complex from Nannochloropsis oceanica. Biochim. Biophys. Acta - Bioenerg. 1857, 370–379. https://doi.org/10.1016/j.bbabio.2015.12.011

Ketheesan, B., Nirmalakhandan, N., 2012. Feasibility of microalgal cultivation in a pilot-scale airlift-driven raceway reactor. Bioresour. Technol. 108, 196–202. https://doi.org/10.1016/j.biortech.2011.12.146

Key, T., McCarthy, A., Campbell, D.A., Six, C., Roy, S., Finkel, Z. V., 2010. Cell size trade-offs govern light exploitation strategies in marine phytoplankton. Environ. Microbiol. 12, 95–104. https://doi.org/10.1111/j.1462-2920.2009.02046.x

Khatoon, H., Haris, H., Rahman, N.A., Zakaria, M.N., Begum, H., Mian, S., 2018. Growth, Proximate Composition and Pigment Production of Tetraselmis chuii Cultured with Aquaculture Wastewater. J. Ocean Univ. China 17, 641–646. https://doi.org/10.1007/s11802-018-3428-7

Khozin-Goldberg, I., Didi-Cohen, S., Shayakhmetova, I., Cohen, Z., 2002. Biosynthesis of eicosapentaenoic acid (epa) in the freshwater Eustigmatophyte Monodus subterraneus (Eustigmatophyceae). J. Phycol. 38, 745–756. https://doi.org/10.1046/j.1529-8817.2002.02006.x

Kilian, O., Benemann, C.S.E., Niyogi, K.K., Vick, B., 2011. High-efficiency homologous recombination in the oil-producing alga Nannochloropsis sp. Proc. Natl. Acad. Sci. 108, 21265–21269. https://doi.org/10.1073/pnas.1105861108

Kim, C.W., Moon, M., Park, W.-K., Yoo, G., Choi, Y.-E., Yang, J.-W., 2014. Energy-efficient cultivation of Chlamydomonas reinhardtii for lipid accumulation under flashing illumination conditions. Biotechnol. Bioprocess Eng. 19, 150–158. https://doi.org/10.1007/s12257-013-0468-0

Kim, D.G., Choi, Y.-E., 2014. Microalgae Cultivation Using LED Light. Korean Chem. Eng. Res. 52, 8–16. https://doi.org/10.9713/kcer.2014.52.1.8

Kim, D.G., Hur, S.B., 2013. Growth and fatty acid composition of three heterotrophic Chlorella species. Algae 28, 101–109. https://doi.org/10.4490/algae.2013.28.1.101

Kim, E., Archibald, J.M., 2009. Diversity and Evolution of Plastids and Their Genomes, in: Sandelius, A.S., Aronsson, H. (Eds.), The Chloroplast: Interactions with the Environment.

Springer Berlin Heidelberg, Berlin, Heidelberg, pp. 1–39. https://doi.org/10.1007/978-3-540-68696-5_1

Kim, G., Mujtaba, G., Lee, K., 2016. Effects of nitrogen sources on cell growth and biochemical composition of marine chlorophyte Tetraselmis sp. for lipid production. ALGAE 31, 257–266. https://doi.org/10.4490/algae.2016.31.8.18

Kim, Z.-H., Kim, S.-H., Lee, H.-S., Lee, C.-G., 2006. Enhanced production of astaxanthin by flashing light using Haematococcus pluvialis. Enzyme Microb. Technol. 39, 414–419. https://doi.org/10.1016/j.enzmictec.2005.11.041

Kindle, K.L., 1990. High-frequency nuclear transformation of Chlamydomonas reinhardtii. Proc. Natl. Acad. Sci. 87, 1228–1232. https://doi.org/10.1073/pnas.87.3.1228

Komolafe, O., Velasquez Orta, S.B., Monje-Ramirez, I., Noguez, I.Y., Harvey, A.P., Orta Ledesma, M.T., 2014. Biodiesel production from indigenous microalgae grown in wastewater. Bioresour. Technol. 154, 297–304. https://doi.org/10.1016/j.biortech.2013.12.048

Koyande, A.K., Chew, K.W., Rambabu, K., Tao, Y., Chu, D.-T., Show, P.-L., 2019. Microalgae: A potential alternative to health supplementation for humans. Food Sci. Hum. Wellness 8, 16–24. https://doi.org/10.1016/j.fshw.2019.03.001

Kropat, J., Hong-Hermesdorf, A., Casero, D., Ent, P., Castruita, M., Pellegrini, M., Merchant, S.S., Malasarn, D., 2011. A revised mineral nutrient supplement increases biomass and growth rate in Chlamydomonas reinhardtii. Plant J. 66, 770–780. https://doi.org/10.1111/j.1365-313X.2011.04537.x

Kumar, K., Mishra, S.K., Shrivastav, A., Park, M.S., Yang, J.-W., 2015. Recent trends in the mass cultivation of algae in raceway ponds. Renew. Sustain. Energy Rev. 51, 875–885. https://doi.org/10.1016/j.rser.2015.06.033

Kumar, S.V., Misquitta, R.W., Reddy, V.S., Rao, B.J., Rajam, M.V., 2004. Genetic transformation of the green alga—Chlamydomonas reinhardtii by Agrobacterium tumefaciens. Plant Sci. 166, 731–738. https://doi.org/10.1016/j.plantsci.2003.11.012

Kurashige, M., Okimasu, E., Inoue, M., Utsumi, K., 1990. Inhibition of oxidative injury of biological membranes by astaxanthin. Physiol Chem Phys Med NMR. 22, 27–38.

La Rocca, N., Andreoli, C., Giacometti, G.M., Rascio, N., Moro, I., 2009. Responses of the Antarctic microalga Koliella antarctica (Trebouxiophyceae, Chlorophyta) to cadmium contamination. Photosynthetica 47, 471–479. https://doi.org/10.1007/s11099-009-0071-y

Lamers, P.P., Janssen, M., De Vos, R.C.H., Bino, R.J., Wijffels, R.H., 2012. Carotenoid and fatty acid metabolism in nitrogen-starved Dunaliella salina, a unicellular green microalga. J. Biotechnol. 162, 21–27. https://doi.org/10.1016/j.jbiotec.2012.04.018

Lang, I., Hodac, L., Friedl, T., Feussner, I., 2011. Fatty acid profiles and their distribution patterns in microalgae: a comprehensive analysis of more than 2000 strains from the SAG culture collection. BMC Plant Biol. 11, 124. https://doi.org/10.1186/1471-2229-11-124

Latowski, D., Kuczyńska, P., Strzałka, K., 2011. Xanthophyll cycle – a mechanism protecting plants against oxidative stress. Redox Rep. 16, 78–90. https://doi.org/10.1179/174329211X13020951739938

Lau, P.S., Tam, N.F.Y., Wong, Y.S., 1996. Wastewater Nutrients Removal by Chlorella vulgaris: Optimization Through Acclimation. Environ. Technol. 17, 183–189. https://doi.org/10.1080/09593331708616375

Lauersen, K.J., Berger, H., Mussgnug, J.H., Kruse, O., 2013a. Efficient recombinant protein production and secretion from nuclear transgenes in Chlamydomonas reinhardtii. J. Biotechnol. 167, 101–110. https://doi.org/10.1016/j.jbiotec.2012.10.010

Lauersen, K.J., Vanderveer, T.L., Berger, H., Kaluza, I., Mussgnug, J.H., Walker, V.K., Kruse, O., 2013b. Ice recrystallization inhibition mediated by a nuclear-expressed and -secreted recombinant ice-binding protein in the microalga Chlamydomonas reinhardtii. Appl. Microbiol. Biotechnol. 97, 9763–9772. https://doi.org/10.1007/s00253-013-5226-x

Lautenschläger, H., 2003. Essential fatty acids - cosmetic from inside and outside, in: Beauty Forum. pp. 54–56.

Lee, C.-G., 1999. Calculation of light penetration depth in photobioreactors. Biotechnol. Bioprocess Eng. 4, 78–81. https://doi.org/10.1007/BF02931920

Lee, R.E., 2008. Basic characteristics of the algae, in: Phycology. Cambridge University Press, Cambridge, pp. 3–30. https://doi.org/10.1017/CBO9780511812897.002

Lee, Y.-K., Chen, W., Shen, H., Han, D., Li, Y., Jones, H.D.T., Timlin, J.A., Hu, Q., 2013. Basic Culturing and Analytical Measurement Techniques, in: Handbook of Microalgal Culture. John Wiley & Sons, Ltd, Oxford, UK, pp. 37–68. https://doi.org/10.1002/9781118567166.ch3

Lewicka, K., Siemion, P., Kurcok, P., 2015. Chemical Modifications of Starch: Microwave Effect. Int. J. Polym. Sci. 2015, 1–10. https://doi.org/10.1155/2015/867697

Li-Beisson, Y., Shorrosh, B., Beisson, F., Andersson, M.X., Arondel, V., Bates, P.D., Baud, S., Bird, D., DeBono, A., Durrett, T.P., Franke, R.B., Graham, I.A., Katayama, K., Kelly, A.A., Larson, T., Markham, J.E., Miquel, M., Molina, I., Nishida, I., Rowland, O., Samuels, L., Schmid, K.M., Wada, H., Welti, R., Xu, C., Zallot, R., Ohlrogge, J., 2013. Acyl-Lipid Metabolism, in: The Arabidopsis Book. BioOne, p. e0161. https://doi.org/10.1199/tab.0161

Li-Beisson, Y., Thelen, J.J., Fedosejevs, E., Harwood, J.L., 2019. The lipid biochemistry of eukaryotic algae. Prog. Lipid Res. 74, 31–68. https://doi.org/10.1016/j.plipres.2019.01.003

Li, D.-W., Balamurugan, S., Zheng, J.-W., Yang, W.-D., Liu, J.-S., Li, H.-Y., 2020. Rapid and Effective Electroporation Protocol for Nannochloropsis oceanica, in: Methods in Molecular Biology (Clifton, N.J.). pp. 175–179. https://doi.org/10.1007/978-1-4939-9740-4_19

Li, J., Han, D., Wang, D., Ning, K., Jia, J., Wei, L., Jing, X., Huang, S., Chen, J., Li, Y., Hu, Q., Xu, J., 2014. Choreography of Transcriptomes and Lipidomes of Nannochloropsis Reveals the Mechanisms of Oil Synthesis in Microalgae. Plant Cell 26, 1645–1665. https://doi.org/10.1105/tpc.113.121418

Li, Z., Wakao, S., Fischer, B.B., Niyogi, K.K., 2009. Sensing and Responding to Excess Light. Annu. Rev. Plant Biol. 60, 239–260. https://doi.org/10.1146/annurev.arplant.58.032806.103844

Liang, J., Wen, F., Liu, J., 2019. Transcriptomic and lipidomic analysis of an EPA-containing Nannochloropsis sp. PJ12 in response to nitrogen deprivation. Sci. Rep. 9, 4540. https://doi.org/10.1038/s41598-019-41169-2

Lichtenthaler, H., 2004. Evolution of carotenoid and isoprenoid biosynthesis in photosynthetic and non photosynthetic organisms, in: 16th International Plant Lipid Symposium, Budapest, Hungary.

Lichtenthaler, H.K., Wellburn, A.R., 1983. Determinations of total carotenoids and chlorophylls a and b of leaf extracts in different solvents. Biochem. Soc. Trans. 11, 591–592. https://doi.org/10.1042/bst0110591

Lima, S., Grisafi, F., Scargiali, F., Caputo, G., Brucato, A., 2018. Growing Microalgae in a "Quasi-isoactinic" Photobioreactor, in: Chemical Engineering Transactions. pp. 673–678. https://doi.org/10.3303/CET1864113

Lin, S., 2005. Algal culturing techniques, Journal of Phycology. https://doi.org/10.1111/j.1529-8817.2005.00114.x

Litvín, R., Bína, D., Herbstová, M., Gardian, Z., 2016. Architecture of the light-harvesting apparatus of the eustigmatophyte alga Nannochloropsis oceanica. Photosynth. Res. 130, 137–150. https://doi.org/10.1007/s11120-016-0234-1

Lizzul, A., Lekuona-Amundarain, A., Purton, S., Campos, L., 2018. Characterization of Chlorella sorokiniana, UTEX 1230. Biology (Basel). 7, 25. https://doi.org/10.3390/biology7020025

López-Rosales, L., Sánchez-Mirón, A., Contreras-Gómez, A., García-Camacho, F., Battaglia, F., Zhao, L., Molina-Grima, E., 2019. Characterization of bubble column photobioreactors for shear-sensitive microalgae culture. Bioresour. Technol. 275, 1–9. https://doi.org/10.1016/j.biortech.2018.12.009

Lourenço, S.O., Barbarino, E., Lavín, P.L., Lanfer Marquez, U.M., Aidar, E., 2004. Distribution of intracellular nitrogen in marine microalgae: Calculation of new nitrogen-to-protein conversion factors. Eur. J. Phycol. 39, 17–32. https://doi.org/10.1080/0967026032000157156

Lumbreras, V., Stevens, D.R., Purton, S., 1998. Efficient foreign gene expression in Chlamydomonas reinhardtii mediated by an endogenous intron. Plant J. 14, 441–447. https://doi.org/10.1046/j.1365-313X.1998.00145.x

Lunka, A.A., Bayless, D.J., 2013. Effects of flashing light-emitting diodes on algal biomass productivity. J. Appl. Phycol. 25, 1679–1685. https://doi.org/10.1007/s10811-013-0044-1

Lv, X., Zou, L., Sun, B., Wang, J., Sun, M.-Y., 2010. Variations in lipid yields and compositions of marine microalgae during cell growth and respiration, and within intracellular structures. J. Exp. Mar. Bio. Ecol. 391, 73–83. https://doi.org/10.1016/j.jembe.2010.06.010

Lyon, B.R., Mock, T., 2014. Polar microalgae: new approaches towards understanding adaptations to an extreme and changing environment. Biology (Basel). 3, 56–80. https://doi.org/10.3390/biology3010056

Lyons, N.M., O'Brien, N.M., 2002. Modulatory effects of an algal extract containing astaxanthin on UVA-irradiated cells in culture. J. Dermatol. Sci. 30, 73–84.

Ma, R., Zhao, X., Xie, Y., Ho, S.-H., Chen, J., 2019. Enhancing lutein productivity of Chlamydomonas sp. via high-intensity light exposure with corresponding carotenogenic genes expression profiles. Bioresour. Technol. 275, 416–420. https://doi.org/10.1016/j.biortech.2018.12.109

Ma, X.-N., Chen, T.-P., Yang, B., Liu, J., Chen, F., 2016. Lipid Production from Nannochloropsis. Mar. Drugs 14, 61. https://doi.org/10.3390/md14040061

Ma, X., Yu, J., Zhu, B., Pan, K., Pan, J., Yang, G., 2011. Cloning and characterization of a delta-6 desaturase encoding gene from Nannochloropsis oculata. Chinese J. Oceanol. Limnol. 29, 290–296. https://doi.org/10.1007/s00343-011-0048-0

Ma, Y., Wang, Z., Yu, C., Yin, Y., Zhou, G., 2014. Evaluation of the potential of 9 Nannochloropsis strains for biodiesel production. Bioresour. Technol. 167, 503–509. https://doi.org/10.1016/j.biortech.2014.06.047

Maffei, G., Bracciale, M.P., Broggi, A., Zuorro, A., Santarelli, M.L., Lavecchia, R., 2018. Effect of an enzymatic treatment with cellulase and mannanase on the structural properties of Nannochloropsis microalgae. Bioresour. Technol. 249, 592–598. https://doi.org/10.1016/j.biortech.2017.10.062

Marotta, G., Pruvost, J., Scargiali, F., Caputo, G., Brucato, A., 2017. Reflection-refraction effects on light distribution inside tubular photobioreactors. Can. J. Chem. Eng. 95, 1646–1651. https://doi.org/10.1002/cjce.22811

Marshall, O.J., 2004. PerlPrimer: cross-platform, graphical primer design for standard, bisulphite and real-time PCR. Bioinformatics 20, 2471–2472. https://doi.org/10.1093/bioinformatics/bth254

Mata, T.M., Martins, A.A., Caetano, N.S., 2010. Microalgae for biodiesel production and other applications: A review. Renew. Sustain. Energy Rev. 14, 217–232. https://doi.org/10.1016/j.rser.2009.07.020

Mathews, F.S., Gordon, M.M., Chen, Z., Rajashankar, K.R., Ealick, S.E., Alpers, D.H., Sukumar, N., 2007. Crystal structure of human intrinsic factor: cobalamin complex at 2.6-A resolution. Proc. Natl. Acad. Sci. U. S. A. 104, 17311–6. https://doi.org/10.1073/pnas.0703228104

Mathieu-Rivet, E., Kiefer-Meyer, M.-C., Vanier, G., Ovide, C., Burel, C., Lerouge, P., Bardor, M., 2014. Protein N-glycosylation in eukaryotic microalgae and its impact on the production of nuclear expressed biopharmaceuticals. Front. Plant Sci. 5, 359. https://doi.org/10.3389/fpls.2014.00359

Mathieu-Rivet, E., Scholz, M., Arias, C., Dardelle, F., Schulze, S., Le Mauff, F., Teo, G., Hochmal, A.K., Blanco-Rivero, A., Loutelier-Bourhis, C., Kiefer-Meyer, M.-C., Fufezan, C., Burel, C., Lerouge, P., Martinez, F., Bardor, M., Hippler, M., 2013. Exploring the N -glycosylation Pathway in Chlamydomonas reinhardtii Unravels Novel Complex Structures. Mol. Cell. Proteomics 12, 3160–3183. https://doi.org/10.1074/mcp.M113.028191

Matos, Â.P., Feller, R., Moecke, E.H.S., de Oliveira, J.V., Junior, A.F., Derner, R.B., Sant'Anna, E.S., 2016. Chemical Characterization of Six Microalgae with Potential Utility for Food Application. JAOCS, J. Am. Oil Chem. Soc. 93, 963–972. https://doi.org/10.1007/s11746-016-2849-y

Matthijs, H.C.P., Balke, H., Van Hes, U.M., Kroon, B.M.A., Mur, L.R., Binot, R.A., 1996. Application of light-emitting diodes in bioreactors: Flashing light effects and energy economy in algal culture (Chlorella pyrenoidosa). Biotechnol. Bioeng. 50, 98–107. https://doi.org/10.1002/(SICI)1097-0290(19960405)50:1<98::AID-BIT11>3.0.CO;2-3

Maul, J.E., Lilly, J.W., Cui, L., dePamphilis, C.W., Miller, W., Harris, E.H., Stern, D.B., 2002. The Chlamydomonas reinhardtii Plastid Chromosome. Plant Cell 14, 2659–2679. https://doi.org/10.1105/tpc.006155

Mayers, J.J., Flynn, K.J., Shields, R.J., 2013. Rapid determination of bulk microalgal biochemical composition by Fourier-Transform Infrared spectroscopy. Bioresour. Technol. 148, 215–220. https://doi.org/10.1016/j.biortech.2013.08.133

Mayfield, S.P., Franklin, S.E., 2005. Expression of human antibodies in eukaryotic micro-algae. Vaccine 23, 1828–1832. https://doi.org/10.1016/j.vaccine.2004.11.013

Mayfield, S.P., Manuell, A.L., Chen, S., Wu, J., Tran, M., Siefker, D., Muto, M., Marin-Navarro, J., 2007. Chlamydomonas reinhardtii chloroplasts as protein factories. Curr. Opin. Biotechnol. 18, 126–133. https://doi.org/10.1016/j.copbio.2007.02.001

McBride, H.M., Neuspiel, M., Wasiak, S., 2006. Mitochondria: More Than Just a Powerhouse. Curr. Biol. 16, R551–R560. https://doi.org/10.1016/j.cub.2006.06.054

Meijer, A.H., Van Dijk, E.L., Hoge, J.H.C., 1996. Novel members of a family of AT hook-containing DNA-binding proteins from rice are identified through their in vitro interaction with consensus target sites of plant and animal homeodomain proteins. Plant Mol. Biol. 31, 607–618. https://doi.org/10.1007/BF00042233

Mendoza, J.L., Granados, M.R., de Godos, I., Acién, F.G., Molina, E., Heaven, S., Banks, C.J., 2013. Oxygen transfer and evolution in microalgal culture in open raceways. Bioresour. Technol. 137, 188–195. https://doi.org/10.1016/j.biortech.2013.03.127

Meng, Y., Jiang, J., Wang, H., Cao, X., Xue, S., Yang, Q., Wang, W., 2015. The characteristics of TAG and EPA accumulation in Nannochloropsis oceanica IMET1 under different nitrogen supply regimes. Bioresour. Technol. 179, 483–489. https://doi.org/10.1016/j.biortech.2014.12.012

Merchant, S.S., Prochnik, S.E., Vallon, O., Harris, E.H., Karpowicz, S.J., Witman, G.B., Terry, A., Salamov, A., Fritz-Laylin, L.K., Marechal-Drouard, L., Marshall, W.F., Qu, L.-H., Nelson, D.R., Sanderfoot, A.A., Spalding, M.H., Kapitonov, V. V., Ren, Q., Ferris, P., Lindquist, E., Shapiro, H., Lucas, S.M., Grimwood, J., Schmutz, J., Cardol, P., Cerutti, H., Chanfreau, G., Chen, C.-L., Cognat, V., Croft, M.T., Dent, R., Dutcher, S., Fernandez, E., Fukuzawa, H., Gonzalez-Ballester, D., Gonzalez-Halphen, D., Hallmann, A., Hanikenne, M., Hippler, M., Inwood, W., Jabbari, K., Kalanon, M., Kuras, R., Lefebvre, P.A., Lemaire, S.D., Lobanov, A. V., Lohr, M., Manuell, A., Meier, I., Mets, L., Mittag, M., Mittelmeier, T., Moroney, J. V., Moseley, J., Napoli, C., Nedelcu, A.M., Niyogi, K., Novoselov, S. V., Paulsen, I.T., Pazour, G., Purton, S., Ral, J.-P., Riano-Pachon, D.M., Riekhof, W., Rymarquis, L., Schroda, M., Stern, D., Umen, J., Willows, R., Wilson, N., Zimmer, S.L., Allmer, J., Balk, J., Bisova, K., Chen, C.-J., Elias, M., Gendler, K., Hauser, C., Lamb, M.R., Ledford, H., Long, J.C., Minagawa, J., Page, M.D., Pan, J., Pootakham, W., Roje, S., Rose, A., Stahlberg, E., Terauchi, A.M., Yang, P., Ball, S., Bowler, C., Dieckmann, C.L., Gladyshev, V.N., Green, P., Jorgensen, R., Mayfield, S., Mueller-Roeber, B., Rajamani, S., Sayre, R.T., Brokstein, P.,

Dubchak, I., Goodstein, D., Hornick, L., Huang, Y.W., Jhaveri, J., Luo, Y., Martinez, D., Ngau, W.C.A., Otillar, B., Poliakov, A., Porter, A., Szajkowski, L., Werner, G., Zhou, K., Grigoriev, I. V., Rokhsar, D.S., Grossman, A.R., 2007. The Chlamydomonas Genome Reveals the Evolution of Key Animal and Plant Functions. Science (80-.). 318, 245–250. https://doi.org/10.1126/science.1143609

Merchuk, J., Gluz, M., Mukmenev, I., 2000. Comparison of photobioreactors for cultivation of the red microalga Porphyridium sp. J. Chem. Technol. Biotechnol. 75, 1119–1126. https://doi.org/10.1002/1097-4660(200012)75:12<1119::AID-JCTB329>3.0.CO;2-G

Merchuk, J.C., Asenjo, J.A., 1994. Communication to the Editor The Monod Equation and Mass Transfer. Biotechnol. Bioeng. 45, 91–94.

Messina, C., Renda, G., Laudicella, V., Trepos, R., Fauchon, M., Hellio, C., Santulli, A., 2019. From Ecology to Biotechnology, Study of the Defense Strategies of Algae and Halophytes (from Trapani Saltworks, NW Sicily) with a Focus on Antioxidants and Antimicrobial Properties. Int. J. Mol. Sci. 20, 881. https://doi.org/10.3390/ijms20040881

Metcalf, Eddy, 2003. Wastewater Engineering Treatment and Reuse, 4th ed. New York.

Metsoviti, M.N., Katsoulas, N., Karapanagiotidis, I.T., Papapolymerou, G., 2019. Effect of nitrogen concentration, two-stage and prolonged cultivation on growth rate, lipid and protein content of Chlorella vulgaris. J. Chem. Technol. Biotechnol. 94, 1466–1473. https://doi.org/10.1002/jctb.5899

Michels, M.H.A., Camacho-Rodríguez, J., Vermuë, M.H., Wijffels, R.H., 2014. Effect of cooling in the night on the productivity and biochemical composition of Tetraselmis suecica. Algal Res. 6, 145–151. https://doi.org/10.1016/j.algal.2014.11.002

Mitra, M., Shah, F., Bharadwaj, S.V.V., Patidar, S.K., Mishra, S., 2016. Cultivation of Nannochloropsis oceanica biomass rich in eicosapentaenoic acid utilizing wastewater as nutrient resource. Bioresour. Technol. 218, 1178–1186. https://doi.org/10.1016/j.biortech.2016.07.083

Moazami, N., Ashori, A., Ranjbar, R., Tangestani, M., Eghtesadi, R., Nejad, A.S., 2012. Large-scale biodiesel production using microalgae biomass of Nannochloropsis. Biomass and Bioenergy 39, 449–453. https://doi.org/10.1016/j.biombioe.2012.01.046

Mohammadi, M., Kazeroni, N., Baboli, M.J., 2015. Fatty acid composition of the marine micro alga Tetraselmis chuii Butcher in response to culture conditions. J. Algal Biomass Util. 6, 49–55.

Molazadeh, M., Ahmadzadeh, H., Pourianfar, H.R., Lyon, S., Rampelotto, P.H., 2019. The Use of Microalgae for Coupling Wastewater Treatment With CO2 Biofixation. Front. Bioeng. Biotechnol. 7. https://doi.org/10.3389/fbioe.2019.00042

Molina, E., Contreras, A., Chisti, Y., 1999. Gas Holdup, Liquid Circulation and Mixing Behaviour of Viscous Newtonian Media in a Split-Cylinder Airlift Bioreactor. Food Bioprod. Process. 77, 27–32. https://doi.org/10.1205/096030899532222

Molina, E., Fernández, J., Acién, F.G., Chisti, Y., 2001. Tubular photobioreactor design for algal cultures. J. Biotechnol. 92, 113–131. https://doi.org/10.1016/S0168-1656(01)00353-4

Monod, J., 1949. The Growth of Bacterial Cultures. Annu. Rev. Microbiol. 3, 371–394. https://doi.org/10.1146/annurev.mi.03.100149.002103

Moody, J.W., McGinty, C.M., Quinn, J.C., 2014. Global evaluation of biofuel potential from microalgae. Proc. Natl. Acad. Sci. 111, 8691–8696. https://doi.org/10.1073/pnas.1321652111

Morowvat, M.H., Ghasemi, Y., 2016. Developing a robust method for quantification of β-carotene in Dunaliella salina biomass using HPLC method. Int. J. Pharm. Clin. Res.

Mouget, J.-L., Legendre, L., de la Noüe, J., 1995. Long-term acclimatization of Scenedesmus bicellularis to high-frequency intermittent lighting (100 Hz). II. Photosynthetic pigments, carboxylating enzymes and biochemical composition. J. Plankton Res. 17, 875–890. https://doi.org/10.1093/plankt/17.4.875

Mühlroth, A., Li, K., Røkke, G., Winge, P., Olsen, Y., Hohmann-Marriott, M., Vadstein, O., Bones, A., 2013. Pathways of Lipid Metabolism in Marine Algae, Co-Expression Network, Bottlenecks and Candidate Genes for Enhanced Production of EPA and DHA in Species of Chromista. Mar. Drugs 11, 4662–4697. https://doi.org/10.3390/md11114662

Mulders, K.J.M., Lamers, P.P., Martens, D.E., Wijffels, R.H., 2014. Phototrophic pigment production with microalgae: biological constraints and opportunities. J. Phycol. 50, 229–242. https://doi.org/10.1111/jpy.12173

Murdock, J.N., Wetzel, D.L., 2009. FT-IR Microspectroscopy Enhances Biological and Ecological Analysis of Algae. Appl. Spectrosc. Rev. 44, 335–361. https://doi.org/10.1080/05704920902907440

Murphy, D., 2001. The biogenesis and functions of lipid bodies in animals, plants and microorganisms. Prog. Lipid Res. 40, 325–438. https://doi.org/10.1016/S0163-7827(01)00013-3

Mussgnug, J.H., 2015. Genetic tools and techniques for Chlamydomonas reinhardtii. Appl. Microbiol. Biotechnol. 99, 5407–5418. https://doi.org/10.1007/s00253-015-6698-7

Naguib, Y.M., 2000. Antioxidant activities of astaxanthin and related carotenoids. J. Agric. Food Chem. 48, 1150–4.

Nasri, H., Baradaran, A., Shirzad, H., Rafieian-Kopaei, M., 2014. New concepts in nutraceuticals as alternative for pharmaceuticals. Int. J. Prev. Med. 5, 1487–99.

Nedbal, L., Tichý, V., Xiong, F., Grobbelaar, J.U., 1996. Microscopic green algae and cyanobacteria in high-frequency intermittent light. J. Appl. Phycol. 8, 325–333. https://doi.org/10.1007/BF02178575

Nelson, N., 2009. Plant Photosystem I – The Most Efficient Nano-Photochemical Machine. J. Nanosci. Nanotechnol. 9, 1709–1713. https://doi.org/10.1166/jnn.2009.SI01

Neupert, J., Karcher, D., Bock, R., 2009. Generation of Chlamydomonas strains that efficiently express nuclear transgenes. Plant J. 57, 1140–1150. https://doi.org/10.1111/j.1365-313X.2008.03746.x

Ng, I.-S., Tan, S.-I., Kao, P.-H., Chang, Y.-K., Chang, J.-S., 2017. Recent Developments on Genetic Engineering of Microalgae for Biofuels and Bio-Based Chemicals. Biotechnol. J. 12, 1600644. https://doi.org/10.1002/biot.201600644

Nielsen, A.Z., Mellor, S.B., Vavitsas, K., Wlodarczyk, A.J., Gnanasekaran, T., Perestrello Ramos H de Jesus, M., King, B.C., Bakowski, K., Jensen, P.E., 2016. Extending the biosynthetic repertoires of cyanobacteria and chloroplasts. Plant J. 87, 87–102. https://doi.org/10.1111/tpj.13173

Nielsen, M.J., Rasmussen, M.R., Andersen, C.B.F., Nexø, E., Moestrup, S.K., 2012. Vitamin B12 transport from food to the body's cells—a sophisticated, multistep pathway. Nat. Rev. Gastroenterol. Hepatol. 9, 345–354. https://doi.org/10.1038/nrgastro.2012.76

Nishino, H., Murakoshi, M., Tokuda, H., Satomi, Y., 2009. Cancer prevention by carotenoids. Arch. Biochem. Biophys. 483, 165–168. https://doi.org/10.1016/j.abb.2008.09.011

Niu, J., Zhu, B., Cai, J., Li, P., Wang, L., Dai, H., Qiu, L., Yu, H., Ha, D., Zhao, H., Zhang, Z., Lin, S., 2014. Selection of Reference Genes for Gene Expression Studies in Siberian Apricot (Prunus sibirica L.) Germplasm Using Quantitative Real-Time PCR. PLoS One 9, e103900. https://doi.org/10.1371/journal.pone.0103900

Nutraceuticals Market Size, Share & Trends | Industry Analysis, 2022 [WWW Document], n.d. URL https://www.alliedmarketresearch.com/nutraceuticals-market (accessed 9.12.19).

Nwoba, E.G., Parlevliet, D.A., Laird, D.W., Alameh, K., Moheimani, N.R., 2019. Light management technologies for increasing algal photobioreactor efficiency. Algal Res. 39, 101433. https://doi.org/10.1016/j.algal.2019.101433

O'Neill, E.C., Kelly, S., 2017. Engineering biosynthesis of high-value compounds in photosynthetic organisms. Crit. Rev. Biotechnol. 37, 779–802. https://doi.org/10.1080/07388551.2016.1237467

Ojha, A., 2016. Advancing microalgae culturing via bubble dynamics, mass transfer, and dynamic growth investigations. Dr. Diss.

Ojha, A., Al-Dahhan, M., 2018. Local gas holdup and bubble dynamics investigation during microalgae culturing in a split airlift photobioreactor. Chem. Eng. Sci. 175, 185–198. https://doi.org/10.1016/j.ces.2017.08.026

Ono, E., Cuello, J.L., 2006. Feasibility assessment of microalgal carbon dioxide sequestration technology with photobioreactor and solar collector. Biosyst. Eng. 95, 597–606. https://doi.org/10.1016/j.biosystemseng.2006.08.005

Oswald, W.J., Asce, A.M., Gotaas, H.B., Asce, M., 1985. Photosynthesis in sewage treatment. Am. Soc. Civ. Eng.

Oukarroum, A., 2016. Change in photosystem II photochemistry during algal growth phases of Chlorella vulgaris and Scenedesmus obliquus. Curr. Microbiol. 72, 692–699. https://doi.org/10.1007/s00284-016-1004-1

Packer, A., Li, Y., Andersen, T., Hu, Q., Kuang, Y., Sommerfeld, M., 2011. Growth and neutral lipid synthesis in green microalgae: A mathematical model. Bioresour. Technol. 102, 111–117. https://doi.org/10.1016/j.biortech.2010.06.029

Palozza, P., Krinsky, N.I., 1992. Astaxanthin and canthaxanthin are potent antioxidants in a membrane model. Arch. Biochem. Biophys. 297, 291–295. https://doi.org/10.1016/0003-9861(92)90675-M

Paniaqua-Michel, J., Olmos-soto, J., Ruiz, M.A., 2012. Microbial carotenoids from bacteria and microalgae, Methods in Molecular Biology. Humana Press, Totowa, NJ. https://doi.org/10.1007/978-1-61779-879-5

Park, K.-H., Lee, C.-G., 2000. Optimization of algal photobioreactors using flashing lights. Biotechnol. Bioprocess Eng. 5, 186–190. https://doi.org/10.1007/BF02936592

Parker, M.S., Mock, T., Armbrust, E.V., 2008. Genomic insights into marine microalgae. Annu. Rev. Genet. 42, 619–645. https://doi.org/10.1146/annurev.genet.42.110807.091417

Pashkow, F.J., Watumull, D.G., Campbell, C.L., 2008. Astaxanthin: a novel potential treatment for oxidative stress and inflammation in cardiovascular disease. Am. J. Cardiol. 101, S58–S68. https://doi.org/10.1016/j.amjcard.2008.02.010

Paul, U.C., Manian, A.P., Široká, B., Bechtold, T., 2014. Quantification of polysaccharide contents with the chemical oxygen demand index (COD), Cellulose Chemistry and Technology.

Pawlak, R., Parrott, S.J., Raj, S., Cullum-Dugan, D., Lucus, D., 2013. How prevalent is vitamin B 12 deficiency among vegetarians? Nutr. Rev. 71, 110–117. https://doi.org/10.1111/nure.12001

Pearson, H.W., Mara, D.D., Bartone, C.R., 1987. Guidelines for the minimum evaluation of the performance of full-scale waste stabilization pond systems. Water Res. 21, 1067–1075. https://doi.org/10.1016/0043-1354(87)90028-5

Pereira, H., Barreira, L., Mozes, A., Florindo, C., Polo, C., Duarte, C. V., Custódio, L., Varela, J., 2011. Microplate-based high throughput screening procedure for the isolation of lipid-rich marine microalgae. Biotechnol. Biofuels 4, 61. https://doi.org/10.1186/1754-6834-4-61

Pereira, H., Custódio, L., Rodrigues, M., de Sousa, C., Oliveira, M., Barreira, L., Neng, N., Nogueira, J., Alrokayan, S., Mouffouk, F., Abu-Salah, K., Ben-Hamadou, R., Varela, J., 2015. Biological activities and chemical composition of methanolic extracts of selected autochthonous microalgae strains from the Red Sea. Mar. Drugs 13, 3531–3549. https://doi.org/10.3390/md13063531

Phillips, J.N., Myers, J., 1954. Growth Rate of Chlorella in Flashing Light. Plant Physiol. 29, 152–161. https://doi.org/10.1104/pp.29.2.152

Pierucci, S., Klemeš, J.J., Piazza, L., Bakalis, S., Visca, A., Di Caprio, F., Spinelli, R., Altimari, P., Cicci, A., Iaquaniello, G., Toro, L., Pagnanelli, F., 2017. Microalgae cultivation for lipids and carbohydrates production. Chem. Eng. Trans. 57, 127–132. https://doi.org/https://doi.org/10.3303/CET1757022

Pirt, S.J., Lee, Y.-K., Richmond, A., Pirt, M.W., 1980. The photosynthetic efficiency of Chlorella biomass growth with reference to solar energy utilisation. J. Chem. Technol. Biotechnol. 30, 25–34. https://doi.org/10.1002/jctb.503300105

Plaza, M., Cifuntes, A., Ibanez, E., 2008. In the search of new functional food ingredients from algae. Trends Food Sci. Technol. 19, 31–39. https://doi.org/10.1016/j.tifs.2007.07.012

Plaza, M., Herrero, M., Cifuentes, A., Ibáñez, E., 2009. Innovative natural functional ingredients from microalgae. J. Agric. Food Chem. 57, 7159–7170. https://doi.org/10.1021/jf901070g

Posten, C., 2009. Design principles of photo-bioreactors for cultivation of microalgae. Eng. Life Sci. 9, 165–177. https://doi.org/10.1002/elsc.200900003

Priyadarshani, I., Rath, B., 2012. Commercial and industrial applications of micro algae-A review. J. Algal Biomass Utln 3, 89–100.

Procházková, G., Brányiková, I., Zachleder, V., Brányik, T., 2014. Effect of nutrient supply status on biomass composition of eukaryotic green microalgae. J. Appl. Phycol. 26, 1359–1377. https://doi.org/10.1007/s10811-013-0154-9

Pulz, O., 2001. Photobioreactors: production systems for phototrophic microorganisms. Appl. Microbiol. Biotechnol. 57, 287–293. https://doi.org/10.1007/s002530100702

Qin, S., Liu, G.X., Hu, Z.Y., 2008. The accumulation and metabolism of astaxanthin in Scenedesmus obliquus (Chlorophyceae). Process Biochem. 43, 795–802. https://doi.org/10.1016/j.procbio.2008.03.010

Raabe, E.W., 1968. Biochemical oxygen demand and degradation of lignin in natural waters. J. (Water Pollut. Control Fed. 40, 145–150.

Radakovits, R., Jinkerson, R.E., Fuerstenberg, S.I., Tae, H., Settlage, R.E., Boore, J.L., Posewitz, M.C., 2012. Draft genome sequence and genetic transformation of the oleaginous alga Nannochloropsis gaditana. Nat. Commun. 3, 686. https://doi.org/10.1038/ncomms1688

Ramos-Martinez, E.M., Fimognari, L., Sakuragi, Y., 2017. High-yield secretion of recombinant proteins from the microalga Chlamydomonas reinhardtii. Plant Biotechnol. J. 15, 1214–1224. https://doi.org/10.1111/pbi.12710

Rao, N., Vidyapeeth, D.Y.P., 2013. Algal Database-Bioprospecting indigenous algae for industrial application. Indian J. Biotechnol. 12, 548–549.

Rasala, B.A., Lee, P.A., Shen, Z., Briggs, S.P., Mendez, M., Mayfield, S.P., 2012. Robust expression and secretion of xylanase1 in Chlamydomonas reinhardtii by fusion to a selection gene and processing with the FMDV 2A peptide. PLoS One 7. https://doi.org/10.1371/journal.pone.0043349

Rasala, B.A., Mayfield, S.P., 2015. Photosynthetic biomanufacturing in green algae; production of recombinant proteins for industrial, nutritional, and medical uses. Photosynth. Res. 123, 227–239. https://doi.org/10.1007/s11120-014-9994-7

Rasoul-Amini, S., Montazeri-Najafabady, N., Shaker, S., Safari, A., Kazemi, A., Mousavi, P., Mobasher, M.A., Ghasemi, Y., 2014. Removal of nitrogen and phosphorus from wastewater using microalgae free cells in bath culture system. Biocatal. Agric. Biotechnol. 3, 126–131. https://doi.org/10.1016/j.bcab.2013.09.003

Rastogi, R.P., Madamwar, D., Pandey, A., 2017. Algal green chemistry : recent progress in biotechnology. Elsevier.

Raux, E., Lanois, A., Levillayer, F., Warren, M.J., Brody, E., Rambach, A., Thermes, C., 1996. Salmonella typhimurium cobalamin (vitamin B12) biosynthetic genes: functional studies in S. typhimurium and Escherichia coli. J. Bacteriol. 178, 753–767. https://doi.org/10.1128/jb.178.3.753-767.1996

Rebolloso-Fuentes, M.M., Navarro-Pérez, A., García-Camacho, F., Ramos-Miras, J.J., Guil-Guerrero, J.L., 2001. Biomass Nutrient Profiles of the Microalga Nannochloropsis. J. Agric. Food Chem. 49, 2966–2972. https://doi.org/10.1021/jf0010376

Rebolloso Fuentes, M., 2000. Biomass nutrient profiles of the microalga Porphyridium cruentum. Food Chem. 70, 345–353. https://doi.org/10.1016/S0308-8146(00)00101-1

Redding, K.E., Cole, D.G., 2008. Chlamydomonas: a sexually active, light-harvesting, carbon-reducing, hydrogen-belching 'planimal'. EMBO Rep. 9, 1182–1187. https://doi.org/10.1038/embor.2008.205

Regad, F., Hervé, C., Marinx, O., Lescure, B., Bergounioux, C., Tremousaygue, D., 1995. The tef1 box, a ubiquitous cis-acting element involved in the activation of plant genes that are highly expressed in cycling cells. Mgg Mol. Gen. Genet. 248, 703–711. https://doi.org/10.1007/BF02191710

Rengel, A., Zoughaib, A., Dron, D., Clodic, D., 2012. Hydrodynamic study of an internal airlift reactor for microalgae culture. Appl. Microbiol. Biotechnol. 93, 117–129. https://doi.org/10.1007/s00253-011-3398-9

Reyimu, Z., Özçimen, D., 2017. Batch cultivation of marine microalgae Nannochloropsis oculata and Tetraselmis suecica in treated municipal wastewater toward bioethanol production. J. Clean. Prod. 150, 40–46. https://doi.org/10.1016/j.jclepro.2017.02.189

Richmond, A., Hu, Q., 2013. Handbook of microalgal culture, handbook of microalgal culture: applied phycology and biotechnology. Second Edition. John Wiley & Sons, Ltd, Oxford, UK. https://doi.org/10.1002/9781118567166

Rismani, S., Shariati, M., 2017. Changes of the total lipid and omega-3 fatty acid contents in two microalgae Dunaliella salina and Chlorella vulgaris under salt stress. Brazilian Arch. Biol. Technol. 60. https://doi.org/10.190/1678-4324-2017160555

Robles-Medina, A., González-Moreno, P.A., Esteban-Cerdán, L., Molina-Grima, E., 2009. Biocatalysis: Towards ever greener biodiesel production. Biotechnol. Adv. 27, 398–408. https://doi.org/10.1016/j.biotechadv.2008.10.008

Rocha, J.M.S., Garcia, J.E.C., Henriques, M.H.F., 2003. Growth aspects of the marine microalga Nannochloropsis gaditana. Biomol. Eng. 20, 237–242. https://doi.org/10.1016/S1389-0344(03)00061-3

Rochaix, J.-D., 2011. Regulation of photosynthetic electron transport. Biochim. Biophys. Acta - Bioenerg. 1807, 878–886. https://doi.org/10.1016/j.bbabio.2011.05.009

Rodolfi, L., Chini Zittelli, G., Bassi, N., Padovani, G., Biondi, N., Bonini, G., Tredici, M.R., 2009. Microalgae for oil: Strain selection, induction of lipid synthesis and outdoor mass cultivation in a low-cost photobioreactor. Biotechnol. Bioeng. 102, 100–112. https://doi.org/10.1002/bit.22033

Ruiz, J., Arbib, Z., Álvarez-Díaz, P.D., Garrido-Pérez, C., Barragán, J., Perales, J.A., 2013. Photobiotreatment model (PhBT): a kinetic model for microalgae biomass growth and nutrient removal in wastewater. Environ. Technol. 34, 979–991. https://doi.org/10.1080/09593330.2012.724451

Ruiz, J., Olivieri, G., de Vree, J., Bosma, R., Willems, P., Reith, J.H., Eppink, M.H.M., Kleinegris, D.M.M., Wijffels, R.H., Barbosa, M.J., 2016. Towards industrial products from microalgae. Energy Environ. Sci. 9, 3036–3043. https://doi.org/10.1039/C6EE01493C

Rumeau, D., Peltier, G., Cournac, L., 2007. Chlororespiration and cyclic electron flow around PSI during photosynthesis and plant stress response. Plant. Cell Environ. 30, 1041–1051. https://doi.org/10.1111/j.1365-3040.2007.01675.x

Sadeghizadeh, A., Farhad dad, F., Moghaddasi, L., Rahimi, R., 2017. CO2 capture from air by Chlorella vulgaris microalgae in an airlift photobioreactor. Bioresour. Technol. 243, 441–447. https://doi.org/10.1016/j.biortech.2017.06.147

Samer, M., 2015. Biological and Chemical Wastewater Treatment Processes, in: Wastewater Treatment Engineering. InTech. https://doi.org/10.5772/61250

Samson, R., Leduy, A., 1985. Multistage continuous cultivation of blue-green alga Spirulina maxima in the flat tank photobioreactors with recycle. Can. J. Chem. Eng. 63, 105–112. https://doi.org/10.1002/cjce.5450630117

Sánchez Mirón, A., García Camacho, F., Contreras Gómez, A., Grima, E.M., Chisti, Y., 2000. Bubble-column and airlift photobioreactors for algal culture. AIChE J. 46, 1872–1887. https://doi.org/10.1002/aic.690460915

Santocono, M., Zurria, M., Berrettini, M., Fedeli, D., Falcioni, G., 2007. Lutein, zeaxanthin and astaxanthin protect against DNA damage in SK-N-SH human neuroblastoma cells induced by reactive nitrogen species. J. Photochem. Photobiol. B Biol. 88, 1–10. https://doi.org/10.1016/j.jphotobiol.2007.04.007

Sanz-Luque, E., Chamizo-Ampudia, A., Llamas, A., Galvan, A., Fernandez, E., 2015. Understanding nitrate assimilation and its regulation in microalgae. Front. Plant Sci. 6. https://doi.org/10.3389/fpls.2015.00899

Saracco, G., 2017. Chimica verde 2.0: Impariamo dalla natura come combattere il riscaldamento globale. Zanichelli.

Sathasivam, R., Radhakrishnan, R., Hashem, A., Abd_Allah, E.F., 2019. Microalgae metabolites: A rich source for food and medicine. Saudi J. Biol. Sci. 26, 709–722. https://doi.org/10.1016/j.sjbs.2017.11.003

Scaife, M.A., Nguyen, G.T.D.T., Rico, J., Lambert, D., Helliwell, K.E., Smith, A.G., 2015. Establishing Chlamydomonas reinhardtii as an industrial biotechnology host. Plant J. 82, 532–546. https://doi.org/10.1111/tpj.12781

Schreiber, U., Bilger, W., Neubauer, C., 2012. Chlorophyll Fluorescence as a Nonintrusive Indicator for Rapid Assessment of In Vivo Photosynthesis. Ecophysiol. Photosynth. 49–70. https://doi.org/10.1007/978-3-642-79354-7_3

Schüler, L.M., Schulze, P.S.C., Pereira, H., Barreira, L., León, R., Varela, J., 2017. Trends and strategies to enhance triacylglycerols and high-value compounds in microalgae. Algal Res. 25, 263–273. https://doi.org/10.1016/j.algal.2017.05.025

Schulze, P.S.C., Carvalho, C.F.M., Pereira, H., Gangadhar, K.N., Schüler, L.M., Santos, T.F., Varela, J.C.S., Barreira, L., 2017a. Urban wastewater treatment by Tetraselmis sp. CTP4 (Chlorophyta). Bioresour. Technol. 223, 175–183. https://doi.org/10.1016/j.biortech.2016.10.027

Schulze, P.S.C., Guerra, R., Pereira, H., Schüler, L.M., Varela, J.C.S., 2017b. Flashing LEDs for microalgal production. Trends Biotechnol. 35, 1088–1101. https://doi.org/10.1016/j.tibtech.2017.07.011

Schulze, P.S.C., Barreira, L.A., Pereira, H.G.C., Perales, J.A., Varela, J.C.S., 2014. Light emitting diodes (LEDs) applied to microalgal production. Trends Biotechnol. 32, 422–430. https://doi.org/10.1016/j.tibtech.2014.06.001

Serôdio, J., Vieira, S., Cruz, S., Coelho, H., 2007. Rapid light-response curves of chlorophyll fluorescence in microalgae: relationship to steady-state light curves and non-photochemical quenching in benthic diatom-dominated assemblages. Photosynth. Res. 90, 29–43. https://doi.org/10.1007/s11120-006-9105-5

Sforza, E., Pastore, M., Santeufemia Sanchez, S., Bertucco, A., 2018a. Bioaugmentation as a strategy to enhance nutrient removal: Symbiosis between Chlorella protothecoides and Brevundimonas diminuta. Bioresour. Technol. Reports 4, 153–158. https://doi.org/10.1016/j.biteb.2018.10.007

Sforza, E., Pastore, M., Spagni, A., Bertucco, A., 2018b. Microalgae-bacteria gas exchange in wastewater: how mixotrophy may reduce the oxygen supply for bacteria. Environ. Sci. Pollut. Res. 25, 28004–28014. https://doi.org/10.1007/s11356-018-2834-0

Sforza, E., Simionato, D., Giacometti, G.M., Bertucco, A., Morosinotto, T., 2012. Adjusted light and dark cycles can optimize photosynthetic efficiency in algae growing in photobioreactors. PLoS One 7, e38975. https://doi.org/10.1371/journal.pone.0038975

Shah, A.R., Ahmad, A., Srivastava, S., Jaffar Ali, B.M., 2017. Reconstruction and analysis of a genome-scale metabolic model of Nannochloropsis gaditana. Algal Res. 26, 354–364. https://doi.org/10.1016/j.algal.2017.08.014

Sierra, E., Acién, F.G., Fernández, J.M., García, J.L., González, C., Molina, E., 2008. Characterization of a flat plate photobioreactor for the production of microalgae. Chem. Eng. J. 138, 136–147. https://doi.org/10.1016/j.cej.2007.06.004

Simionato, D., Basso, S., Giacometti, G.M., Morosinotto, T., 2013a. Optimization of light use efficiency for biofuel production in algae. Biophys. Chem. 182, 71–78. https://doi.org/10.1016/j.bpc.2013.06.017

Simionato, D., Block, M.A., La Rocca, N., Jouhet, J., Maréchal, E., Finazzi, G., Morosinotto, T., 2013b. The Response of Nannochloropsis gaditana to nitrogen starvation includes de novo biosynthesis of triacylglycerols, a decrease of chloroplast galactolipids, and reorganization of the photosynthetic apparatus. Eukaryot. Cell 12, 665–676. https://doi.org/10.1128/EC.00363-12

Singh, D., Nedbal, L., Ebenhöh, O., 2018. Modelling phosphorus uptake in microalgae. Biochem. Soc. Trans. 46, 483–490. https://doi.org/10.1042/BST20170262

Solovchenko, A., Khozin-Goldberg, I., Recht, L., Boussiba, S., 2011. stress-induced changes in optical properties, pigment and fatty acid content of Nannochloropsis sp.: Implications for non-destructive assay of total fatty acids. Mar. Biotechnol. 13, 527–535. https://doi.org/10.1007/s10126-010-9323-x

Solovchenko, A.E., Khozin-Goldberg, I., Didi-Cohen, S., Cohen, Z., Merzlyak, M.N., 2008. Effects of light and nitrogen starvation on the content and composition of carotenoids of the green microalga Parietochloris incisa. Russ. J. Plant Physiol. 55, 455–462. https://doi.org/10.1134/S1021443708040043

Stehfest, K., Toepel, J., Wilhelm, C., 2005. The application of micro-FTIR spectroscopy to analyze nutrient stress-related changes in biomass composition of phytoplankton algae. Plant Physiol. Biochem. 43, 717–726. https://doi.org/10.1016/j.plaphy.2005.07.001

Steinbrenner, J., Sandmann, G., 2006. Transformation of the Green Alga Haematococcus pluvialis with a Phytoene Desaturase for Accelerated Astaxanthin Biosynthesis. Appl. Environ. Microbiol. 72, 7477–7484. https://doi.org/10.1128/AEM.01461-06

Stevens, D.R., Purton, S., Rochaix, J.-D., 1996. The bacterial phleomycin resistance geneble as a dominant selectable marker in Chlamydomonas, MGG Molecular & General Genetics. Springer-Verlag.

Su, X., Xu, J., Yan, X., Zhao, P., Chen, J., Zhou, C., Zhao, F., Li, S., 2013. Lipidomic changes during different growth stages of Nitzschia closterium f. minutissima. Metabolomics 9, 300–310. https://doi.org/10.1007/s11306-012-0445-1

Subashchandrabose, S.R., Ramakrishnan, B., Megharaj, M., Venkateswarlu, K., Naidu, R., 2011. Consortia of cyanobacteria/microalgae and bacteria: Biotechnological potential. Biotechnol. Adv. 29, 896–907. https://doi.org/10.1016/j.biotechadv.2011.07.009

Sukenik, A., Livne, A., Neori, A., Yacobi, Y.Z., Katcoff, D., 1992. Purification and characterization of a light-harvesting chlorophyll-protein complex from the marine Eustigmatophyte Nannochloropsis sp. Plant Cell Physiol. 33, 1041–1048. https://doi.org/10.1093/oxfordjournals.pcp.a078354

Sulaiman Al-Zuhair, 2007. Production of biodiesel: possibilities and challenges. Biofuels, Bioprod. Biorefining 1, 57–66. https://doi.org/10.1002/bbb

Supeng, L., Guirong, B., Hua, W., Fashe, L., Yizhe, L., 2012. TG-DSC-FTIR Analysis of Cyanobacteria Pyrolysis. Phys. Procedia 33, 657–662. https://doi.org/10.1016/j.phpro.2012.05.117

Suzuki, H., Hulatt, C.J., Wijffels, R.H., Kiron, V., 2019. Growth and LC-PUFA production of the cold-adapted microalga Koliella antarctica in photobioreactors. J. Appl. Phycol. 31, 981–997. https://doi.org/10.1007/s10811-018-1606-z

Takache, H., Pruvost, J., Marec, H., 2015. Investigation of light/dark cycles effects on the photosynthetic growth of Chlamydomonas reinhardtii in conditions representative of photobioreactor cultivation. Algal Res. 8, 192–204. https://doi.org/10.1016/j.algal.2015.02.009

Tanaka, R., Tanaka, A., 2007. Tetrapyrrole Biosynthesis in Higher Plants. Annu. Rev. Plant Biol. 58, 321–346. https://doi.org/10.1146/annurev.arplant.57.032905.105448

Tanaka, T., Makita, H., Ohnishi, M., Mori, H., Satoh, K., Hara, A., 1995. Chemoprevention of Rat Oral Carcinogenesis by Naturally Occurring Xanthophylls, Astaxanthin and Canthaxanthin. Cancer Res. 55, 4059–4064.

Tapia, C., Fermoso, F.G., Serrano, A., Torres, Á., Jeison, D., Rivas, M., Ruiz, G., Vílchez, C., Cuaresma, M., 2019. Potential of a local microalgal strain isolated from anaerobic digester effluents for nutrient removal. J. Appl. Phycol. 31, 345–353. https://doi.org/10.1007/s10811-018-1546-7

Thangavel, P., Sridevi, G., 2015. Environmental Sustainability, Environmental Sustainability: Role of Green Technologies. Springer India, New Delhi. https://doi.org/10.1007/978-81-322-2056-5

Thornber, J.P., 1986. Biochemical Characterization and Structure of Pigment-Proteins of Photosynthetic Organism, in: Photosynthesis III. Springer Berlin Heidelberg, Berlin, Heidelberg, pp. 98–142. https://doi.org/10.1007/978-3-642-70936-4_3

Tibbetts, S.M., Milley, J.E., Lall, S.P., 2015. Chemical composition and nutritional properties of freshwater and marine microalgal biomass cultured in photobioreactors. J. Appl. Phycol. 27, 1109–1119. https://doi.org/10.1007/s10811-014-0428-x

Toseland, A., Daines, S.J., Clark, J.R., Kirkham, A., Strauss, J., Uhlig, C., Lenton, T.M., Valentin, K., Pearson, G.A., Moulton, V., Mock, T., 2013. The impact of temperature on marine phytoplankton resource allocation and metabolism. Nat. Clim. Chang. 3, 1–6. https://doi.org/10.1038/nclimate1989

Tran, M., Van, C., Barrera, D.J., Pettersson, P.L., Peinado, C.D., Bui, J., Mayfield, S.P., 2013. Production of unique immunotoxin cancer therapeutics in algal chloroplasts. Proc. Natl. Acad. Sci. 110, E15–E22. https://doi.org/10.1073/pnas.1214638110

Tredici, M.R., Materassi, R., 1992. From open ponds to vertical alveolar panels: the Italian experience in the development of reactors for the mass cultivation of phototrophic microorganisms, Journal of Applied Phycology.

Tredici, M.R., Zittelli, G.C., 1998. Efficiency of sunlight utilization: Tubular versus flat photobioreactors. Biotechnol. Bioeng. 57, 187–197. https://doi.org/10.1002/(SICI)1097-0290(19980120)57:2<187::AID-BIT7>3.0.CO;2-J

Trevelyan, W.E., Forrest, R.S., Harrison, J.S., 1952. Determination of Yeast Carbohydrates with the Anthrone Reagent. Nature 170, 626–627. https://doi.org/10.1038/170626a0

Ugwu, C.U., Aoyagi, H., Uchiyama, H., 2008. Photobioreactors for mass cultivation of algae. Bioresour. Technol. 99, 4021–4028. https://doi.org/10.1016/j.biortech.2007.01.046

Vahrenholz, C., Riemen, G., Pratje, E., Dujon, B., Michaelis, G., 1993. Mitochondrial DNA of Chlamydomonas reinhardtii: the structure of the ends of the linear 15.8-kb genome suggests mechanisms for DNA replication. Curr. Genet. 24, 241–7. https://doi.org/10.1007/bf00351798

Van Amerongen, H., Croce, R., 2013. Light-harvesting in photosystem II. Photosynt Res 116. https://doi.org/10.1007/s11120-013-9824-3

Vandesompele, J., De Preter, K., Pattyn, F., Poppe, B., Van Roy, N., De Paepe, A., Speleman, F., 2002. Accurate normalization of real-time quantitative RT-PCR data by geometric averaging of multiple internal control genes. Genome Biol. 3, research0034.1. https://doi.org/10.1186/gb-2002-3-7-research0034

Vanier, G., Hempel, F., Chan, P., Rodamer, M., Vaudry, D., Maier, U.G., Lerouge, P., Bardor, M., 2015. Biochemical Characterization of Human Anti-Hepatitis B Monoclonal Antibody Produced in the Microalgae Phaeodactylum tricornutum. PLoS One 10, e0139282. https://doi.org/10.1371/journal.pone.0139282

Varela, J.C., Pereira, H., Vila, M., León, R., 2015. Production of carotenoids by microalgae: achievements and challenges. Photosynth. Res. 125, 423–436. https://doi.org/10.1007/s11120-015-0149-2

Varshavsky, A., 2017. The Ubiquitin System, Autophagy, and Regulated Protein Degradation. https://doi.org/10.1146/annurev-biochem

Vazhappilly, R., Chen, F., 1998. Eicosapentaenoic Acid and Docosahexaenoic Acid Production Potential of Microalgae and Their Heterotrophic Growth. J. Am. Oil Chem. Soc. 75, 393–397.

Vejrazka, C., Janssen, M., Streefland, M., Wijffels, R.H., 2012. Photosynthetic efficiency of Chlamydomonas reinhardtii in attenuated, flashing light. Biotechnol. Bioeng. 109, 2567–2574. https://doi.org/10.1002/bit.24525

Villalobos, A., Ness, J.E., Gustafsson, C., Minshull, J., Govindarajan, S., 2006. Gene Designer: a synthetic biology tool for constructing artificial DNA segments. BMC Bioinformatics 7, 285. https://doi.org/10.1186/1471-2105-7-285

Vitamin B12 (Cobalamin, Cyanocobalamin) Market Value to boost by 400 million US in 2025 [WWW Document], n.d. URL https://www.reuters.com/brandfeatures/venture-capital/article?id=58074 (accessed 9.12.19).

Wada, M., Yasuno, R., Wada, H., 2001. Identification of an Arabidopsis cDNA encoding a lipoyltransferase located in plastids. FEBS Lett. 506, 286–90. https://doi.org/10.1016/s0014-5793(01)02932-5

Walker, T.L., Purton, S., Becker, D.K., Collet, C., 2005. Microalgae as bioreactors. Plant Cell Rep. 24, 629–641. https://doi.org/10.1007/s00299-005-0004-6

Wang, L., Min, M., Li, Y., Chen, P., Chen, Y., Liu, Y., Wang, Y., Ruan, R., 2010. Cultivation of Green Algae Chlorella sp. in Different Wastewaters from Municipal Wastewater Treatment Plant. Appl. Biochem. Biotechnol. 162, 1174–1186. https://doi.org/10.1007/s12010-009-8866-7

Warren, M.J., Raux, E., Schubert, H.L., Escalante-Semerena, J.C., 2002. The biosynthesis of adenosylcobalamin (vitamin B12). Nat. Prod. Rep. 19, 390–412. https://doi.org/10.1039/b108967f

Wells, M.L., Potin, P., Craigie, J.S., Raven, J.A., Merchant, S.S., Helliwell, K.E., Smith, A.G., Camire, M.E., Brawley, S.H., 2017. Algae as nutritional and functional food sources: revisiting our understanding. J. Appl. Phycol. 29, 949–982. https://doi.org/10.1007/s10811-016-0974-5

Wiktorowska-Owczarek, A., Berezińska, M., Nowak, J., 2015. PUFAs: Structures, Metabolism and Functions. Adv. Clin. Exp. Med. 24, 931–941. https://doi.org/10.17219/acem/31243

Wilkie, A.C., Edmundson, S.J., Duncan, J.G., 2011. Indigenous algae for local bioresource production: Phycoprospecting. Energy Sustain. Dev. 15, 365–371. https://doi.org/10.1016/j.esd.2011.07.010

Wood, B.J.B., 1974. Fatty acids and saponifiable lipids, in: Algal Physiology and Biochemistry. Blackwell Scientific Publications Oxford, pp. 236–265.

Wu, K.-C., Yau, Y.-H., Ho, K.-C., 2017. Capability of microalgae for local saline sewage treatment towards biodiesel production. IOP Conf. Ser. Earth Environ. Sci. 82, 012008. https://doi.org/10.1088/1755-1315/82/1/012008

Wu, X., Merchuk, J.C., 2004. Simulation of algae growth in a bench scale internal loop airlift reactor. Chem. Eng. Sci. 59, 2899–2912. https://doi.org/10.1016/j.ces.2004.02.019

WWAP, 2017. Wastewater : the untapped resource : the United Nations world water development report 2017.

Xu, L., Weathers, P.J., Xiong, X.R., Liu, C.Z., 2009. Microalgal bioreactors: Challenges and opportunities. Eng. Life Sci. 9, 178–189. https://doi.org/10.1002/elsc.200800111

Xue, S., Su, Z., Cong, W., 2011. Growth of Spirulina platensis enhanced under intermittent illumination. J. Biotechnol. 151, 271–277. https://doi.org/10.1016/j.jbiotec.2010.12.012

Yaakob, Z., Ali, E., Zainal, A., Mohamad, M., Takriff, M., 2014. An overview: biomolecules from microalgae for animal feed and aquaculture. J. Biol. Res. 21, 6. https://doi.org/10.1186/2241-5793-21-6

Yan, N., Fan, C., Chen, Y., Hu, Z., 2016. The Potential for Microalgae as Bioreactors to Produce Pharmaceuticals. Int. J. Mol. Sci. 17, 962. https://doi.org/10.3390/ijms17060962

Yarnold, J., Ross, I.L., Hankamer, B., 2016. Photoacclimation and productivity of Chlamydomonas reinhardtii grown in fluctuating light regimes which simulate outdoor algal culture conditions. Algal Res. 13, 182–194. https://doi.org/10.1016/j.algal.2015.11.001

Yasuno, R., Wada, H., 2002. The biosynthetic pathway for lipoic acid is present in plastids and mitochondria in Arabidopsis thaliana. FEBS Lett. 517, 110–4. https://doi.org/10.1016/s0014-5793(02)02589-9

Yoshida, H., Yanai, H., Ito, K., Tomono, Y., Koikeda, T., Tsukahara, H., Tada, N., 2010. Administration of natural astaxanthin increases serum HDL-cholesterol and adiponectin in subjects with mild hyperlipidemia. Atherosclerosis 209, 520–523. https://doi.org/10.1016/j.atherosclerosis.2009.10.012

Yoshioka, M., Yago, T., Yoshie-Stark, Y., Arakawa, H., Morinaga, T., 2012. Effect of high frequency of intermittent light on the growth and fatty acid profile of Isochrysis galbana. Aquaculture 338–341, 111–117. https://doi.org/10.1016/j.aquaculture.2012.01.005

Yu, H., Kim, J., Lee, C., 2019. Potential of mixed-culture microalgae enriched from aerobic and anaerobic sludges for nutrient removal and biomass production from anaerobic effluents. Bioresour. Technol. 280, 325–336. https://doi.org/10.1016/j.biortech.2019.02.054

Yu, W.-L., Ansari, W., Schoepp, N.G., Hannon, M.J., Mayfield, S.P., Burkart, M.D., 2011. Modifications of the metabolic pathways of lipid and triacylglycerol production in microalgae. Microb. Cell Fact. 10, 91. https://doi.org/10.1186/1475-2859-10-91

Yuan, G., Zhang, Wenlei, Xu, X., Zhang, Wei, Cui, Y., Liu, T., 2018. Biolistic transformation of Haematococcus pluvialis with constructs based on the flanking sequences of its endogenous alpha tubulin gene. bioRxiv 420711. https://doi.org/10.1101/420711

Yuan, J.-P., Chen, F., 2000. Purification of trans-astaxanthin from a high-yielding astaxanthin ester-producing strain of the microalga Haematococcus pluvialis. Food Chem. 68, 443–448. https://doi.org/10.1016/S0308-8146(99)00219-8

Yun, H.-S., Lee, H., Park, Y.-T., Ji, M.-K., Kabra, A.N., Jeon, C., Jeon, B.-H., Choi, J., 2014. Isolation of novel microalgae from acid mine drainage and its potential application for biodiesel production. Appl. Biochem. Biotechnol. 173, 2054–2064. https://doi.org/10.1007/s12010-014-1002-3

Zedler, J.A.Z., Gangl, D., Guerra, T., Santos, E., Verdelho, V. V., Robinson, C., 2016. Pilot-scale cultivation of wall-deficient transgenic Chlamydomonas reinhardtii strains expressing recombinant proteins in the chloroplast. Appl. Microbiol. Biotechnol. 100, 7061–7070. https://doi.org/10.1007/s00253-016-7430-y

Zedler, J.A.Z., Gangl, D., Hamberger, B., Purton, S., Robinson, C., 2015. Stable expression of a bifunctional diterpene synthase in the chloroplast of Chlamydomonas reinhardtii. J. Appl. Phycol. 27, 2271–2277. https://doi.org/10.1007/s10811-014-0504-2

Zeeman, S.C., Kossmann, J., Smith, A.M., 2010. Starch: Its Metabolism, Evolution, and Biotechnological Modification in Plants. Annu. Rev. Plant Biol. 61, 209–234. https://doi.org/10.1146/annurev-arplant-042809-112301

Zeraatkar, A.K., Ahmadzadeh, H., Talebi, A.F., Moheimani, N.R., McHenry, M.P., 2016. Potential use of algae for heavy metal bioremediation, a critical review. J. Environ. Manage. 181, 817–831. https://doi.org/10.1016/j.jenvman.2016.06.059

Zhang, K., Kurano, N., Miyachi, S., 2002. Optimized aeration by carbon dioxide gas for microalgal production and mass transfer characterization in a vertical flat-plate photobioreactor. Bioprocess Biosyst. Eng. 25, 97–101. https://doi.org/10.1007/s00449-002-0284-y

Zhu, C.J., Lee, Y.K., Chao, T.M., 1997. Effects of temperature and growth phase on lipid and biochemical composition of Isochrysis galbana TK1. J. Appl. Phycol. 9, 451–457. https://doi.org/10.1023/A:1007973319348

Zhu, S., Feng, S., Xu, Z., Qin, L., Shang, C., Feng, P., Wang, Z., Yuan, Z., 2019. Cultivation of Chlorella vulgaris on unsterilized dairy-derived liquid digestate for simultaneous biofuels feedstock production and pollutant removal. Bioresour. Technol. 285, 121353. https://doi.org/10.1016/j.biortech.2019.121353

Zhu, S., Wang, Y., Shang, C., Wang, Z., Xu, J., Yuan, Z., 2015. Characterization of lipid and fatty acids composition of Chlorella zofingiensis in response to nitrogen starvation. J. Biosci. Bioeng. 120, 205–209. https://doi.org/10.1016/j.jbiosc.2014.12.018

Zielińska, A., Nowak, I., 2014. Fatty acids in vegetable oils and their importance in cosmetic industry. Chemik 68, 103–110.

Zou, N., Richmond, A., 2000. Light-path length and population density in photoacclimation of Nannochloropsis sp (Eustigmatophyceae). J. Appl. Phycol. 12, 349–354. https://doi.org/10.1023/A:1008151004317

Zuber, N., Findlay, J.A., 1965. Average Volumetric Concentration in Two-Phase Flow Systems. J. Heat Transfer 87, 453–468. https://doi.org/10.1115/1.3689137

Zuorro, A., Malavasi, V., Cao, G., Lavecchia, R., 2018. Use of cell wall degrading enzymes to improve the recovery of lipids from Chlorella sorokiniana. Chem. Eng. J. https://doi.org/10.1016/j.cej.2018.11.023

Zweytick, D., Athenstaedt, K., Daum, G., 2000. Intracellular lipid particles of eukaryotic cells. Biochim. Biophys. Acta - Rev. Biomembr. 1469, 101–120. https://doi.org/10.1016/S0005-2736(00)00294-7